PhD THESIS in Bio-engineering

Université Catholique de Louvain – Belgian Nuclear Research Centre

Kristel Mijnendonckx

Adaptive silver resistance in *Cupriavidus metallidurans*

Laboratoy of Food and Environmental Microbiology (UCL)

Microbiology Unit (SCK•CEN)

November 7, 2013

PhD defense committee:

Promoter:	Jacques Mahillon	–	UCL (ELIM)
Co-promoter:	Rob Van Houdt	–	SCK•CEN (MIC)
Reviewers:	Isabelle George	–	ULB
	Dirk Springael	–	KULeuven
	Jon Hobman	–	University of Nottingham
Secretary:	Claude Bragard	–	UCL (ELIM)
President:	Pierre Defourny	–	UCL (SST/ELI)

The known is finite, the unknown infinite; intellectually we stand on an island in the midst of an illimitable ocean of inexplicability. Our business in every generation is to reclaim a little more land.

Thomas Henry Huxley
(1825 – 1895)

Acknowledgements

"Eindelijk gedaan met je doctoraat. Dan is het gedaan met het schoon leven en kun je eindelijk beginnen werken" heb ik nog al eens te horen gekregen de laatste tijd ☺. Ik kan bij deze vertellen dat het behalen van een doctoraat inderdaad wel een schoon leven en genieten is, maar ook hard werken, veel bijleren en van tijd tot tijd zwoegen en zweten (vooral als de administratie geregeld moet worden). Ik ben dan ook heel trots op het resultaat van al het werk dat we de laatste 4 jaar verzet hebben en hier voorgesteld wordt. Natuurlijk zou ik dit nooit gekund hebben zonder de hulp en steun van verschillende personen en die verdienen het om eens extra in de bloemetjes gezet te worden.

First, I would to thank Natalie Leys to give me the opportunity to perform my PhD thesis at the MIC unit of SCK•CEN and my promoter Jacques Mahillon for the collaboration with UCL. I also want to thank the members of the examination commission for their critical evaluation of the dissertation.

Ik zou ook graag mijn collega's willen bedanken. Niet alleen voor de raad en me wegwijs te maken in de labo's, maar ook voor de gezellige babbels tijdens de middagpauzes en in het labo. Door de goede sfeer, kom je vanzelf met volle goesting naar het werk. En als je al eens een mindere dag hebt, zorgen de gesprekken tijdens de middag er wel voor dat alles weer voor efkes vergeten is. Een dikke merci dus en hopelijk blijft dit zo nog een tijdje doorgaan!

Een extra bedankje voor Pieter voor al het bio-informatica werk. Je hebt altijd tijd gemaakt voor alle analyses (en het waren er best wel veel) en ik

kon je altijd storen als ik een vraag had. Zonder uw hulp hadden we nooit zover gestaan in het zilver verhaal!

De collega's van de SCK volleybalploeg zou ik ook graag willen bedanken. Alhoewel er met de meeste toch een 'klein' verschil is in leeftijd, merk ik dat toch niet (en toch zeker niet aan de toog ☺). Het is de ideale ontspanning op een weekdag, waar ik nog altijd veel bijleer. Maar toch ben ik ook blij dat ik de oudere generatie af en toe ook al eens iets kan bijleren ☺.

Sjerk, Katrien en Floris, Arne, Jef, Nick, Freddy, Evelien voor alle ontspannings- en cafémomenten (en dat zijn er best wel veel), vakantie in Frankrijk, voor de gesprekken over sport en ook de fietsmomenten samen, voor het luisteren naar men gezaag,… Hoewel jullie waarschijnlijk niet echt begrepen waar het over ging, luisterden jullie toch altijd met veel interesse (of jullie deden toch goed alsof ☺) en dat doet toch veel plezier. Ik hoop dat onze vriendschap nog blijft!

Katrien, Sabine en Anne voor de voortzetting van de gezellige momenten die al begonnen zijn op kot.

Caroline, An, Thomas en Maarten: hoewel we maar een jaar hebben samengewerkt, is de band toch groot genoeg geworden om regelmatig te blijven afspreken en bij te kletsen en heel hard voor elkaar te supporteren als er eens iemand iets zot doet. De spelletjes namiddagen mogen ook zeker op regelmatige basis blijven duren als het van mij afhangt!

Ik zal waarschijnlijk nog wat mensen vergeten te vermelden zijn, dus bij deze ook aan hen een dikke merci.

Dan zijn er nog een paar speciale personen die extra in de verf gezet mogen worden.

Mijn familie, schoonfamilie, broers en zussen voor alle steun en de leuke momenten samen. Gezelligheid, genoeg eten en drinken zijn altijd gegarandeerd. Ik zou me geen betere familie kunnen voorstellen!

Rob, mijn begeleider tijdens mijn doctoraat. Amaj, ik kon me op voorhand geen betere begeleider voorstellen. Je zijt precies een wandelende encyclopedie. Voor alles wist je wel een oplossing en je stond ook altijd direct klaar als ik hulp nodig had met iets. Ik heb zoveel bijgeleerd tijdens de laatste 4 jaar en daar ben jij toch voor het grootste deel verantwoordelijk voor. Als ik ooit de helft zou weten wat jij allemaal weet, zou ik al heel blij zijn. Naast het urenlange overleg over het werk, komen we ook op persoonlijk vlak overeen (vooral door de gedeelde interesse voor de fiets), wat heel de periode des te aangenamer heeft gemaakt. Ik wens iedereen een begeleider als jij toe tijdens hun doctoraat, dan kan het niet mislopen.

Kristof: ik denk niet dat er veel woorden voor nodig zijn. Je hebt altijd voor me klaargestaan de laatste 4 jaar. Niet alleen voor mijn doctoraat en de tijd die daar in kroop, maar ook toen ik het vorig jaar in mijn kop kreeg om intensiever te gaan sporten en daar bijna al mijn vrije tijd in kroop. Hoewel wij op veel vlakken toch heel verschillend zijn, kan ik tegen je zagen en klagen, kunnen we veel plezier maken samen en gezellige babbels hebben. En je kunt nog eens lekker koken ook, wat wilt een mens nog meer ☺. Ik zou me moeilijk nog een leven zonder jou kunnen voorstellen.

En dan de laatste, maar de belangrijkste persoon die ik zou willen bedanken, is mijn moeder. Hoewel het zeker niet de gemakkelijkste oplossing was, ben ik zo blij dat je me een tweede kans hebt gegeven toen mijn eerste jaar op de universiteit niet echt een succes was. Had ik die niet gekregen, had ik nooit gestaan waar ik nu sta. Van kindsbeen af leg je ons zo hard je kunt in de watten en nu hetzelfde met je kleinkinderen. Je staat altijd direct klaar en steunt ons altijd door dik en dun. "Wacht maar tot je zelf kinderen hebt, dan

doe je juist hetzelfde" zeg je altijd. Ik hoop het. Ik zou echt een even goeie moeder voor mijn kinderen willen zijn als jij voor ons bent, want ge zijt de beste moeder die er is (hoewel we van tijd toch denken dat er ergens een klein hoekse af is ☺)!

Table of Contents

Abstract

During long-term manned spaceflight, controlling microbial contamination is of paramount importance as it can cause problems for the astronaut's health – well documented to have a decreased immunity – and the infrastructure of the space station. Strains from the β-proteobacterial genera *Cupriavidus* and *Ralstonia* have been identified and isolated during numerous monitoring campaigns from different space-related environments. This study aimed to gather more insights in the ability of these genera to thrive in these environments.

Several *C. metallidurans* and *R. pickettii* isolates from space-related environments were characterized in detail. Our results revealed that extreme resistance is not required to withstand the disinfection and sterilization procedures implemented in the International Space Station and space industry. All isolates acquired moderate to high tolerance against several stressors (antibiotics, silver and other metals, UV-C) and can grow in oligotrophic conditions, putatively enabling them to persist in these environments.

An important part of this study investigated the silver resistance mechanisms of the *C. metallidurans* and *R. pickettii* isolates, as silver is used to sanitize space water sources. All isolates tolerated silver concentrations higher than those measured regularly in the drinking water aboard the ISS and survived a 23 months exposure to 2 µM $AgNO_3$ in drinking water. In addition, at least all *C. metallidurans* isolates carried efflux systems involved in silver detoxification.

Furthermore, rapid evolution towards significantly increased silver resistance (> 10-fold compared to the parental strain) was observed with *C.*

metallidurans strains. Interestingly, the identified silver efflux pumps did not participate in this adaptive evolution. Whole-genome gene expression profiling and Illumina resequencing indicated the involvement of an uncharacterized protein that belongs to a unique group of ca. 20 homologous proteins distributed over the *C. metallidurans* genome. In addition, the data also indicated the putative involvement of the two-component regulatory system AgrR/S.

Finally, as Insertion Sequence elements were involved in the above described adaptive evolution, all IS elements in type strain *C. metallidurans* CH34 were characterized and classified. Our observations indicated that these IS elements indeed play an active role in the lifestyle of CH34, including its metabolic potential and adaptation under selective pressure.

Preamble

This PhD thesis was supported by the European Space Agency (ESA-PRODEX) and the Belgian Science Policy (Belspo) through the COMICS project and an AWM PhD grant from the Belgian Nuclear Research Centre (SCK•CEN). This PhD was a collaboration between the Laboratory of Food and Environmental Microbiology of the Catholique University of Louvain-la-Neuve and the Unit of Microbiology of SCK•CEN. Research was performed at SCK•CEN.

The initial objective of this project was to characterize *C. metallidurans* and *R. pickettii* isolates from different space-related environments in detail (Chapter 4). The observations that all *C. metallidurans* isolates contained several silver resistance mechanisms and their abiltiy to survive long time-periods in water supplemented with silver nitrate, prompted the study of the silver resistance mechanisms in *C. metalldiruans* more in detail (Chapter 5). This led to the discovery of a novel type of silver resistance, in which insertion sequence elements played a role. Therefore, the last chapters (Chapter 6 and 7) of this work discuss the presence and role of insertion sequence elements in *C. metallidurans* CH34. Moreover, the mobility and metal resistance capacity of plasmids present in all *C. metallidurans* isolates was investigated.

This thesis contains a series of five manuscripts (one added as Appendix A) describing work performed in collaboration with other scientists. In addition, several sections of this work have been communicated to different scientific meetings, as posters and oral communications (Appendix B).

Included manuscripts

1. **Microbial contamination monitoring and control during human space missions** Van Houdt R., Mijnendonckx K., Leys N. *Planetary and Space Science* 60(1):115-120, 2012
2. **Antimicrobial silver: uses, toxicity and potential for resistance** Mijnendonckx K., Leys N., Mahillon J., Silver S., Van Houdt R. *Biometals* 26 (3), 2013
3. **Characterization of the Survival Ability of *Cupriavidus metallidurans* and *Ralstonia pickettii* from Space-Related Environments** Mijnendonckx K., Provoost A., Ott C., Venkateswaran K., Mahillon J., Leys N., Van Houdt R. *Microbial Ecology* 65(2): 347-360, 2013
4. **Insertion sequence elements in *Cupriavidus metallidurans* CH34: Distribution and role in adaptation** Mijnendonckx K., Provoost A., Monsieurs P., Leys N., Mergeay M., Mahillon J., Van Houdt R. *Plasmid* 65(3): 193-203, 2011
5. **Variation in genomic islands contribute to genome plasticity in *Cupriavidus metallidurans*** Van Houdt R., Monsieurs P., Mijnendonckx K., Provoost A., Janssen A., Mergeay M., Leys N *BMC Genomics* (13): 111, 2012

List of Figures

List of Tables

List of Acronyms

AC	amorphous carbon
Amp	ampicillin
AgNP	silver nanoparticle
ATR	attenuated total reflection
CDS	coding sequence
CFU	colony forming unit
CGH	comparative whole genome hybridization
CHR1	chromosome 1
CHR2	chromosome 2
Cm	chloramphenicol
COG	cluster of orthologous groups
CWC	contingency water container
DR	direct repeat
ERIC-PCR	enterobacterial repetitive intergenic consensus PCR
ESI	electrospray ionization
FTIR	fourier transform infrared spectroscopy
GI	genomic island
HME-RND	heavy metal efflux – resistance nodulation cell division
ICE	integrative and conjugative element
IR	inverted repeat
IMAC	immobilized metal affinity chromatrography
IPTG	isopropyl-β-D-1-thiogalactopyranoside
IS	insertion sequence
ISS	International Space Station
ISS MORD	International Space Station Medical Operations Requirements
Km	kanamycin
LB	lysogeny-Broth
LOCAD-PTS	Lab-On-a-Chip application development portable test System
MEGA	molecular evolutionary genetics analysis
MGE	mobile genetic element

MIC	minimal inhibitory concentration
MS	mass spectrometry
MTC	maximum tolerable concentration
ND	not determined
ORF	open reading frame
PHA	polyhydroxyalkanoates
PHB	polyhydroxybutyrate
SEC	size exclusion chromatography
TEM	transmission electron microscopy
PVP	polyvinylpyrrolidone
ROS	reactive oxygen species
Tc	tetracycline
Tm	trimethoprim
WRS	water recovery system

PART I

INTRODUCTION AND OBJECTIVES

Chapter 1

Microbial contamination monitoring and control during human space missions

The ubiquity and resilience of microorganisms makes them unavoidable in most environments including space habitats. The impaired immune system of astronauts in flight raises the level of concern about disease risk during human space missions and additionally these biological contaminants may affect life support systems and hardware. In this chapter, the microbial contamination observed in manned space stations and in particular, the International Space Station will be discussed, demonstrating that it is a microbiologically safe working and living habitat. Microbial contamination levels were in general below the implemented quality standards, although, occasional contamination hazard reports indicate that the current prevention and monitoring strategies are a strict minimum.

This chapter is based on the following publication:

Van Houdt R., Mijnendonckx K., Leys N. (2012) Microbial contamination monitoring and control during human space missions *Planetary and Space Science* 60(1):115-120

1.1 Introduction

The International Space Station (ISS) is an exceptional work and living place. This state-of-the-art small-enclosed volume accommodates alternating crews with 3 to 10 members. Astronauts on mission face unique circumstances including high working pressure, defined diet and restricted hygienic practices, microgravity and radiation. These factors affect the immune system of astronauts (reviewed by [1]) and increased susceptibility to infection in space analogous environments has been shown [2, 3].

The microbial population in these man-made environments mainly comes from the crew (skin, upper respiratory tract, mouth, and gastrointestinal tract) but also environmental microorganisms are present. This microbial population is further shaped both in diversity and mass by the unique combination of environmental factors (e.g. restricted hygienic practices, confinement, microgravity, radiation). Although most of these microorganisms do not pose severe risks for healthy people, the hampered immune system of astronauts combined with limited treatment and isolation possibilities, and no immediate return to Earth reinforces the requirement to control microbial contamination stringently. Therefore, the contamination level as well as its diversity needs to be controlled, to guarantee adequate living quality and reduce the risks of harmful effects on the crew. It is obvious that (opportunistic) pathogens, which are capable of causing infections and disease, take a dominant part in these preventive measures. Therefore, international microbiological quality standards for food, air, surfaces and water have been defined and prevention, monitoring and mitigation measures are implemented by the space agencies.

1.2 International environmental quality standards for the ISS

The maximal concentration of bacteria and fungi allowed in water, air and on surfaces in the living and working areas of the ISS were internationally defined to ensure the indoor environmental quality in space stations and are described in the ISS Medical Operations Requirements Document (ISS MORD) [4, 5]. The threshold levels are a trade-off between acceptable risk and realizable levels with the current prevention and monitoring technologies available and applicable for space (Table 1.1). Threshold levels are scored by the maximum total number of aerobic and heterotrophic viable cells of bacteria or fungi, counted as colony forming units on a rich agar medium.

Table 1.1: Environmental microbial quality standards for air, surfaces and water in the ISS

		Maximum for bacteria	Maximum for fungi
Pre-flight	Air	300 CFU/m^3	50 CFU/m^3
	Internal surfaces	500 CFU/100 cm^2	10 CFU/100 cm^2
	Potable water*	50 CFU/ml	ND
In-flight	Air	1000 CFU/m^3	100 CFU/m^3
	Internal surfaces	10,000 CFU/100 cm^2	100 CFU/100 cm^2
	Potable water*	50 CFU/ml	ND

ND = not determined, CFU = Colony Forming Unit, *Coliforms may not be detected.

The in-flight air quality standards in the ISS are equivalent to limits frequently implemented for healthy offices [6, 7] and in general similar to those used to assess indoor air quality in Europe [8]. Based on the classification of the European Collaborative Action "Indoor Air Quality and its Impact on Man" for bacteria and fungi in homes and offices, the ISS threshold levels fall in the category intermediate for bacteria and low for

fungi [9]. Similarly, ISS drinking water standards are comparable to World Health Organization guidelines [10] and Earthly US standards [11]. For surfaces there are few published standards or guidelines on what are acceptable levels of microbial contamination. The European Commission Decision laid down that cleaned and disinfected surfaces in establishments for the production and marketing of fresh meat have an acceptable range when total viable counts are between 0-10 CFU/cm^2 (equivalent to 0-1,000 CFU/100 cm^2) (2001/471/EC). For hand contact surfaces in hospitals, the total viable count should be less than 2.5 CFU/cm^2 (equivalent to 250 CFU/100 cm^2) [12]. Therefore, ISS surface standards for bacterial contamination are less stringent than standards for food contact surfaces or hand contact surfaces in hospitals. The ISS surface standard for fungal contamination is comparable to those described in the Australian Mould Guidelines. The latter rates the hygiene of indoor surfaces normal when viable fungal concentration is between 50 and 105 CFU/100 cm^2 [13].

1.3 Microbial contamination control in the ISS

1.3.1 Air

Airborne microorganisms can be dispersed through different routes including talking, coughing, sneezing, and sewage removal, and can cause irritation, respiratory infections and allergic diseases [14]. Dispersion and disposition of airborne particles is complex as particles are subjected to Brownian motion, gravity, electrical forces, thermal gradients, electromagnetic radiation, turbulent diffusion, inertial forces, and relative humidity [15, 16]. In addition, the ability of microorganisms to survive in droplets and on dust particles is affected by relative humidity, temperature, atmosphere composition (pollutants, oxygen), UV light and residence time [17-19].

In an orbiting spacecraft, airborne microorganisms (and dust) do not settle due the absence of gravity and thermodiffusion or electrostatic forces gain in importance. This results in a more persistent (bio)aerosol and higher microbial contamination levels in cabin air and thus a continuous active removal of the aerosols from the air is necessary. Therefore, it is evident that the design and operational characteristics of a confined space station have an important impact on the spread of (bio)aerosols [20].

In space, the air in the ISS is continuously filtered to guarantee that the microbial levels remain below the thresholds and to prevent spread of microorganisms through bioaerosols. Different filters are used in the ISS: while the air in the U.S. Segment of the ISS (Nodes 1, 2, and 3, Lab, Airlock, Japanese Experiment module JEM-PM, and Columbus) is filtered through High Efficiency (HEPA) filters (Duane L. Pierson, pers. comm.), the Russian Segment (Service Module, Functional Cargo Block FGB, and Mini-Research Modules 1 & 2) uses pleated woven (accordian structure) filters. However, both filter fine aerosols (from 0.3 µm) and constantly reduce the levels of dust particles and associated microorganisms in the air (99.97% efficiency for the HEPA filters) [21]. Although filters continuously scavenge, they do not inactivate microbial cells and need to be replaced when saturated. The POTOK 150MK Russian air filtration and disinfection systems do provide inactivation by using electrostatic pulses and charged ions followed by filtration with an efficiency up to 99% for particle sizes ranging from 0.01 µm to 10 µm [22]. Two POTOK systems are currently implemented in the ISS, one in Zvezda module and a second one in the Zarya module.

To evaluate the airborne microbial population, air samples from different sites of the U.S. and Russian segments are collected regularly (once every 90 days) within the framework of the standard on-board procedure "Control of Environmental Microecosphere" (MO-21). In the U.S. segment, two samples

are collected in each module with the U.S.-supplied Microbial Air Sampler Kit [23], one on a media plate for bacterial analysis and one for fungal analysis. In the Russian segment, the Ecosphera kit is used, which includes a SAS air sampling device (PBI International, Italy) that uses an aspiration/sedimentation method to collect air samples on petri dishes with trypcase soy agar and Czapek's medium for bacteria and fungi, respectively. In both cases, evaluation of the airborne microbial contamination (sample collection, incubation, data recording and interpretation) is performed by the crew aboard ISS and transmitted later to Earth by radio communication.

1.3.2 Surface

Most microorganisms are able to adhere to surfaces and form biofilms. This process promotes persistence and resilience of microbial contamination and has major implications for many industrial activities. For instance, biofilm formation in potable water distribution systems and on food and food contact surfaces constitutes an increased risk for product contamination with spoilage or pathogenic microorganisms [24, 25].

In space vehicles, microbial contamination levels on surfaces and instrumentation are minimized pre-flight with different methods such as heat, radiation or chemicals depending on surface-cleaning method compatibility [26]. In flight, surfaces burdened with contamination levels above the threshold levels are wiped with disinfectant wipes according to the guidelines until a decrease of the contamination below the acceptability limits is obtained. The active ingredient in these disinfectant wipes is either a quaternary ammonium compound (supplied by U.S.) or a mixture of hydrogen peroxide and a quaternary ammonium compound (supplied by Russia). When cleaning fails repeatedly removal and replacement of the contaminated surfaces is the final countermeasure.

To evaluate the microbial contamination of surfaces aboard ISS, samples from different sites of the U.S. and Russian segments are collected regularly within the framework of the standard on-board procedure "Sanitary-Epidemiological Status Monitoring" (MO-22). In the U.S. segment, two sites are sampled once every 90 days in each module with the U.S.-supplied Surface Sampler Kit (SSK) [27], one on a media plate for bacterial analysis and one for fungal analysis. If the designated crew member observes that the acceptability limit is exceeded, a digital image of the sample will be downlinked and evaluated by NASA and RSA microbiologists. In addition, samples are further analysed post-flight and detection of clinically significant organism is reported. In the Russian segment, the Test Tube Kit for Microbiological Sampling is used, which is a pouch holding fluoroplastic test tubes with preservative impregnated pads. Sample collection is done by swabbing a 10 by 10 cm surface area within 1 to 2 days before completion of each mission and sample return to the laboratory simultaneous with crew return. Post-flight, bacterial and fungal numbers are analysed and morphologically-different isolates are identified. If acceptability limits are exceeded, recommendations to the crew are transmitted. Thus, evaluation of the microbial contamination of surfaces differs slightly between the U.S. and Russian segments, while for the U.S. samples are processed and evaluated aboard, the Russian segment relies solely on post-flight analysis.

1.3.3 Water

Microbial contamination of drinking water is a well-known hazard, both from a health perspective as well as for microbial-mediated corrosion [28, 29]. In drinking water storage and distribution systems, microorganisms often develop into biofilms. These sessile communities facilitate the persistence of pathogens and show an increased resistance to disinfectants [24, 30-32]. The latter can be due to different mechanisms such as a slow or incomplete penetration of the biocide into the biofilm, an altered physiology

of the biofilm cells, expression of an adaptive stress response by some cells, or differentiation of a small subpopulation of cells into persister cells [24]. Appropriate monitoring and disinfection methods are therefore essential to mitigate the risks to crew health and hardware disintegration.

The ISS is provided with potable water through different supplies. The Russian PROGRESS, European ATV and American Shuttle vehicles provide ground-supplied water [33-35]. However, it's expensive to ship water from Earth to space as transport costs to deliver items to the ISS run up to 10,000 Euros per kilogram [36]. This emphasizes the necessity to recycle water in space. Water from the Shuttle fuel cells is collected in Contingency Water Containers (CWC) during flight and transferred to the ISS upon arrival [33-35]. Aboard the ISS, humidity condensate, which mainly originates from the crew's breath and sweat, is collected and purified by the Russian SRV-K system located in the Service Module [34]. In addition since May 2009, humidity condensate and urine distillate are being recycled by the U.S. Water Recovery System (WRS) (U.S. Segment) into potable water, which is then distributed by the Potable Water Dispenser.

Microbial contamination of the potable water sources in ISS is prevented by the addition of silver (4.6 µM) pre- and in-flight. Potable water collected in CWC during Shuttle flight is disinfected by the addition of iodine (15.8 - 39.4 µM), which is removed and replaced by silver before being dispended for consumption [34].

The quality of potable water from different ports in the Russian (SRV-K, SVO-ZV, CWC) and U.S. segment (WRS) are checked once every three months and each month, respectively. The samples are processed in-flight with the U.S.-supplied Water Microbiology Kit [5, 37] for the quantification of heterotrophic bacteria and for the U.S segment also for the presence of coliforms. In addition, samples are regularly archived for further analysis

post-flight. The sampling schedule and frequency is adjusted when recommended by U.S. and Russian experts to ensure water quality aboard the ISS.

1.3.4 Food

Finally, also food processing (production and packaging) is rigorously tested and controlled pre-flight to guarantee that contamination levels comply with the implemented standards for space flight foods [5, 38, 39]. Noteworthy, the Hazard Analysis Critical Control Point management system applied in the food industry is designed to identify and prevent microbial and other hazards in food production and was initially developed by the Pillsbury Company while working on producing foods for NASA for space flights in the early 1960s [40].

Commercially sterile food, which by definition is free of microorganisms capable of reproducing in the food under normal non-refrigerated conditions of storage and distribution, is checked for package integrity. Foods for space flights that are not commercially sterile are analysed at the stage of raw materials (before packaging) for certain specific microorganisms depending on the product (5 samples from each lot) and after flight packaging (finished goods) for total aerobic count (one sample from each daily production) (Table 1.2) [39].

1.4 The environmental microbial contamination detected aboard the ISS

1.4.1 Air

The airborne bacterial and fungal contamination levels were already monitored during the occupation of the Mir space station (1986-2001). In general (95% of the samples) the air contained less than 500 bacterial CFU

per m^3 of air and occasional increases were due to human exercise [41]. The concentration of fungi in the air ranged from 2 up to 10,000 fungal CFU per m^3 of air [41]. Although the fungal concentrations fluctuated strongly, an initial build-up was observed probably due to fungal accumulation on different locations and equipment inside the station [41]. Later, a comparable survey was performed aboard the ISS (from the year 1998 to 2005) and showed that the airborne bacterial and fungal contamination were low with a maximum of 710 and 44 CFU/m^3, respectively [42] (Table 1.3). These levels were well within the acceptable levels defined by the current threshold limits aboard the ISS (1,000 bacterial and 100 fungal CFU/m^3). The improved microbial air quality in the ISS compared to Mir was largely caused by the installation of the efficient Russian air disinfection and filtration system POTOK 150MK. A similar increase in microbial air quality was noticed in Mir after installation of this system in January 1998 [41]. This illustrates (and as mentioned above) that rational habitat design is essential and probably most cost-effective in the long-term.

Table 1.2: Microbial testing procedure for foods that are not commercially sterile

Test	Item is rejected
Total aerobic count	If > 20,000 CFU/g in a sample or If > 10,000 CFU/g in more than 1 sample
Yeast and moulds	If > 1,000 CFU/g in a sample or If > 100 CFU/g in more than 1 sample
Coliform	If > 100 CFU/g in a sample or If > 10 CFU/g in more than 1 sample
Coagulase-positive staphylococci	If > 100 CFU/g in a sample or If > 10 CFU/g in more than 1 sample
Salmonella	If > 0 CFU/g in a sample

The observed airborne contamination levels were generally within the acceptable levels (see above), however, these absolute numbers do not necessarily reveal the associated risks since no information is provided about

the pathogenic potential of the contaminants. Identification of the microorganisms that make up the contamination is thus an essential supplement to their numbers, to be able to truly asses the risks associated to such contamination. *Staphylococcus* and *Bacillus* spp. were found to be the dominant bacterial species in the air aboard ISS [43], which is similar to other surveys in non-space related confined environments such as airplanes [44] and polar stations [45]. *Staphylococcus aureus*, which colonizes naturally the skin and nose of healthy people, but also can cause a range of illnesses, was observed occasionally (in 3.2% of the cases). Exchange of *S. aureus* strains among crewmembers was also observed in previous missions [46]. The dominant fungal species were *Penicillium* and *Aspergillus* [42], which are xerophilic and primary colonizers of indoor environments [9, 47, 48] and may trigger hypersensitivity reactions such as rhinitis, sinusitis or asthma [49].

Table 1.3: Environmental microbial contamination reported for air, surfaces and water in the ISS

In-flight	Bacteria	Fungi	Reference
Air	< 710 CFU/m^3 Dominant: *Staphylococcus* and *Bacillus* spp.	< 44 CFU/m^3 Dominant: *Penicillium* and *Aspergillus* spp.	[42]
Internal surfaces	24 – 43,000 CFU/100 cm^2 Dominant: *Staphylococcus* and *Bacillus* spp.	25 - 300,000 CFU/100 cm^2 Dominant: *Penicillium* and *Aspergillus* spp.	[42]
Potable Water	Often >100 CFU/100 ml Dominant: *Methylobacterium*, *Ralstonia*, *Sphingomonas* and *Pseudomonas* spp.	ND	[50]

1.4.2 Surface

A large survey performed aboard the ISS (from the year 1998 to 2005), which included 243 swab samples, showed that the bacterial and fungal

contamination ranged from 25 to 43,000/100 cm^2 and from 25 to 300,000/100 cm^2, respectively [42] (Table 1.3). These contamination levels varied strongly but were in most cases low and below the implemented threshold limits (i.e. 10,000 bacterial and 100 fungal CFU/100 cm^2) [42].

Some surfaces were apparently more prone to an occasional rise in bacterial and fungal contamination such as a panel of the ventilation screen and the table surface in the Service Module, or behind panels of the Functional Cargo Blok [35, 42]. Despite the drop in contamination levels after disinfection (as described above), the resilience of contamination at certain locations could indicate either a resistance to the used disinfectants, favourable growth conditions (e.g. humidity), or both.

All data collected were based on the current implemented procedures, which are culture-dependent analyses. These labour-intensive and time-consuming analyses with a bias towards the culturable fraction of the population motivate the need to develop new rapid monitoring systems. One of these new techniques that has been tested aboard the ISS is the Lab-On-a-Chip Application Development Portable Test System (LOCAD-PTS), which is based on the *Limulus* Amebocyte Lysate assay [51, 52]. In this system, the presence of endotoxin (lipopolysaccharides), lipoteichoic acid and β-1.3-glucan activates and cleaves a colorimetric substrate, resulting in a quantifiable color, enabling the detection and quantification of Gram-negative, Gram-positive bacteria and fungi, respectively. However, it cannot distinguish between live and dead organisms. Recent analyses aboard ISS with the LOCAD-PTS indicated that the highest endotoxin levels were found on surfaces associated with human activity such as exercise, hygienic, dining and sleeping areas [51, 52].

1.4.3 Water

A four-year monitoring campaign (27 sampling times spread over the period 2000-2004) was performed on the the ISS SVO-ZV system, which dispenses at ambient temperature both the Russian ground-supplied and the CWC water for consumption. These in-flight analyses showed that bacterial contamination levels were above the former acceptability limit of 100 CFU/100 ml in 16 cases (60%) [34]. Most of the recovered isolates were typical waterborne gram-negative bacteria, including the genera *Methylobacterium*, *Ralstonia*, *Sphingomonas* and *Pseudomonas*. Most of these bacteria are non-pathogenic and only some members of these groups are recognized as opportunistic pathogens. Therefore, this contamination does not pose an immediate risk to the astronauts. Nevertheless, consumption of this contaminated potable water is prohibited, as currently the identification methods that are available for in-flight screening of the water quality are not fully validated. Thus, clearly, these types of water contamination waste large amounts of crew time and Earth-based resources and require more materials to be transferred both to and from the ISS, which is very costly.

A series of remediation actions were initiated to combat this recurrent water contamination, however, contamination levels increased again above the threshold limit shortly afterwards [34]. The observed resilience could be due to a number of factors. For instance, the contaminating bacterial population could be adapted to survive in these oligotrophic conditions by the formation of a starved and non-culturable but metabolic active fraction of the population (VBNC) or by the formation of persister cells, which are both more resistant to disinfectants. A small McAlister and colleagues [53] showed that *Ralstonia* sp. isolated from ultrapure water systems were able to survive in such ultrapure water for up to 6 months. *Ralstonia solanacearum* was even able to survive over 4 years in river water [54]. In addition, the

bacterial population could be equipped with resistance mechanisms towards silver, which is the designated biocide in the ISS potable water [33]. Isolates recovered from ISS water indeed showed the presence of large plasmids similar to the plasmids of *Cupriavidus metallidurans* strain CH34 [55], which could be indicative for the presence of silver resistance mechanisms. *C. metallidurans* strain CH34 (formerly *Ralstonia metallidurans* CH34) has been studied intensively for its resistance towards multiple heavy metals including silver, for which the genetic determinants are mostly carried by one of its large plasmids [56, 57]. Finally, certain parts in the water system could be prone to bacterial adherence and subsequent biofilm formation, which could augment the aspects described above.

1.5 Conclusions

The combined effort of the different space agencies to evaluate the microbial contamination aboard ISS continuously, which is in-flight for almost ten years, showed that it is a microbiologically safe working and living habitat. Nevertheless, multiple reported contamination events indicate that the current prevention, monitoring and disinfection methods are the strict minimum to control the microbial contamination in manned space stations. The current efforts and limitations even motivate further development and improvement of these or new methods.

As prevention is the first step, it will be an essential element in the design of (future) orbital and planetary space stations, which should integrate, next to thermal, mechanical and chemical resistance of equipment and utensils, also the hygienic properties (e.g. biofouling or antimicrobial surface properties). A rational habitat design that integrates both constructional and health-related parameters is essential and probably most cost-effective in the long-term.

In addition, monitoring tools could be optimized by developing online detection tools that are capable of simultaneous quantification and identification. These molecular, non-culture dependent assays would be less time consuming for the astronauts, bypass the necessity for post-flight analyses, and allow quick and autonomous decisions by the crew resulting in an accurate assessment and remediation of contamination problems aboard space stations. However, development of new techniques should be continued and stimulated since each culture-independent monitoring system has its own drawbacks (e.g. sensitivity, selectivity and reliability).

Chapter 2

Antimicrobial silver: uses, toxicity and potential for resistance

---

This chapter gives a comprehensive overview of the widespread use and toxicity of silver compounds in many biological applications. Moreover, the bacterial silver resistance mechanisms and their spread in the environment are discussed. This chapter shows that it is important to understand in detail how silver and silver nanoparticles exert their toxicity and to understand how bacteria acquire silver resistance. Silver ions have shown to possess strong antimicrobial properties but cause no immediate and serious risk for human health, which led to an extensive use of silver-based products in many applications. However, the risk of silver nanoparticles is not yet clarified and their widespread use could increase silver release in the environment, which can have negative impacts on ecosystems. Moreover, it is shown that silver resistance determinants are widely spread among environmental and clinically relevant bacteria. These resistance determinants are often located on mobile genetic elements, facilitating their spread. Therefore, detailed knowledge of the silver toxicity and resistance mechanisms can improve its applications and lead to a better understanding of the impact on human health and ecosystems.

This chapter is based on the following publication:

Mijnendonckx K., Leys N., Mahillon J., Silver S., Van Houdt R. (2013) Antimicrobial silver: uses, toxicity and potential for resistance *Biometals* 26 (3)

2.1 Introduction

The transition metal silver, both a precious and an industrial metal, is mined with an estimated production of 24,000 tons in 2012 and has a wide range of applications. Silver is used for coin and metal fabrication, in electrical and electronic compounds and for jewelry. In addition, the broad-spectrum antimicrobial effects of silver are well documented. Already the ancient Greeks used silver preparations for the treatment of ulcers, to stimulate wound healing and as preservative for food and water [58]. In fact, silver was perhaps the most important antimicrobial compound before the introduction of antibiotics in the 1940s and is still used today in a wide range of medical applications because of its antibacterial effects and low toxicity to human cells. Examples are the use of silver preparations as topical cream in the treatment of burn wounds [59], in dental amalgams, in preventative eye care and the use of silver-impregnated polymers to prevent bacterial (biofilm) growth on medical devices such as catheters and heart valves. Silver is also widely used as a (co-)disinfectant of water systems such as swimming pool water, hospital hot water systems and potable water systems. For these purposes, silver has the advantages that it has no unfavourable effect on the colour, taste and odour of water [60]. Silver is even used as an alternative to detergents for laundry [61]. The increase in occurrence and number of antibiotic-resistant strains revived the interest in the antimicrobial effects of silver and its compounds. However, concerns are being stated about whether excessive clinical use of silver compounds possibly results in silver-resistant bacteria [62], as reported several times [63, 64]. Silver-resistant bacteria also have been isolated from non-clinical environments where silver is present. Silver is naturally found in association with other metals to form minerals, as trace elements in gold, lead, zinc and copper ores, or can be introduced in the environment through industrial wastewater [65, 66]. So far, the mechanisms of silver resistance have not been fully

elucidated yet and different preventive strategies have been suggested. Here, an overview of understanding silver toxicity to human cells and the antimicrobial activity of silver ions and silver nanoparticles will be presented. In addition, resistance mechanisms against silver in bacteria are discussed.

2.2 Human toxicity of silver

Recently, the use of silver in antibacterial and antifungal agents in wound care products, medical devices, textiles, cosmetics and domestic appliances had a tremendous boost [62, 64]. This raised issues about the safety aspects and potential risks associated with the absorption of Ag^+ into the human body [67, 68]. Human toxicology of silver is not well documented. Relevant experimental studies in animal models that are reported openly and epidemiological studies evaluating people that come into contact with silver are rather limited [67, 68]. It seems that health risks associated with systemic absorption of silver ions are rather low [67, 68]. The most common observable changes associated with prolonged exposure to silver compounds are argyria and argyrosis, characterized by an irreversible deposition of silver selenide and silver sulfide precipitates in the skin and the eyes, respectively. The affected area becomes bluish-gray and it becomes worse in the presence of sunlight. However, argyria and argyriosis are not life threatening and are not associated with irreversible tissue damage [67-69]. Like most other xenobiotic metals, silver can elicit delayed contact hypersensitivity reactions and allergy in rare predisposed persons. However, the extent of the risk is until now not known [68].

There are several recommended exposure limits and guidelines for silver, but the values vary according to the reference agency that promulgates recommendations. The World Health Organization decided that a lifetime intake of about 10 g of silver can be considered the human no observable

adverse effect level [70]. The National Institute for Occupational Safety and Health (USA) set current exposure limits for silver compounds in air at 0.093 µM and in drinking water at 0.93 µM. The American Conference on Governmental Industrial Hygienists set exposure limits in environmental exposures and drinking water regulations at 0.93 µM. The European Commission recommended an 8 hour time-weighted average of 0.93 µM total silver dust as occupational exposure limit [67, 70]. This suggests that humans are unlikely to be exposed to sufficient amounts of silver in their lifetime to provoke symptoms of argyria [70]. However, care should be taken when using commercially available silver products containing unspecified levels of ionizable silver, e.g. 'Jintan Silver Pills', an inventive Japanese remedy for heartburn, nausea, vomiting, motion sickness, hangover, dizziness, bad breath, choking, indisposition and sunstroke (according to the label) [64, 68]. People living in highly polluted areas with silver residues from factory wastes (e.g. the San Francisco Bay) have also an increased risk to develop argyria as silver enters the food chain [71].

2.3 Antimicrobial activity of silver ions

The antimicrobial activity of silver compounds has been studied for many decades [72-74]. Reports were not always conclusive about the mechanism of action. An overview of the successive steps how silver exerts its antibacterial effect is shown in Figure 2.1.

Silver rapidly interacts with sulfhydryl groups on the surface of microorganisms by replacing the hydrogen atoms, which results in the formation of an S-Ag bond. This completely blocks respiration and electron transfer, hampering the induction of successful rescue mechanisms [74, 75]. In addition, blocking respiration and electron transfer causes a collapse of the proton motive force, resulting in de-energizing the membrane and ultimately leading to cell death [76]. In *Escherichia coli*, a collapse of the

proton motive force and subsequent cell death was observed after addition of $AgNO_3$ [77]. Similarly, in *Vibrio cholerae*, low concentrations of Ag^+ led to massive proton leakage through the membrane [76]. In *V. cholerae* this effect was independent of the presence of the Na^+-translocating NADH-ubiquinone oxidoreductase [76], previously thought to be one of the primary targets of Ag^+ ions [78-80], suggesting that other membrane proteins modified by Ag^+ can cause proton leakage.

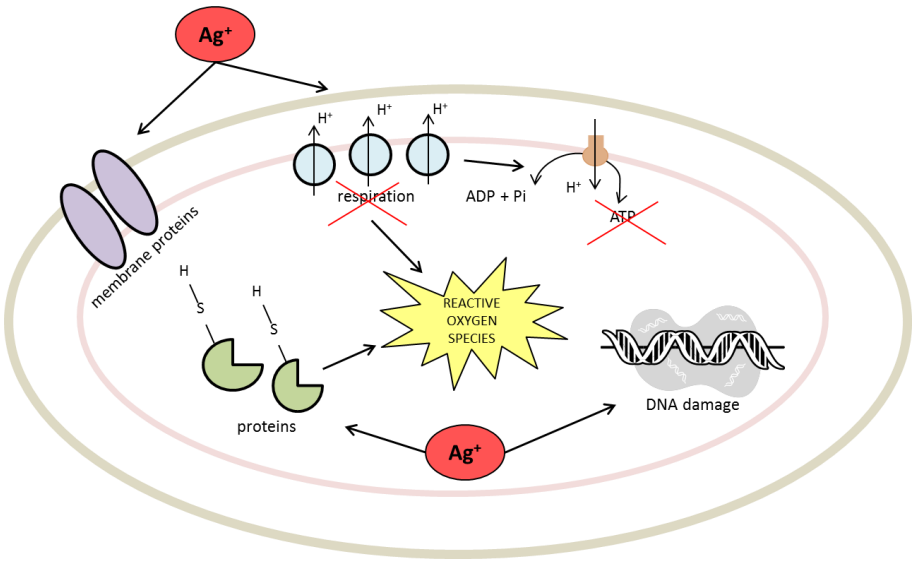

Figure 2.1: Antimicrobial effects of Ag^+. Interaction with membrane proteins and blocking respiration and electron transfer; inside the cell, Ag^+ ions interact with DNA, proteins and induce ROS production.

Disruption of the cell membrane results in the entrance of Ag^+ in the cytoplasm where it can exert additional damage at many stages. Ag^+ ions are able to form complexes with nucleic acids and preferentially interact with the nucleosides rather than with the phosphate groups of nucleic acids. Binding to the guanine base (N^7 atom), which is affected by methylation, enhances pyrimidine dimerization and interferes with DNA replication [74]. Nevertheless, it is hypothesized that the most profound effect of silver ions is

their interaction with thiol groups [74, 75, 77]. Since the thiol group of cysteine residues is necessary for the activity of many enzymes, interaction leads to conformational changes and to inactivation of enzymatic functions. Liau, et al. [81] showed that the activity of silver nitrate against *Pseudomonas aeruginosa* PAO1 was neutralized by cysteine and other thiol compounds (e.g. sodium thioglycolate) contrary to amino acids containing disulfide bonds, non-sulfur containing amino acids and other sulfur-containing compounds such as cystathionine, cysteic acid, methyl cysteine, methionine, taurine, sodium bisulfite and sodium thiosulfate.

All aerobic organisms produce Reactive Oxygen Species (ROS) as a by-product of aerobic respiration. ROS are short-lived reactive oxidants that are highly toxic as they cause damage to proteins, DNA, RNA and lipids [82]. Recent work showed that Ag^+ treatment promotes ROS production and, in that way, the antibacterial effect can be enhanced [75, 83]. SoxR-mediated transcription of *soxS* was induced after silver treatment in a similar way to that after treatment with paraquat, a known superoxide-radical generator [83]. Superoxide anions can cause liberation of iron from iron-sulfur clusters of the respiratory chain enzymes, which in turn can induce the production of hydroxyl radicals through the Fenton reaction [75]. The activity of anti-oxidative enzymes depends on thiol groups, which are blocked by Ag^+. Therefore, these enzymes are probably not able to detoxify the generated ROS. In addition, anaerobically grown bacteria are often less susceptible to Ag^+ ions putatively reflecting the influence of ROS production on the antibacterial activity of Ag^+ [83, 84]. However, a significant difference in silver toxicity is not always observed under aerobic and anaerobic conditions indicating that other factors are at play. For instance, a rapid decrease in viable cells of *E. coli* was observed with silver zeolite in aerobic conditions while it was not seen in anaerobic conditions, while treatment with $AgNO_3$ resulted in a rapid decrease of viable cells in both conditions [84]. Xiu and

colleagues [85] also observed that oxygen did not affect the toxicity of $AgNO_3$ to *E. coli* K12.

Kim and colleagues [86] showed that the toxic effect of silver ions on *E. coli* and on MS2 phages significantly increased in the presence of UV-A and visible light irradiation. Possibly, photochemical destruction of the silver-cysteine complex and subsequent formation of monosulfide radicals are at the basis of this observation [86]. Similar to ROS, these radicals may directly interact with polyunsaturated fatty acids in membranes and initiate lipid peroxidation. Consequently, a decrease in membrane fluidity occurs, which alters membrane properties and can disrupt membrane bound proteins [82].

The toxicity of silver compounds depends on the bioavailability of Ag^+ ions and (among other) on the amount of halides in the growth medium [87]. A large fraction of Ag^+ rapidly binds to proteins, hence it use as general protein stain, and forms complexes with free chloride, phosphate and sulfate ions. Therefore, to sustain antimicrobial activity, Ag^+ should be released slowly and continuously [88]. Several studies showed that the difference in silver resistance and sensitivity was more explicit in the presence of Cl^- [87, 89]. Moderate levels of Cl^- interact with Ag^+ and precipitate as AgCl thereby decreasing available Ag^+. However, higher levels of Cl^- bring back the Ag^+ in solution as $AgCl_2^-$ making it available again. Br^- has a similar effect but as AgBr is less soluble than AgCl, it functions at lower concentrations. I^- removes Ag^+ into a non-bioavailable 1:1 AgI precipitate [64, 87]. Besides implications for laboratory studies, this affects also environmental studies, as soil and aqueous environments contain several ligands able to complex Ag^+.

2.4 Silver nanoparticles

Silver nanoparticles (AgNPs) are particles of $Ag^{(0)}$ with a size ranging from 1 to 100 nm. This small size gives them specific physiochemical characteristics different from those of bulk materials of the same composition, mainly due to the high surface-area-to-volume ratio [90]. As of March 2011, AgNP-containing products constitute the largest group of all the nano-based commercial products available on the market. It is mentioned in 313 products while the second best, carbon-based nanoparticles, is only mentioned in 91 product descriptions. The specific characteristics of AgNPs, makes them interesting to use in inks [91], microelectronics [92] and medical imaging [93]. However, the broad-spectrum antibacterial activities of AgNPs made them very popular in several medical applications, in milk bottles and toys for children, clothing, sheets and pillows, cosmetics, refrigerators, vacuum cleaners, washing machines, plenty of personal care applications and many others. This extensive use leads to an increased release of AgNPs (and Ag^{+} ions) in the environment, which consequently might have harmful ecological effects [94, 95]. Therefore, detailed knowledge about the toxicity mechanism and behaviour of AgNPs is necessary. Moreover, this will help to improve the antimicrobial applications of AgNPs.

The toxic effect of AgNPs against a broad spectrum of Gram-negative and Gram-positive bacteria [reviewed in 90] and viruses [96-98] has been reported. However, the mechanism how AgNPs exert their toxicity is not yet completely known. The shape of AgNPs and more specific their effective surface area in terms of active facets is important for their toxicity as triangular particles seem to be more effective than spherical particles, which are again more effective than rod shaped particles [99]. Another study showed that the surface charge is the most important factor in toxicity [100]. *Bacillus* spp. were less susceptible to more negatively-charged AgNPs than

to more positively-charged AgNPs, due to the high degree of repulsion between the negatively-charged membrane and the negatively-charged AgNPs. Positively-charged AgNPs are attracted by the cell membrane allowing a higher degree of interaction, resulting in higher toxicity [100].

As indicated above, several studies suggest that the toxicity of AgNPs is affected by their size, which is responsible for their specific physiochemical characteristics. The smaller the nanoparticles are, the larger the surface available for interaction is, resulting in a higher specific activity [101-103]. In addition, compared to larger AgNPs, small AgNPs release more Ag^+ ions [102, 104] and consequently exhibit stronger antimicrobial activities. When larger AgNPs are used, microbial growth is inhibited due to the particle itself rather than to the Ag^+ ions [102]. Moreover, it is shown that the type of capping agent used to prevent aggregation of the nanoparticles, and environmental conditions such as pH, ionic strength and electrolyte type influence the aggregation potential and toxicity of AgNPs [85, 105]. However, Xiu *et al.* [104] recently showed that particle properties affect the toxicity of AgNPs only in an indirect manner through mechanisms that influence the rate, extent, location and/or timing of Ag^+ release, which is the only factor responsible for the antimicrobial activity of AgNPs. Their hypothesis was confirmed by testing the antimicrobial activity of self-made glycol-thiol coated AgNPs (PEG-AgNPs) and commercially available polyvinylpyrrolidone-coated AgNPs (PVP-AgNPs) of different sizes and with different surface charges. No significant difference between the dose-response patterns of the tested AgNPs expressed as a function of the released Ag^+ concentration and the dose-response pattern of cells exposed to ionic Ag^+ was observed. In addition, when PEG-AgNPs of 5 or 11 nm were prepared anaerobically and thus no Ag^+ ions were released, no measurable toxic effect on *E. coli* K-12 was observed (the highest concentration reached in the chamber was 158 mg/l for 5 nm and 195 mg/l for 11 nm particles)

[104]. In a previous experiment with commercially available AgNPs coated with amorphous carbon (AC-AgNPs), toxicity also increased after exposure to air [85]. However, in this study, a 98 % mortality was observed after treatment of *E. coli* K-12 with anaerobically prepared AC-AgNPs [85] contrary to PEG-AgNPs [104]. Therefore, next to the release of Ag^+ from AgNPs, the influence of the capping agent cannot be ignored (Figure 2.2). Notably, hormesis has been observed when *E. coli* K-12 and *Cupriavidus necator* H16 were exposed to sublethal concentrations of AgNPs [104, 106]. This stimulatory effect could be elicited by the residual Ag^+ in the AgNPs stock suspension [104] and is of significant importance to consider in antimicrobial applications of AgNPs.

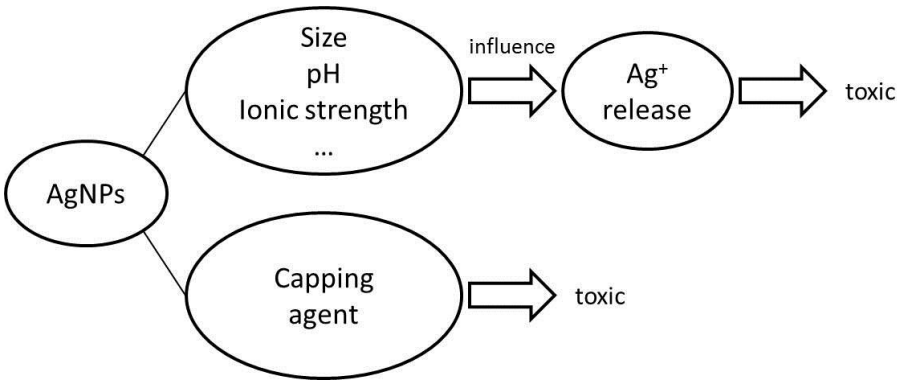

Figure 2.2: The antimicrobial effects of AgNPs depend on 1) their size and environmental conditions, which influence release of Ag+ release, and 2) the capping agent.

Many chemical and physical methods exist to produce AgNPs. The most common method is chemical reduction from Ag^+ to Ag^0 with a chemical reducing agent (e.g. $NaBH_4$,) together with a stabilizer (e.g. PVP) to prevent aggregation. However, with this method, it is difficult to control the size of the AgNPs, the process is expensive, and the reducing agents can be toxic for the environment [101]. Therefore, "green synthesis" of AgNPs is of increased interest. It has been shown that the use of bacteria has potential in

the eco-friendly production of AgNPs. Extracellular AgNPs were produced using the culture supernatant of *Staphylococcus aureus* [107], *Bacillus megaterium* [108], *P. aeruginosa* [109], *Klebsiella pneumoniae* [110] and many other bacteria. Formation of intracellular Ag-based crystals was observed in *Pseudomonas stutzeri* AG259 [111]. In addition, a silver-binding peptide selected from a combinatorial phage display and fixed on the *E. coli* maltose-binding protein, promotes silver tolerance and the formation of periplasmic AgNPs [112]. These observations indicate that bacteria can be of interest for the biological synthesis of silver nanomaterials and also for bioremediation of toxic silver waste.

Although there is a large amount of data available about the usefulness and toxicity of AgNPs, there is no standardization of the preparation method of AgNPs, nor for toxicity studies [94]. Moreover, the mechanism of killing can differ depending on the studied organism. In multicellular organisms, there can be an organism-specific immune response to different nanoparticle morphologies leading to different observations, making it difficult to extrapolate results to different biological systems [104].

2.5 Silver resistance mechanisms

The first silver-resistant bacteria were identified and isolated in the 1960s from a burn wound that was treated with silver nitrate [113]. Since then, silver-resistant bacteria were repeatedly isolated from clinical environments, burn wounds and even teeth [63, 114, 115]. Silver resistant microorganisms were recovered also from environments with naturally occurring silver. For example, a *P. stutzeri* strain was isolated from the soil of a silver mine in Utah [65] and the yeast *Candida argentea* was obtained from the sediments of a disused metal mine in the UK [116].

The first described, and to date best-characterized silver resistance mechanism, is encoded on plasmid pMG101 of *Salmonella enterica* serovar Typhimurium. This strain led to closure of the Massachusetts General Hospital burn ward as it killed several patients [63]. The 180 kb pMG101 plasmid belongs to the IncHI incompatibility group and confers resistance to silver, mercury, tellurite as well as to several antibiotics [117]. The region that is responsible for silver resistance, *silCFBA(ORF105aa)PRSE*, comprises 9 genes of which 8 are characterized primarily based on homologies with other known metal resistance determinants [64, 118] (Figure 2.3). SilP, a P-type ATPase efflux pump, transports silver ions from the cell cytoplasm to the periplasm. SilF, a periplasmic protein that probably functions as chaperone, transports Ag^+ from SilP to the SilCBA complex. This complex forms a three-polypeptide membrane-potential dependent cation/proton antiporter system that spans the entire cell membrane and belongs to the Heavy Metal Efflux - Resistance Nodulation cell Division (HME-RND) family of efflux pumps. The complex consisting of a transmembrane efflux pump (SilA), an outermembrane factor (SilC), and a membrane fustion protein (SilB), pumps $Ag^+$from the periplasm and the cytoplasm to the exterior of the cell (Figure 2.3) [64, 119]. The gene *orf105* is located between *silA* and *silP* and putatively codes for an uncharacterized protein of 105 amino acids [117]. The *silCFBA(ORF105aa)P* genes are transcriptionally controlled by *silRS*, encoding a two-component regulatory system consisting of a transmembrane histidine kinase SilS and a response regulator SilR. The proteins are homologous to other two-component regulatory system involved in regulation of metal resistance determinants. The *silE* gene, encoding a periplasmic protein, is located downstream of *silRS*. The gene is under control of its own promoter and is strongly induced during growth in the presence of Ag^+. Although the precise role of SilE in silver resistance is not yet experimentally validated, one SilE molecule can bind up to 38 Ag^+ ions depending on the experimental conditions [66].

Therefore, SilE could provide the first line of defense by binding Ag^+ in the periplasm before Ag^+ enters the cytoplasm. A homologous protein, PcoE, has 48 % identity with SilE. PcoE is part of the large plasmid-borne *pcoABCDRSE* cluster that confers periplasmic copper resistance and acts as a 'metal sponge' by its ability to bind multiple Cu^+ and Ag^+ ions. Analysis of clinical isolates showed that *silCFBA(orf105)* and *silRS* genes are more conserved than *silP* and *silE* [64].

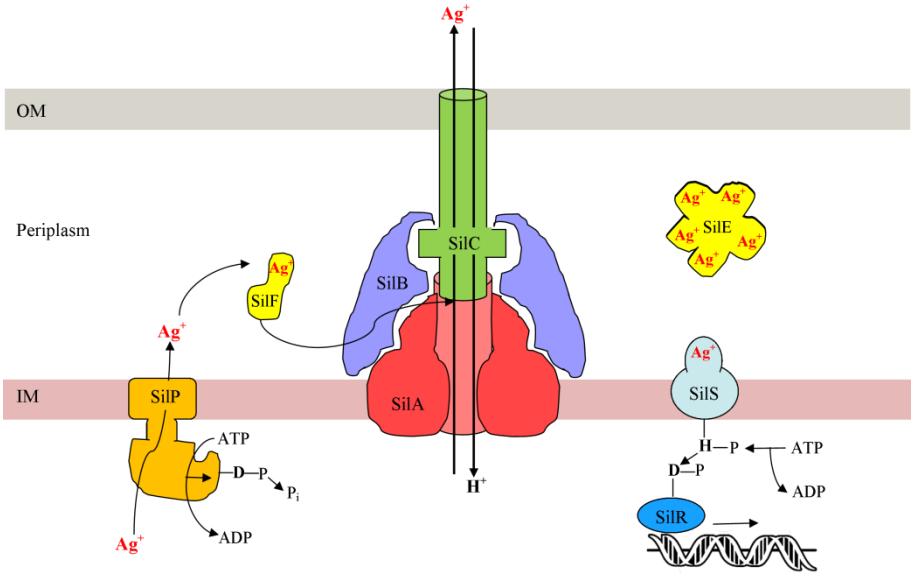

Figure 2.3: Model of silver resistance conferred by the *sil* gene cluster from plasmid pMG101 (based on [64, 119]).

Chromosomally-located sequences that are homologues to the *sil* determinants have been found in all *E. coli* strains. Although the *cusCFBARS* gene cluster is mainly involved in copper resistance [120], it was shown to also confer a certain degree of silver resistance, since deletion of *cusA* resulted in silver sensitivity [121]. CusCFBARS comprises of a tri-component HME-RND efflux system (CusCBA), a small periplasmic Cu^+ and Ag^+ binding protein (CusF), and a two-component regulatory system CusRS [122]. It seems that CusA can efflux metal ions from both the periplasm and the cytoplasm and uses methionine amino acid pairs or

clusters to export Cu^+ and Ag^+ [123]. The promoter region of *cusC* contains a highly conserved palindrome sequence that is present upstream of several copper- and silver responsive promoters [122]. This copper box is probably the binding site for CusR and is also found in the promoter region of *pcoE*, which is regulated by CusR [122]. Although overexpression of PcoE alone has little effect on overall copper resistance, it is expressed rapidly in response to the *cusRS* system and therefore can act as a first line of defense while expression of the other resistance proteins proceeds [124].

Lok *et al.* [125] demonstrated that CusB and CusF were constitutively expressed in a silver resistant *E coli* strain, isolated by stepwise selection of increasing concentrations of silver, while both were undetectable in the silver sensitive parent strain. Deletion of *cusF* in the silver resistant mutant abolished the silver resistance: the minimal inhibitory concentration dropped from more than 1 mM $AgNO_3$ in M9 mineral medium to 12 µM, compared to 3 µM for the parent strain. However, the role of CusB remains unclear. No differential expression was observed for CusC and CusA, presumably because these hydrophobic membrane-associated components may not be readily resolved by standard two-dimensional gel electrophoresis procedures used in their study [125]. Sequencing of the regulatory system c*usRS* showed that there was a single point mutation in *cusS*, which resulted in a change of threonine-17 to proline in the N-terminal protein region. This mutation probably locks CusS in an autophosphorylation state, resulting in constitutive and Ag^+-independent activation of *cusCFBA* [126]. Previous studies on the same silver resistant mutant already showed that Ag^+ is actively pumped out the cell. Yet, the exact molecular mechanism was has not been elucidated [89]. In addition, this mutant strain was deficient in the outer membrane porin OmpF and consequently showed a decrease in outer membrane permeability. Although this alone did not cause the silver resistance, it probably acts synergistically to raise the level of resistance. In

addition, it may contribute to the observed low-level cross-resistance between Ag^+ and cephalosporins (β-lactam antibiotics) [89].

Cross-resistance to silver caused by alteration of the membrane permeability was also observed after induction with low levels of the β-lactam amoxicillin [127]. Another mechanism shown to confer cross-resistance to silver and antibiotics is co-regulation. Overexpression of *soxS*, a transcription factor involved in the response to oxidative stress, or *robA*, also encoding a DNA-binding protein, resulted in an increased resistance to Ag^+ but also to Hg^{2+} and Cd^{2+} and to the antibiotics tetracycline, kanamycin, chloramphenicol and novobiocin [128]. Another widely observed phenomenon, of which examples are presented throughout this chapter, is the physical linkage of genes involved in silver and antibiotic resistance. The study of cross-regulation is of paramount importance as silver is ubiquitously present in the environment as a consequence of the numerous applications of Ag^+ and AgNPs in clinical and non-clinical environments. In general, the structural and functional characteristics of metal resistance share common themes with those conferring antibiotic resistance [reviewed in 129]. Therefore, metal contaminated soils can be a putative reservoir of harmful, antibiotic resistant strains. The long term effects on the environment and human health of this possible cross-resistance are not yet known but are an important aspect to take into consideration in future studies.

2.6 Mobile genetic elements and horizontal transfer of silver resistance

The *sil* gene cluster is highly conserved in several other plasmids of the incHI-2 incompatibility group such as plasmids MIP233, MIP235 and WR23 of various *Salmonella* serovars and plasmids pR47b and pR478 of *Serratia marcescens* [130]. In *Enterobacter cloacae*, the major difference between virulent and avirulent genotypes appears to be the presence of a large

plasmid that also belongs to the IncHI-2 incompatibility group, which contains, besides several antibiotic resistant determinants, a functional *sil* gene cluster [114]. The 83-kb plasmid pJT1 of *E. coli* R1, isolated from patients with burn wounds, conferred resistance up to 1 mM $AgNO_3$ [131]. Plasmid mediated silver resistance is also reported in environmental organisms. The environmental isolate *Acinetobacter baumannii* BL88 harbours plasmid pUPI199 that can tolerate up to 0.75 mM $AgNO_3$ and contains, in addition, resistance determinants for 13 different metals and 10 antibiotics [132]. In *P. stutzeri* AG259, isolated from the soil of a silver mine, silver resistance was also mediated by one of its plasmids [65]. This strain was able to grow on rich medium with 50 mM $AgNO_3$ by accumulation of Ag and Ag_2S crystals in its periplasm [111].

In *Delftia acidovorans* and *Bordetella petrii*, *silCBA* is located on an Integrative and Conjugative Element (ICE) belonging to the Tn*4371* family. This family refers to a group of mobile genetic elements that carry functional modules involved in conjugative transfer, integration, maintenance/stability and accessory genes conferring a special phenotype to the host bacteria [133]. All together, in many strains, the silver-resistant determinants are located on mobile genetic elements, facilitating the spread of these traits to other members of the population.

In natural environments, microorganisms are frequently exposed to elevated concentrations of silver. Estuarine and coastal waters exposed to anthropogenic inputs, including those from wastewater effluents (e.g. industry, hospitals, dental offices, etc.) and water flow from metal mines, are an important source of silver, while in pristine freshwaters, the concentrations of dissolved silver are generally low [134]. Wastewater discharges from hospitals, photographic and electronic industries are shown to be at the basis for the enhanced silver concentrations found in the San Francisco Bay. Active efforts to reduce discharges and more stringent

discharge regulations have resulted in a decrease in silver concentrations over the last two to three decades. However, silver contamination is still a matter of concern [71]. In estuarine waters contaminated with metal-mine wastes in southwest England, silver concentrations 400 times higher than background levels were reported in sediments and in residing organisms [135]. Elevated silver concentrations were also observed in Atlantic coastal waters receiving untreated municipal wastewater, while the lowest concentrations where found in the Gullmard Fjord, without major sources of water pollution [134]. Although the emergence of digital photography and improvements to wastewater treatments resulted in reduced silver inputs over the last decades, extended use of silver and AgNPs in commercial products will lead again to an increase of silver in the environment. Moreover, sediments will likely remain as a secondary source of silver to marine waters for some time [134]. The use of sewage sludge as fertilizer or as organic soil improver can also lead to the spread of silver in the environment [136]. Silver resistant determinants are present in many environmental bacteria and frequently located on mobile genetic elements, which can be horizontally transferred at higher frequencies in particular conditions within natural ecosystems (e.g. in nutritional hot spots such as manure-applied soils) [Reviewed in 137]. Furthermore, this could diversify mobile genetic elements and disseminate novel phenotypes among bacterial populations [138]. These observations highlight the necessity to control the release of silver in the environment as this can putatively facilitate the dissemination of silver resistance determinants among environmental microorganisms and to clinically important organisms.

2.7 Silver resistance determinants in *C. metallidurans*

Cupriavidus metallidurans is specialized in metal resistance and is often associated with industrial sites linked to mining, metallurgical and chemical industries [139] but is also isolated from different spacecraft-related environments [140, 141], from patients with cystic fibrosis [142] or as the causative agent of an invasive human infection [143]. Type strain *C. metallidurans* CH34 harbours resistance determinants for at least 20 different metal ions [56], mainly located on its two megaplasmids [57], although chromosomally-encoded metal responsive clusters have also been identified [144]. *C. metallidurans* CH34 carries a number of systems putatively involved in silver detoxification, based on homologies with described silver resistance systems. The *silDCBA* and *cusDCBAF* operons, which encode proteins that belong to the HME-RND transporter family, are located on a genomic island present on pMOL30 and the chromid [56, 145], respectively. The *cupRAC* operon that codes for a P-type ATPase is located on chromosome 1 [56]. Moreover, expression of all three operons (except *silA*) was induced after 30 min exposure to 0.25 µM Ag^+ [144]. The SilB, SilC, CusB and CusC proteins were also induced after growth in the presence of 1 µM $AgNO_3$ [146, 147]. In addition, overexpression of SilCBA could increase silver resistance of *E. coli* GR17 (4 µM compared to 1.7 µM). Moreover, it was shown that the C-terminal domain of SilB is able to bind Ag^+ [148].

In addition to Sil and Cus, proteomic data revealed the induction of AgrR after growth of CH34 in the presence of 1 µM $AgNO_3$ [147]. AgrR is part of a two-component system AgrR-AgrS, which comprises a histidine kinase AgrS that act as sensor and transmits the signal through a phosphorylation cascade to the cytoplasmic transcriptional response regulator AgrR. This two-component system is associated with an RND-efflux system encoded by *agrCBA* of which the function is still unknown (Figure 2.4). It shows

characteristics of heavy metal efflux systems as well as hydrophilic/amphiphilic compounds efflux systems. Induction of AgrR by silver may indicate that this efflux pump could be involved in silver resistance.

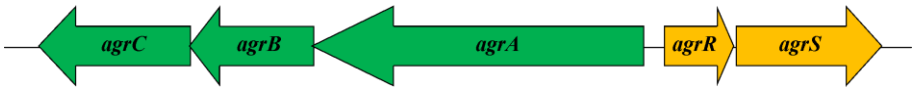

Figure 2.4: Orientation of the *agr* gene cluster in *C. metallidurans* CH34. The genes encoding for the efflux pump are presented in green, while the genes comprising the two-component regulatory system are shown in orange.

Comparative whole genome hybridization (CGH) between 16 different *C. metallidurans* strains isolated from diverse biotopes and *C. metallidurans* CH34 showed that the metal resistance determinants, including the silver resistant gene clusters, are highly conserved [149]. Recent analysis of *C. metallidurans* isolates from different potable water management systems of the International Space Station and from the air of the Kennedy Space Center Payload Hazardous Servicing Facility during assembly of the Mars Exploration Rover indicated that each isolate harbours at least one megaplasmid. Moreover, PCR analysis of the plasmid extracts showed that the *silCBA* operon is located on one of the megaplasmids [150]. Among others, the presence of the *sil* gene cluster in the potable water isolates gives them the ability to withstand the sanitation procedure in which silver is used [150].

2.8 Conclusions

We reviewed the current insights into toxicity of and bacterial resistance to silver ions and nanoparticles, which are widely used in many biological applications. Although the antimicrobial activity of silver ions has not yet been fully elucidated, they probably interact with the cytoplasmic membrane

where they compromise electron transfer and the proton motive force, ultimately resulting in cell death. In addition, ionic silver interacts with enzymes and ionic silver exposure is able to promote the production of reactive oxygen species. Silver nanoparticles basically ferry silver ions to bacteria, which are released and exert their action, although other factors cannot be excluded at this point.

Silver resistance determinants are widely spread among environmental and clinically relevant bacteria. Next to chemical detoxification, for instance by precipitation in the periplasm via reduction to elemental silver or the formation of Ag_2S crystals, bacterial silver resistance mechanisms result from active efflux systems. Efflux pumps are either P-type ATPases, which pump Ag^+ from the cell cytoplasm to the periplasmm, or three-polypeptide membrane-potential dependent cation/proton antiporters (HME-RND family), which pump Ag^+ from the periplasm to the exterior of the cell. These resistance mechanisms are often located on mobile genetic elements, facilitating their spread. This is of concern because the extensive use of silver-based products will increase the release of silver in the environment, putatively inducing the dissemination of silver resistance (and thereby cross-resistance to antibiotics). Future studies need to tackle the precise mechanism of Ag^+ and AgNPs toxicity and resistance. Detailed knowledge of all these factors can lead to an improvement of the many applications of silver (e.g. antimicrobial, bioremediation, nanomaterials) and, to a better estimation of the risks associated with human health and ecosystems.

Chapter 3

Objectives

Strains from the closely related β-proteobacterial genera *Cupriavidus* and *Ralstonia* have been identified and isolated during numerous monitoring campaigns from different space-related environments. Although these microorganisms do not pose a treath for healthy people, the decreased immune system of the astronauts makes it necessary to limit possible microbial contaminations. Moreover, microorganisms can cause damage to the infrastructure of the space station. Therefore, we aimed to gather more insights in the ability of these genera to thrive in these environments.

The first objective is to characterize the *Cupriavidus metallidurans* and *Ralstonia pickettii* isolates from different space-related environments in detail to have more knowledge about their general tolerance mechanisms towards several stressors. All isolates will be screened for their tolerance to several metals, antibiotics and UV-C irradiation. Moreover, their potential to form biofilms on polysterene will be investigated and their plasmid profile will be determined. All results will be compared with their type strains to elucidate the factors contributing to their survival in harsh and strictly controlled space-related environments.

As silver is used to sanitize potable water sources in the ISS, the silver resistance mechanisms of the isolates are studied more in detail. All isolates will be screened for the presence of genetic determinants related to silver resistance in type strain *C. metallidurans* CH34. Moreover, the genomic location of these gene clusters will be determined to evaluate their mobility throughout the population. Furthermore, the survival capability of all isolates in water with and without the disinfectant silver will be examined. In

addition, the adaptive response to toxic silver concentrations will be evaluated. In case mutants with increased resistance to silver are obtained, the underlying mechanisms and regulatory circuit will be elucidated.

It is known that next to mutations, horizontal gene transfer mediated by mobile genetic elements, plays an important role in the evolution and adaptation of microorganisms. Therefore, a detailed study of the insertion sequence (IS) elements present in type strain *C. metallidurans* CH34 will be performed. All the IS elements are characterized and classified. All fully sequenced bacterial genomes were scrutinized for the occurrence of these IS elements. In addition, transposition and induction of these IS elements in different conditions were scrutinized as well as genetic rearrangements and gene activation. In this way, the role of IS elements in the metabolism of CH34 will be investigated. In the last chapter, the plasmid mobility of the plasmids present in the *C. metallidurans* isolates will be investigated and their ability to transfer metal resistance will be studied.

PART II

RESULTS

Chapter 4

Characterization of the survival ability of *Cupriavidus metallidurans* and *Ralstonia pickettii* from space-related environments

---

In this part, several *C. metallidurans* and *R. pickettii* isolates from space-related environments were characterized in detail. All isolates were screened for their plasmid content, their tolerance to different antiobiotics, metals and UV-C irradiation and their potential to form biofilms was investigated. The results are compared with their type strains to gain more insights in the factors contributing to their survival in these harsh and strictly controlled environments.

This chapter is based on the following publication:

Mijnendonckx K., Provoost A., Ott C., Venkateswaran K., Mahillon J., Leys N., Van Houdt R. (2013) Characterization of the Survival Ability of *Cupriavidus metallidurans* and *Ralstonia pickettii* from Space-Related Environments *Microbial Ecology* 65(2): 347-360.

4.1 Introduction

Human space exploration can only be successful if protection of the explorers is secured. To ensure this, rational habitat design together with efficient life support systems guaranteeing the quantity, quality and recycling of air, water, food and waste are essential. Continuous monitoring of vital parameters and contaminants is consequently a requirement. One important aspect herein is monitoring microbial contaminants [151]. Earth-borne microorganisms are ubiquitous and thus also present in spacecraft and space station environments [42, 43, 151, 152]. In these confined space habitats the prevailing microbial population in the air and on surfaces originates mainly from human activity [42, 45], while contamination of potable water sources originates mostly from the environmental flora of the water source or the system itself [50]. It is shown that in such confined environments, microorganisms can harm the integrity of the spacecraft hardware by causing biodegradation of structural spacecraft components [152]. In addition, microbial contaminations can cause problems for the health of the astronauts, as the human immune system is depressed in confined habitats [153].

Strains from the closely related β-proteobacterial genera *Ralstonia* and *Cupriavidus* have been identified and isolated during numerous monitoring campaigns from different space-related environments. They have been found in the air of the Kennedy Space Center Payload Hazardous Servicing Facility (PHSF) during assembly of the Mars Exploration Rover [154] and on the surface of the Mars Odyssey Orbiter prior to flight in the Kennedy Space Center Spacecraft Assembly and Encapsulation Facility II [140, 155]. They have been found in cooling and drinking water from the Mir space station [141, 156], the Shuttle [152], and the ISS [141, 156]. How these strains are able to persist in these strictly controlled and oligothrophic environments, remains unclear. *Cupriavidus* and *Ralstonia* strains were already isolated

from harsh man-made environments such as non-ferrous industry, mine areas and metal factories [139], from highly controlled clean environments such as hospitals [157], and from ultrapure industrial water systems [158]. In water systems, *R. pickettii* strains often form biofilms, making them more resistant to biocides and consequently more difficult to eradicate [30, 159]. Moreover, these strains often contain mobile genetic elements (plasmids, transposons, genomic islands) that carry determinants allowing the strains to specifically adapt to their environment [160, 161]. For example, *C. metallidurans* CH34 carries many determinants for metal resistance on its megaplasmids pMOL28 and pMOL30 [57, 160], *C. eutrophus* H16 contains plasmid pHG1, with genes involved in chemolitotrophy and anaerobic growth on nitrates [162], and the catabolic plasmid pJP4 of *C. pinatubonensis* JMP134 carries genes involved in the degradation of aromatic pollutants [163].

In this chapter, 4 different *C. metallidurans* and 8 *R. pickettii* isolates from different space-related environments (space industry or ISS) were compared to the respective type strains, *C. metallidurans* CH34 (from metal polluted soil origin) [164] and *R. pickettii* ATCC27511 (from human tissue clinical origin) [165]. All isolates were screened for their potential to form biofilms, for their tolerance to UV-C irradiation, different antibiotics and metal ions and for the presence of plasmids. Their survival capacities in potable water, with and without the disinfectant silver, were investigated.

4.2 Materials and Methods

4.2.1 Bacterial isolates, strains and growth conditions

Bacterial isolates and type strains used in this study are listed in Table 4.1. Isolates and strains were grown in liquid Lysogeny-Broth (LB) medium or

Table 4.1: Overview of all bacterial strains used in this study.

Strain	Name	Origin	Reference
Escherichia coli	MG1655	Laboratory strain	[166]
Cupriavidus metallidurans	CH34^T	Decantation tank of Belgian Zinc factory	[164]
	NA1	Water sample, ISS SVO-ZV returned on Space Shuttle mission STS-104 (2001) (original code: 0103380-2)	[167]
	NA2	Water sample, ISS Contingency water container S/N 5076 (2002) (original code: 0200393-2)	[167]
	NA4	Water sample, ISS SRV-K filter reactor effluent returned on Soyuz 10S (2004) (original code: 0502478-1)	[167]
	NE12	Air filter sample, Northeast corner KSC-PHSF, FL (original code: NE12)	[154]
Ralstonia pickettii	ATCC27511^T	Cystic fibrosis patient who had undergone tracheotomy	[165]
	SSH1	Surface sample, Mars Odyssey orbiter, JPL-SAE-II, CA (original code: 31V3)	[140]
	SSH2	Surface sample, Mars Odyssey orbiter, JPL-SAE-II, CA (original code: 46V1)	[140]
	SSH3	Surface sample, Mars Odyssey orbiter, JPL-SAE-II, CA (original code: 48V1)	[140]
	SSH4	Surface sample, Mars Odyssey orbiter, JPL-SAE-II, CA (original code: 49V2)	[140]
	CW1	Water sample, American segment of the ISS cooling system (original code: R21D)	[168]
	CW2	Water sample, American segment of the ISS cooling system (original code: R21F)	[168]
	CW3	Water sample, American segment of the ISS cooling system (original code: R21I1)	[168]
	CW4	Water sample, American segment of the ISS cooling system (original code: R42JB)	[168]

T: type strain; SVO-ZV: System for water storage and dispensing; SRV-K: System for regeneration of condensate water; KSC-PHSF: Kennedy Space Center Payload Hazardous Servicing Facility; JPL-SAE-II: Jet Propulsion Laboratory Spacecraft assembly and encapsulation facility II; SSH: surface space hardware; CW: cooling water.

mineral salts 284 medium (MM284) supplemented with 0.2% (wt/vol) gluconate as sole carbon source [169]. Cultures were grown in the dark at 30°C on a rotary shaker at 150 rpm. For autotrophic growth, the carbon source was excluded from solid MM284 agar medium and plates were incubated in a jar with a gas atmosphere containing a mixture of H_2, CO_2 and O_2 (72%, 18%, 10%). For anaerobic growth, 20 mM KNO_3 was added to solid MM284 agar medium and plates were incubated in an anoxic atmosphere using the Anaerocult® A system (Merck, Germany). To determine the survival frequency of a *C. metallidurans* isolate at 37°C, the ratio of the viable counts at 37°C and 30°C was determined. To this end, 100 µl of serial dilutions of an overnight LB culture (30°C, 10^9 CFU/ml) was spread on LB agar plates and colonies were counted after incubation for 3 days at 37°C and 30°C, respectively. For each replicate of each isolate, 95 colonies were selected, dissolved in 150 µl 10 mM $MgSO_4$ and replica plated on the following media: MM284 agar, LB agar, MM284 + 1 mM $NiCl_2$ and MM284 + 0.8 mM $CuSO_4$. Growth was scored after 3 days incubation at 30°C.

4.2.2 DNA extraction

Genomic DNA was isolated using the QIAamp DNA mini kit (Qiagen, The Netherlands).

4.2.3 Phylogenetic analysis

PCR amplification of the 16S rRNA gene was performed with the 8-forward and 926-reverse primer pair (Table 4.2). The conditions for the PCR reaction were the following: 5 min at 95°C followed by 25 cycles of 45 s at 95°C, 30 s at 55°C and 1 min at 72°C each and a final extension at 72°C for 10 min. The length of the generated fragments was 893 bp. The PCR products were purified with the Wizard® SV Gel and PCR Clean-Up System (Promega, USA) and were sequenced with the 8-forward primer. Sequence alignments

and phylogenetic analysis of the 16S rRNA gene sequence similarities was performed on a 692 bp fragment with the Molecular Evolutionary Genetics Analysis (MEGA) 5.01 software (www.megasoftware.net). Analysis was based on the Maximum Likelihood method with 1000 bootstrap repetitions. The 16S rRNA gene sequences obtained in this study, were submitted to the Genbank database under accession numbers JN637298 to JN637308 (Figure 4.1). The accession numbers used from Genbank were: *C. metallidurans* CH34^T (Y10824), *Cupriavidus necator* LMG8453^T, *Cupriavidus pinatubonensis* 1245^T (AB121221), *Cupriavidus laharis* 1263a^T (AB054961), *Cupriavidus taiwanensis* LMG19424^T (AF30032), *Cupriavidus pauculus* LMG3413^T (AF139173), *Cupriavidus respiraculi* AU3313^T (AF500583), *Cupriavidus campinensis* WS2^T (AF312020), *Cupriavidus gilardii* LMG5886^T (AF076645), *Cupriavidus oxalatica* Ox1^T (AF155567), *Cupriavidus basilensis* LMG189901^T (AF312022), *Ralstonia mannitolilytica* LMG6866^T (AJ270258), *Ralstonia insidiosa* AU2944^T (AF488779), *Ralstonia solanacearum* GMI1000^T (X67036), *Ralstonia syzygii* ATCC49543^T (AB021403), (AF191737), *R. pickettii* ATCC27511^T (X67042), *R.pickettii* SSH1 (AF526914), *R. pickettii* 12J (CP001068), *R. pickettii* 12D (CP001644), *Escherichia coli* ATCC11775^T (X80725). For all 12 isolates, Enterobacterial repetitive intergenic consensus (ERIC) sequences were investigated by PCR (Table 4.2) [170]. PCR conditions were the following: 7 min at 95°C followed by 30 cycles of 1 min at 94°C, 1 min at 52°C and 8 min at 65°C and a final extension of 16 min at 65°C. DNA was analysed by horizontal gel electrophoresis for 20 hours at 80 V in a precooled electrophoresis chamber at 4°C. After electrophoresis, DNA was stained with ethidium bromide (0.3 µg/ml TBE) for 30 min and destained overnight at 4°C in ultrapure water.

Table 4.2: Primers used in this study

Name	Oligonucleotide sequence 5' – 3'	Length
silA_Forward	GGATCTTGCCACGAATCATATAGC	3562 bp
silC_Reverse	ACGTCAGCGTGGAGTTGATGTA	
agrA_Reverse	CCCAGGAGTGAGCTTCTCATTT	3277 bp
agrC_Forward	GCCGAAACACGACGTTCTACT	
cusC_Forward	GATCTCTAGACGGAGGCTTTATGTCATTCC	6413 bp
cusA_Reverse	GATCCTGCAGCAAACCATCCCGGTCGTC	
8 Forward	AGAGTTTGATCCTGGCTCAG	893 bp
926 Reverse	CCGTCAATTCCTTTGAGTTT	
czcN_Forward	TCGGATGAAGACCGCTTTC	10573 bp
czcE_Reverse	AGCCAAGGTCCACACTCGTATC	
ERIC_FW	AGTAAGTGACTGGGGTGAGCG	
ERIC_RV	ATGTAAGCTCCTGGGGATTCAC	

4.2.4 Plasmid profiling

The extraction of large plasmids was based on the method of Andrup *et al.* [171]. DNA was analysed by horizontal gel electrophoresis in 0.5% Certified Megabase agarose gel (Bio-Rad, USA) with 1 x TBE buffer for 20 hours at 100 V in a precooled electrophoresis chamber at 4°C. After electrophoresis, DNA was stained with ethidium bromide (0.3 µg/ml TBE) for 30 min and destained overnight at 4 °C in ultrapure water. Plasmid DNA was further processed when used for PCR. Briefly, 150 µl of the plasmid extract was put on a 100 kDa Amicon filter (Millipore, USA) and centrifuged for 2 min at 11,300 g. The samples were washed twice with 150 µl ultrapure water and centrifuged each time for 2 min at 11,300 g. The concentrated plasmid DNA was recovered by inverting the filter in a new eppendorf tube and centrifuged 2 min at 100 g followed by a drop dialysis. To remove the remaining chromosomal DNA in the plasmid extract, the sample was treated with Plasmid-Safe™ ATP-Dependent DNase (Epicentre Biotechnologies, USA). A reaction mixture of 42 µl plasmid extract, 2 µl ATP (25 mM), 5 µl Reaction buffer (10 x concentrated) and 1 µl Plasmid-Safe DNase was

incubated 4 h at 37°C followed by 30 min at 70°C. This sample was again purified and concentrated with a 100 kDa Amicon filter. Chromosomally located genes could not be amplified with this plasmid DNA as starting material (data not shown).

4.2.5 Biofilm formation

For each strain, the capacity to form a biofilm on polystyrene was investigated [172, 173]. To this end, 10^7 CFU/ml were washed with 10 mM $MgSO_4$, resuspended in LB medium and transferred to a 96-well plate. After 7 days incubation at 30°C on a rotary shaker, the amount of biofilm formation was measured. For this, the culture was removed and the plate was washed 3 times with 10 mM $MgSO_4$. Then, the biofilm was stained with a 0.03% crystal violet solution for 5 min. After that, the wells were washed with 10 mM $MgSO_4$ until the wash solution was clear. Ethanol was added to dissolve the crystal violet and after 5 min, the absorbance at 530 nm was measured. Biofilm-forming capacity for each isolate was expressed relative to the average value for uninoculated growth medium. A student T-test was performed on the data (n = 9) to check if there was significant biofilm formation compared to uninoculated growth medium.

4.2.6 UV-C treatment

For measuring UV-C resistance, serial dilutions of the isolates and *E. coli* MG1655 were plated on LB agar and irradiated in the UV-C oven after 30 minutes [174]. The UV oven (HL-2000 Hybrilinker, UVP) used for these tests was equipped with 5 lamps of 8 Watt each, emitting light with a peak at 254 nm. The distance between the lamps and the surface of the plates (on which the bacterial cells were spread) was approximately 7 cm. The UV doses that were programmed were 0 (not exposed to UV-C), 25, 50, 75, 100, 150 and 200 J/m² and the dose rate was 30 J/m² s. After irradiation, the plates were further incubated for 48 hours at 30°C in the dark. After 48

hours, the colonies were counted and D_{10}-values (the dose that kills 90% of the population) were calculated according the method of Coohill and Sagripanti (2008) [175]. A student T-test was performed to calculate significant differences ($p < 0.05$) between the D_{10}-values ($n = 3$) of the isolates and their type strain.

4.2.7 Antibiotic resistance

The resistance of the isolates against several antibiotics was investigated, including the (1) aminoglycoside-type kanamycin 50 µg/ml (Km50) and kasugamycin 50 µg/ml (Ksg50), (2) polyketide tetracycline 20 µg/ml (Tc20), and (3) chloramphenicol 30 µg/ml (Cm30), 100 µg/ml (Cm100) and 150 µg/ml (Cm150), all binding the bacterial ribosome subunit leaving the bacterium unable to synthesize proteins, and (4) the penicillin-type ampicillin 100 µg/ml (Amp100) and carbenicillin 100 µg/ml (Cb100), that interfere with the synthesis of the peptidoglycan layer of bacterial cell walls, and (5) trimethoprim 100 µg/ml (Tm100) that inhibits folate synthesis, necessary for nucleic acids synthesis. To this end, of each isolate, one single colony was selected, dissolved in saline (0.85% NaCl) and streaked onto LB agar media containing the different antibiotics. The isolates were scored as antibiotic resistant positive (+) if visible colonies appeared after 3 days incubation at 30°C, or negative (-) if not.

4.2.8 Metal ion resistance

A stationary phase culture (OD_{600} of ca. 1, representing 10^9 CFU/ml) of each isolate in MM284 was diluted 50 times in double concentrated MM284 medium. Of this, 100 µl was added in a 96-well plate to 100 µl of an aqueous solution containing twice the metal concentration of interest, resulting in a start concentration of ca. 10^7 CFU/ml. The plates were incubated at 30°C for 48 hours in the dark on a rotary shaker. At different time points, bacterial growth was measured by determination of the optical

density at 595 nm. The MIC values were determined for the following metal solutions: $CdCl_2$, $CoCl_2$, $CuSO_4$, $ZnSO_4$, $NiCl_2$, $HgCl_2$ and $AgNO_3$.

4.2.9 PCR amplification of genes involved in heavy metal tolerance

PCR amplification of the *czcNICBADRSE* gene cluster involved in Cd^{2+}, Zn^{2+}, Co^{2+} resistance in *C. metallidurans* CH34 was performed on the *R. pickettii* isolates with primers based on the sequence of CH34 (Table 4.2). The conditions for the PCR reaction were the following: 10 min at 94°C followed by 10 cycles of 20 s at 94°C, 30 s at 56°C and 10 min at 68°C each, then 15 cycles of 20 s at 94°C, 30 s at 56°C and 10 min plus 5 s extra per cycle at 68°C and a final extension of 10 min at 68°C. The length of the obtained fragment in CH34 is 10573 bp. PCR amplification of the genes known to be involved in silver resistance in *C. metallidurans* CH34, i.e. *silCBA*, *agrCBA* and *cusCBA*, was performed on genomic DNA and plasmid DNA extracted from all isolates with primers based on the sequence of CH34 (Table 4.2). The conditions for the PCR reactions with *silCBA* and *agrCBA* primers were the following: 5 min at 95°C followed by 25 cycles of 45 s at 95°C, 30 s at 55°C and 3 min at 72°C each and a final extension at 72°C for 10 min. The length of the generated fragments generated was 3562 bp for *silCBA* and 3277 bp for *agrCBA.* For PCR amplification of *cusCBA*, the settings were as follows: 2 min at 94°C followed by 10 cycles of 45 s at 94°C, 30 s at 55°C and 7 min at 68°C each, then 15 cycles of 45 s at 94°C, 30 s at 55°C and 7 min plus 10 s extra per cycle at 68°C and a final extension of 10 min at 68°C. The length of this fragment is 6413 bp. The presence of these fragments was analysed by horizontal gel electrophoresis in a 0.8% agarose gel, running at 100 V during 1 hour. The positive PCR products were purified with the Wizard® SV Gel and PCR Clean-Up System (Promega, USA). The samples were sequenced with the *agrA* reverse and *silA* forward primer and fragments of 1022 bp and 1059 bp respectively,

were used for sequence alignments and phylogenetic analysis was performed with the MEGA 5.01 software. Analysis was based on the neighbour-joining method with 1000 bootstrap repetitions. The obtained sequences were submitted to Genbank under the following accession numbers: *agrA* from JQ294044 to JQ294052 and *silA* from JQ294034 to JQ294043 (also specified in Figure 4.7).

4.2.10 Survival in potable water, with silver

For each isolate, a culture in MM284 was prepared. Cells were harvested, washed 2 times in saline solution, and resuspended to a final cell density of 10^9 CFU/ml in 2 ml sterilized potable water (Chaudfontaine) with and without 2 µM $AgNO_3$. The samples were incubated stationary at 20°C in the dark. At different time points, the number of viable cells was determined by plate count on MM284 after 48 h of growth at 30°C.

4.3 Results and Discussion

4.3.1 Phylogeny

Initially, the different samples were analysed by heterotrophic plate counts. After 7 days, the colonies were counted and purified. Tentative identification was based on analysis of the 16S rRNA gene sequence [50, 140, 154, 168]. Here, we describe the 16S rRNA gene sequences of 12 different isolates, which were subsequently subjected to a phylogenetic analysis (Figure 4.1). Four isolates harbour a 16S rRNA gene sequence that is more than 98% identical to type strain *C. metallidurans* CH34. The 16S rRNA gene sequence of eight isolates is more than 98% identical to type strain *R. pickettii* ATCC27511 (Figure 4.1).

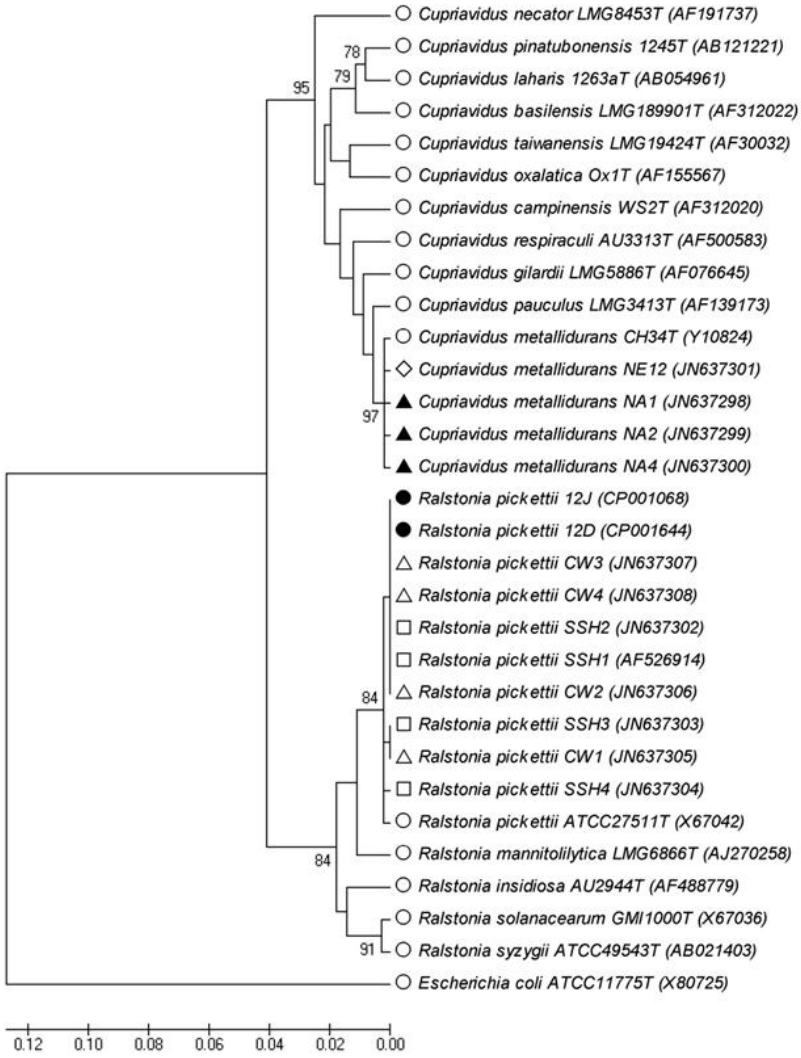

Figure 4.1**:** Maximum likelihood phylogenetic tree based upon 16S rRNA gene sequence similarities, showing the place of the space isolates within the *Cupriavidus* and *Ralstonia* genera. *Escherichia coli* ATCC11775 was included as outgroup. Numbers at the branches represent percentages of 1000 bootstrap repetitions (only values above 50% are shown). Symbols for each strain: type strains ○; *Ralstonia pickettii* 12D and 12J ●; isolates from the ISS potable water ▲; ISS cooling water Δ; an air filter of the PHSF assembly facility ◊ and the surface of the Mars orbiter □. GenBank accession numbers are shown in parentheses.

Their clonal relationship was investigated by ERIC-PCR (Figure 4.2). The *C. metallidurans* isolates are clearly clonally distinct. The *R. pickettii* water isolates also showed distinct ERIC-PCR fingerprints, except isolates CW1 and CW4. The ERIC-PCR fingerprints of the *R. pickettii* surface isolates are the same for SSH2, SSH3 and SSH4. However, differences in plasmid profiles and phenotypes (see below) indicated that neither CW1 and CW4, nor SSH2, SSH3 and SSH4 are clonal. Finally, the close relationship between *Ralstonia pickettii* and *Cupriavidus metallidurans* (previously *Ralstonia metallidurans* [139]) is evidenced by similar ERIC-PCR fingerprints. We focussed in particular on these closely related β-proteobacterial genera *Ralstonia* and *Cupriavidus*, which thrive in many different natural environments, as they appeared in the intersection of all samples. This indicated that they are also ubiquitously present in space-related environments (space industry and ISS). The ISS potable water systems were mostly contaminated with *Methylobacterium, Ralstonia* and *Sphingomonas*, which are typical water-borne microorganisms [50]. The predominant genera in the air of spacecraft assembly facilities before human activity were *Burkholderia*, *Afipia* and *Cupriavidus* [154, 176]. *Ralstonia*, *Microbacterium* and *Bacillus* were, together with the fungus *Aureobasidium*, the main fraction of cultivable species isolated from the surface of the Mars Odyssey Orbiter [140]. The route of contamination by *Ralstonia* and *Cupriavidus* spp. is most likely through water and air exchange and not via human activity, which is a source of contamination by human commensals and/or (opportunistic) pathogens such as *Staphylococcaceae* and *Streptococcaceae* [176]. The ability to withstand the prevailing conditions and implemented cleaning and sanitation plan will facilitate their persistence and will allow transmission of contamination to the operational spacecraft in space. However, as non-spore-forming bacteria, they are not considered the most likely candidates to survive in extra-terrestrial environments [177, 178].

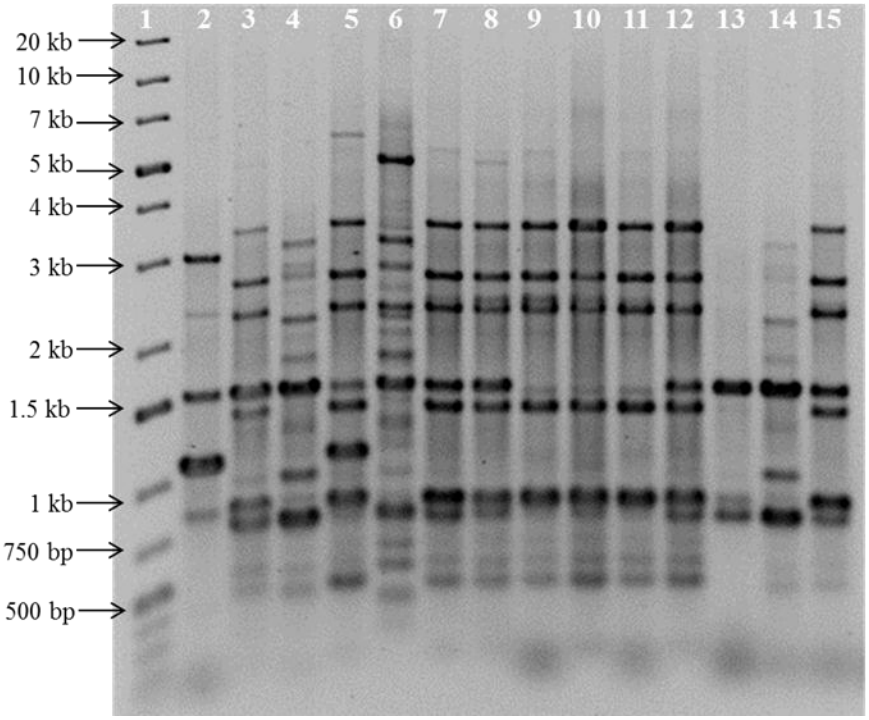

Figure 4.2: ERIC-PCR for the different *C. metallidurans* (2-6) and *R. pickettii* (7-15) isolates showing their clonal relationship. (1) GeneRuler™ 1 kb plus DNA Ladder; (2) *C. metallidurans* CH34; (3) NA1; (4) NA2; (5) NA4; (6) NE12; (7) *R. pickettii* ATCC27511; (8) SSH1; (9) SSH2; (10) SSH3; (11) SSH4; (12) CW1; (13) CW2; (14) CW3; (15) CW4.

4.3.2 Growth requirements and limits

An interesting feature of many *C. metallidurans* strains is that they display a 'mutator phenotype' at 37°C, also termed temperature-induced mortality and mutagenesis or TIMM [56, 179-181], which has been used as a diagnostic for *C. metallidurans* [179]. Survival of many *C. metallidurans* strains is very low at 37°C, with a frequency of survivors around 10^{-6} to 10^{-3} compared to the viable count at 30°C [182-184]. As for type strain CH34, isolates NA4 and NE12 showed hampered growth in rich LB medium at 37°C with a frequency of survivors ranging from 10^{-2} to 10^{-4}, while strains NA1 and NA2

grew equally well at 37°C and 30°C (Table 4.3). For NA4, NE12 and CH34, a large fraction of survivors, ranging from 2 to 42%, showed mutations such as auxotrophy and loss of heavy metal resistance (Ni^{2+} and Cu^{2+}) (Table 4.3). Overall, the mutation frequency of NA4 was lower than of NE12 and CH34 (Table 4.3). Until now, the precise mechanism of this TIMM is not yet known and is beyond the scope of this study. However, it would be interesting for further studies as it reflects the ability of these strains to cope with changing temperature conditions.

Table 4.3: Survival and mutation frequency of *C. metallidurans* isolates at 37 °C.

Isolate	**Survival frequency[a]**	**Auxotrophy[b]**	**Loss of Ni^{2+} resistance[b]**	**Loss of Cu^{2+} resistance[b]**
$CH34^T$	$2.03 \times 10^{-4} \pm 6.18 \times 10^{-5}$	15.43 ± 7.43	26.63 ± 15.25	19 ± 5.87
NA1	$9.13 \times 10^{-1} \pm 9.11 \times 10^{-2}$	0	0	0
NA2	$1.14 \pm 3.70 \times 10^{-2}$	0	0	0
NA4	$1.75 \times 10^{-2} \pm 2.45 \times 10^{-2}$	4.21 ± 6.4	2.46 ± 0.61	16.8 ± 5.86
NE12	$3.31 \times 10^{-4} \pm 3.07 \times 10^{-4}$	14.09 ± 3.47	20 ± 10.04	42.5 ± 15.77

[a]Survival frequency is calculated as viable count on LB agar at 37°C divided by viable count at 30°C (n = 3). [b]Mutation frequency is given in percentage of analysed colonies (n = 285) transferred from LB agar incubated at 37°C on 284 MM, 284 MM + 1 mM Ni^{2+} and 284 MM + 0.8 mM Cu^{2+}, respectively.

At this moment, it is not yet clear whether *C. metallidurans* is able to cause a human infection. As many strains are not able to grow at 37°C, it is unlikely that they will cause a human disease. In addition, although *C. metallidurans* strains have been isolated from patients with cystic fibrosis, it remains unclear if these strains were causing an active infection or intervened only as secondary opportunistic pathogens [142]. Nevertheless, recently, a first case of invasive human infection caused by *C. metallidurans* was reported [185].

All *R. pickettii* isolates were able to grow at 37°C. *R. pickettii* strains have been reported to be opportunistic human pathogens [157, 186], and such contamination in drinking water could pose a potential threat for astronauts as the human immune system is depressed in space conditions [153]. Therefore, it is important to find proper methods for prevention of contamination but maybe even more important to develop adequate and fast identification tools. Although most contaminants including *Cupriavidus* and *Ralstonia* isolates pose no immediate threat to the astronauts, contaminated water in the ISS is often rejected for consumption, as currently no identification method is available during flight. This type of contamination wastes tremendous amounts of crew time and Earth-based resources. In addition, these water contamination events require materials to be transferred both to and from the ISS, with transport costs to deliver items to the ISS running up to 10,000 Euros per kilogram [36].

All *R. pickettii* isolates and *C. metallidurans* NE12 were able to grow anaerobically in the presence of nitrate. To carry out this function, strain CH34 harbours the *nar*, *nas* and *nap* genes encoding different nitrate reductases [56]. Several genes coding for nitrate reductases, which are highly similar to the *nar, nas* and *nap* genes of *C. metallidurans* CH34, are also present on the genome of *R. pickettii* strain 12J. This function is presumably not essential to survive in these space-related environments, as *C. metallidurans* NA1, NA2 and NA4 were not able to grow anaerobically.

None of the tested *R. pickettii* and *C. metallidurans* isolates were able to grow autotrophically on H_2 and CO_2. In *C. metallidurans* CH34, this trait is located on genomic islands that belong to the family of Tn*4371*-like Integrative and Conjugative Elements (ICE) [133, 161]. Analysis of multiple *C. metallidurans* isolates by comparative whole genome hybridisation showed that these elements are absent in the *C. metallidurans* space isolates [187].

All isolates, except *C. metallidurans* NA1, *R. picketti* SSH2 and type strain ATCC27511, were able to form biofilms on polystyrene (Table 4.4).

Table 4.4: Ability of the isolates to form biofilms on polystyrene

	Isolate	**Mean OD_{530}[a]**	**Ratio[b]**
C. metallidurans	CH34	0.079	1.403*
	NA1	0.066	1.185
	NA2	0.071	1.274*
	NA4	0.200	3.573*
	NE12	0.225	4.020*
R. pickettii	ATCC27511	0.137	2.440
	SSH1	0.525	9.383*
	SSH2	0.122	2.177
	SSH3	0.286	5.105*
	SSH4	0.307	5.474*
	CW1	0.320	5.714*
	CW2	0.182	3.252*
	CW3	0.162	2.895*
	CW4	0.742	13.244*
E.c coli	MG1655	0.270	4.829*

[a]Data represent the mean (n = 3) amount of crystal violet retained by the biofilm as measured by absorbance at 530 nm. [b]Biofilm-forming capacity for each isolate was expressed relative to the average value for uninoculated growth medium.
*Significant biofilm formation compared to uninoculated LB ($p < 0.05$).

The biofilm-forming capacity of the *R. picketti* isolates was in general higher than that of the *C. metallidurans* isolates. The biofilm-forming capacity of *Escherichia coli* MG1655, which was included for comparison, situated between the *R. pickettii* and *C. metallidurans* isolates (Table 4.4). Biofilm formation of *R. pickettii* was already shown in plastic water piping (PVC) commonly used to distribute water in pharmaceutical, industrial and hospital water systems [188]. It is hypothesized that *R. pickettii* may be able to scavenge from the polymers in the plastic piping [189]. Biofilm-forming capacity can affect the persistence of microbial contaminants as cells within

a biofilm are more resistant to antibiotics, cleaning reagents and other biocides than their planktonic counterparts [reviewed in159].

4.3.3 Plasmid profiles

Strains from the *Cupriavidus* and *Ralstonia* genera typically carry two chromosomes and often one or more megaplasmids. These megaplasmids carry specific traits that allow adaptation to or survival in different ecological niches. For instance, plasmid pRALTA of *C. taiwanensis* LMG19424 carries genes involved in legume symbiosis and nitrogen fixation [190], while the catabolic plasmid pJP4 of *C. pinatubonensis* JMP134 carries genes involved in degradation of aromatic pollutants [163]. *C. metallidurans* CH34 contains two megaplasmids that are especially involved in metal resistance: pMOL28 (171 kb) and pMOL30 (234 kb). Plasmid pMOL28 carries determinants for resistance to mercury, chromate, nickel and cobalt, while plasmid pMOL30 enables resistance to copper, cadmium, zinc, cobalt, lead, mercury, and silver [56, 57, 160]. Large plasmid extractions showed that each isolate carried at least one megaplasmid (Figure 4.3). With the method used here, only covalently closed circular plasmid DNA will be isolated [171]. The size of the fragments was compared relative to a BAC-Tracker™ Supercoiled DNA Ladder (Epicentre Biotechnologies, USA).

C. metallidurans NA1 and NA4 carry 2 plasmids similar in size to pMOL28 and pMOL30 of *C. metallidurans* CH34. NA4 carries in addition a smaller plasmid with a size around 95 kb. *C. metallidurans* NA2 and NE12 carry a single megaplasmid: that of NA2 is comparable in size to pMOL28, while the one of NE12 is comparable in size to pMOL30. *R. pickettii* isolates SSH2, SSH3, SSH4, CW1 and CW2 carry one plasmid, which is larger than the plasmid observed in type strain ATCC27511 and than pMOL30 of *C. metallidurans* CH34. *R. pickettii* isolates SSH1 and CW4 also harbour one

plasmid, similar in size to pMOL30 but larger than the plasmid observed in type strain *R. pickettii* ATCC27511. Both strain SSH2 and SSH4 carry two additional smaller plasmids, one with a size around 95 kb and the other around 65 kb. *R. pickettii* CW3 carries only one smaller plasmid of approximately 45 kb. These differences in plasmid profiles could be partially responsible for the further discussed differences in the resistance characteristics.

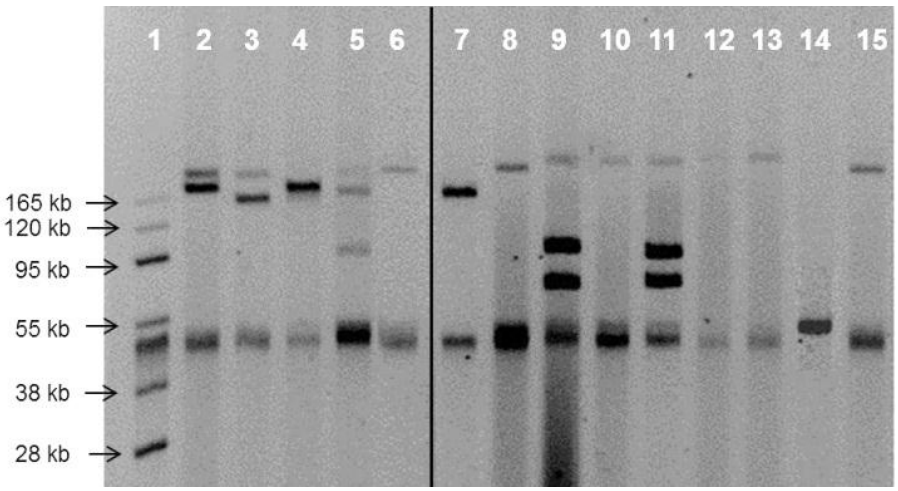

Figure 4.3: Megaplasmids in the different *C. metallidurans* (2-6) and *R. pickettii* (7-15) isolates. (1) BAC-Tracker™ Supercoiled DNA Ladder; (2) *C. metallidurans* CH34; (3) NA1; (4) NA2; (5) NA4; (6) NE12; (7) *R. pickettii* ATCC27511; (8) SSH1; (9) SSH2; (10) SSH3; (11) SSH4; (12) CW1; (13) CW2; (14) CW3; (15) CW4.

4.3.4 UV-C resistance

Several chemical antimicrobial agents as well as physical cleaning methods are used to control microbial contamination on spacecraft hardware surfaces during (and after) assembly [26, 151]. In addition, assembly facilities such as the JPL spacecraft assembly facility and the PHSF facility of the Kennedy Space Center are classified as 100000 (US standard, equal to ISO 8). This means that a maximum of 100,000 particles with a size greater than 0.5 µm

per ft³ of air or 3,520,000 particles per m^3 of air is accepted in these clean rooms. Air entering through HEPA filters installed in the ceilings of the clean rooms are tested and guaranteed as class air 5000. Furthermore, temperature and humidity are highly controlled and cleanrooms and surfaces are subjected to extensive cleaning [176]. One sterilization/ cleaning method used is UV-C irradiation. Each isolate was screened for its resistance against different doses (from 25 until 200 J/m²) of UV-C 254 nm radiation. The dose needed to kill 90% of the population (D_{10}-values) was determined (Table 4.5).

Table 4.5: UV-C 254 nm resistance of *C. metallidurans* and *R. pickettii* isolates and species type strains(T).

Source	**Species**	**Strain**	**D_{10} value[a]**
Intestine	*E. coli*	MG1655	36.7 ± 4.1
Metal polluted soil	*C. metallidurans*	CH34T	22.1 ± 4.7
Human tissue clinical origin	*R. pickettii*	ATCC27511T	11.1 ± 1.0
Surface	*R. pickettii*	SSH1	27.3 ± 6.2*
	R. pickettii	SSH2	9.1 ± 1.6
	R. pickettii	SSH3	29.7 ± 9.9*
	R. pickettii	SSH4	26.2 ± 4.4*
Air filter	*C. metallidurans*	NE12	24.0 ± 5.0
Potable water	*C. metallidurans*	NA1	27.5 ± 2.6
	C. metallidurans	NA2	36.1 ± 2.7*
	C. metallidurans	NA4	22.9 ± 2.7
Cooling water	*R. pickettii*	CW1	10.5 ± 5.0
	R. pickettii	CW2	10.3 ± 1.4
	R. pickettii	CW3	27.8 ± 1.7*
	R. pickettii	CW4	13.9 ± 1.6

[a]D_{10} values are mean values (n = 3) with standard deviation. *Significant difference ($p < 0.05$) between an isolate and its respective type strain.

In general, the *R. pickettii* and *C. metallidurans* isolates and type strains are relatively sensitive to UV-C (compared to *E. coli* MG1655). The D_{10}-values of the *R. pickettii* surface isolates (except for SSH2) were 2.5 times higher

compared to *R. pickettii* ATCC27511 and to the *R. pickettii* isolates from the cooling water (except CW3). Also *C. metallidurans* NA2 was significantly more resistant to UV-C radiation than *C. metallidurans* CH34. The cooling water isolates were equally resistant as the type strain, except for *R. pickettii* CW3, which displayed a D_{10}-value 2.5 times higher. As expected, the D_{10}-values of the isolates are much lower than those of endospores from *Bacillus* spp. isolated from cleanroom environments [191, 192], indicating that extreme resistance is not necessary to escape from the cleaning and sanitation plan used in such facilities. A disadvantage of sterilization by UV radiation is that subtle variations in the surface can create small areas that shelter microorganisms [178].

4.3.5 Antibiotic resistance

Each isolate was screened for its resistance against several antibiotics (Table 4.6). *R. pickettii* ATCC27511 was resistant to 5 of the 7 antibiotics tested. This feature is likely reminiscent of the clinical origin of the strain. All isolates, except *R. pickettii* CW3, grew in the presence of kanamycin (50 µg/ml). Although the *R. pickettii* isolates formed smaller colonies compared to the *C. metallidurans* isolates. All *C. metallidurans* isolates, except NA4, were also resistant to kasugamycin (50 µg/ml), while none of the *R. pickettii* isolates was able to resist this concentration. The *C. metallidurans* isolates were also more resistant to chloramphenicol than the *R. pickettii* isolates. *C. metallidurans* isolates were able to grow at concentrations up to 150 µg/ml, while the *R. pickettii* isolates were only able to grow at a concentration of 30 µg/ml. *R. pickettii* ATCC27511 and all surface isolates (*R. pickettii* SSH1, SSH2, SSH3 and SSH4) were able to grow on carbenicillin (100 µg/ml). Only *C. metallidurans* CH34 and NA4 were sensitive to ampicillin (100 µg/ml). None of the isolates grew in the presence of trimethoprim (100 µg/ml) or tetracycline (20 µg/ml).

4.3.6 Metal resistance

To flourish successfully in highly polluted metal-rich environments, many *R. pickettii* and *C. metallidurans* strains have acquired several metal detoxification mechanisms [56, 57, 146]. The most frequent mechanism is pumping out ions via efflux pumps [193] and interplay between different types of efflux pumps can result in higher resistance and better detoxification [56]. Other detoxification mechanisms are reduction to a less toxic state or sequestration of the metal intracellular or at the cell surface [193]. In this study, each isolate was screened for its resistance against Ag^{+}, Hg^{2+}, Cd^{2+}, Co^{2+}, Zn^{2+}, Cu^{2+} and Ni^{2+} ions in a Tris-buffered mineral medium with gluconate as carbon source. The minimal inhibitory concentration (MIC) – the lowest concentration that inhibits visible growth – was determined after 48 hours (Table 4.7). Silver and mercury were the most toxic. Together with cadmium, these two metals have no beneficial biological role what makes resistance systems necessary. The other metals are micronutrients, thus it is essential that bacteria can react to limiting amounts but also to an excess of these metals [194]. Generally, *C. metallidurans* isolates were more resistant to Hg^{2+}, Zn^{2+}, and Cu^{2+} but more sensitive to Ni^{2+} than the *R. pickettii* isolates. Among the *C. metallidurans* isolates, only subtle differences in metal susceptibility were observed.

Table 4.6: Antibiotic resistance of *C. metallidurans* and *R. pickettii* isolates and species type strains(T).

	Isolate	Km50	Ksg50	Cm30	Cm100	Cm150	Cb100	Amp100	Tc20	Tm100
C. metallidurans	CH34^T	+++	+	+++	+++	+++	-	-	-	-
	NA1	+++	+	+++	+++	+++	-	+++	-	-
	NA2	+++	+	+++	+++	+++	-	+++	-	-
	NA4	+++	-	+++	+++	+++	-	-	-	-
	NE12	+++	+	+++	+++	+++	-	+++	-	-
R. pickettii	ATCC27511^T	+++	+++	+++	-	-	+++	+++	-	-
	SSH1	+++	-	+++	-	-	+++	+++	-	-
	SSH2	+++	-	+++	-	-	+++	+++	-	-
	SSH3	+++	-	+++	-	-	+++	+++	-	-
	SSH4	+++	-	+++	-	-	+++	+++	-	-
	CW1	+++	-	+++	-	-	-	+++	-	-
	CW2	+	-	+++	-	-	-	+++	-	-
	CW3	-	-	+++	-	-	-	+++	-	-
	CW4	+++	-	+++	-	-	-	+++	-	-

(Km) kanamycin, (Ksg) kasugamycin, (Cm) chloramphenicol, (Amp) ampicillin, (Cb) carbenicillin, (Tc) tetracycline, (Tm) trimethoprim. The number represents the concentration in µg/ml. Symbols: (+++) very good growth, (+) slight growth, (-) no growth.

One noticeable difference is the MIC of Ni^{2+} for *C. metallidurans* NA4: 40 mM compared to 4 mM for the other *C. metallidurans* isolates. A possible explanation for this could be that *C. metallidurans* NA4 carries a functional *nccCBA* locus, which has been shown to be responsible for higher Ni^{2+} resistance in other *C. metallidurans* strains [195]. In contrary, in type strain CH34 this locus is not functional due to a frame shift mutation in *nccB* [57].

The *R. pickettii* isolates were also more or less equally resistant against the tested metals. The MIC values for Cd^{2+}, Co^{2+} and Zn^{2+} of *R. pickettii* SSH1, CW3 and CW4 were in the same range of that of *C. metallidurans* CH34. In all the other *R. pickettii* isolates, the MIC values for those metals (especially for Zn^{2+}) were lower. In *C. metallidurans* CH34, Cd^{2+}, Co^{2+} and Zn^{2+} resistance is conferred by the *czcMNICBADRSEJ ompP czcP* gene cluster located on plasmid pMOL30 and probably obtained by horizontal transfer [56, 57]. A similar *czc* gene cluster was also found in *R. pickettii* 12J [161] and PCR amplification (with primers based on the sequence of CH34) could confirm the presence of this cluster in *R. pickettii* SSH1 and CW4. However, no amplification could be observed for CW3 (Figure 4.4). It could be that resistance to these metals is conferred by other gene clusters or that the primers were not optimal for this strain. In the Zn-sensitive *R. pickettii* isolates, no amplification could be observed indicating the absence of this cluster as it is the case for *R. pickettii* 12D [161]. Further studies are necessary to determine if these metal resistant clusters are chromosomally located or on their megaplasmids. In addition, it cannot be excluded that the differences in MIC values between the isolates could be due to the fact that other metal resistant gene clusters are present.

Table 4.7: Metal ion MIC-values in mM for *C. metallidurans* and *R. pickettii* isolates and species type strains(T)

	Isolate	Ag^{+}	Hg^{2+}	Cd^{2+}	Co^{2+}	Zn^{2+}	Cu^{2+}	Ni^{2+}
C. metallidurans	CH34^{T}	0.001	0.0027	1	12.5	12	6	4
	NA1	0.0005	0.0027	0.5	12.5	12	6	4
	NA2	0.0005	0.0013	0.5	6.25	12	6	4
	NA4	0.001	0.0027	0.5	12.5	12	6	40
	NE12	0.004	0.0054	1	12.5	12	1.5	4
R. pickettii	ATCC27511^{T}	0.001	0.0013	0.25	3.125	3	0.75	1
	SSH1	0.002	0.0054	1	12.5	24	1.5	4
	SSH2	0.001	0.00068	0.25	6.25	3	1.5	4
	SSH3	0.001	0.00068	0.5	6.25	3	1.5	4
	SSH4	0.001	0.00068	0.5	6.25	3	0.75	8
	CW1	0.002	0.0013	0.5	3.125	3	1.5	8
	CW2	0.002	0.0013	0.5	3.125	3	1.5	8
	CW3	0.002	0.0054	0.5	12.5	6	1.5	8
	CW4	0.002	0.0054	0.5	12.5	12	1.5	8

[a]MIC-values were scored in 284MM medium supplemented with 0.2% gluconate as carbon source at 30°C after 48 h

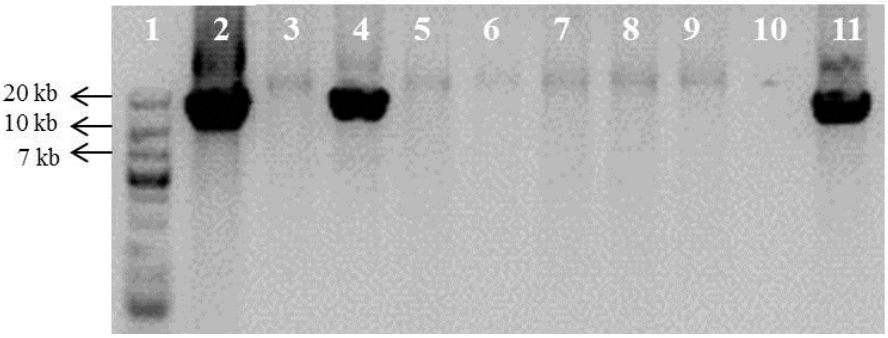

Figure 4.4: Presence of the *czcNICBADRSE* gene cluster in *C. metallidurans* CH34 (10573 bp) and the different *R. pickettii* (3-11) isolates. (1) GeneRuler™ 1 kb plus DNA Ladder; (2) *C. metallidurans* CH34; (3) *R. pickettii* ATCC27511; (4) SSH1; (5) SSH2; (6) SSH3; (7) SSH4; (8) CW1; (9) CW2; (10) CW3; (11) CW4.

Stainless steels are used for many applications because of their stability, cleanability and high resistance to corrosion. However, care should be taken as many factors such as inorganic anions and inorganic acids/bases which are present in many disinfectants can cause pitting, a localized and intense form of galvanic corrosion [196]. These pits can facilitate bacterial adhesion and biofilm formation what, on its turn leads to a higher corrosion rate [196]. This phenomenon was also observed in the water system of the ISS, where the concentration of dissolved nickel ions increased in time probably as a result of galvanic corrosion of the surfaces in the presence of water containing silver ions [197]. Consequently, metal tolerance can be an advantage to survive in these space-related environments. In addition, the mechanisms necessary to resist metals are generally the same as those of antibiotic resistance [198] and co-selection between them has been frequently reported [for a comprehensive overview, see 129]. So, their tolerance to heavy metals can be an additional advantage as it can putatively influence antibiotic resistance and vice versa.

Finally, resistance to silver is of special interest as it is used as water disinfectant in the ISS (see next paragraph).

4.3.7 Silver resistance

Silver ions are widely used for their antibacterial effects [64, 74]. Next to clinical applications (e.g. burn wound treatment, silver-coated catheters or silver filling amalgams) [199], silver compounds are used as (co-)disinfectant to control infectious agents in water management systems (e.g. swimming pools or hospitals) [60, 200]. In the ISS, all sources of water are sanitized with silver ions [50]. The ISS MORD identifies 4.6 µM as the maximum tolerated silver concentration in potable water. However, chemical analysis of samples returned from the ISS indicated that the dissolved silver concentration in SRV-K potable water was always below 0.86 µM and in SVO-ZV potable water this concentration ranged from 0.21 to 2.61 µM (both measured from Oct 2006 to Oct 2007) [201]. This decrease seems to be due to a rapid deposition of silver onto the metallic surfaces of the water distribution systems, which makes it unavailable for microbial control [197]. An additional problem is that phosphate is added to the water to prevent corrosion [197] and already small amounts of phosphate in water lead to an increase in microbial growth [202, 203]. Silver ions have a broad spectrum of activities: they have a high affinity to sulfhydryl groups in proteins leading to conformational changes and inactivation of enzymes, they block the respiratory chain and are able to bind with DNA resulting in inhibition of proliferation [74].

For *C. metallidurans* CH34, the MIC for silver after 7 days was 4 µM in mineral medium (MM284) compared to 800 µM in complex rich medium (LB) (data not shown). Thus, the use of mineral medium for the MIC determination strongly decreases the MIC compared to a complex rich medium. However, it better reflects the potable water conditions and the

bioavailability of the metal. In liquid medium, addition of silver resulted in a delay of the exponential growth phase by prolonging the lag phase. Therefore, the time point of determination appeared to be an important factor. The minimal inhibitory $AgNO_3$ concentrations ranged from 0.5 to 4 µM after 2 days (Table 4.7) and from 1 µM to 8 µM after 7 days (data not shown). The MIC values of the *R. pickettii* isolates from the cooling water were higher compared to those of the surface isolates (except SSH1) and the type strain (Table 4.7). Putatively they have acquired different or more resistance markers, which can be an advantage to survive in (the ISS) water sources. After 7 days of exposure to a silver concentration equal to the MIC, half of the isolates (NA2, NA4, SSH2, SSH3, SSH4, CW4) were able to resuscitate after transfer to fresh MM284 medium. A fraction of cells was not killed by silver but putatively entered a 'dormant' (persistent) state that allows them to survive but not proliferate in the presence of silver. This phenomenon is known, and these persister cells are more resistant to stressors and are able to resuscitate and reproduce when more favourable conditions arrive [204]. The observed MIC concentrations for silver were thus often higher than the concentration used in ISS. Therefore, this will not inhibit growth when organic material is present nor eradicate the contamination.

C. metallidurans CH34 carries a number of systems putatively involved in silver detoxification. The *silDCBA*, *agrCBA*, and *cusDCBAF* operons, which encode proteins that belong to the RND family of transporters, are located on pMOL30, chromosome 1 and 2, respectively. The *cupRAC* operon that codes for a P-type ATPase is located on chromosome 1 [56]. PCR amplification using CH34-based primers showed the presence of the *agrCBA*, *silCBA*, and *cusCBA* operons in almost all isolates except for the *R. pickettii* isolates SSH2, SSH3 and SSH4 (Figure 4.5), although their MIC (after 48 h) was the same as that of CH34 (Table 4.7).

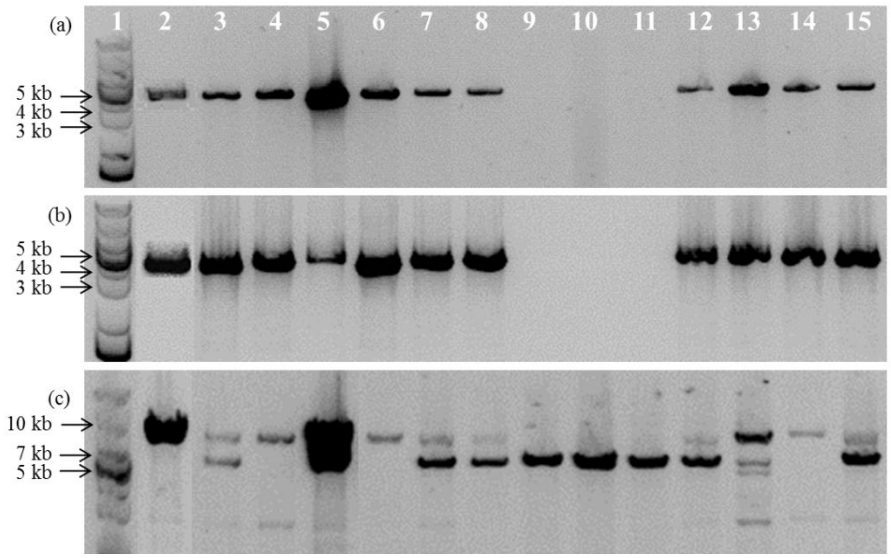

Figure 4.5: Presence of the (a) *agrCBA* (3277 bp) (b) *silCBA* (3562 bp) and (c) *cusCBA* (6413 bp) operon in the different *C. metallidurans* (2-6) and *R. pickettii* (7-15) isolates and species type strains. (1) GeneRuler™ 1 kb plus DNA Ladder; (2) *C. metallidurans* CH34; (3) NA1; (4) NA2; (5) NA4; (6) NE12; (7) *R. pickettii* ATCC27511; (8) SSH1; (9) SSH2; (10) SSH3; (11) SSH4; (12) CW1; (13) CW2; (14) CW3; (15) CW4.

Putatively, these fragments were not present in these isolates and silver resistance was conferred by other resistance determinants, or it could be that annealing of the primers, which were based on the gene sequences of CH34, was not optimal for these *R. pickettii* isolates. PCR amplification on plasmid extracts showed that in all *C. metallidurans* isolates and almost all *R. pickettii* isolates, the *silCBA* cluster is located on one of their megaplasmids, while *agrCBA* is chromosomally located as it is the case for *C. metallidurans* CH34 (Figure 4.6).

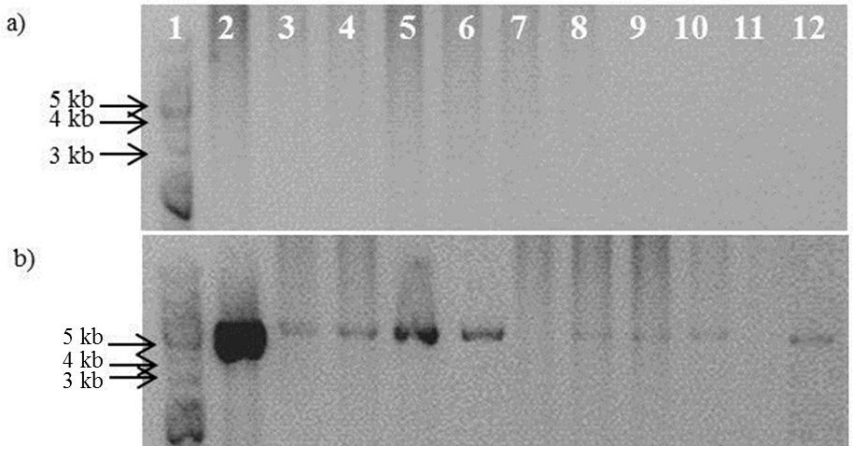

Figure 4.6: Presence of the (a) *agrCBA* (3277 bp) and (b) *silCBA* (3562 bp) operon on plasmid DNA in the different *C. metallidurans* (2-6) and *R. pickettii* (7-12) isolates and species type strains. (1) GeneRuler™ 1 kb plus DNA Ladder; (2) *C. metallidurans* CH34; (3) NA1; (4) NA2; (5) NA4; (6) NE12; (7) *R. pickettii* ATCC27511; (8) SSH1; (9) CW1; (10) CW2; (11) CW3; (12) CW4.

The sequence of *silA* (if present) is highly conserved (98% - 99% identical), while the *agrA* sequence showed more variation between the isolates (Figure 4.7). For *R. pickettii* CW4, the amplified *silA* sequence was more similar to *hmyA* of CH34, which encodes a paralogous efflux pump [56].

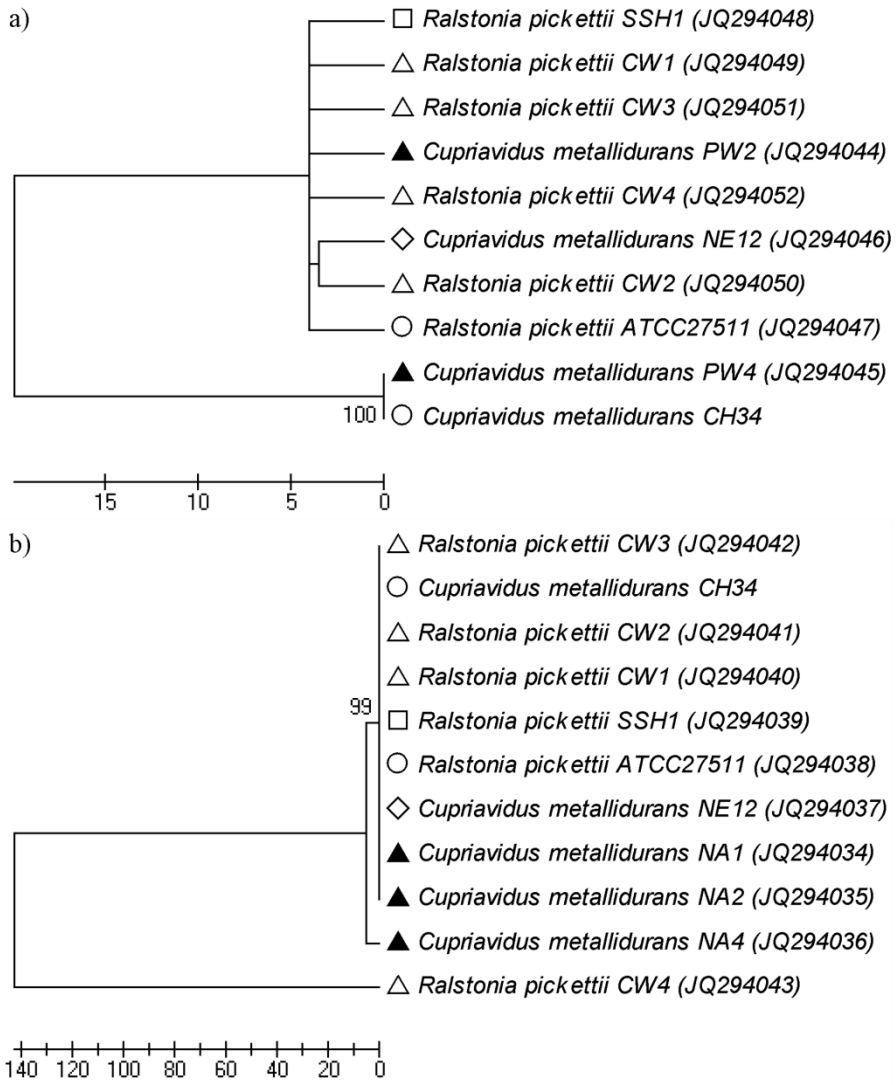

Figure 4.7: Neighbour-joining phylogenetic tree based upon a) *agrA* and b) *silA* gene sequence similarities. Numbers at the branches represent percentages of 1000 bootstrap repetitions (only values above 50 % are shown). Symbols for each strain: type strains ○; isolates from the ISS potable water ▲; ISS cooling water Δ; an air filter of the PHSF assembly facility ◊ and the surface of the Mars orbitor □. GenBank accession numbers are shown in parentheses.

4.3.8 Survival in potable water

All isolates survived for at least 23 months in potable water with or without 2 µM $AgNO_3$, and could be resuscitated and proliferated afterward (Figure 4.8 and Figure 4.9). During this period, the viable fraction decreased on average from 10^9 CFU/ml to 10^6 CFU/ml.

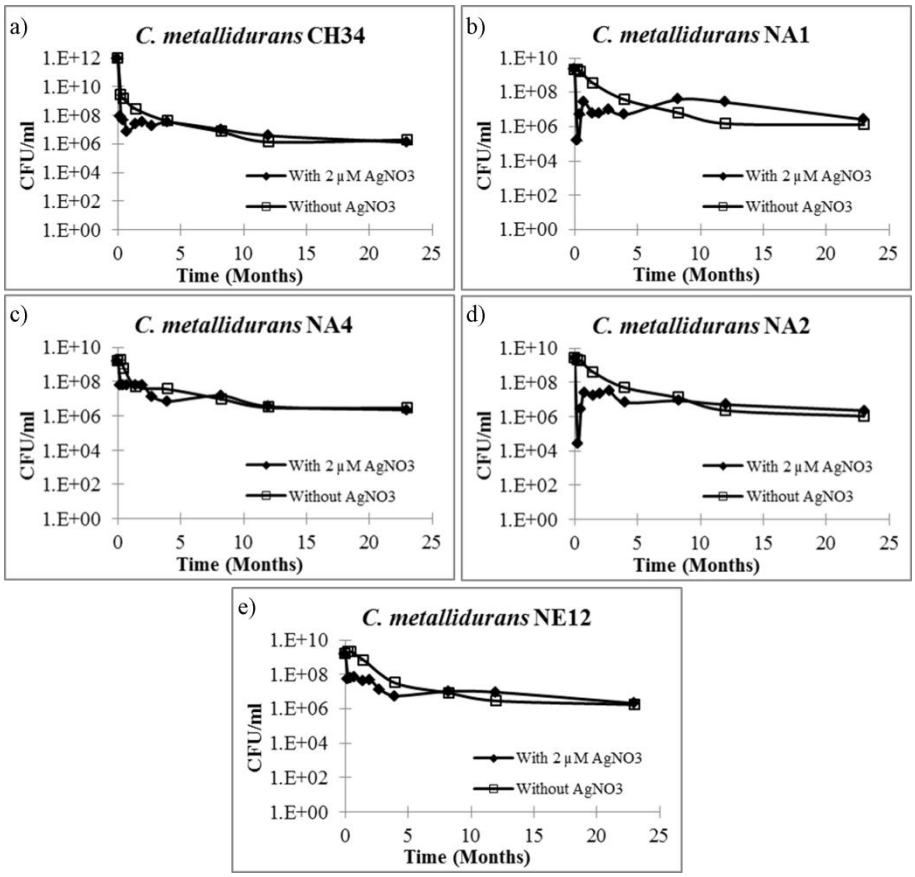

Figure 4.8: Survival of *C. metallidurans* isolates and species type strain in potable water without (open squares) and with (full diamonds) 2 µM AgNO3 during a period of 23 months. a) *C. metallidurans* CH34; b) NA1; c) NA2; d) NA4; e) NE12.

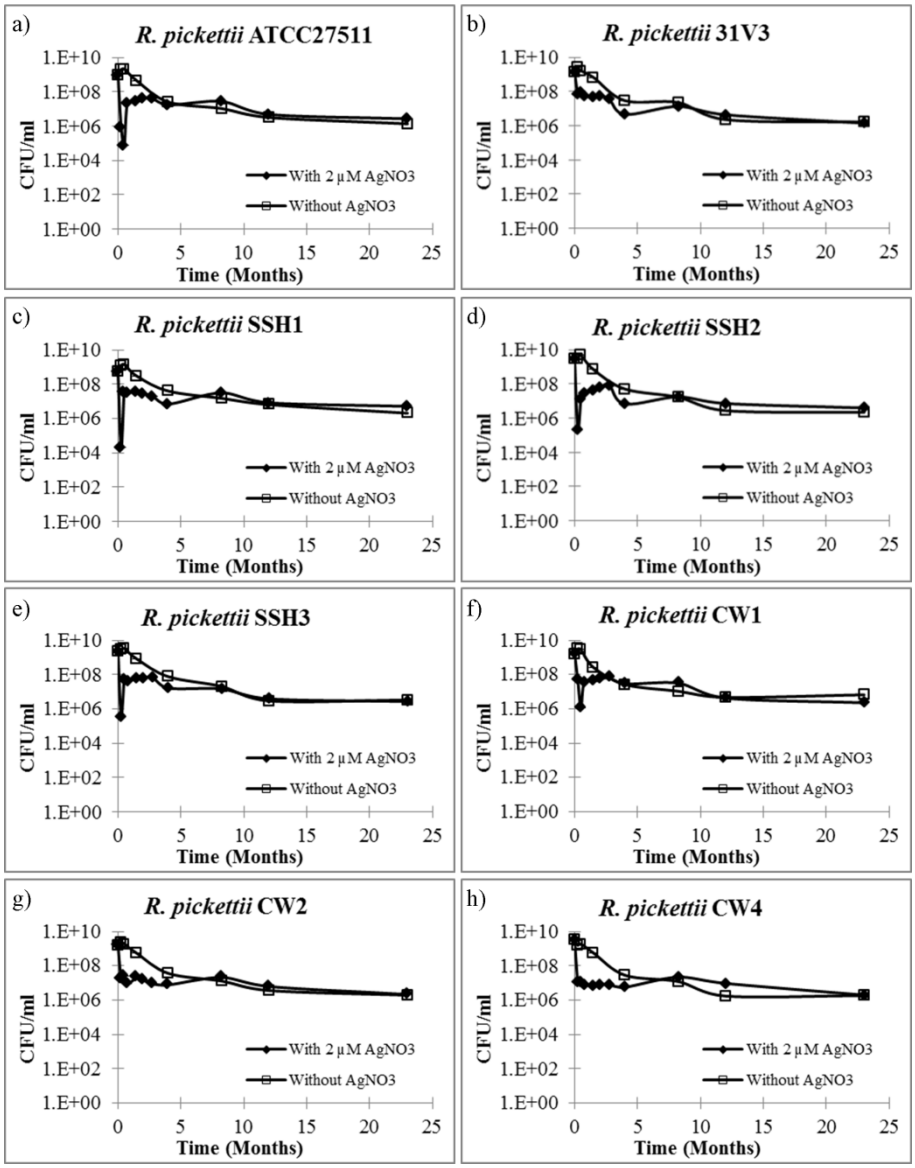

Figure 4.9: Survival of *R. pickettii* isolates and species type strain in potable water without (open squares) and with (full diamonds) 2 µM AgNO3 during a period of 23 months. a) *R. pickettii* ATCC27511; b) SSH1; c) SSH2; d) SSH3; e) SSH4; f) CW1; g) CW2; h) CW4.

4.4 Conclusions

The presence of *Ralstonia pickettii* and *Cupriavidus metallidurans* in space-related environments such as spacecraft assembly facilities, robot surfaces and the ISS is not an isolated observation neither in location nor frequency. For instance concerning frequency, the ISS SVO-ZV water storage and dispensing system was monitored 27 times over a 4-year period (2001-2004) and bacterial levels above the acceptability limit of 100 CFU/100 ml were detected in 16 cases (60%), with high incidence of *R. pickettii* and *C. metallidurans* [50]. Although these recurrent contaminations elicited a series of remediation actions, contamination levels always increased above the acceptability limit soon afterward [50].

Our results provide insights in the factors causing this resilience of the contamination. First of all, it appears that most of the analysed phenotypes are common to *R. pickettii* and *C. metallidurans* as isolate phenotypes were similar to that of their respective type strains, isolated from different environments. Survival in oligotrophic environments such as on surfaces, in air and in water (even when supplemented with disinfectant) is certainly a beneficial trait. Correspondingly, *Ralstonia* spp. isolated from ultrapure water were previously shown to survive in such water for at least 6 months [53]. *Ralstonia solanacearum* was even able to survive over 4 years in river water [205]. Acquired resistance (UV-C radiation, antibiotics, and heavy metals) can also aid their survival and persistence.

Resistance to silver is of special interest taking into account its use as water disinfectant aboard the ISS. Furthermore, since at least part of these silver resistance mechanisms are located on their megaplasmids, they could be disseminated to different members of the contaminating population [137, 206]. It is therefore essential that the silver concentrations aboard the ISS are continuously monitored and maintained close to the maximum allowed

levels. In addition, alternative disinfectants could be studied to obtain improved control and prevention strategies. Finally, the persistence of contamination and its resistance to disinfectants can be promoted by biofilm formation [32, 159]. Preventing, through adequate design, and identifying critical points in the environment or system that are potentially prone to contamination build-up and biofilm formation are critical. Many isolates from space-related environments are extremely resistant such as *Bacillus* spores to UV-C and *Acinetobacter radioresistens* to dessication and H_2O_2 [140]. However, our results indicate that extreme resistance is not essential for surviving these harsh and oligotrophic environments with dedicated cleaning and sanitation plans.

Chapter 5

Genetic adaptation of *Cupriavidus metallidurans* in response to silver toxicity

---

Silver is used to sanitize potable water systems aboard the ISS. In the previous chapter, it was shown that the *C. metallidurans* and *R. pickettii* isolates harbour several resistance mechanisms and that they were able to withstand silver concentrations higher than the concentrations measured in the potable water systems aboard the ISS. Moreover, they were able to survive during a long time-period in potable water supplemented with silver nitrate. Therefore, in this chapter, the silver resistance mechanisms are studied in more detail. Silver resistant mutants are generated and the underlying genetic circuit is investigated.

This chapter is based on the following publication:

Mijnendonckx K., Monsieurs P., Leys N., Mahillon J., Van Houdt R. Genetic adaptation of *Cupriavidus metallidurans* in response to silver toxicity reveals a novel silver resistance mechanism. *In preparation*

5.1 Introduction

Silver is widely used as a (co-)disinfectant of water systems such as swimming pools, hospital hot water systems and potable water systems due to its broad-spectrum antimicrobial properties. In fact, silver is also used aboard the ISS in the three main water systems on the Russian side. Despite repeated disinfection and remediation actions, contamination of these water systems is not an exceptional event. A four-year monitoring campaign of the Russian storage and dispensing system (SVO-ZV) showed that bacterial contamination levels were above the acceptability limit of 100 CFU/100 ml in 16 of 27 sampling times [50]. The most dominant species were typical water-borne microorganisms such as *Methylobacterium*, *Sphingomonas* and *Ralstonia*, however, also *C. metallidurans* was recurrently detected [50].

C. metallidurans strains are frequently isolated from metal-contaminated industrial sites linked to mining, metallurgic, and chemical industries [139], and are characterized by multiple metal-resistances [56]. However, *C. metallidurans* isolates are increasingly being recovered from other anthropogenic environments not typified by metal contamination such as different spacecraft-related environments (Chapter 4) and medically relevant sources such as patients with cystic fibrosis [142] and human cerebrospinal fluid (Appendix A). Recently, a first case of invasive infection by *C. metallidurans* was reported [143]. Results described in Chapter 4 showed that *C. metallidurans* strains isolated from different sources of the potable water management system of the ISS were able to tolerate silver concentrations higher than concentrations measured in the ISS potable water. Moreover, isolates were able to survive during a long time-period in water supplemented with silver nitrate. All isolates contain a number of systems that are putatively involved in silver detoxification, facilitating their survival in these water systems.

In this study, the silver resistance mechanisms of *C. metallidurans* were explored. To this end, independent spontaneous silver resistant mutants of type strain *C. metallidurans* CH34, its plasmidless derivative AE104 and *C. metallidurans* NA4, isolated from the Russian condensate recycle system SRV-K aboard the ISS, were obtained. The involved mechanisms and underying genetic circuit was studied in detail.

5.2 Materials and Methods

5.2.1 Bacterial strains, media, plasmids and culture conditions

C. metallidurans CH34, its plasmidless derivative AE104 and *C. metallidurans* NA4, isolated from the Russian condensate recycle system SRV-K aboard the ISS, were cultured in Tris salt mineral medium (MM284) supplemented with 0.2% (wt/vol) gluconate as carbon source [169]. Liquid cultures were grown in the dark at 30°C on a rotary shaker at 150 rpm. *E. coli* strains were grown in LB medium at 37°C. When appropriate, media were supplemented with antibiotics at the following concentrations: kanamycin (50 µg/ml for *E. coli* or 1500 µg/ml for *C. metallidurans*), chloramphenicol (30 µg/ml), tetracycline (20 µg/ml) and ampicillin (100 µg/ml). All strains and plasmids used in this study are presented in Table 5.1.

Table 5.1: Bacterial strains and plasmids used in this study.

Strain/Plasmid	Relevant genotype or description	Reference
Escherichia coli		
DG1	*mcrA* Δ(*mrr-hsdRMS-mcrBC, modification-, restriction-*) Φ80*LacZ* Δ*M15* Δ*LacX74 recA1 araD139* Δ(*ara-leu*)*7697 galU galK rpsL endA1 nupG*	Eurogentec, Belgium
BL21 (DE3)	F^-, *ompT, gal, dcm, lon, hsdS*$_B$($r_B^- m_B^-$) λ(DE3 *[lac, lacUV5-T7, gene 1, ind1, sam7, nin5*])	Novagen, Germany
C. metallidurans		
CH34^T	Decantation tank of Belgian Zinc factory	[164]
AE104	Plasmidless derivative of *C. metallidurans* CH34	[169]
NA4	Water sample, ISS SRV-K filter reactor effluent returned on Soyuz 10S (2004) (original code: 0502478-1)	[167]
CH34M1	*C. metallidurans* CH34 spontaneous silver resistant mutant, Ag^R	This study
CH34M2	*C. metallidurans* CH34 spontaneous silver resistant mutant, Ag^R	This study
AE104M	*C. metallidurans* AE104 spontaneous silver resistant mutant, Ag^R	This study
NA4M	*C. metallidurans* NA4 spontaneous silver resistant mutant, Ag^R	This study
NA4Δ*agrRS*	*C. metallidurans* NA4 *agrRS*::*tet*, Tc^R	This study
NA4Δ*agrS*	*C. metallidurans* NA4 *agrS*::*tet*, Tc^R	This study
NA4Δ*mmmQ*	*C. metallidurans* NA4 *mmmQ*::*tet*, Tc^R	This study
NA4Δ*czcL*	*C. metallidurans* NA4 *czcL*::*tet*, Tc^R	This study
NA4MΔ*agrRS*	*C. metallidurans* NA4M *agrRS*::*tet*, Tc^R	This study

NA4MΔ*agrS*	*C. metallidurans* NA4M *agrS*::*tet*, Tc^R	This study
NA4MΔ*mmmQ*	*C. metallidurans* NA4M *mmmQ*::*tet*, Tc^R	This study
NA4MΔ*czcL*	*C. metallidurans* NA4M *czcL*::*tet*, Tc^R	This study
Plasmids		
pK18*mob*	pMB1 ori, *mob*$^+$, *lacZ*, Km^R	[207]
pBBR1MCS-2	pBBR1 ori, *mob*$^+$, *lacZ*, *Km*^{R}	[208]
pPROBE-TT	pBBR1 ori, *mob*$^+$, promoterless *gfp*, Tc^R	[209]
pPROBE-TT'	pBBR1 ori, *mob*$^+$, promoterless *gfp*, Tc^R, reversed MCS of pPROBE-TT	[209]
pBAD33	p15A ori, P_{araBAD}, *araC*, Cm^R	[210]
pLATE31	pMB1 ori, *lacI*, rrnBT1-T2 transcription terminator, *lacO*, T7 RNA polymerase promoter, C-terminal polyhistidine tag, P_{tet} in opposite direction of T7 promoter, T7 terminator, Amp^R	Thermo Scientific, Belgium
pSCK1	*agrRS* gene region of *C. metallidurans* NA4 in pK18*mob*, Km^R	This study
pSCK2	*mmmQ* - *czcL* gene region of *C. metallidurans* NA4 in pK18*mob*, Km^R	This study
pSCK3	*agrRS*::*tet* in pK18*mob*, Km^R, Tc^R	This study
pSCK4	*agrS*::*tet* in pK18*mob*, Km^R, Tc^R	This study
pSCK5	*mmmQ*::*tet* in pK18*mob*, Km^R, Tc^R	This study
pSCK6	*czcL*::*tet* in pK18*mob*, Km^R, Tc^R	This study
pBBR-*agrRS*	*agrRS* of *C. metallidurans* NA4 in pBBR1MCS-2, Km^R	This study
pBBR-$agrRS_M$	*agrRS* of *C. metallidurans* NA4M in pBBR1MCS-2, Km^R	This study
pBBR-*mmmQ*	*mmmQ of C. metallidurans* NA4 in pBBR1MCS-2, Km^R	This study

pPTT-*agrR*	Promoter region *agrR* of *C. metallidurans* CH34 in pPROBE-TT, Tc^R	This study
pPTT-*czcR*$_2$	Promoter region *czcR*$_2$ of *C. metallidurans* CH34 in pPROBE-TT, Tc^R	This study
pPTT-*mmmQ*	Promoter region *mmmQ* of *C. metallidurans* CH34 in pPROBE-TT, Tc^R	This study
pPTT-*czcL*	Promoter region *czcR*$_2$ of *C. metallidurans* CH34 in pPROBE-TT', Tc^R	This study
pPTT-*agrA*	Promoter region *agrR* of *C. metallidurans* CH34 in pPROBE-TT', Tc^R	This study
pBAD-*agrRS*	*agrRS* of *C. metallidurans* CH34 in pBAD33, Cm^R	This study
pBAD-*agrR*	*agrR* of *C. metallidurans* CH34 in pBAD33, Cm^R	This study
pBAD-*agrRS*$_M$	*agrRS* of *C. metallidurans* AE104M in pBAD33, Cm^R	This study
pBAD-*czcR*$_2$*S*$_2$	*czcR*$_2$*S*$_2$ of *C. metallidurans* CH34 in pBAD33, Cm^R	This study

(tet) tetracycline, (Ag^R) silver resistant, (Km^R) kanamycine resistant, (Tc^R) tetracycline resistant, (Cm^R) chloramphenicol resistant, (Amp^R) ampicillin resistant, (P_{araBAD}) arabinose inducible promoter, (P_{tet}) tetracycline regulated promoter

5.2.2 Generation of spontaneous silver resistant mutants

Spontaneous silver resistant mutants of *C. metallidurans* CH34, its plasmidless derivative AE104 and *C. metallidurans* NA4 were generated by exposure to a toxic concentration of $AgNO_3$ (Table 5.2).

Table 5.2: Spontaneous silver resistant mutants of *C. metallidurans*

Name	Parent strain	Selected on
CH34M1	*C. metallidurans* CH34	LB agar + 0.5 mM $AgNO_3$
CH34M2	*C. metallidurans* CH34	LB agar + 2 mM $AgNO_3$
AE104M	*C. metallidurans* AE104	MM284 + 3 µM $AgNO_3$
NA4M	*C. metallidurans* NA4	MM284 + 8 µM $AgNO_3$

5.2.3 Metal ion resistance

A stationary phase culture (OD_{600} of ca. 1, representing 10^9 CFU/ml) of each strain grown in MM284, was diluted 100-fold in 2 ml MM284 medium with different concentrations of the metals of interest. The lowest concentration that inhibits visible growth was defined as MIC. The MIC values were determined for the following metal solutions: $AgNO_3$, $CdCl_2$, $CoCl_2$, $CuSO_4$, $ZnSO_4$, $NiCl_2$, KCr_2O_4, Cl_4NA_2Pd and $HAuCl_4$.

5.2.4 Transmission electron microscopy

Dr. Peter Baatsen from the electron microscopy facility of VIB/KULeuven performed transmission electron microscopy (TEM) analysis on mutant *C. metallidurans* AE104M after growth in the presence of 80 µM $AgNO_3$. The cells were pelleted at 10,000 g for 5 min, washed twice with 10 mM $MgSO_4$, and resuspended in 1 ml $MgSO_4$ (10 mM). A drop of each sample was spotted onto a carbon-coated copper mesh TEM grid and dried in a vacuum. The grid was inserted into the TEM and pictures were recorded.

5.2.5 Gene expression analysis

Gene expression in the different spontaneous silver resistant mutants was compared with the parent strain in basic growth conditions. To this end, 3 independent stationary phase cultures of *C. metallidurans* CH34, AE104, NA4 and the spontaneous silver resistant mutants CH34M1, CH34M2, AE104M and NA4M, were diluted 1/500 in 25 ml MM284. These subcultures were allowed to grow until a cell density of 5 x 10^8 CFU/ml (OD_{600} = 0.5) was reached. Each culture was fractionated in 2 ml portions, and cells were harvested by centrifugation for 2 min at 10,000 g. Bacterial pellets were flash frozen by immersion into liquid nitrogen and were kept frozen at -80°C at all times. Microarrays were based on the genome of *C. metallidurans* CH34. RNA extraction, labelling and hybridization, microarray spotting, scanning and data analysis was performed according to the work of [144].

5.2.6 Illumina whole genome sequencing

Whole genome (re)sequencing was performed by BaseClear (Leiden, The Netherlands), and comprised of a 50 bp paired-end sequencing approach with 300 bp insert size on the Illumina GAIIx platform.

5.2.7 General cloning procedures

Standard molecular biology procedures were employed during this study, unless mentioned specifically. All oligonucleotides in this study were supplied by Eurogentec (Seraing, Belgium) and are listed in Table 5.3.

Table 5.3: Oligonucleotides used in this study. Restriction sites introduced for cloning are underlined.

Primer name	Primer Sequence from 5' to 3'
FW1	CATGGGATCCGGAAGGAAAAATGTCTGTCG
REV1	AGTCGAATTCCTTCATGTTTTCATCCTCAGC
FW2	GACTGGATCCATTGCTTCCGTCAATTCG
REV2	GATCGAATTCTGCGCATGTTGGTTCACT
FW3	GATCGGATCCCTCAGACTCGGACATGACTCAT
REV3	CTAGGAGCTCGATGGTTCGCATCTTGGAAT
FW4	GATCGAATTCACCGTATGGCAGAGGAATTG
REV4	GACTAAGCTTCTTGACCGAGCCATACGAAC
FW5	GATCGGATCCACGCGAGCTACTTCTTCGAG
REV5	CTAGAAGCTTGGTGTTGCTGTCGAAGTTCA
FW6	GACTACTAGTGTTTTCATCCTCAGCTGCACG
REV6	GACTCTTAAGGCAACATCGTCGCTATCCGT
FW7	TCGAACTAGTCAAGACTGTCGGTTCTCAAGGA
FW8	TTATCTTAAGCTTGGAATCCTCTTCGTGA
REV8	GGTCACTAGTTACAGGATGTCGCTCGAT
FW9	CTAGACTAGTGGCGGTTTCAAGTCCAAGTG
REV9	CTAGACTAGTCAGCCAATGATGCCGATACA
FW10	GATCACTAGTTCAGCCCCATACGATATAAG
REV10	TTATCTTAAGTGGAGTGGTGAATCCGTTAG
FW11	GACGATGAGCGCATTGTTAG
REV11	TCAGGGACAGCTTCAAGGAT
FW12	CATGGGATCCGGAAGGAAAAATGTCTGTCG
REV12	TCAGAAGCTTTCAGGTATGCGGAATTGTC
FW13	GATCGGATCCCTCAGACTCGGACATGACTCAT
REV13	CTAGAAGCTTTCAGGCCCCGTCGGTGAACACGTC
FW14	CGATTAAGTTGGGTAACGCC
REV14	ATTAGGCACCCCAGGCTTTA
FW15	GATCTCTAGAGTGCAGCTGAGGATGAAAACAT
REV15	GATCAAGCTTTCAAGACTGTCGGTTCTCAAG
FW17	CTGATCTAGACCGGCTTGGAAGTGAACC
REV17	GATCAAGCTTTTATGCGCCTGCCCTACTG

5.2.8 Construction of plasmids

The *agrRS* and *mmmQ-czcL* gene regions, including 0.5 kb up- and downstream, from *C. metallidurans* NA4 were amplified by PCR (DreamTaq polymerase, Fermentas, Belgium) using the primer pairs FW4-REV4 and FW5-REV5, providing *Eco*RI/*Hin*dIII and *Bam*HI/*Hin*dIII recognition sites, respectively. The amplicons were subsequently cloned in pK18*mob* digested with *Eco*RI/*Hin*dIII and *Bam*HI/*Hin*dIII, respectively. The resulting constructs pSCK1 and pSCK2 were transformed to *E. coli* DG1 electrocompetent cells (Eurogentec, Belgium). Next, inverse PCR was performed with the primers FW6-REV6, FW6-REV7, FW8-REV8, and FW-9-REV9 to amplify the flanking regions of the gene of interest including the pK18*mob* vector. Afterwards, a tetracycline resistance cassette, amplified from pACY184 with primers FW10 and REV10, was cloned as a *Bsp*TI/*Bcu*I fragment in each *Bsp*TI/*Bcu*I digested amplicon. The resulting constructs pSCK3, pSCK4, pSCK5 and pSCK6 were transformed to *E. coli* DG1 electrocompetent cells (Eurogentec, Belgium). All plasmids were confirmed by sequencing with outward tetracycline primers (primer FW11 and REV11).

PCR amplification (DreamTaq polymerase, Fermentas, Belgium) of the genes *agrRS* and *mmmQ* and their promoter region was done on genomic DNA from *C. metallidurans* NA4 and NA4M with the primer pair FW12-REV12 and on the genomic DNA from *C. metallidurans* NA4 with the primer pair FW13-REV13, respectively. Afterwards, these PCR products were cloned as a *Bam*HI/*Hin*dIII fragment in the vector pBBR1MCS-2. The resulting vectors pBBR-*agrRS*, pBBR-$agrRS_M$ and pBBR-*mmmQ* were transformed in *E. coli* DG1 competent cells. Sequences of the plasmids were confirmed with the primers FW14 and REV14.

The genes *agrR*, *agrRS* and *czcR$_2$S$_2$* from type strain *C. metallidurans* CH34 and *agrRS* from mutant AE104M were amplified by PCR (DreamTaq polymerase, Fermentas, Belgium) with primer pairs FW15-REV15, FW15-REV12, FW16-REV16 and FW15-REV12, respectively, providing *Bam*HI/*Hin*dIII recognition sites. These amplicons were subsequently cloned in pBAD33 [211], and transformed to *E. coli* DG1 competent cells resulting in the plasmids pBAD-*agrRS*, pBAD-*agrR*, pBAD-*agrRS*$_M$ and pBAD-*czcR$_2$S$_2$*, respectively.

Transcriptional promoter-*gfp* fusions were constructed according to the following procedure. A ca. 0.3 kb fragment upstream the *agrR*, *czcR$_2$* and *mmmQ* start codon was amplified by PCR (DreamTaq polymerase, Fermentas, Belgium) using the primer pairs FW1-REV1, FW2-REV2 and FW3-REV3, providing *Bam*HI/*Eco*RI, *Bam*HI/*Eco*RI and *Bam*HI/*Xba*I recognition sites, respectively. The amplicons were subsequently cloned into pPROBE-TT [209] containing a promoterless *gfp* and transformed in *E. coli* DG1 competent cells, resulting in the vectors pPTT-*agrR*, pPTT-*czcR$_2$* and pPTT-*mmmQ*. The amplicons of *agrR* and *czcR$_2$* were also cloned in pPROBE-TT' [209], carrying an inversed multiple cloning site compared to pPROBE-TT, consequently providing the promotor region of *agrA* and *czcL* in the vectors pPTT-*agrA* and pPTT-*czcL*, respectively.

5.2.9 Insertion mutagenesis

For insertion mutagenesis, pSCK3, pSCK4, pSCK5 and pSCK6 were conjugated into *C. metallidurans* NA4 and NA4M with *E. coli* HB101 pRK600 as helper. For each mutant, a tetracycline-resistant and kanamycin-sensitive exconjugant was selected, and confirmed being a genuine mutant by PCR and sequencing with outward tetracycline primers (primer FW11 and REV11), yielding NA4Δ*agrRS*, NA4Δ*agrS*, NA4Δ*mmmQ*, NA4Δ*czcL*,

and NA4MΔ*agrRS*, NA4MΔ*agrS*, NA4MΔ*mmmQ*, NA4ΔM*czcL*, respectively.

5.2.10 Complementation

The vectors pBBR1MCS-2, pBBR-*agrRS* and pBBR-$agrRS_M$ were electroporated in insertion mutants NA4Δ*agrRS* and NA4MΔ*agrRS* and selected on MM284 + kanamycin 1500 µg/ml. The vectors pBBR1MCS-2 and pBBR-*mmmQ* were electroporated in the insertion mutant NA4MΔ*mmmQ* and selected on MM284 + kanamycin 1500 µg/ml. The survival of all constructs on LB agar and LB agar supplemented with 0.5 mM $AgNO_3$ was scored. To this end, 100 µl of serial dilutions of an onvernight LB culture (10^9 CFU/ml) were spread on LB agar and LB agar + 0.5 mM $AgNO_3$ plates. After 3 days, colonies on both conditions were counted.

5.2.11 *In vivo* cross-regulation

In order to confirm the possible cross-regulations identified by the phylogenetic footprinting approach, the arabinose inducible expression vector pBAD33 [211] was combined with pPROBE-TT [209], which contains promoterless gfp, in *E. coli* DG1. To this end, electrocompetent cells of the cultures pBAD-*agrRS*, pBAD-*agrR*, pBAD-$agrRS_M$ and pBAD-$czcR_2S_2$, were made. First, 6 ml liquid exponential phase LB cultures of each strain were distributed in 4 tubes containing each 1.5 ml culture. These cultures were washed twice with 300 mM sucrose. Finally, the pellets were pooled in 200 µl sucrose (300 mM). Purified vectors pPTT-*agrR*, pPTT-$czcR_2$, pPTT-*mmmQ*, pPTT-*agrA* and pPTT-*czcL* were electroporated in each electrocompetent culture of pBAD-*agrRS*, pBAD-*agrR*, pBAD-$agrRS_M$ and pBAD-$czcR_2S_2$. In this way, in total 20 different combinations were made. Possible cross-regulations were tested by comparing Gfp production in each construct, either induced or un-induced with 0.2% arabinose. To this

end, overnight LB cultures supplemented with Tc (20 µg/ml) and Cm (30 µg/ml), were diluted 10 times in 2 ml LB with the same antibiotics and with 0.2% arabinose on the one hand and water on the other hand. These cultures were incubated for 6 hours at 30°C and after that, Gfp production was measured by flow cytometry.

5.2.12 Flow cytometry

Flow cytometry was used to measure Gfp production. To this end, an overnight LB culture was diluted 100-fold in 10 mM $MgSO_4$ (filtered with 0.2 µm filter), and analysed with an BD Accuri C6 flow cytometer (BD Biosciences, Belgium). Gfp production was measured with filter FL1 (excitation 488 nm/emission 533/30 nm) and at least 80,000 cells were recorded. The respective cell populations were delimited to eliminate background signals originating from cell debris. All data analysis was performed with the CFlow Software.

5.2.13 Phylogenetic footprinting

A phylogenetic footprinting approach with the promoter region of *agrR* was performed *in silico* by Pieter Monsieurs (SCK•CEN). By combining the output of different motif detection algorithms (MotifSampler, AlignACE, MEME, Weeder and RSAT) followed by a Markov clustering of the output motif models, the regulatory motif of *agrRS* was defined. This model was used for a genome wide screening of all upstream regions in type strain *C. metallidurans* CH34 to identify possible binding sites for AgrR.

5.2.14 MmmQ protein expression and purification

The coding sequence of MmmQ corresponding to the protein with its signal peptide was amplified by PCR using genomic DNA from *C. metallidurans* CH34 as template. A 3C-protease cleavage site was introduced at the C-terminus of MmmQ. The PCR product was cloned into a pLATE31 vector

(Thermo Scientific, Belgium) upstream of a 6 His-tag coding sequence. The pLATE31_*mmmQ* vector was transferred into an *E. coli* strain BL21 (DE3) (Novagen, Germany) for expression. Cells were grown at 37°C in LB medium to an OD_{600nm} of 0.7. Expression was induced by 0.5 mM isopropyl-β-D-1-thiogalactopyranoside (IPTG) for 3 hours and cells were collected by centrifugation at 5,000 g for 15 min at 4°C.

Cell pellets were suspended in chilled purification buffer A (20 mM HEPES pH 8, 0.3 mM NaCl) containing 10 mM imidazole, and protease inhibitors (Complete, Roche, Belgium). Cells were lysed in an EmulsiFlex (Avestin, Germany) at 4°C and incubated with 20 µg/ml DNase for 15 min. Cell debris were removed by centrifugation at 10,000 g for 15 min at 4°C. Supernatant was incubated with Ni-NTA resin (Thermo Scientific, Belgium) for 1 hour at 4°C under gentle agitation. After collecting the flow-through, the resin was washed with chilled purification buffer A containing 10 mM (wash L1) and 40 mM (wash L2) imidazole, respectively. The protein was eluted in the same buffer containing 250 mM imidazole (elutions E1, E2 and E3). The protein sample was loaded onto a PD-10 desalting column (GE Healthcare, Belgium) using storage buffer (20 mM HEPES pH 7.5, 150 mM NaCl). The 6 His-tag was removed by overnight digestion with 3C-protease at 4°C. Sample was fractioned on a Superdex 200 10/300 GL size exclusion column using an ÄKTA purifier system (GE Healthcare, Belgium). This chromatography step was also used to exchange the buffer of the protein sample.

5.2.15 Mass spectrometry

For accurate molecular mass determination, the protein sample was desalted on ZipTipC_{18} (Merck Millipore, Germany) and solubilized in 50% acetonitrile/1% formic acid (v/v). The protein solution was loaded into gold-palladium coated borosilicate nano-electrospray capillaries (Thermo

Scientific, Belgium). Mass spectra were acquired on a Q-Tof Ultima API mass spectrometer (Waters, France), equipped with a Z-spray nano-electrospray source and operating in positive ion mode. Capillary voltages of 1.8 - 2.0 kV and cone voltage of 50 V typically were used. The source temperature was kept at 80°C and the time-of-flight analyser was operated in the V mode. Data acquisition was performed using a MassLynx 4.0 system. The spectra represent the combination of 1-sec scans. The molecular mass was determined after MaxEnt1 deconvolution of the m/z raw data (Waters, France).

For the metal binding experiments, the buffer of protein sample was exchanged to 10 mM ammonium acetate, pH 6.9 by size exclusion chromatography (SEC). The protein was incubated at a final concentration of 5 µM in the presence of Ag^{+} for 10 min at 22°C. Parameters used for binding experiments were set on following values: capillary voltage 1.6 kV, cone voltage 50 V, source block temperature 20°C, pirani pressure 2.2 mbar.

5.2.16 Fourier transform infrared spectroscopy

Prior to Fourier transform infrared spectroscopy (FTIR) analysis, the buffer of the protein sample was exchanged to 5 mM HEPES, pH 7.5 on a Micro Bio-Spin 6 column (Bio-Rad, Belgium). Attenuated total reflection infrared (ATR-FTIR) spectra were obtained at a resolution of 2 cm^{-1} on a Bruker IFS55 FTIR spectrophotometer equipped with a MCT detector. The spectrophotometer continuously was purged with dry air (Whatman, Belgium). Measurements were carried out at 20°C. Thin protein films were obtained by slowly evaporating 1 µl of protein solution on the diamond ATR element under a stream of nitrogen. Spectra represent the average of 256 scans for each time point. For hydrogen/deuterium exchange, nitrogen gas saturated with D_2O was flushed on the sample during 15 min.

MmmQ purification, mass spectrometry and FTIR analysis were performed by Dr. Guy Vandenbussche from ULB.

5.3 Results

5.3.1 Spontaneous silver resistant mutants

Independent spontaneous of *C. metallidurans* CH34, AE104 and NA4 were obtained by exposure to a toxic concentration of $AgNO_3$ (Table 5.2). The MIC values of $AgNO_3$ for the wild-type and mutant strains are presented in Figure 5.1. Mutants CH34M1 and CH34M2 were 4 times more resistant compared to wild-type CH34, mutant AE104M was ± 30 times more resistant than wild-type AE104 and mutant NA4M was ± 10 times more resistant compared to wild-type NA4.

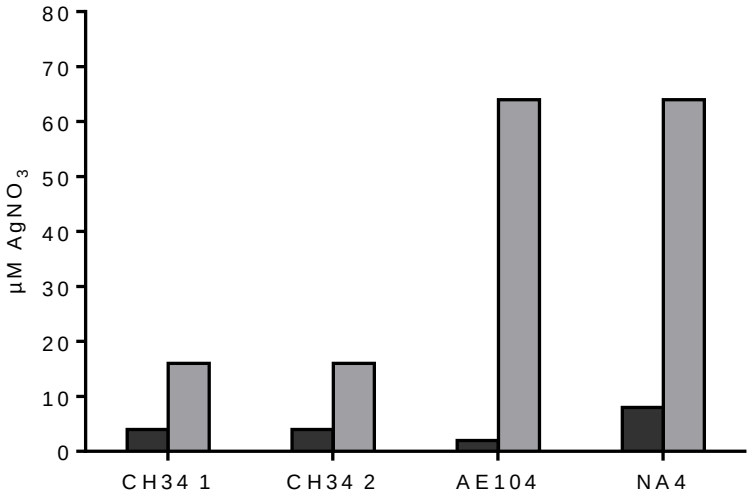

Figure 5.1: MIC of $AgNO_3$ after 7 days for wild-type (dark grey bars) compared to silver mutants (light grey bars) of *C. metallidurans* type strain CH34, its plasmidless derivative AE104 and *C. metallidurans* NA4.

Cross-resistance of the mutants for Cu^{2+}, Zn^{2+}, Cd^{2+}, Co^{2+}, Ni^{2+}, Cr^{2+}, Sr^{2+}, Pd^{2+} and Au^{3+} was tested. No noticeable differences in resistance for those metals were observed, except for Au^{3+} (Figure 5.2). CH34M1 was 4 times less resistant to Au^{3+} compared CH34, while AE104M was 4 times more resistant compared to AE104. For CH34M2 and NA4M, no difference in Au^{3+} resistance compared to respectively CH34 and NA4 was observed.

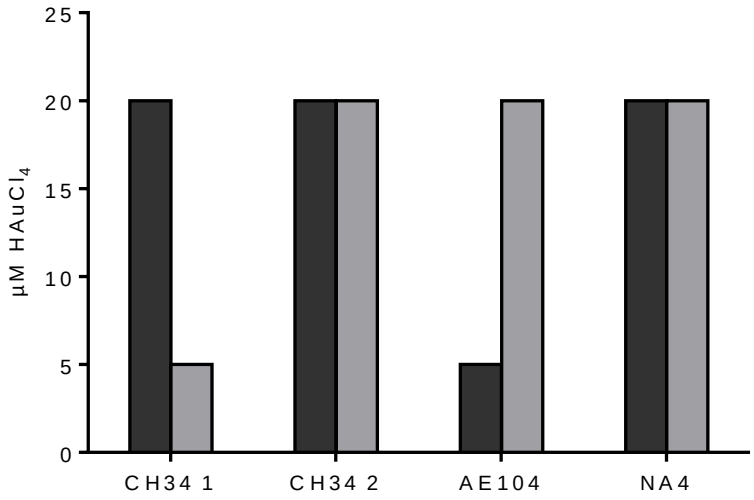

Figure 5.2: MIC of $HAuCl_4$ after 3 days for wild-type (dark grey bars) compared to silver mutants (light grey bars) of *C. metallidurans* type strain CH34, its plasmidless derivative AE104 and *C. metallidurans* NA4.

5.3.2 TEM analysis

TEM analysis on AE104M performed after growth in the presence of 80 µM $AgNO_3$, showed the presence of electron dense granules, putatively indicating that some cells are able to produce Ag nanoparticles (Figure 5.3).

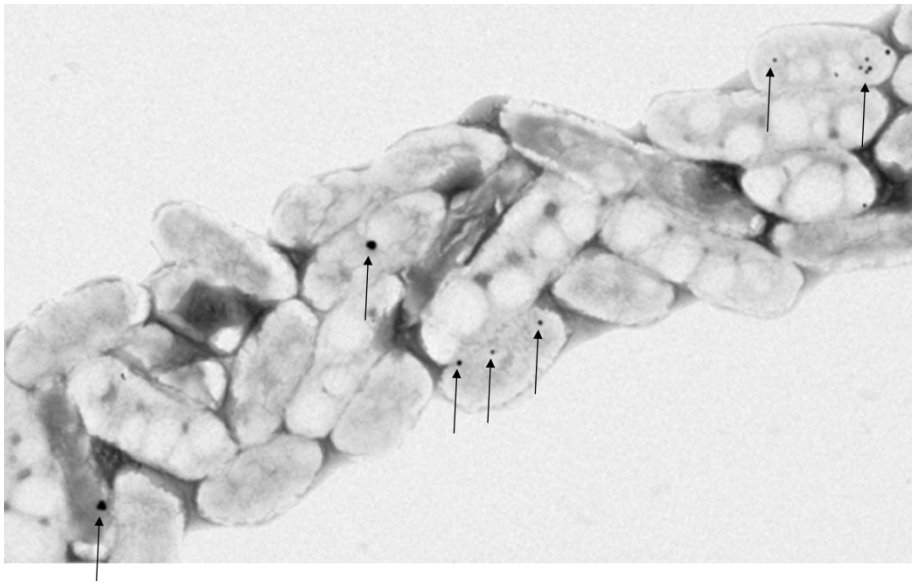

Figure 5.3: TEM picture of *C. metallidurans* AE104M after growth in the presence of 80 µM $AgNO_3$. Putative nanoparticles are pointed by arrows.

5.3.3 Whole genome expression analysis

Whole genome expression analysis of the different silver resistant mutants compared to their respective wild-type strain in basic growth conditions was performed. Genes were considered as differentially expressed as fold change ratios were above 2 or below 0.5 with adjusted P-values below 0.05. In CH34M1, 301 genes were differentially expressed (133 up- and 168 down-regulated), 293 genes (158 up- and 135 down-regulated) in CH34M2, 179 genes (75 up- and 104 down-regulated) in AE104M and 348 genes (204 up- and 104 down-regulated) in NA4M (Figure 5.4). Eight up-regulated genes were common in all mutants, while no common down-regulated genes were found (Table 5.4, Figure 5.4). These genes code for an outer membrane protein, a two-component regulatory system and proteins of unkown function (Table 5.4). The sensor kinase (AgrS) and response regulator (AgrR) of the two-component system are associated with an RND-efflux

pump (AgrCBA) of unknown specificity (see also Figure 2.4). Two other genes, *mmmQ* and *czcL* also belong to a larger gene cluster that is highly conserved among *C. metallidurans* (Figure 5.5).

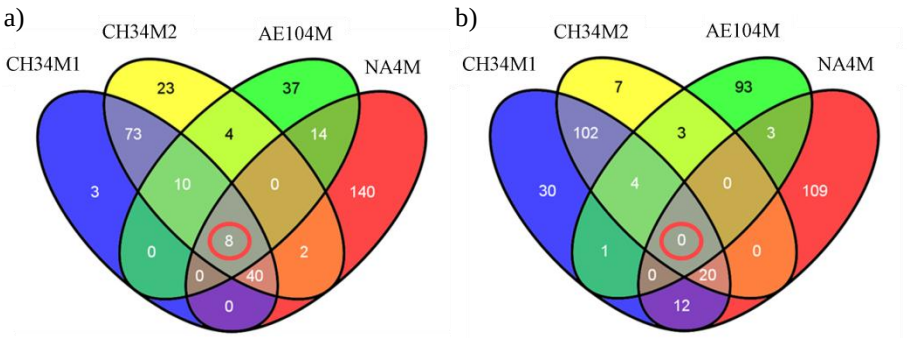

Figure 5.4: Venn diagrams showing the number of common a) up-regulated and b) down-regulated genes in each mutant compared to the other. A red line surrounds the number of common differentially expressed genes between all mutants.

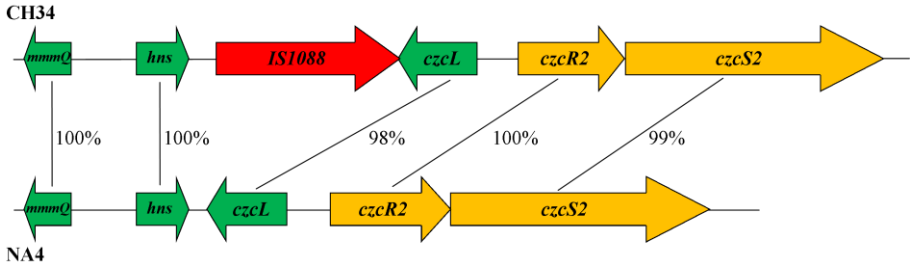

Figure 5.5: Genetic organization of the gene cluster comprising *mmmQ* and *czcL* in *C. metallidurans* CH34 (upper) and *C. metallidurans* NA4 (lower). In CH34, the IS element *IS1088* (red) is located between *hns* and *czcL*. Sequence similarities are shown at protein level.

Table 5.4: Common differentially expressed genes in all mutants. Values represent fold change ratios compared to the wild-type strains.

Locus	**Function**	**CH34M1**	**CH34M2**	**AE104M**	**NA4M**
Rmet_0477	Conserved hypothetical protein, CopQ-like	9.0	9.1	3.9	15.8
Rmet_1751	DNA-binding response regulator, AgrR	78.5	65.4	81.0	54.2
Rmet_1752	signal transduction histidine kinase, AgrS	44.4	38.0	30.4	16.2
Rmet_3571	protein involved in metal response (CopQ-like), MmuQ	23.8	22.0	21.2	2.9
Rmet_4461	protein involved in metal response (CopQ-like), MmmQ	81.0	88.6	106.6	26.2
Rmet_4464	Conserved hypothetical protein, CzcL	5.1	4.9	2.1	2.8
Rmet_4595	Conserved hypothetical protein, CzcI-like	7.7	8.2	3.1	2.7
Rmet_5118	Outer membrane protein (porin), OmpC family	8.6	9.0	5.8	3.6

5.3.4 Confirmation of the gene expression data

Plasmid-borne *gfp* transcriptional fusions to the *agrR*, *mmmQ* and *czcR*$_2$ promoter region were electroporated into NA4 and NA4M and tested for Gfp production by flow cytometry. There was a clear shift in Gfp production in NA4M compared to NA4 for all three promoters (Figure 5.6), confirming the microarray data. For *agrR* and *mmmQ* the NA4M population is a mixture of fluorescent and non-fluorescent cells, which was also observed in colonies on solid medium. For both, the same result was obtained when the experiment started from a fluorescent colony or a non-fluorescent one.

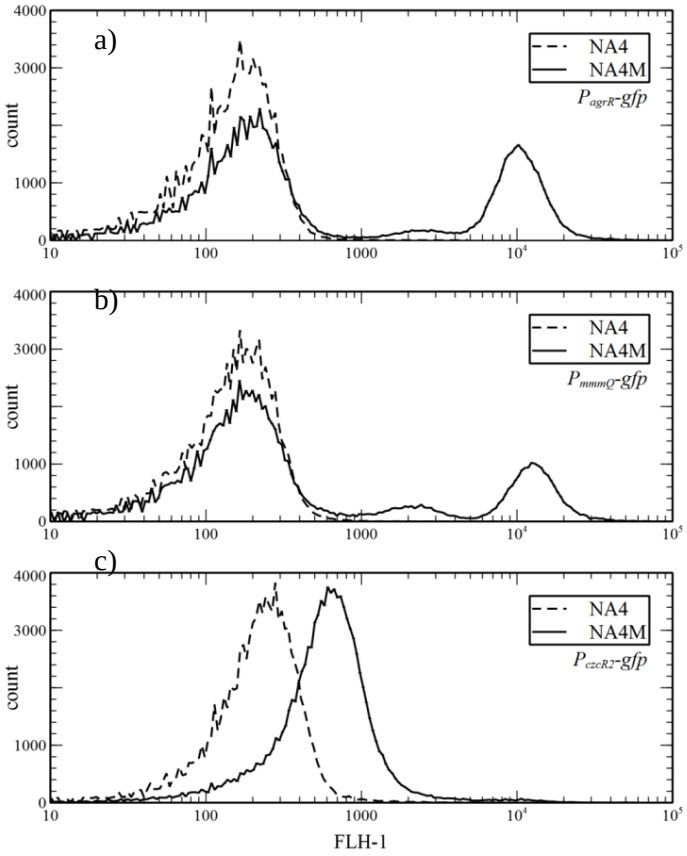

Figure 5.6: Gfp production measured with flow cytometry in mutant NA4M (full line) compared to wild-type NA4 (dotted line) for a) Promoter region *agrR* (pPTT-*agrR*) b) Promoter region *mmmQ* (pPTT-*mmmQ*) and c) Promoter region *czcR*$_2$ (pPTT- *czcR*$_2$).

5.3.5 Whole genome sequencing of mutants

The genomes of CH34M1, CH34M2 and NA4M were sequenced and compared to type strain CH34 and NA4, respectively. In CH34M1, IS*Rme3* was transposed from its original position in the 3' region of *agrS*, while in CH34M2, IS*1086* was transposed from its original position into the 5' region of *agrS* (Figure 5.7). In CH34M1, one additional event caused by IS elements occurred, namely, IS*Rme3* transposed into Rmet_2171 (integrase). In CH34M2, IS*Rme15* transposed in Rmet_2992 (hypothetical protein) and IS*Rme5* in *cupA*. However, none of these three genes was differentially expressed in these mutants. In addition to the mutations caused by IS elements, both CH34M1 and CH34M2 showed insertions of one nucleotide, and single nucleotide polymorphisms in coding or promoter regions. CH34M1 and CH34M2 have 15 mutations in common, however, none of the affected genes are differentially expressed in both mutants. In NA4M, three mutations caused by an IS element or transposon occurred but either in genes that were not differentially expressed in all *C. metallidurans* mutants or in genes that are absent in CH34M1 and CH34M2. Screening for point mutations showed one C in T substitution in *agrS*, which resulted in an arginine to cysteine substitution at residue 412 (Figure 5.7).

Thus, all resequenced mutants showed mutations in *agrS*. Also in AE104M, analysis of the *agrRS* region showed an insertion of IS*Rme3* in *agrS*. In addition to *agrS*, the efflux pump coded by *agrCBA* is also affected in all mutants. In CH34M1, there is a duplication of 7 bp in the promoter region of *agrCBA*, affecting the expression of *agrCBA*. In CH34M2, there is a 4 bp duplication in *agrA*, resulting in an early stop codon and thus disfunctional AgrA and in NA4M, *agrA* is disrupted by a transposase (also present in wild-type NA4) (Figure 5.7).

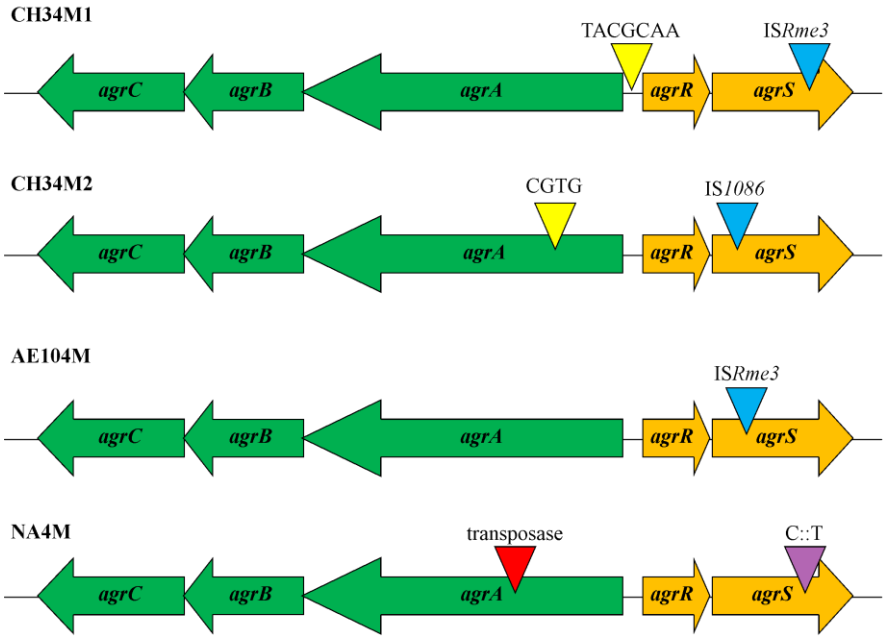

Figure 5.7: Schematic representation of all mutations that occurred in the *agrCBARS* gene cluster. Mutations occurred by IS elements are presented as blue triangles, duplications are presented as yellow triangles and sinlge nucleotide substitutions are shown as purple triangles. The transposase in NA4M (red triangle) is already present in wild-type NA4.

5.3.6 Influence of *agrRS*, *agrS*, *mmmQ* and *czcL* knockout on silver resistance

All experiments were performed with AE104M and NA4M but only the results of NA4M are presented in detail, as it is the most relevant strain for this study. To investigate the role of the upregulated genes, *agrRS*, *agrS*, *mmmQ* or *czcL* were deleted in NA4M. In all of these deletion mutants, silver resistance decreased again to wild-type level or less (NA4MΔ*agrRS*) (Figure 5.8). As control, a random gene was deleted (*acxR*, coding for an alcohol dehydrogenase), showing no effect on silver resistance (data not shown).

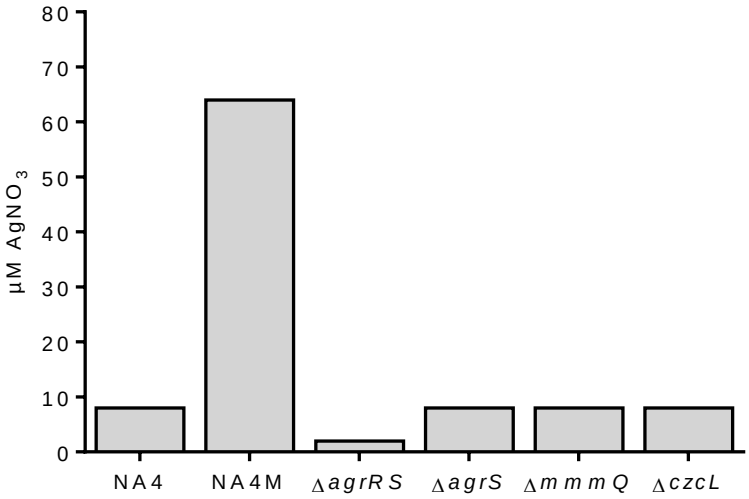

Figure 5.8: MIC for $AgNO_3$ after 7 days for NA4, NA4M, NA4MΔ*agrRS* (Δ*agrRS*), NA4MΔ*agrS* (Δ*agrS*), NA4MΔ*mmmQ* (Δ*mmmQ*) and NA4MΔ*czcL* (Δ*czcL*).

5.3.7 Complementation of *agrRS* and *mmmQ*

NA4MΔ*agrRS* and NA4MΔ*mmmQ* were complemented with pBBR-$agrRS_M$ and pBBR-*mmmQ*, respectively, but silver resistance could not be restored for pBBR-$agrRS_M$. By constrast, silver resistance could be restored after plasmid-mediated complementation with *mmmQ* (Figure 5.9). This graph shows that the number of NA4M surviving 0.5 mM $AgNO_3$ is not equal to the unexposed control. Plasmid pBBR-*mmmQ* is partially able to complement silver resistance, although the number of NA4MΔ*mmmQ*_pBBR-*mmmQ* surviving 0.5 mM $AgNO_3$ is approximately 1000 fold less compared to NA4M.

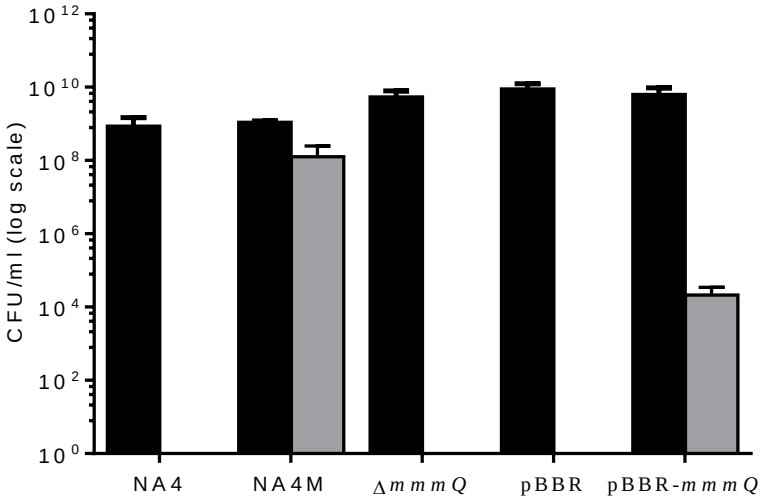

Figure 5.9: Survival of NA4, NA4M, NA4M*ΔmmmQ* (*ΔmmmQ*), NA4M*ΔmmmQ*_pBBR (pBBR) and NA4M*ΔmmmQ*_pBBR-*mmmQ* (pBBR-*mmmQ*) on LB agar plates (black bars) and on LB agar plates supplemented with 0.5 mM $AgNO_3$ (grey bars). Values represent the average of three independent experiments.

In addition, for plasmid-mediated *mmmQ* complementation, the level of *mmmQ* expression was measured in each construct with RT-PCR. This clearly showed up-regulation of *mmmQ* expression in NA4M compared to NA4 (confirmation of microarray and data transcriptional *gfp* fusion), loss of *mmmQ* expression in NA4MΔ*mmmQ* and NA4MΔ*mmmQ*_pBBR, and restoration of *mmmQ* expression levels in NA4MΔ*mmmQ*_pBBR-*mmmQ* to NA4M levels (Figure 5.10), confirming the important role of *mmmQ* in the adaptive response to silver toxicity.

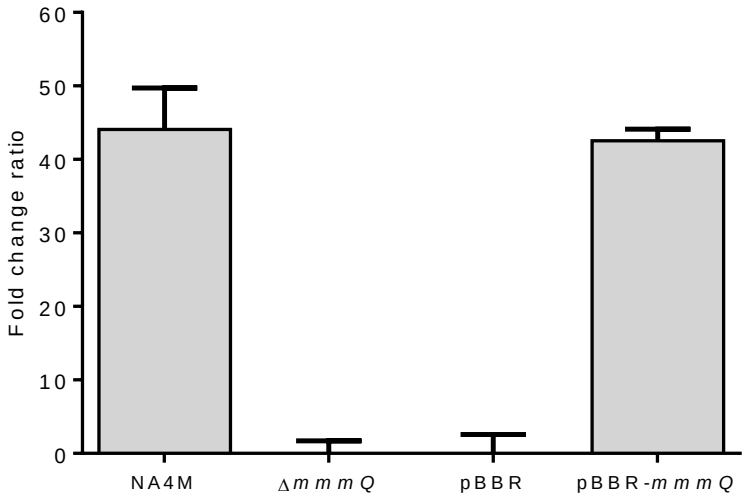

Figure 5.10: Expression level of *mmmQ* in the different strains. Expression levels are normalized compared to expression levels of *uvrD* and fold change ratios between NA4M, NA4MΔ*mmmQ*, NA4MΔ*mmmQ*_pBBR, NA4MΔ*mmmQ*_pBBR-*mmmQ* and NA4 are presented.

5.3.8 Phylogenetic footprinting

To detect possible binding sites of the transcription factor AgrR, a phylogenetic footprinting approach was followed. In first instance, the promoter region of *agrR* from closely and more distantly related species was compared by several motif detection tools, followed by clustering analysis on the outcome of the models. In this way, a possible regulatory motif for *agrR* was found (Figure 5.11). A clear similarity was observed between the regulatory motif of *agrR* and the putative motif found in other transcriptional involved in metal resistance, such as $czcR_2$, $copR_2$ (both chromosomally located) and $copR_1$ (plasmid located).

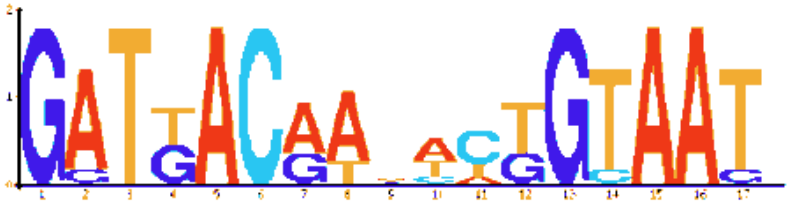

Figure 5.11: Logo of the proposed regulatory motif found of *agrR*.

In a second step, this regulatory motif was used to perform a genome-wide screening of all upstream regions in *C. metallidurans* CH34 to detect possible binding sites for AgrR. This illustrated next to a possible binding site for AgrR upstream its own associated efflux pump *agrCBA*, possible binding sites upstream genes associated with metal resistance (e.g. *copC*$_1$*B*$_1$*A*$_1$*R*$_1$*S*$_1$, *czcR*$_2$*S*$_2$, *chrF*$_2$, *chrA*$_2$, *chrB*$_2$, *czcM*, *czcE)*. In addition, possible binding sites were discovered in the promoter region of 4 genes, commonly up-regulated in all mutants, namely, Rmet_0477, Rmet_4461 (*mmmQ*), Rmet_4464 (*czcL*) and Rmet_4595 (*czcI*$_2$).

5.3.9 *In vivo* cross-regulation

In addition to the theoretical predicted interactions of AgrR with other genes, it was tested if this cross-regulation could be confirmed *in vivo*. To this end, combinations were made in *E. coli* DG1 with *agrR*, *agrRS* and *agrRS* of AE104M under control of an arabinose inducible promoter in pBAD33 and *gfp* under control of the promoter region of *agrA*, *agrR*, *mmmQ*, *czcL* and *czcR*$_2$ in pPROBE-TT and pPROBE-TT'. There was clear Gfp production observed when *agrRS* was combined with the promoter region of *mmmQ* (Figure 5.12). When only *agrR* was combined with *mmmQ* promoter region, Gfp production could also be observed although less pronounced. However, this indirectly indicates the binding of AgrR to *mmmQ*. No other positive combinations were observed.

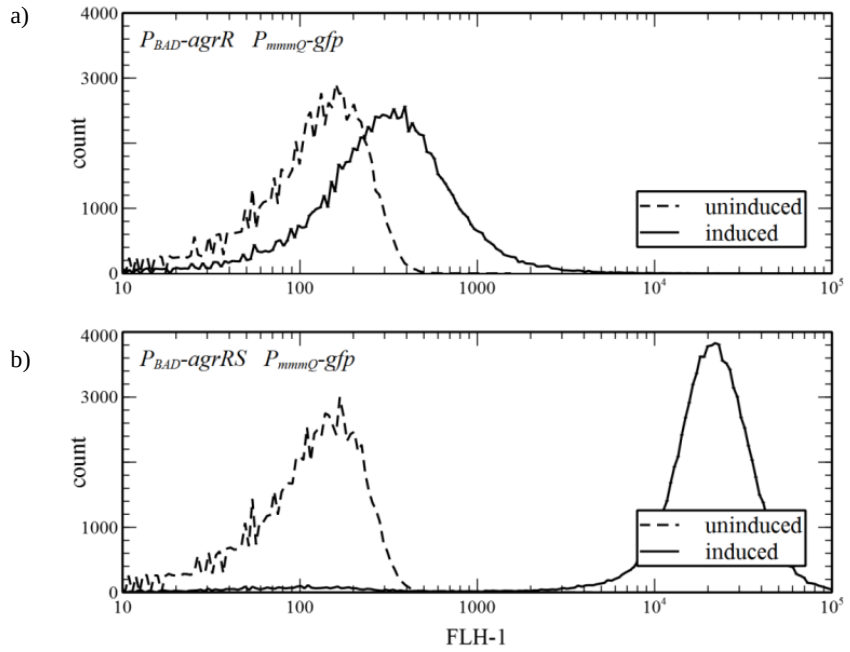

Figure 5.12: *In vivo* cross-regulation in *E. coli* DG1 between a) pBAD-*agrR* and pPTT-*mmmQ* and b) pBAD-*agrRS* and pPTT-*mmmQ*. Gfp production is compared between uninduced (dashed line) and induced (full line) samples.

5.3.10 MmmQ protein purification

Recombinant 6His-MmmQS was overexpressed in *E. coli* BL21 (DE3). The protein was purified by immobilized metal affinity chromatrography (IMAC) on a Ni-NTA column (Thermo Scientific, Belgium). The 6His-tag was removed by 3C-protease digestion. The different purification fractions were analysed by SDS-PAGE, and showed that MmmQ migrated on SDS-PAGE at a higher apparent molecular mass than expected (Figure 5.13).

After cleavage with 3C-protease of the 6His-tag, MmmQ was separated from the other components (protease and cleaved 6His-tag) by SEC (Figure 5.14). This last purification step was also used to exchange the purification buffer for 10 mM ammonium acetate, pH 6.75 that is compatible with mass spectrometry measurements.

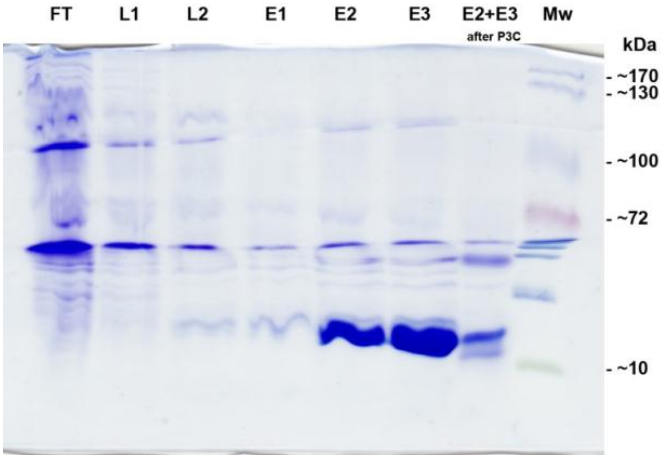

Figure 5.13: Analysis by SDS-PAGE of the different IMAC purification fractions of recombinant MmmQ. Lane FT: flow-through; lane L1: wash with purification buffer A containing 10 mM imidazole; lane L2: wash with purification buffer containing 40 mM imidazole; lanes E1, E2, and E3: sequential elution with purification buffer A containing 250 mM imidazole; lane E2+E3 after P3C: mixture of fractions E2 and E3 after cleavage with 3C-protease of the 6His-tag; lane Mw: molecular mass standards.

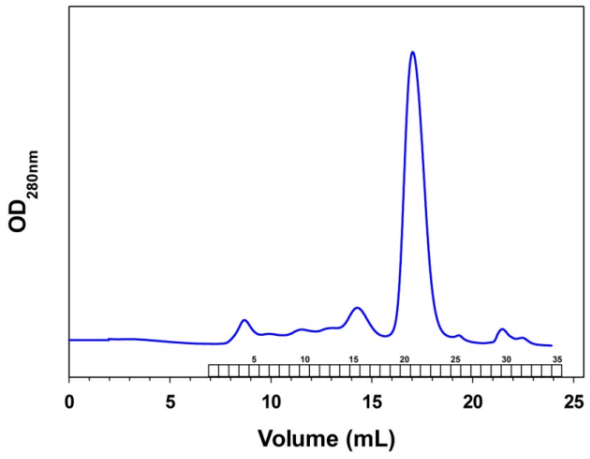

Figure 5.14: Size exclusion chromatogram of MmmQ on a SDX-200 column in 10 mM ammonium acetate, pH 6.75. The small bars numbered from 1 to 35 represent the different collected fractions. The protein eluted as a symmetric peak mainly in the fractions 20 to 22.

5.3.11 MmmQ Mass spectrometry analysis

The purified MmmQ was analysed by mass spectrometry to assess the integrity of the protein. The experimental mass (7328.7 Da) determined by electrospray ionization-mass spectrometry (ESI-MS) was in good agreement with the theoretical molecular mass (7328.9219 Da) calculated from MmmQ sequence devoid of its sequence signal as predicted by the SignalP 4.1 server (Figure 5.15).

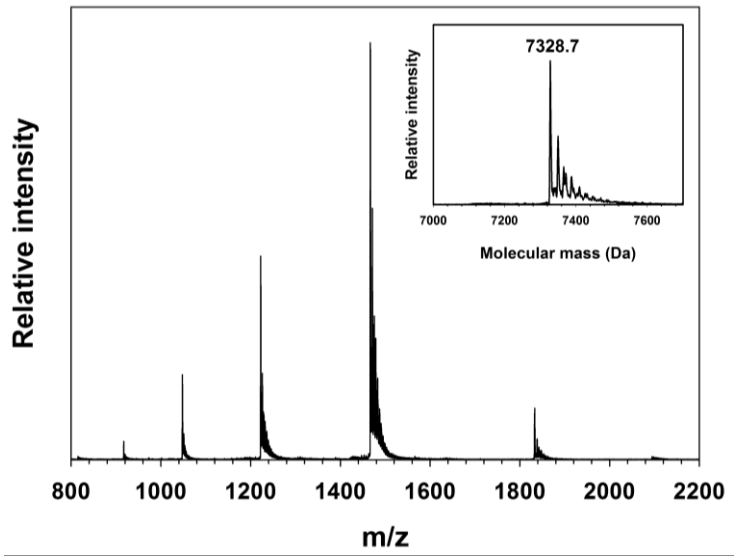

Figure 5.15: ESI-MS spectrum of purified MmmQ (SEC fraction 21). The inset represents the MaxEnt1 deconvolution of the m/z raw data.

The binding of silver ions on MmmQ was monitored by mass spectrometry under non-denaturing conditions to preserve the potential protein-ion complexes. Mass spectra were recorded after incubation of the protein with 1 or 2 molar equivalents of Ag^+ (Figure 5.16). No mass shift was observed upon addition of Ag^+ indicating that no specific binding of silver ions had occurred.

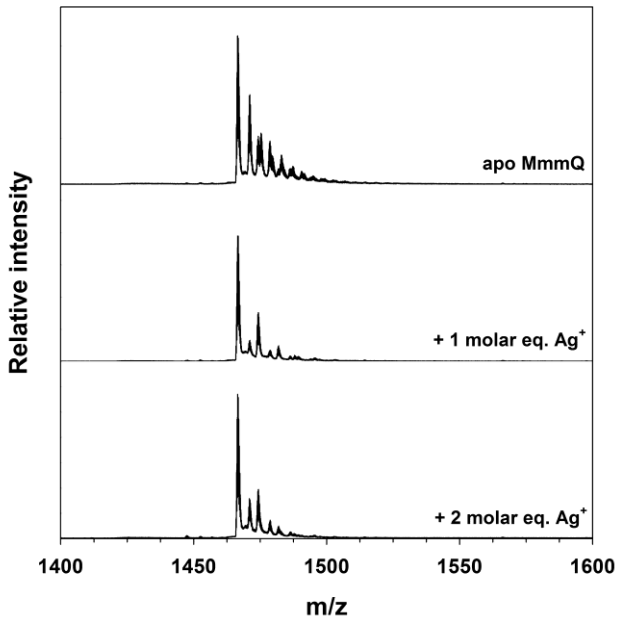

Figure 5.16: ESI-MS spectra of apo-MmmQ, and of MmmQ incubated with 1 or 2 molar equivalents of Ag^+. Intensities were normalized.

5.3.12 Fourier transform infrared spectroscopy

The structure of purified MmmQ was determined by ATR-FTIR. This technique is based on the changes that occur in a totally, internally reflected infrared beam when the beam comes into contact with a sample. For this purpose, the protein sample buffer was exchanged for 5 mM HEPES, pH 7.5 (Figure 5.17). The two major protein absorption bands Amide I and Amide II are observed in the region 1800-1400 cm^{-1}. The Amide I band is associated to the υ(C=O) vibration and Amide II results from δ(N-H) and υ(C-N) vibration of the peptide bond [212]. The shape of these bands are closely related to the secondary structure of the protein. The maximum of the Amide I band was observed at 1650 cm^{-1} but shifted to 1639 cm^{-1} upon 15 min hydrogen/deuterium exchange. In addition, during the H/D exchange, the Amide II band rapidly shifted from 1537 cm^{-1} to 1452 cm^{-1}. This fast

exchange and the position of the Amide I band maximum after H/D exchange indicate that the protein adopts a random-coil conformation.

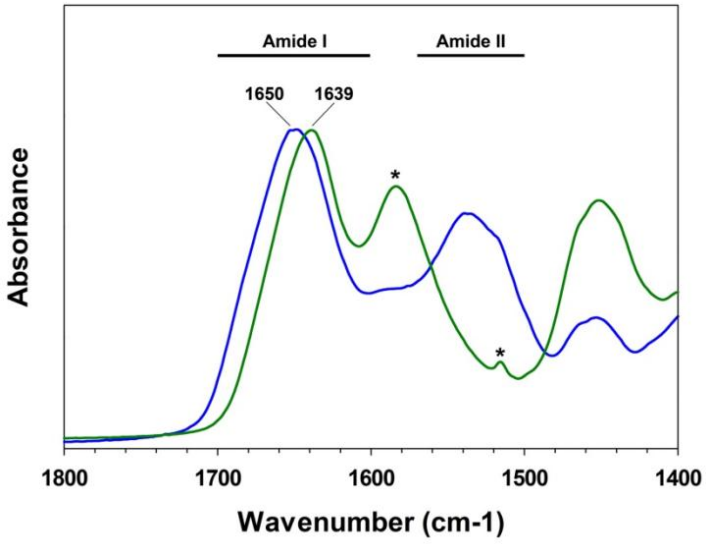

Figure 5.17: ATR-FTIR spectra of purified MmmQ (SEC fraction 21) before (blue) and after (green) 15 min hydrogen/deuterium exchange in 5 mM HEPES, pH 7.5. The spectra are represented in the 1800-1400 cm^{-1} region and the intensities were normalized. The stars indicate contribution of amino acid lateral chains.

5.4 Discussion

Independent silver resistant mutants of type strain *C. metallidurans* CH34, its plasmidless derivative AE104 and NA4, an isolate from the potable water system aboard the ISS, were obtained by exposure to a toxic silver concentration. The level of resistance is 4 to 30 fold higher compared to their parent strain (Figure 5.1). The high resistance could be facilitated by the formation of electron dense granules observed in AE104M after growth in the presence of $AgNO_3$ (Figure 5.3). This putatively indicates that some cells are able to accumulate silver ions and reduce them to Ag nanoparticles, making them unable to exert their action.

In *C. metallidurans* CH34, different silver resistance mechanisms have been identified. They comprise two RND-driven efflux pumps encoded by the *silDCBA* and *cusDCBAF* operons located respectively on plasmid pMOL30 and the chromid, and a P-type ATPase efflux pump encoded by the *cupRAC* operon located on chromosome 1 [56]. However, the *silDCBA* operon is not present in *C. metallidurans* AE104 (and AE104M) and whole-genome expression profiling indicated that none of these determinants are up-regulated in all mutants (compared to their parent strain). Furthermore, whole-genome expression profiling and resequencing indicated that *agrS*, coding for a histidine kinase of the two-component efflux system AgrRS, was affected in all mutants, either via disruption by an IS element or by point mutation. Furthermore, *agrS* and *agrR* were together with 6 other genes commonly upregulated in all mutants (compared to their parent strain) and deletion of *agrRS* resulted in complete loss of silver resistance (Figure 5.8).

The *agrRS* operon codes for a typical two-component system, which comprises a histidine kinase AgrS that act as sensor and transmits the signal through a phosphorylation cascade to the cytoplasmic transcriptional response regulator AgrR. These systems play an important role in the ability of organisms to adapt to specific environments, as they are able to modify gene expression levels in response to changing stimuli [213]. In type strain CH34, there are 56 two-component pairs of adjacent genes distributed in its genome, of which several are involved in metal resistance [56]. Untill now, the two-component system AgrRS was not linked to metal resistance [144]. The system is associated with an RND-driven efflux pump AgrCBA of which the specificity is not yet known as it harbours characteristics of both heavy metal efflux and hydrophilic and amphiphilic compounds efflux systems. Nevertheless, our results indicated that this efflux pump is not involved in the observed increase in silver resistance as it is either not differentially expressed or inactivated by mutation.

The effect of *agrS* mutation is not yet elucidated, however, it can influence the phosphorylation state of AgrR thereby affecting its activation. Similarly, a silver resistant mutant of *E. coli* contained a single point mutation in *cusS*, encoding the sensor kinase of the two-component system CusRS, which plays a role in silver resistance. This mutation (T17P) locks CusS in an autophosphorylation state, resulting in constitutive and Ag^+ independent activation of *cusCFBA* [126]. The fact that IS elements are involved, showed that mobile genetic elements (MGEs) are of importance in the adaptation to different stressors and reflects the flexibility of *C. metallidurans* in its adaptation to changing environments.

A phylogenetic footprinting approach was performed with the promoter region of *agrRS* to identify the regulatory motif of AgrR (Figure 5.11). This showed similarity of the AgrR regulatory motif to that of other transcriptional regulators involved in metal resistance (such as $CzcR_2$, $CopR_1$ and $CopR_2$). Screening the genome of CH34 identified possible AgrR binding sites (among other) in the promoter region of *agrA* and *czcR*$_2$ but also in the promoter regions of *mmuQ*, *mmmQ* and *czcL*. The latter three were commonly upregulated in all mutants (compared to their parent strain), with *mmmQ* upregulated the most in AE104M and NA4M. *In vivo* experiments indirectly indicated possible cross-regulation between AgrR and *mmmQ* in *E. coli* (Figure 5.12). A complex cross-regulation was also observed in *P. aeruginosa* after growth in the presence of 5 mM $ZnCl_2$. Exposure to Zn^{2+} resulted in the induction of the two-component system *czcRS*. CzcR then promotes expression of the metal efflux pump *czcCBA*, and als negatively regulates the expression of *oprD*, a gene coding for a porin through which carpabenems (class of β-lactam antibiotics) enter the cells [214, 215]. In addition, CzcR is involved in the regulation of genes involved in virulence processes and biofilm formation [215].

The mmmQ gene codes for an uncharacterized small protein and belongs to a unique group of ca. 20 homologous proteins (including MmuQ and Rmet_0477) distributed over the genome of *C. metallidurans*. These small proteins, which range in size from 69 to 165 amino acid residues and carry a distinctive signal peptide, are apparently conserved only in *Cupriavidus* and *Ralstonia* species as no homologs have been found in current databases [56]. Previous studies showed that the expression of many of these small genes is induced by exposure to heavy metals [216]. Deleting the *mmmQ* gene resulted in loss of the increased silver resistance, indicating that it has an important role in the resistance mechanism. Although, preliminary experiments indicated that purified MmmQ was unable to bind Ag^+ *in vitro* (Figure 5.16), silver resistance could be restored after plasmid-mediated *mmmQ* complementation (Figure 5.9). Structure analysis of MmmQ showed that it is an intrinsically disordered protein and consequently adopts a random-coil conformation (Figure 5.17). Such disordered proteins are common in nature, although more widespread in eukaryotes compared to prokaryotes [217]. They appear to play a role in a wide range of biological processes, such as regulation, recognition, cell signalling and cell cycle thereby complementing the function of ordered proteins and structured domains [218]. In the presence of the right partner molecule, the protein often undergoes induced folding and acquires a well-defined 3D-structure [217]. Therefore, if MmmQ would need to bind Ag^+ to exert its role in the increased silver resistance, it could be that another protein or factor is necessary to facilitate binding of Ag^+ to MmmQ. For instance, the protein coded by *czcL*, for which expression is up-regulated in all mutants and its promoter carries a predicted AgrR biding site. Furthermore, silver resistance was lost when the gene was inactivated by insertion mutagenesis (Figure 5.8). CzcL is a periplasmic protein with uncharacterized function and homologs seem to be conserved only in a few *Cupriavidus* and *Ralstonia* species. However, at this moment, the precise role of MmmQ and CzcL in

the silver resistance mechanism still needs to be elucidated and more research about possible interactions of each protein should be performed.

5.5 Conclusions

All together, our data indicate that *C. metallidurans* is able to adapt rapidly to toxic silver concentrations without mediation of its known silver efflux pumps. Instead, the involvement of a two-component system that cross-regulated different small uncharacterized proteins was discovered. Our hypothesis is that mutation of *agrS* leads to induction of *agrR*, which in turn affects expression of (among other) *mmmQ* resulting in an increased resistance against silver. The study revealed a putative role and function of a particular group of homologous proteins that is apparently only present in *Cupriavidus* and *Ralstonia*. Moreover, this system seems to be much more efficient as it gives the strains the ability to withstand much higher silver concentrations. The latter could be facilitated by the accumulation of silver ions and their reduction in nanoparticles making them unable to exert their action. Although the importance of some genes and proteins could be illustrated, their precise role and interactions need to be studied more in detail.

If these data are evaluated in the context of space exploration, it further emphasizes the fact that it is very important to develop proper monitoring and identification tools in the potable water systems aboard the ISS that are sanitized with $AgNO_3$ [50]. Results discussed in Chapter 4 already demonstrated that *C. metallidurans* isolates were able to withstand silver concentrations higher than concentrations often measured in the potable water systems aboard the ISS. This is partially due to the fact that silver concentrations quickly decrease after transportation in stainless steel containers. However, the results discussed here indicate that the problem will not be solved as silver concentrations are kept at their maximum levels

during the whole mission. Moreover, as the two-component system and the small proteins are present in all *C. metallidurans* isolates, they all have the potential to become highly resistant against silver and consequently, remediation actions with silver disinfection will not be useful. In the long-term it will putatively more suitable to find alternative disinfection methods, however, this will not be an easy challenge as silver has a lot of advantageous for these purposes. It has no unfavourable effect on odour, taste and colour of the water and most importantly, it does not cause immediate and serious risks for human health (Chapter 2). Consequently, it does not need to be removed before consumption and thus no specific equipment is necessary.

Chapter 6

Insertion Sequence elements in *Cupriavidus metallidurans* CH34: distribution and role in adaptation

Mobile genetic elements are one of the key factors in microbial evolution and adaptation. One of the features of type strain *C. metallidurans* CH34 is that it harbours a substantial amount of different mobile genetic elements such as genomic islands, transposons, megaplasmids, integrative and conjugative elements and insertion sequence elements. Since the genome sequence of CH34 is known and annotated, detailed studies have been performed to unravel the origin and function of these mobile genetic elements. Up to now, no detailed studied was performed on the insertion sequence elements present in this strain and their role in the metabolism of the strain. As insertion sequence elements were involved in the novel resistance mechanism discussed in previous chapter, insertion sequence elements present in CH34 are identified and characterized.

This chapter was based on the following publication:

Mijnendonckx K., Provoost A., Monsieurs P., Leys N., Mergeay M., Mahillon J., Van Houdt R. (2011) Insertion sequence elements in Cupriavidus metallidurans CH34: Distribution and role in adaptation *Plasmid* 65(3): 193-203

6.1 Introduction

After the isolation of *Cupriavidus metallidurans* CH34 (formerly *Ralstonia metallidurans*) from metallurgical sediments in Belgium [169], the strain attracted attention mainly because of two interesting features. First, the strain exhibited resistance to a wide range of different heavy metals mediated by efflux, complexation, and reduction [56, 57, 146]. In addition, it showed great adaptive potential. The latter became clear through its ability to accept and express foreign genes [182], for instance by capturing new broad-host range plasmids by exogenous plasmid isolation [219, 220] especially those expressing their accessory genes for the degradation of xenobiotics [221], or through its successful role as host for functional metagenomics [222, 223]. Recently, CH34 is also being used as a model to study the impact of challenging environments related to space exploration on microbial behaviour [224]. All species from the closely related genera *Cupriavidus* and *Ralstonia* carry two chromosomes and in addition often one or more large plasmids [225]. These plasmids often have specific traits linked to their ecological niche. For *C. metallidurans* CH34, the two megaplasmids pMOL28 and pMOL30 contain most of the heavy metal resistance determinants [57, 160]. Another interesting feature of many *C. metallidurans* strains is that they display a mutator phenotype, also termed temperature-induced mortality and mutagenesis or TIMM [179, 180, 226, 227]. In a temperature window between 36°C (with maximal viable counts) and 38°C (resulting in complete mortality) cells survived with a frequency of 10^{-4}-10^{-5} compared to viable count at 30°C and showed different mutations like deficiency in autotrophy or requirement for lysine [182, 183, 227].

Although some insertion sequence (IS) elements have already been described in *C. metallidurans* CH34, a detailed and comprehensive survey of the IS elements, their role in the metabolism of *C. metalliduran*s CH34, and their occurrence in other bacteria has until now not been performed. These

small elements (typically less than 3 kb) carry one or more open reading frames (ORFs) encoding for products essential for their mobility and generally no other functions are encoded. IS elements are flanked by short inverted repeat (IR) sequences and generate short directly repeated (DR) sequences of the target DNA at the point of insertion, which are 2 to 14 bp in size and specific for a certain element [228]. IS elements have been implicated in the evolution of the host as they contribute to diverse genomic rearrangements [229, 230]. Furthermore, transposition could lead to altered gene expression, which could be advantageous for the survival or the expression of newly acquired genetic traits under certain conditions [231, 232]. IS elements are therefore seen as a significant force in the adaptive and evolutionary response of their host, conferring genome plasticity that allows rapid adaptation to new environments [233, 234].

In this chapter, all IS elements in *C. metallidurans* CH34 were characterized and classified. All fully sequenced bacterial genomes were scrutinized for the occurrence of these IS elements. Finally, transposition and induction of these IS elements in different conditions were scrutinized as well as genetic rearrangements and gene activation.

6.2 Material and Methods

6.2.1 Media, strains, plasmids, and culture conditions

C. metallidurans CH34 and its derivatives were cultured in Tris salt mineral medium (MM284) supplemented with 0.2% (wt/vol) gluconate as described previously [169]. Liquid cultures were grown at 30°C on a rotary shaker at 150 rpm. Plasmid pGBG1 was a kind gift of Dominique Schneider [235] and was propagated in *E. coli* DH5α. Plasmid pGBG1 was introduced in *C. metallidurans* CH34 by electroporation as described by Choi *et al*. [236]. Selection was done on chloramphenicol (1000 µg/ml). IS elements from *C.*

metallidurans CH34 were trapped in pGBG1 by selection on tetracycline (20 µg/ml).

6.2.2 Molecular analysis

Standard techniques were used for isolation of chromosomal DNA, electroporation, PCR and agarose gel electrophoresis. The oligonucleotides used in this study were synthesized by Eurogentec (Seraing, Belgium) and are listed in Table 6.1. Detection of a part of the integrase module of CMGI-3 was done by PCR amplification of a 490 bp DNA fragment with primers PC_F and PC_R (starting material was CH34 genomic DNA). IS*1071*-mediated excision was detected by PCR amplification of a 3,450 bp junction fragment generated by this event (primers P_F and P_R used on CH34 genomic DNA) (Figure 6.5). *C. metallidurans* clones carrying a tetracycline-resistant pGBG1 were analysed by PCR with primers pGBG1_11 and pGBG1_12 and fragments were subsequently sequenced (Macrogen, Amsterdam, The Netherlands).

Table 6.1: PCR primers used in this study

Name	Sequence (from 5' to 3')	Reference
PC_F	ATACCAGCTTGCCGACGA	This study
PC_R	GGGCTTGCAGTTCCTTTGAC	This study
P_F	ATACCAGCTTGCCGACGA	This study
P_R	GGGCTTGCAGTTCCTTTGAC	This study
pGBG1_G11	TATCAGCTATGCGCCGACCAGAAC	[235]
pGBG1_G12	GCCAATCCCCATGGCATCGAGTAA	[235]

6.2.3 Analysis of IS elements and survey with IScan

Previously, the full genome (4 replicons) of *C. metallidurans* CH34 was manually annotated via the MaGe platform [56, 237] and deposited in the NCBI database (http://www.ncbi.nlm.nih.gov/genbank/) under the GenBank accession numbers NC_007971 (for pMOL30), NC_007972 (for pMOL28), NC_007973 (for chromosome 1), and NC_007974 (for chromosome 2). All

C. metallidurans CH34 project data are freely available through MaGe (https://www.genoscope.cns.fr/agc/microscope/home/index.php).

Analysis of the IS elements (terminal inverted repeats, direct targets repeats, potential DDE catalytic motifs, family classification) was done via ISFinder [238], the PALINDROME algorithm of the EMBOSS package [239], BLASTP and BLASTN (http://blast.ncbi.nlm.nih.gov/Blast.cgi), and manual curation. The IScan tool [240] was used to search for IS elements, related to the 21 distinct elements identified in *C. metallidurans* CH34 (Table 6.2), in 970 curated bacterial genomes available from GenBank. Only those BlastP hits to IS ORFs were retained with an *E*-value of 1e-20 and at least a 35% amino acid identity between IS ORFs and a BlastP hit measured over at least 50% of the smallest protein. For the other parameters, the default settings of the IScan tool were used.

6.2.4 Microarray data mining

Different data sets from transcriptomic analyses using microarrays were specifically scrutinized for IS-related gene expression. These data sets are available through the Gene Expression Omnibus repository (http://www.ncbi.nlm.nih.gov/geo/) under accession numbers GSE7272, GSE14049 and GSE23876.

6.3 Results and discussion

6.3.1 Identification and distribution of IS in CH34 genome

Fifty-seven intact IS elements were found in CH34, representing identical copies of 21 distinct IS elements (Table 6.2). These copies were dispersed over the four replicons with most of the elements located on chromosome 1 (30 copies) (Figure 6.1 and Figure 6.2). IS*Rme3* and IS*1088* were most abundant with 10 and 9 copies, respectively. Four elements (IS*Rme9*, IS*Rme10*, IS*Rme18* and IS*Rme19*) were only found on the two plasmids

(Figure 6.1, Table 6.2). The active center of the transposase, represented by three conserved acidic amino acids, D, D, and E, constituting the DDE motif, was identified in each element (Table 6.3) and all IS elements were placed into 10 families. The IS*3*, IS*30*, and IS*5* family were most abundant with 18, 13 and 5 copies, respectively (Figure 6.3). The IS*3* and IS*5* family are in fact the most abundant families among bacterial genomes (together with IS*1* and IS*481*) [240, 241].

Table 6.2 Distribution of IS elements in *C. metallidurans* CH34

IS element	**Family (sub-)**	**Length (bp)**	**CHR1**	**CHR2**	**pMOL28**	**pMOL30**
IS*Rme4*	IS*21*	2469	2			
IS*Rme9*	IS*21*	2688			1	
IS*Rme20*	IS*21*	1977	1			
IS*1090*	IS*256*	1343	4			
IS*Rme11*	IS*3* (IS*150*)	1231		2		
IS*Rme12*	IS*3* (IS*150*)	1454	1			
IS*Rme17*	IS*3* (IS*150*)	1678	1			
IS*1087B*	IS*3* (IS*2*)	1330	2			
IS*Rme3*	IS*3* (IS*3*)	1288	3	5		2
IS*Rme15*	IS*3* (IS*51*)	1325		1		1
IS*1086*	IS*30*	1106	1	1	1	
IS*1088*	IS*30*	1103	3	6		
IS*Rme10*	IS*30*	1063				1
IS*Rme8*	IS*4*	1455	1	1		
IS*Rme5*	IS*481*	1041	3	1		
IS*Rme1*	IS*5* (IS*427*)	1331	2	2		
IS*Rme6*	IS*5* (IS*427*)	913	1			
IS*Rme7*	IS*6*	840	2			
IS*Rme19*	IS*66*	2227				1
IS*1071*	Tn*3*	3204	3		1*	
IS*Rme18*	Tn*3*	ND			1	

*Copy inactivated by Tn*6049.*

Table 6.3: DDE motif of the IS elements in *C. metallidurans* CH34. Amino acids part of the catalytic site are shown in bold, other indicate conservation within a family. The numbers in parentheses indicate the distance in amino acids between the residues of the catalytic site.

IS element	Family (sub)	DDE motif*		
IS*Rme4*	IS*21*	---**D**W-- (57)	-I-**D**N-K---- (46)	--------KG-I**E**
IS*Rme9*	IS*21*	---**D**F-- (65)	-V-**D**N-R---- (45)	-R------KA-V**E**
IS*Rme20*	IS*21*	---**D**W-- (57)	-L-**D**N-K---- (48)	--------KG-V**E**------R
IS*1090*	IS*256*	---**D**A-- (65)	---**D**G--G--- (107)	-----I-TTN--**E**-----L**R**
IS*Rme11*	IS*3* (IS*150*)	WV-**D**-TY (59)	-HS**D**-G-Q--S (35)	---G---DNA-A**E**------**K**
IS*Rme12*	IS*3* (IS*150*)	W-T**D**VTE (59)	-HS**D**QGW-Y-- (35)	S-RGNC-DN---**E**-FF--L**K**
IS*Rme17*	IS*3* (IS*150*)	W-T**D**ITE (60)	-HS**D**-G---Y- (35)	S-KG---DN---**E**-FF--L**K**
IS*1087B*	IS*3* (IS*2*)	WCS**D**GFE (65)	-LS**D**NGS-Y-- (35)	T-V-SPQSNG-A**E**-FVKT-**K**
IS*Rme3*	IS*3* (IS*3*)	W--**D**ITY (59)	-HT**D**RGS-Y-S (35)	S--G---DN---**E**S----L**K**
IS*Rme15*	IS*3* (IS*51*)	WV-**D**-TY (61)	HHS**D**RG-QY-S (35)	GS-GDSYDNALA**E**-ING-Y**K**
IS*Rme10*	IS*30*	WE-**D**L-- (56)	-T-**D**-G-EMA- (33)	--P--P-QR--N**E**--N--V**R**
IS*1086*	IS*30*	WE-**D**L-- (56)	-T-**D**-G-EMA- (33)	--P--P-QR---**E**--N--L**R**
IS*1088*	IS*30*	WE-**D**L-- (59)	-T-**D**-G-EMA- (33)	--P--P-QR---**E**--N--L**R**
IS*Rme8*	IS*4* (IS*4*)	--L**D**--- (76)	-L-**D**—F----- (103)	-----Y--RW-I**E**--F---**K**
IS*Rme5*	IS*481*	-HI**D**-K- (60)	---**D**NG--F-- (48)	-----PQTNG--**E**RF--R-----R
IS*Rme1*	IS*5* (IS*427*)	---**D**-T- (113)	--A**D**G—YD--- (52)	--------R--I**E**--F---**K**
IS*Rme6*	IS5 (IS*427*)	--I**D**-S- (65)	--A**D**--YD--- (39)	-------K-R-V**E**-----LH
IS*Rme7*	IS*6*	WR-**D**ETY (56)	V-I**D**K------ (32)	-----KYLNN--**E**-DH--I**K**
IS*Rme19*	IS*66*	-HA**D**--- (60)	L--**D**-F-GY-- (51)	-AL--I--LY-I**E**
IS*Rme18*	Tn*3*	AS-**D**-M- (70)	---**D**T-G--D- (129)	-R------LNRG**E**--H-V-**R**
IS*1071*	Tn*3*	AS-**D**-M- (69)	---**D**T-G--D- (129)	-R------LNRG**E**---A--**R**

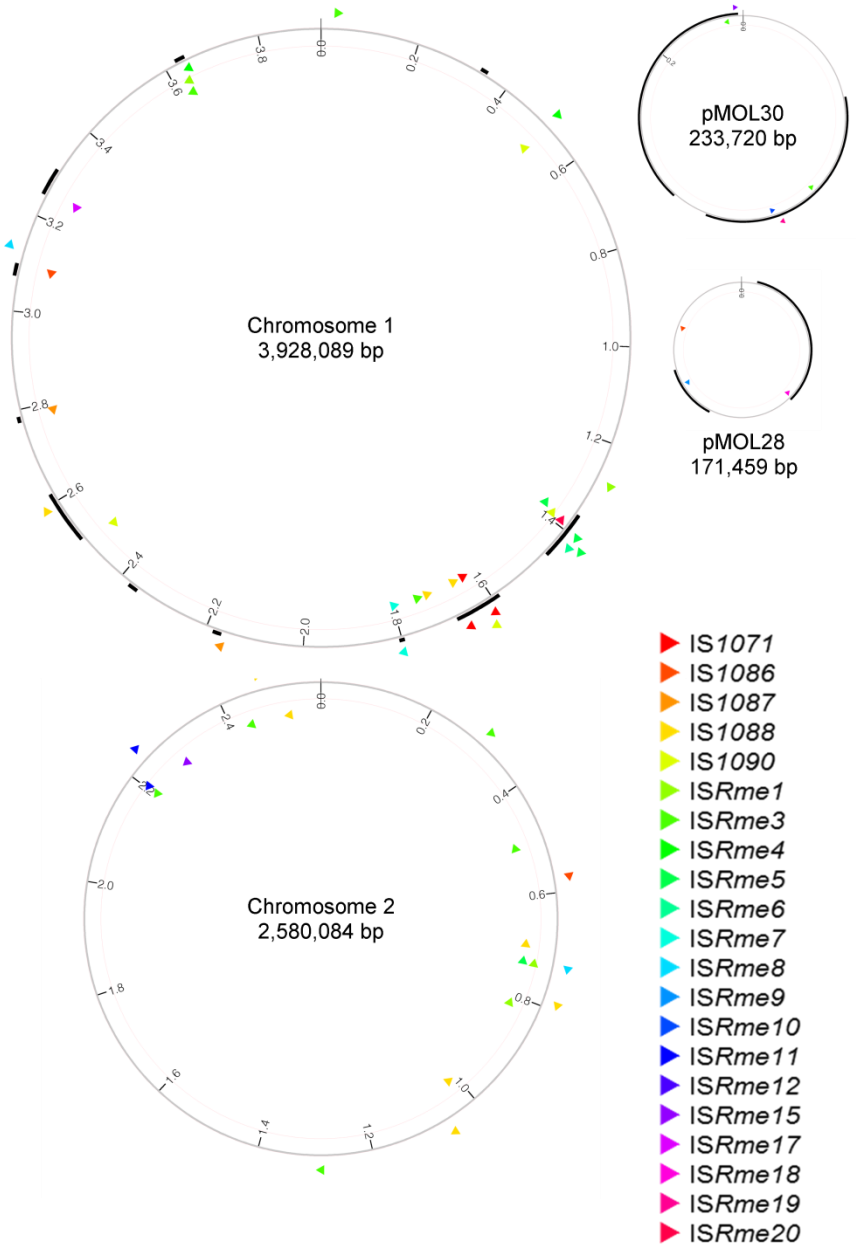

Figure 6.1: Distribution of the 57 copies representing 21 distinct IS elements in *C. metallidurans* CH34. Circular representation of the 4 replicons with the distribution of the different IS elements (coloured triangles). Genomic islands are indicated in black solid bars.

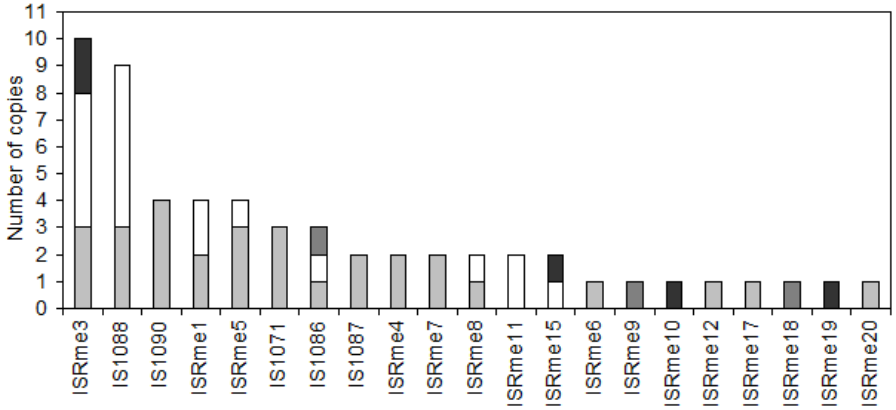

Figure 6.2: Copy number of the IS elements in *C. metallidurans* CH34. The stacked bars represent the number of copies of each IS element over the 4 replicons: chromosome 1 (light grey), chromosome 2 (white), plasmid pMOL28 (dark grey) and plasmid pMOL30 (black).

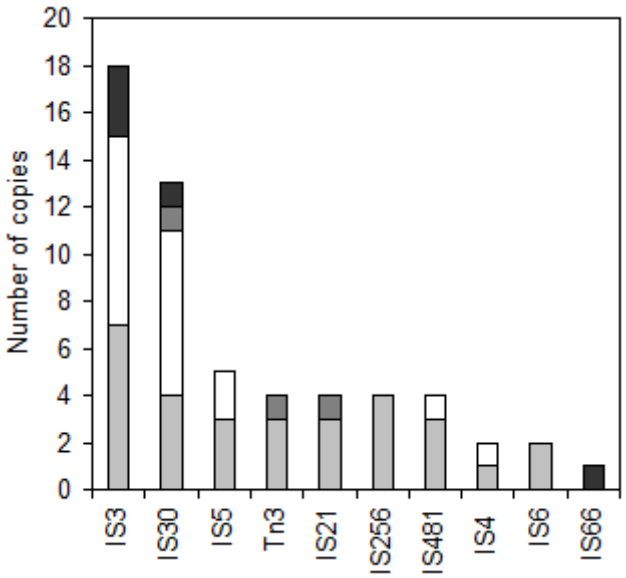

Figure 6.3: Distribution of the 10 IS families in *C. metallidurans* CH34. The stacked bars represent the distribution of the IS families over the 4 replicons: chromosome 1 (light grey), chromosome 2 (white), plasmid pMOL28 (dark grey) and plasmid pMOL30 (black).

6.3.2 IS dispersion in sequenced prokaryotic genomes

Touchon and Rocha [241] showed that in general genome size was the only significant predictor of IS abundance in prokaryotic genomes. Nevertheless, for the 4 sequenced *Cupriavidus* strains the number of genes annotated as related to transposable elements fluctuated strongly. *Cupriavidus taiwanensis* LMG19424 carried 222 transposase-related genes, followed by *C. metallidurans* CH34 with 145. Both contained a markedly higher number than *C. euthrophus* H16 (52) and *Cupriavidus pinatubonensis* JMP134 (25). This result in a density per Mb of 34.3 for LMG19424 and 21.0 for CH34 compared to 7.0 and 3.4 for H16 and JMP134, respectively. For JMP134, as well as for CH34, a significant number of these genes related to transposable elements, 93.2 and 55.5% respectively, are located on MGEs (plasmids or integrated genomic islands) or remnants hereof. Therefore, horizontal acquisition and spread could (have) be(en) mediated by these MGEs.

IScan [240] was applied to scrutinize 970 completely sequenced bacterial genomes for the presence of insertion sequences related to the IS elements of CH34 (Figure 6.4). Most relatives were observed in the β-proteobacteria class and *Burkholderiacea* family to which the *Cupriavidus* genus belongs. Interestingly, 100% conserved equivalents were found for IS*Rme3* in the genomes of *Ralstonia pickettii* 12D (two copies) and *R. pickettii* 12J (one copy), for IS*Rme8* in *Burkholderia vietnamiensis* G4 [equivalent to IS*Bvi1* [242]], for IS*Rme17* in *Delftia acidovorans* SPH-1 and *Comamonas testosteroni* KF-1 (only partial IS). These 100% conserved elements suggest recent interaction and horizontal transfer between these strains. Not only genetic relatedness, but also co-inhabitation significantly enhances the probability of gene acquisition by horizontal gene transfer [243].

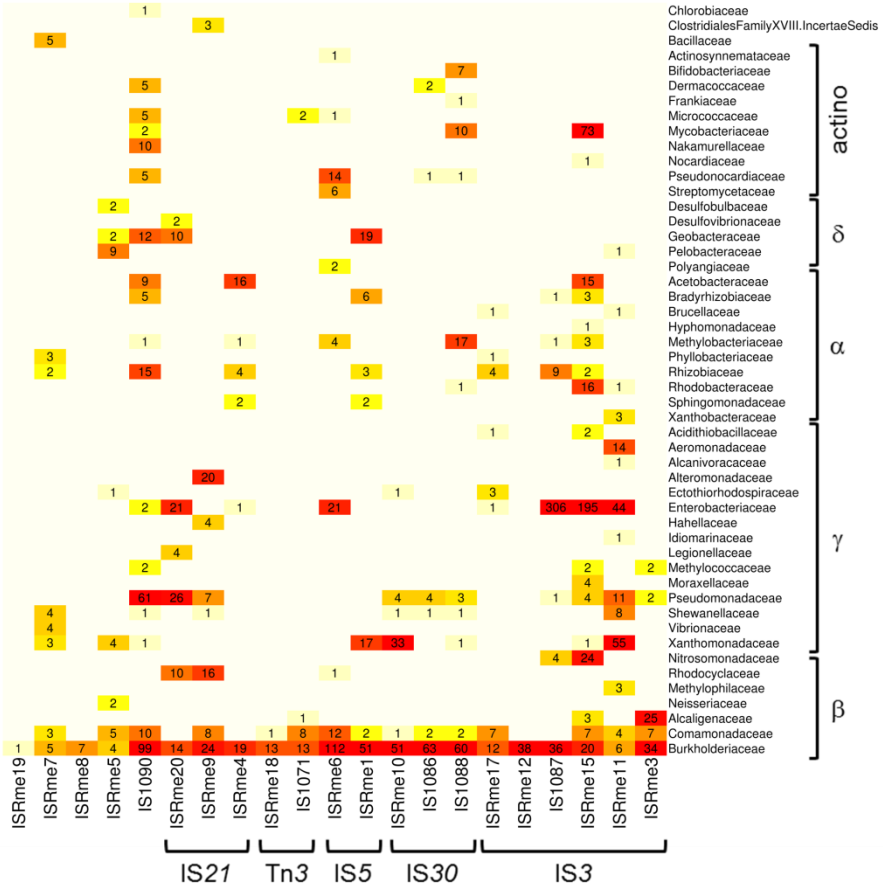

Figure 6.4: Dispersion of CH34 IS elements in sequenced bacterial genomes. Schematic representation of insertion sequences related to the IS elements of CH34 in all completely sequenced bacterial genomes. The number corresponds to the number of IS elements related to a particular IS element of CH34 (X-axis, grouped by IS family) in a certain bacterial family (Y-axis, grouped by bacterial class). The colour code grades the total number of IS in a particular bacterial family divided by the number of sequenced species herein.

In this respect, all strains were isolated from anthropogenic and polluted environments. *C. metallidurans* CH34 was isolated from sediments of a decantation basin of a zinc factory [169], *R. pickettii* 12J and 12D were

isolated from copper-contaminated lake sediments [244], *B. vietnamiensis* G4 was isolated from an industrial waste treatment facility for its trichloroethene oxidizing ability [245], *D. acidovorans* SPH-1 and *C. testosteroni* KF-1 were isolated from a sewage treatment plant and are part of a defined three-member bacterial community which completely mineralises linear alkylbenzenesulfonate surfactants [246]. Moreover, IS*Rme17* is part of a much larger gene cluster of 12 kb carrying genes involved in methionine biosynthesis and phosphite metabolism, which is almost 100% conserved among *C. metallidurans* CH34, *D. acidovorans* SPH-1 and *C. testosteroni* KF-1. This indicates recent horizontal gene transfer of a much larger gene cluster.

6.3.3 Genetic rearrangements through IS elements

The three intact copies of IS*1071* are located in genomic island CMGI-3 [161], which carries genes involved in carbon dioxide fixation and hydrogenotrophy. Temperature-induced mortality and mutagenesis at 37°C frequently yielded *C. metallidurans* CH34 mutants unable to grow autotrophic. Next to gene inactivation due to mutations, loss of the genes involved in autotrophy could be mediated either by excision of the whole genomic island CMGI-3 (Tn*4371* family) or by excision mediated by two IS*1071* copies flanking the complete region (Figure 6.5). Eight different TIMM mutants deficient in autotrophic growth were analysed using PCR assays that allowed detection of a part of the integrase module of CMGI-3 and of the junction generated by IS*1071*-mediated excision (Figure 6.5).

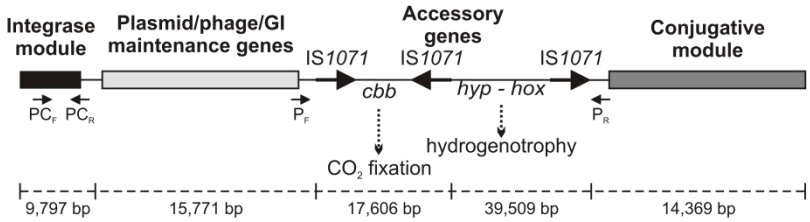

Figure 6.5: Schematic representation of the genomic island CMGI-3 and the copies of IS*1071* therein. The different modules of the Tn*4371*-family island are represented as boxes. The IS*1071* transposase genes and corresponding transcription orientation are shown as large arrows. Primers (small arrows) are indicated below. The island carries genes involved in CO_2 fixation (Calvin-Benson-Bassham (CBB) cycle) and hydrogenotrophy (*hy*drogenase *p*leiotropic and *h*ydrogen *ox*idation genes). The scheme is not drawn to scale.

For all mutant strains and wild-type CH34 the integrase module of CMGI-3 was detected. For all mutant strains but not for wild-type CH34, a 3,450 bp junction fragment was detected (Figure 6.6). These results indicated loss through IS*1071*-mediated excision in all cases rather than excision of the whole CMGI-3 element. This is the third observation that IS*1071*-mediated rearrangements alter the metabolic potential of the host as previously described for *Comamonas* sp. strain JS46 [247] and *C. pinatubonensis* JMP134 strain. These rearrangements with IS*1071* provide the first molecular explanation of the observations associated with TIMM. It may be hypothesized that the control on the stability of some transposable elements would be relieved under stress (e.g. near-lethal growth temperature), allowing increased transposition events, excessive recombination and genome destabilization. It will be of interest to examine if (other) IS elements or transposons would be involved in other events elicited by the mutator phenotype of *C. metallidurans*.

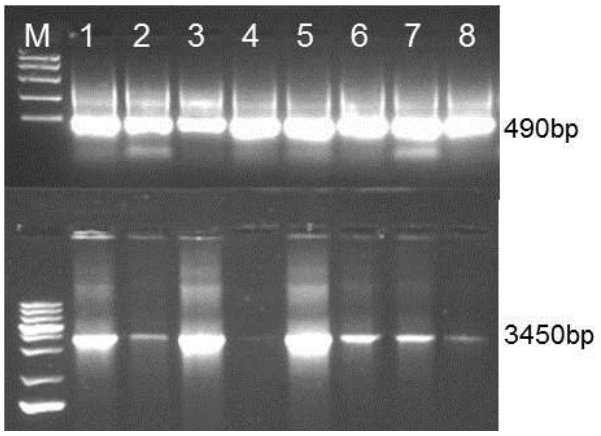

Figure 6.6: PCR analysis of IS*1071*-mediated loss of autotrophy. PCR analyses of 8 mutants derived from *C. metallidurans* CH34 that are deficient in autotrophic growth. upper: PCR amplification of CMGI-3 fragment (490 bp; primers PC_F and PC_R), lower: PCR amplification of junction IS*1071*-mediated excision (3450 bp; primers P_F and P_R). No amplification with primers P_F and P_R was observed for wild-type CH34

6.3.4 Transposition of IS elements

For a number of the identified IS elements transposition has been reported previously and was confirmed in this study. Transposition of IS*1086* and IS*Rme1* was detected in CH34 by positive selection on sucrose and tetracycline by inactivation of the *sacB* gene on vector pJV240 [184] and the λ CI repressor controlling expression *tetA* on vector pGBG1 [235], respectively. Excision of IS*1086* was observed in the rearranged derivative of pMOL28 obtained after exposure to 37°C [180]. IS*1087* was identified in a spontaneous zinc resistant mutant of strain AE126, which is a derivative of CH34 normally sensitive to zinc as it only carries plasmid pMOL28 and not plasmid pMOL30 (associated with resistance to zinc) [248-250]. The increased level of zinc resistance was due to insertion of IS*1087* in *cnrY*, which encodes an anti-sigma factor, resulting in constitutive expression of the the *cnr* cobalt and nickel resistance determinant and in increased

(nonspecific) Zn efflux [248-250]. IS*1088* and IS*1090* were identified by introducing the *czr* (cadmium zinc resistance) operon of *Pseudomonas aeruginosa* CMG103 in *C. metallidurans* AE104, which lacks both plasmids pMOL28 and pMOL30. Expression of the *P. aeruginosa* CMG103 *czr* operon was low in *C. metallidurans* AE104, resulting in a low resistance to Zn (0.8 mM). However, mutants with increased resistance to Zn (up to 1.5 mM) that carried IS*1088* or IS*1090* in the promoter region of *czr* were readily observed (at frequency of ca. 10^{-4} transposition event/cell/generation) [251].

In an attempt to monitor the transposition of other IS elements, pGBG1-mediated IS trapping was performed again [235]. This identified again the transposition of IS*1086* (data not shown). In addition, analysis of 4 different silver resistant mutants from *C. metallidurans* CH34 indicated the transposition of IS*1086* and IS*1087B* in the *agr* locus. This locus encodes a RND efflux system with its associated two-component regulatory system. However, since this RND likely belongs to the HAE-RND family (*h*ydrophobic and *a*mphiphilic compounds *e*fflux) and not HME-RND family (*h*eavy *m*etal *e*fflux) the involvement of this locus in the increased silver resistance still needs to be determined (K. Mijnendonckx, unpublished results).

6.3.5 Induction of IS elements

C. metallidurans CH34 carries a high number of metal resistance genes and is specifically adapted to survive ecological niches strongly dominated by heavy metal pollution [56]. As model organism it has been used to study microbial heavy metal responses and as a result multiple microarray data sets are publicly available through the Gene Expression Omnibus repository under accession numbers GSE7272, GSE14049 and GSE23876. These data sets were mined for differential expression of the identified IS-bound

transposases after exposure to different heavy metals (Ag^{+}, As^{3+}, Au^{3+}, Cd^{2+}, Co^{2+}, Cr^{6+}, Cs^{+}, Cu^{2+}, Hg^{2+}, Mn^{2+}, Ni^{2+}, Pb^{2+}, Se^{4+}, Sr^{2+}, Tl^{+} and Zn^{2+}). Ten (out of 21) IS elements showed differential expression to one or more metals (Table 6.4).

Since IS mRNAs are generally quite unstable, regulation of transposition is tightly regulated and endogenous promoters driving transposase expression are often inefficient [252], induction of neighbouring genes up- or downstream of IS elements on the corresponding DNA strand was examined [252]. Gene Rmet_6069 on plasmid pMOL30 is inactivated by IS*Rme15* and is also induced by Pb^{2+} (2.1 fold). Differential expression could therefore putatively be driven by the promoter of Rmet_6069 via read-trough transcription. Also Rmet_6072, upstream of IS*Rme3*, was induced by Pb^{2+} (2.6 fold) and As^{3+} (2.5 fold) (possible read-trough). For IS*Rme7* no in-frame stop codon was observed, therefore, the two *ISRme7* copies generated transposases of 792 and 1,026 aa residues. An oligonucleotide probe specific to the IS*Rme7* copy with the transposase of 1,026 aa residues did not show any differential expression after exposure to Cd^{2+}. This indicates that the observed IS*Rme7* expression could putatively be driven by the promoter of Rmet_6461 (directly upstream of the other IS*Rme7* copy) via read-trough transcription. Unfortunately, no probe for Rmet_6461 was available. Also partial IS elements on pMOL30 (see section 6.3.6) were affected. Rmet_5965 and Rmet_5964 were induced by Cd^{2+}, Cu^{2+} (only Rmet_5965), Ni^{2+}, and Zn^{2+}, whereas the partial IS elements (Rmet_5951-Rmet_5952 and Rmet_6153-Rmet_6152) were induced by Cd^{2+}.

Table 6.4: Transcriptomic analysis (via microarrays) of the IS elements in *C. metallidurans* CH34 under different heavy metal challenges[#].

	As^{3+}	**Cd^{2+}**	**Co^{2+}**	**Cr^{6+}**	**Cs^{+}**	**Cu^{2+}**	**Hg^{2+}**	**Ni^{2+}**	**Pb^{2+}**	**Se^{4+}**	**Sr^{2+}**	**Zn^{2+}**
IS*1090*									2.3			
IS*1087B*						0.6*						0.5*
IS*Rme3*	1.8[$]	1.8*				0.5*	0.6*		1.7*			
IS*Rme15*									2.1[$]			
IS*1086*											0.5	
IS*1088*		0.5	0.5		0.5		0.5			0.4		
IS*Rme8*											1.7	
IS*Rme5*	0.6			0.6	0.5	0.6			0.4		0.5	
IS*Rme7*		2.1										
IS*Rme19*		2.1							1.8			

[#]Only metals and IS elements are shown for which at least one oligonucleotide probe showed differential expression with a fold change < 0.6 or > 1.7 and an adjusted P-value < 0.05. For IS elements with two ORFs it is indicated if the probe was for the catalytic(*) or the DNA binding([$]) region.

These microarrays were performed to identify metal responsive gene clusters in *C. metallidurans* CH34 after exposure to non-lethal concentrations. The observed expression response of IS-related genes to heavy metals could therefore be biased due to the used concentration (well below the minimal inhibitory concentration) or the metal challenge time of 30 min. It would be interesting to examine the response of IS-related genes to a metal concentration approaching (or above) the minimal inhibitory concentration. Nevertheless, these results indicate that exposure to heavy metals could affect expression of transposase genes. Increased expression of certain IS elements after exposure to metals has already been described. IS*1246* in *Pseudomonas putida* KT2440 was induced by Zn^{2+}, Ni^{2+} and Cd^{2+} [253] and *insA* (IS*1*) in *E. coli* by Zn^{2+}, Co^{2+} and Cd^{2+} [254]. Also other physical and chemical stresses can elicit increased expression or transposition frequencies. Examples are elevated temperature [255, 256], irradiation [257], magnetic fields [258], and availability of oxygen and nutrients [256, 259]. But also conjugative interactions can induce transposition [260]. The *C. metallidurans* CH34 IS elements affected by heavy metals belong to different IS families, which could indicate that common factors are involved. Another interesting observation is the differential expression of partial IS elements. One of these fragments belongs to the Tn*3* family and is very similar to IS*Rme18* but carries a frameshift mutation in the transposase resulted in two ORFs (Rmet_5951 and Rmet_5952). A partial IS (comprising Rmet_6153 and Rmet_6152) is closely related to IS*Rme15* but has an internal deletion (3' part of *orfA* and 5' part of *orfB*). Both partial IS elements were induced by Cd^{2+} while the intact but very similar IS*Rme15* and IS*Rme18* were not induced. This could be an artifact due to altered mRNA stability or the truncated fragment could actually play a regulatory role, however, the biological relevance remains to be determined.

6.3.6 Gene inactivation by IS elements and inactivated IS elements

At least 32 IS are inserted inside an ORF, thereby inactivating the gene and concurrent gene product. One of the IS*Rme3* elements (Rmet_5679/Rmet_5680) inserted in the gene encoding the pump of a heavy metal tricomponent efflux system (*nimBAC*). Three insertions were in other IS elements. An IS*5* family element was inactivated by an IS*3* family (IS*407* sub-family) element, which in turn was inactivated by insertion of IS*Rme5* (see section 6.3.7). IS*Rme3* (Rmet_3942/Rmet_3943) inactivated an IS*3* family (IS*407* sub-family) element. Element IS*Rme19* and IS*Rme4* (Rmet_0483) inactivated a site-specific recombinase. Inactivated IS elements were also identified. An IS*1071* copy on pMOL28 was inactivated by Tn*6049* and at least 8 fragmented IS elements were found on pMOL30. Two partial IS elements in pMOL30, Rmet_5951/Rmet_5952 and Rmet_6153/Rmet_6152, were similar to IS*Rme18* and IS*Rme15*, respectively (see section 6.3.6). Also noteworthy, an IS*66* family element was inactivated by the recently described RIT element composed out of 3 tyrosine-based site-specific recombinase in tandem [161].

6.3.7 Characterization of IS elements in CH34

In this section, the identified IS elements and their ORFs will be described according to their (dis)similarities to the relevant IS family characteristics. The nucleotide sequences of the terminal inverted repeats of the IS elements are shown in Table 6.5.

Table 6.5: Nucleotide sequences of the terminal inverted repeats of the IS elements in *C. metallidurans* CH34.

Element	Left (LE) (top) and right (RE) (bottom) IS ends
IS*Rme4*	**TG**TTGATTTGCACTGAATCCTGACCCACCCACGGCAGGTATTTGCATCGA
	TGTTGATTTGCACCGAATCCTGACCCACGATTTGCATCGAAAATTGACCC
IS*Rme9*	**TG**CGTATTTCGGGGCGCGTGATCAGCGATTTCGGGGGAACGTGATCACCT
	TGCGGATTTCGGTGAAGGTGATCAGCGGTTTCGGCGAACGTGATCAGGGA
IS*Rme20*	**TG**ACCCAGCGGCAGCACATTGGATTTGACCCACCCGGGTAGGATGGGCCC
	TGACCCTGGGTCAGCGTCAGTTGCTGGCCATCGGTTTCGCCTGACCCAGG
IS*1090*	**GG**GACTGTCGGAGATTTCGTGTTTAAGGCATAACATGCTCCCAAGGAGAA
	GGGGGTGTCAGAATTTCCGTGTTCAAGGCGGGTTGAGAATCACACGGATG
IS*Rme11*	**TG**GACCGGCCAGCCTTTCGTAGACATCTTCGAGCCATAATTTGTGGCAAC
	TGGACCGGCCAGAGTTTCATAGACACTCACGAGCCGTTTAGCGCGTAGCG
IS*Rme12*	**TG**AACTGCACCCCAAAGGTTGGACACCCGTTCAACCTTTGGGGTGTTTTT
	TGAACTGACCCCAAGAAGTTGGACAGTTAAGGCGGTAGGCTAAGCCATAG
IS*Rme17*	**TG**TTGATTTCCACGCAGAACTGACCCGCCGGGGATGCGGACAAAAACTTG
	TGTTGATTTCCACCCAGAAGTGACCCACTAGCCCCCGGTGGGGGTGCGGA
IS*1087B*	**TG**GAGCGGCCCCTTGAATCTCAGGACACCCGGCACCTCTTACAATAAGAG
	TGGAGTTGACCCTGTAACTCAGGACACCCGAACACCGTTAAGTTGATGAT
IS*Rme3*	**TG**AGCTTGCCCCCGCAAAACGAATCCCTTGCTGAGGTTAAACTGAAGCAA
	TGACCTTGCCCCTGTTCCACGAATCCCATAACCGAGGGAATTAGGCAGCC
IS*Rme15*	**TG**AATCGCCCCGGGTTTTGCGGAGGCTCTCACTCTTGAGAGAATGCGAGC
	TGAATCGCCCCGGTTTTCGCGGAGGCTGTTTGGTTAAAGTAAAACGGCCT
IS*1086*	GGCGGCCTCAAATCTGAAGTGCAACACCTTGCCATTCGGTAAGGTGTGGT
	GGCGGTTTCAAGTGCGAAGCGCAACACCCCTTGGTTATTGAACAGGAAGC
IS*1088*	GGCGGCCTCAATTCCGAAGTGCAACACCGAGAATTGAGGCCAAGATGACC
	GGCGGTTTCAAGTCCAAGTGCAACAAAAACTCAATGCACTAAATCCGGCT
IS*Rme10*	GCGGTCTCTAGAATGAAGTGCAACACCCTGATGTTAGGGTGTTGGGATGG
	GCGGTTTCAAGTCTGAGATGCAACACCAGTTCGTAATTTGTTGATCTCTT
IS*Rme8*	C**AAT**ACTGTTCAGATAGTATTTTTAAAGCCATAATCCTCATCCATCGAAG
	A**AAT**ACTGTTCAGATACGAAGCACCGGCACTGGCTGATGCCGCAAATGGA
IS*Rme5*	**TGT**CGTGTCCCTGATGATTGGTTAATTGGTTCACGCCGTGGTTTACTCTT
	TGTCGTGTCCCGGCTGATTGGTAACACGTCTGTTGAACAGTTCGGGGTGT
IS*Rme1*	CAGGCTGCTGAAATACCGGCAGCGAACGTCAGCGCGACGACTTGCTGAAT
	CAGGCTGCTGAAGTACTAGCCGCATAAAAGCGAAGCTTCCCTCTGCAAGG
IS*Rme6*	**GA**GGCCAGTTCAAAAACCCCTGAGGCGGCTGTTTACTTTCTCGGTAAGCT
	GAGGCCAGTTCAAAAAGGCTGCTCCGTACGCCTGAAGATGTTCCAGCAGA
IS*Rme7*	**GG**TTCTGTCGCGCTAAGGGTGCCGGGGTGAGATTTCAGCAGACATTGCCC
	GGTTCTGTCGCGATAAGGCCGGTTGGTCGAAGCCGGTGGGCTGGAGTGCG
IS*Rme19*	**GTAA**GCGCCCGGTGAACCCGTCTTGAAGGGAAGCAGGAGAGCAAGGAGCA
	GTAAGCGCCCGGTGAACCCGTCTCGACGGGGCTACGCAGGAAGGACGGAA
IS*1071*	**GGGG**TCTCCTCGTTTTCAGTGCAA**TAAG**TGACGGTACGCAAAGCTAGCAC
	GGGGTCTCCTCGTTTTCAGTGCAA**TAAG**TGACGGTACGAAAAGCTAGCAC
IS*Rme18*	ND

Characteristics of the IS family indicated in bold.

6.3.7.1 ISRme3, ISRme11, ISRme12, ISRme15, ISRme17, IS1087B (IS3 family)

These elements belong to the IS*3* family (IS*Rme3* to the sub-family IS*3*; IS*Rme11*, IS*Rme12*, IS*Rme17* to sub-family IS*150*; IS*Rme15* to sub-family IS*51*; and IS*1087B* to sub-family IS*2*) with inverted repeats that shared the signature of this family including the characteristic ends (5'-TG and CA-3') (Table 6.5).

The 1,288 bp IS*Rme3* element is with 10 copies the most abundant in CH34. Direct target repeats of 3 bp were observed in 7 cases. It carries two consecutive ORFs with an overlap of 4 bp. OrfA exhibits a N-terminal helix-turn-helix motif and a C-terminal leucine zipper-like motif [L(6)L(6)L], while OrfB displays the catalytic DD(35)E motif. A potential frameshift window (A_7 type) was identified in the element, which could reconstitute an *orfAB* transposase. However, such a fusion protein was never found in the current database of CH34 proteins identified under different growth conditions by shotgun proteome analysis (B. Leroy, pers. comm.). Equivalents of IS*Rme3* that are 100% identical were observed in the genomes of *Ralstonia pickettii* 12D (two copies) and *R. pickettii* 12J (one copy). Outside the *Cupriavidus* and *Ralstonia* genera, the closest relative (81% DNA identity) was a putative IS element from *Burkholderia xenovorans* LB400. One of the IS*Rme3* copies is inserted at the extremity of the genomic island CMGI-30b, which holds genes involved in the response to copper and silver [160].

IS*Rme11*, IS*Rme12* and IS*Rme15* carry two consecutive ORFs with a 1 bp overlap. Relatives of IS*Rme12* (> 35% protein identity) were only found in the *Burkholderiaceae* family. IS*Rme11* showed the highest similarity (ca. 90% protein identity) with an IS from *Burkholderia cenocepacia* MC0-3. The closest relative of IS*Rme15* was identified in *Bordetella petrii* (97% protein identity).

IS*Rme17* carries only one ORF coding for a 512 aa long transposase. An 100% identical copy was found in *D. acidovorans* SPH-1 and *C. testosteroni* KF-1 (only partial IS).

Element IS*1087* was identified in a spontaneous zinc resistant mutant of a derivative CH34 strain lacking pMOL30 (see above) [261]. DNA sequence analysis of the two IS*1087* copies present in CH34 revealed a sequence slightly different from IS*1087* (accession number AJ243722). This element, with a length of 1330 bp, was denoted IS*1087B*. IS*1087B* carries two consecutive and partially overlapping ORFs in the relative translational reading frames 0 and -1 (a general feature for IS*3* members). The closest relative (90% protein identity) was found in *Burkholderia phytofirmans* PsJN.

6.3.7.2 ISRme4, ISRme9 and ISRme20 (IS21 family)

IS*Rme4*, IS*Rme9* and IS*Rme20* are members of the IS*21*-family and are 2,469, 2,688 and 1,977 bp long, respectively. They bear the characteristic 5'-CA-3' end (Table 6.5) and have internal repeats in the L and R end (Table 6.6). OrfA harbours a N-terminal helix-turn-helix and DDE motif. OrfB carries a characteristic ATP binding domain [G----GKT(54)DE]. OrfA and OrfB from IS*Rme4* shared respectively 94% and 97% protein identity with an IS from *R. pickettii* 12D. IS*Rme9*, located on plasmid pMOL28, showed the highest similarity (around 70% protein identity) with IS*408* and IS*Bmu3* from *B. multivorans* ATCC17616. These elements, along with other IS identified in *B. multivorans* ATCC17616, showed an increased transposition frequency under a high-temperature condition of 42°C [255].

Table 6.6: Nucleotide sequences of the repeats internal in the L(eft) and R(ight) end terminal repeats of IS elements in *C. metallidurans* CH34. L1-L2 and R1-R2 indicate internal repeated sequences with corresponding coordinates between brackets. Conserved nucleotides are capitalized.

IS element	L end terminal repeat	R end terminal repeat
IS*Rme4*	L1: ATTTGCActGAATccTGACCCAC (6-28) L2: ATTTGCAtcGAATgtTGACCCAC (40-63)	R1: GATTTGCAcCGAAtccTGACCCAC (2418-2441) R2: GATTTGCAtCGAAaatTGACCCAC (2442-2465)
IS*Rme9*	L1: ATTTCGGGGcgCGTGATCA (6-24) L2: ATTTCGGGGgaaCGTGATCA (28-47)	R1: TTTCGGtgAAgGTGATCAG (2642-2660) R2: TTTCGGcgAAcGTGATCAG (2664-2682)
IS*Rme20*	L1: TGACCCA (1-7) L2: TGACCCA (26-33)	R1: TGACCCtGGGTCA (1965-1977) R2: TGACCCaGGGTCA (1924-1936)

6.3.7.3 ISRme5 (IS481 family)

This element of 1,041 bp belongs to the IS*481*-family and the 4 copies display transposases with different lengths since no transposase in-frame stop codons were observed within the IS. The inverted repeats of the element terminated with the characteristic 5'-CAC-3' end and in 2 cases a direct repeat of 6 bp was observed. Two copies were located in genomic island CMGI-2, which is involved in hydrogenotrophy and the metabolism of aromatic compounds [161], in a region with multiple transposases and fragments hereof (Figure 6.7). Putatively, IS*Rme5*b (Rmet_1280) integrated first into an IS element (comprising Rmet_1279, Rmet_1302 and Rmet_1303), resulting in a transposase ORF that ended at the stop codon present in the flanking sequence (CCTAAT) that was duplicated during insertion. In a next event, integration of a gene cluster involved in hydrogenotrophy (*hy*drogenase *p*leiotropic and *h*ydrogen *ox*idation genes) was assisted by IS*Rme5*c (Rmet_1301). This resulted for Rmet_1301 in an ORF that ended in the sequence originally duplicated by Rmet_1280 (CCTAAT), and for Rmet_1280 in a transposase of 463 aa overlapping the 3' end of *hypE* (Rmet_1281, not shown) with 216 bp. The IS element (Rmet_1279, Rmet_1302 and Rmet_1303) inactivated by these events was already integrated in an IS*5*-family element resulting in the fragments Rmet_1304 and Rmet_1278.

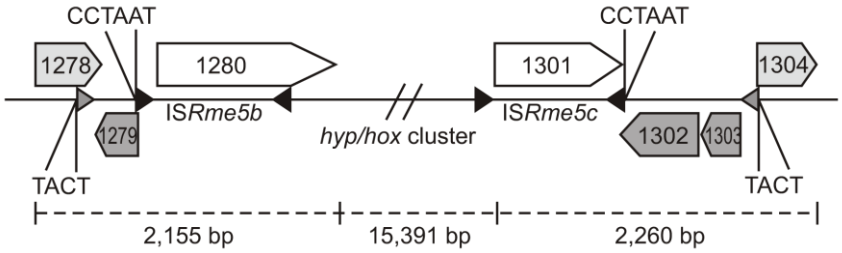

Figure 6.7: Composition of the region flanked by two IS*Rme5* elements in genomic island CMGI-2 of *C. metallidurans* CH34.

This genomic region illustrates that a first insertion event could attract further successive insertion events leading to a region rich in MGEs and possibly prone to attract advantageous features carried by the MGEs. The closest relative in a prokaryotic genome was found in *Brachymonas petroleovorans* (65% protein identity), a recently isolated β-proteobacterium that grows on cyclohexane [262]. However, apparently a 100% identical DNA sequence could be found on 2 different DNA scaffolds from the black cottonwood tree, *Populus trichocarpa* [263] (NCBI Genome Biology BLAST). Scaffold 2473 and 3410 aligned respectively with bp 46 to 1,041 and bp 1 to 453 from IS*Rme5*. Since contamination of prokaryotic IS elements in eukaryotic sequences has been described [264, 265], PCR was performed on genomic DNA of *Populus trichocarpa*. Although, a fragment of approximately 1 kb could be amplified, sequence analysis indicated no similarity to IS*Rme5* (data not shown).

6.3.7.4 ISRme7 (IS6 family)

This 840 bp element (IS*6*-family) is present at two copies with 4 bp that mismatch. No transposase in-frame stop codons were observed within the IS, generating transposases with different lengths of 792 and 1,026 amino acids, respectively. The elements flank the putative genomic island CMGI-11, which contains an operon encoding proteins involved in fimbriae biosynthesis [161]. IS*Bmu21* of *B. multivorans* ATCC17616 was found to be the closest relative (74% protein identity).

6.3.7.5 ISRme18 and IS1071

Element IS*1071* was originally identified in transposon Tn*5271* from *Alcaligenes sp.* BR60 (later *C. testosteroni* BR60), which carried genes involved in chlorobenzoate catabolism [266, 267]. Four copies of this element were identified in CH34, 3 intact elements on chromosome 1 in CMGI-3 and one copy on pMOL28 inactivated by insertion of Tn*6049* [55, 161]. Compared to IS*1071* from *C. testosteroni* BR60 the element in CH34

carries an insertion of 3 bp between position 554 and 555, generating one additional amino acid. Many IS*1071* sequences have been identified next to genes involved in the degradation of xenobiotics on conjugative plasmids from environmental bacteria such as *Pseudomonas* spp. [268], *Comamonas* spp. [269-271], *D. acidovorans* [271, 272], and *C. pinatubonensis* JMP134 [273]. Our IScan analysis also revealed IS*1071* sequences in *Acidovorax* spp. and *Burkholderia* spp. Element IS*Rme18*, which is located on pMOL28, was also identified as a member of the Tn*3* family, although the IRs could not be recognized and therefore IS*Rme18* could be an inactive copy. A fragmented IS element similar to IS*Rme18* (approximately 90% on DNA sequence) was identified on pMOL30 (Rmet_5952 and Rmet_5951). Similar elements were identified in *Burkholderia* spp. (> 60% protein identity) and in *Polaromonas* sp. JS666 (54% protein identity), which is capable of degrading chlorinated ethenes [274].

6.3.7.6 ISRme1 and ISRme6

These IS elements belong to the IS*5* family (IS*427* sub-family) with lengths of 1,331 and 913 bp for IS*Rme1* and IS*Rme6*, respectively. IS*Rme1* was present at 4 copies and was first observed by trapping in a broad-host range vector, which allows positive selection [235]. In CH34, IS*Rme1* generated direct target repeats of 4 bp by duplication of the preferred target sequence YTAR. IS*Rme1* carries one ORF, which shares 93% and 91% protein identity with IS from *C. taiwanensis* RALTA and *C. pinatubonensis* JMP134, respectively. Outside the *Cupriavidus* and *Ralstonia* genera, the closest relative (83% protein identity) was a putative IS element from *Burkholderia phymatum* STM815.

IS*Rme6* contains 2 ORFs, which do not partially overlap like for most of the IS*427* subgroup members. However, a potential -1 frameshift window (5'-GAAAAACTGG-3') was observed at position 435, possibly generating an ORF of 271 aa with 76% protein identity to the fused ORF of IS*JP4*. The

latter element was identified in *C. pinatubonensis* JMP134 where it inactivates the gene encoding for the transcriptional regulator TfdT of the chlorocatechol-degradative operon [275]. IS*Rme6* was also found in a cluster of genes for the degradation of aromatic compounds located on genomic island CMGI-2. It disrupts a glutathione-S-tranferase gene often found along with genes for the degradation of aromatic compounds [276].

6.3.7.7 ISRme8

A 1,455-bp element from the IS*4*-family (subfamily IS*4*) is found twice in CH34 with 10 bp direct target repeats. IS*Rme8* is 100% identical to IS*Bvi1* from *B. vietnamiensis* G4 [242].

6.3.7.8 ISRme10, IS1086, and IS1088

These three IS elements belong to the IS*30*-family with lengths of 1,063, 1,106 and 1,103 bp for IS*Rme10*, IS*1086* and IS*1088*, respectively. IS*Rme10* is located on pMOL30. IS*1086* is found once on pMOL28 and twice in the chromosome (3 bp direct target repeats), which confirmed previous hybridisation experiments [184]. The nine copies of IS*1088* are only present in the 2 chromosomes, not in the megaplasmids, and a direct repeat of 3 bp was generated in 8 cases. The closest relative of IS*Rme10*, IS*1086* and IS*1088* were IS*3091* (54% protein identity) from *Acidithiobacillus ferrooxidans*, an IS (73% protein identity) from *Thiomonas sp.* 3As and an IS (67% protein identity) from *Rhodoferax ferrireducens*, respectively.

6.3.7.9 ISRme19

This 2,227 bp IS belongs to the IS*66* family, indicated by similar IRs (Table 6.5), 8 bp direct target repeats and the presence of multiple ORFs. IS*Rme19* carries putatively 5 ORFs and a similar element, sharing 72% DNA sequence, was detected in *R. pickettii* 12J (3 copies).

6.3.7.10 IS1090

Four copies of this 1,343 bp element, which belongs to the IS*256* family, were identified in CH34. IS*1090* carries the related inverted repeats (Table 6.5) and generated, like most of the IS*256* family members, 8 bp direct target repeats. Close relatives (91% protein identity) were found in *Burkholderia ambifaria* MC40-6 and *B. cenocepacia* MC0-3.

6.4 Conclusions

This study revealed 9 new IS elements in *C. metallidurans* CH34. In total, 57 intact IS copies from 21 distinct IS elements were characterized and classified into 10 different families. A number of these IS elements were associated with genomic islands, gene inactivation and rearrangements that alter the autotrophic growth capacities. The latter provide the first molecular explanation of the observations associated with TIMM in *C. metallidurans*. In addition, differential expression of IS-related genes was found under heavy metal stress, an environmental stress to which *C. metallidurans* CH34 is well adapted. Therefore, these observations indicate that IS elements play an active role in *C. metallidurans* CH34, its metabolic potential and adaptation under selective pressure.

Chapter 7

Plasmid mediated metal resistance in *Cupriavidus metallidurans* space isolates

---

In type strain *C. metallidurans* CH34, a substantial part of its metal resistance is located on the two megaplasmids pMOL28 and pMOL30. For both plasmids, transfer frequencies of Ni^{2+} and Zn^{2+} resistance determinants already have been identified. Chapter 4 showed that the *C. metallidurans* strains isolated frome space-related environments contain at least one megaplasmid. Moreover, all isolates were as metal tolerant as type strain *C. metallidurans* CH34. In this chapter, the transfer of Ni^{2+} resistance determinants to a plasmidless derivative of *C. metallidurans* CH34 and the co-transfer of other metal resistance determinants are investigated.

7.1 Introduction

It is well studied that the transfer of DNA between bacterial cells facilitates microbial resilience and survival in extreme environments. MGEs such as transposons, IS elements, plasmids, genomic islands, allow mobilization and reorganization of genes within a given bacterial genome or between bacterial cells [277]. Furthermore, MGEs often carry key features allowing survival in specific environmental niches such as those exposed to xenobiotic compounds [163, 278], multiple antibiotics [198], heavy metals [57] or even as beneficial plant rhizobacterium [279]. Therefore, they are seen as key players in the reshuffling of genetic material, which in combination with mutations and selection, drive evolution [277].

One of the interesting features of type strain *C. metallidurans* CH34 is that it carries a large diversity of MGEs, including at least 21 genomic islands, 2 integrative and conjugative elements, 19 copies of 5 different transposons, 57 copies of 21 different IS elements (discussed in detail in Chapter 6) and 2 megaplasmids [161, 181]. Both the number and diversity of genes related to MGEs is larger in CH34 than in related strains from other *Cupriavidus* and *Ralstonia* species [161]. The megaplasmids pMOL28 and pMOL30 harbour genomic islands that are highly specialized in metal resistance. They carry resistance determinants at least for, Co^{2+}, Ni^{+2}, Cr^{+4}, Hg^{+2}, Zn^{+2}, Cd^{+2}, Cu^{+2}, Ag^{+}, Pb^{+2} [57]. Although pMOL28 carries a complete set of conjugative genes, which show extensive synteny with the highly self-transferring plasmid pHG1 from *Cupriavidus eutrophus* H16, transfer frequencies of resistance markers were rather low (± 10^{-8} transconjugants per donor cell) [169]. For plasmid pMOL30, which contains very few genes involved in plasmid transfer, resistance determinants are transferred at a frequency of 10^{-8} transconjugants per donor cell [160, 169]. For both plasmids, transfer frequencies could be increased up to 10^{-3} transconjugants per donor cell with the aid of the IncP1 plasmid RP4 as helper strain [169].

In Chapter 4, it was shown that all *C. metallidurans* strains isolated from space-related environments carry at least one megaplasmid and that there were almost no differences in their metal resistance profiles. In this chapter, the mobility of these megaplasmids will be studied as well as the metal resistance determinants they carry.

7.2 Materials and Methods

7.2.1 Media, strains, plasmids, and culture conditions

All *C. metallidurans* strains and isolates were cultured in Tris salt mineral medium (MM284) supplemented with 0.2% (wt/vol) gluconate as carbon source [169]. Liquid cultures were grown in the dark at 30°C on a rotary shaker at 150 rpm. For autotrophic growth, the carbon source was excluded from solid MM284 agar medium and plates were incubated in a jar with a gas atmosphere containing a mixture of H_2, CO_2 and O_2 (72%, 18%, 10%). *E. coli* DH5α was grown in liquid LB medium at 37°C on a rotary shaker at 150 rpm in the dark. When appriopriate, media was supplemented with antibiotics at the following concentrations: trimethoprim (100 µg/ml) and kanamycin (50 µg/ml for *E. coli* or 1500 µg/ml for *C. metallidurans*). Plasmids used in this study are listed in Table 7.1.

Table 7.1: Plasmids used in this study.

Plasmid	Description	Reference
pSCrhaBout*gfp*	pTn*Mod*, *rhaR rhaS* P_{rhaB} *e-gfp*, Tm^R	[280]
pRK2013	ColE1 ori, RK2-Mob^+ RK2-Tra^+, Km^R	[281]
pKT230	RSF1010 based, Tra^-, Mob^+, Km^R from pACYC177	[282]

Tm^R: Trimethoprim resistance; Km^R: Kanamycin resistance.

7.2.2 Molecular analysis

Standard techniques for PCR, Standard techniques were used for isolation of chromosomal DNA, electroporation, PCR and agarose gel electrophoresis

unless stated otherwise. The oligonucleotides used in this study were synthesized by Eurogentec (Seraing, Belgium) and are listed in Table 7.2.

Table 7.2: Primers used in this study.

Name	Sequence 5'→3'	Length
Dam_Fw	CATGGGATCCGCCGGCTTCAATGTAAAGAT	1055 bp
Dam_Rv	GCTAGAATTCCCATCGCTGCACAAGAGTAG	

7.2.3 Random transposon mutagenesis

To construct a suitable recipient strain, a tri-parental mating was performed with the plasmidless *C. metallidurans* AE104, *E. coli* DH5α pSCrhaBout*gfp* and *E. coli* HB101 containing the helper plasmid pRK2013. Transconjugants were selected on MM284 supplemented with 100 µg/ml trimethoprim (Tm). Positive clones were purified on MM284 supplemented with 100 µg/ml Tm and tested for their capability to grow autothropically. Three positive AE104_Tm clones were selected for further experiments.

7.2.4 Conjugations

To investigate the transfer capabilities of the plasmids present in the *C. metallidurans* isolates, bi-parental matings were performed with three independent AE104_Tm strains as recipients and all *C. metallidurans* isolates as donor strains. After 4 days, heterotrophic plate counts were performed to estimate the number of transconjugants. The latter were selected on MM284 + 100 µg/ml Tm + 1 mM $NiCl_2$, donor strains were scored on MM284 + 1 mM $NiCl_2$, while recipient strains were counted on MM284 + 100 µg/ml Tm. To determine the transfer frequency of Ni^{2+} resistance, the ratio between recipients and transconjugants was calculated. Transconjugants were screened to be genuine by analysing their capabilities to grow autothrophically. In addition, the presence of *dam*, which is specific for *C. metallidurans* CH34, was controlled by PCR amplification with primers dam_FW and dam_RV (Table 7.2).

To study the mobilization capacities of the plasmids of *C. metallidurans* NA4, a tri-parental mating was performed with AE104_Tm as recipient, *E. coli* DH5α pKT230 as donor and *C. metallidurans* NA4 as helper strain. After 3 days, heterotrophic plate counts were performed to estimate the number of transconjugants. The latter were selected on MM284 + 100 µg/ml Tm + 1500 µg/ml Km, while recipient strains were counted on MM284 + 100 µg/ml Tm. To determine the mobilization frequency of the plasmid pKT230, the ratio between recipients and transconjugants was calculated. Matings were performed in triplicate.

To explore if one of the plasmids of *C. metallidurans* NA4 is a broad-host range plasmid, a bi-parental mating was setup with *E. coli* DH5α as recipient strain and *C. metallidurans* NA4 as donor strain. After 3 days, heterotrophic plate counts were performed to estimate the number of transconjugants. The latter were selected on M9 mineral medium supplemented with 0.4% glucose and 1 mM thiamine hydrochloride + 1 mM $NiCl_2$, donor strains were counted on MM284 + 1 mM $NiCl_2$, while recipient strains were counted on M9 mineral medium + 0.4% glucose 1 mM thiamine hydrochloride. To determine the transfer frequency of the plasmid, the ratio between recipients and transconjugants was calculated. Matings were performed in triplicate.

7.2.5 Plasmid profiling

The extraction of large plasmids was based on the method of Andrup *et al.* [171]. DNA was analysed by horizontal gel electrophoresis in 0.5% Certified Megabase agarose gel (Bio-Rad, USA) with 1 x TBE buffer for 20 hours at 100 V in a precooled electrophoresis chamber at 4°C. After electrophoresis, DNA was stained with ethidium bromide (0.3 µg/ml TBE) for 30 min and destained overnight at 4°C in ultrapure water.

7.2.6 Metal ion resistance

A stationary phase culture (OD_{600} of ca. 1, representing 10^9 CFU/ml) of each strain in MM284, was diluted 100 times in 2 ml MM284 medium with different concentrations of the metals of interest. The lowest concentration that inhibits visible growth was defined as MIC. The MIC values were determined for the following metal solutions after 3 days: $CoCl_2$, $CuSO_4$, $ZnSO_4$, $NiCl_2$ and KCr_2O_4,

7.3 Results

7.3.1 Transfer frequencies

In a first step, a *C. metallidurans* AE104 recipient strain with an appropriate and selectable marker (resistance to trimethoprim) was constructed via random transposon mutagenesis using a Tn*Mod* minitransposon. To rule out possible effects of the location of the minitransposon, experiments were performed with 3 independent transposon mutants. Transconjugants were screened for the presence of *dam,* which is only present in recipient *C. metallidurans* AE104, and the ability to grow autotrophically, another feature of the recipient strain. For *C. metallidurans* NE12, Ni^{2+} resistance determinants are transferred with the lowest frequency of ± 10^{-5} transconjugants per recipient cell, Ni^{2+} resistance determinants of *C. metallidurans* NA1 and NA2 are transferred with a frequency of ± 10^{-4} and ± 10^{-3} transconjugants per recipient cell, respectively. For *C. metallidurans* NA4, a large difference was observed in transfer frequency for recipients 1 and 3 compared to recipient 2. The frequency for recipients 1 and 3 was ± 10^{-1} transconjugants per recipient cell, while only ± 10^{-5} for recipient 2 (Table 7.3).

Table 7.3: Transfer frequencies of Ni^{2+} resistance determinants per recipient cell in *C. metallidurans*

Transconjugant	Transconjugants/recipient	Average
AE104_1xNA1	9.17×10^{-4}	
AE104_2xNA1	9.50×10^{-4}	6.72×10^{-4}
AE104_3xNA1	1.50×10^{-4}	
AE104_1xNA2	2.88×10^{-3}	
AE104_2xNA2	1.35×10^{-3}	1.87×10^{-3}
AE104_3xNA2	1.38×10^{-3}	
AE104_1xNA4	2.00×10^{-1}	
AE104_2xNA4	6.87×10^{-5}	1.01×10^{-1}
AE104_3xNA4	1.03×10^{-1}	
AE104_1xNE12	5.22×10^{-5}	
AE104_2xNE12	1.45×10^{-4}	7.13×10^{-5}
AE104_3xNE12	1.68×10^{-5}	

7.3.2 Plasmid profiles of the transconjugants

For *C. metallidurans* NA1, NA2 and NE12, 6 suitable transconjugants were screened for their plasmid content. All transconjugants of AE104xNA1 contained the largest plasmid of NA1, while for NA2 and NE12, the only plasmid present was found in all investigated AE104xNA2 and AE104xNE12 transconjugants. One transconjugant of each was selected for further experiments (Figure 7.1). In the case of *C. metallidurans* NA4, 4 transconjugants that each showed a different plasmid profile were selected (Figure 7.1). Apparently, it seems that *C. metallidurans* NA4 harbours an additional fourth plasmid that is ambiguously observed (Figure 7.1, Chapter 4). However, transconjugants AE104_3xNA4_1 and AE104_2xNA4_2 clearly harbour a plasmid that is larger than the other 3 plasmids present in NA4. AE104_3xNA4_1 contains also the smallest plasmid of NA4, while AE104_2xNA4_2 harbours also the second largest plasmid. Transconjugant AE104_3xNA4_2 has only the smallest plasmid of NA4, while AE104_2xNA4_1 holds all plasmids (Figure 7.1).

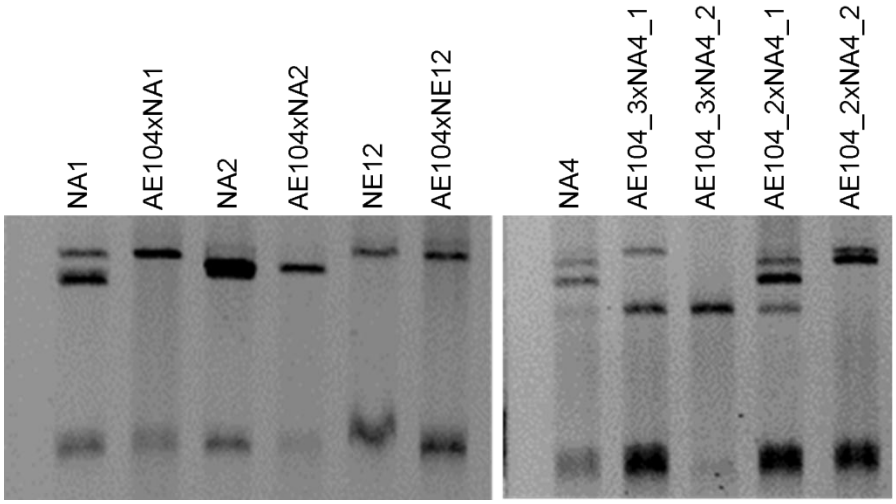

Figure 7.1: Plasmid profile of the different transconjugants. *C. metallidurans* NA1; AE104xNA1; *C. metallidurans* NA2; AE104xNA2; *C. metallidurans* NE12; AE104xNE12; *C. metallidurans* NA4; different NA4 transconjugants AE104_3xNA4_1, AE104_3xNA4_2, AE104_2xNA4_1 and AE104_2xNA4_2.

7.3.3 Metal ion resistance

To explore the metal resistance markers that are located on the transferred plasmids, each transconjugant was screened for its resistance to Ni^{2+}, Co^{2+}, Zn^{2+}, Cu^{2+} and Cr^{4+} ions in a Tris-buffered mineral medium with gluconate as carbon source. MIC values were determined after 3 days (Figure 7.2). For *C. metallidurans* NA1, metal resistance determinants for at least Ni^{2+}, Co^{2+} and Zn^{2+} are located on its largest plasmid, in *C. metallidurans* NA2, resistance determinants for at least Ni^{2+} and partially Co^{2+} and Zn^{2+} are plasmid-borne. The plasmid of *C. metallidurans* NE12 harbours metal resistance determinants for at least Ni^{2+}, Co^{2+}, Zn^{2+} and Cu^{2+}. The smallest plasmid of *C. metallidurans* NA4 can only provide part of the Ni^{2+} resistance. In addition, it provides partial resistance to Zn^{2+} and Cr^{2+}. A combination of the small plasmid with larger plasmid seems to be necessary to obtain full Zn^{2+} resistance while a combination of the 2 largest plasmids

seem needed to acquire full Co^{2+} resistance. The second smallest plasmid seems to provide complete Cu^{2+} and Cr^{4+} resistance (Figure 7.2). However, these data still need to be confirmed.

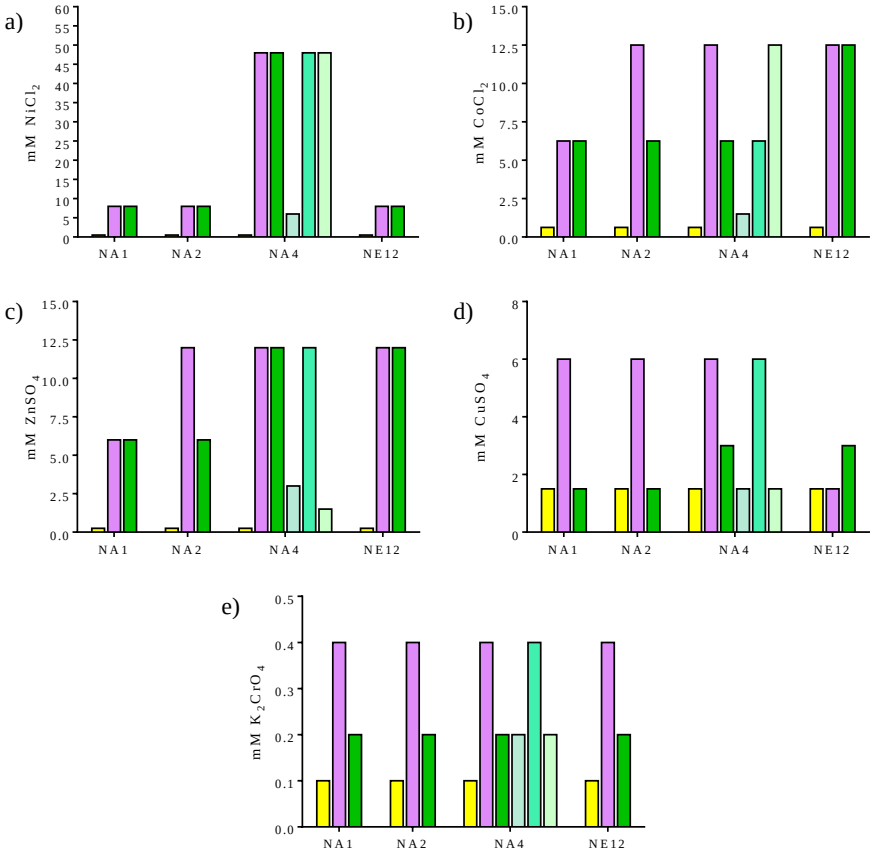

Figure 7.2: Metal ion MIC values in mM for the different transconjugants and *C. metallidurans* isolates after 3 days for a) Ni^{2+}, b) Co^{2+}, c) Zn^{2+}, d) Cu^{2+} and e) Cr^{4+}. Yellow bars represent MIC values for AE104, purple bars represent MIC values of the isolates, and transconjugants are presented as different shades of green.

7.3.4 Mobilization frequency

When *C. metallidurans* NA4 was the donor, many transconjugants contained the smallest plasmid present in NA4. Therefore, it was investigated if NA4 was able to mobilize a broad-host range RSF1010-derived vector to *C.*

metallidurans AE104_Tm. After 3 days, the average frequency of mobilization was 2.25 x 10^{-5} per recipient cell (Table 7.4).

Table 7.4: Mobilization frequency of the plasmid pKT230 with *C. metallidurans* NA4 as helper strain.

	Transconjugants/recipients	**Average**
Conjugation 1	1.73 x 10-5	
Conjugation 2	2.06 x 10-5	2.25 x 10-5
Conjugation 3	2.97 x 10-5	

The plasmid profile of 17 different transconjugants was sreened most of them contained the smallest plasmid (Figure 7.3).

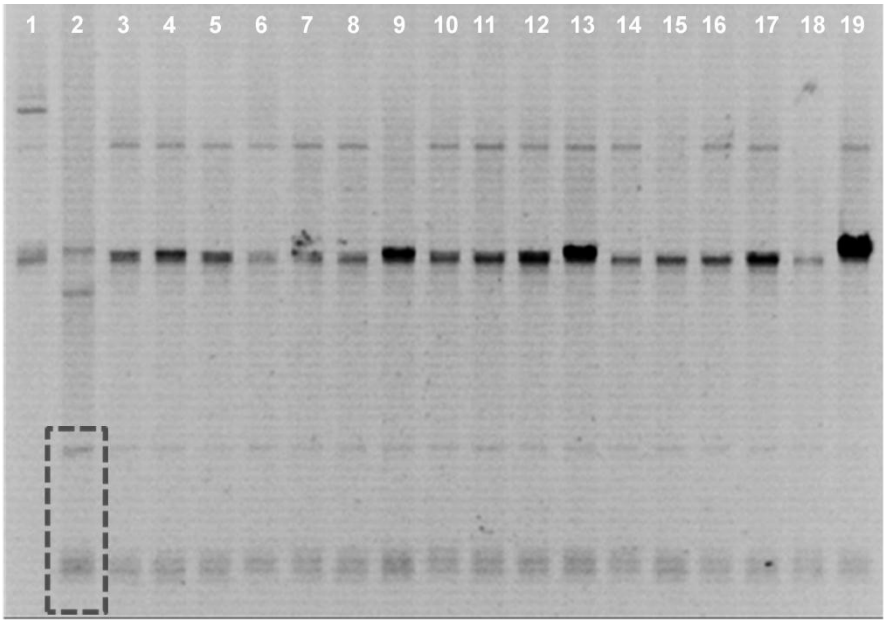

Figure 7.3: Plasmid extraction of transconjugants after mobilization of the pKT230 plasmid. (1) *C. metallidurans* NA4, (2) pKT230, (3-19) transcojugants. Bands representing plasmid pKT230 are surrounded by a dotted frame.

7.3.5 Plasmid stability in *E. coli*

To investigate if the smallest plasmid of *C. metallidurans* NA4 is a broad-host range plasmid, matings were performed between *E. coli* DH5α and NA4. Possible transconjugants were selected on M9 medium supplemented with glucose and thiamine hydrocholoride and 1 mM $NiCl_2$. However, with this experimental setup, no transconjugants were obtained.

7.4 Discussion

The two megaplasmids pMOL28 and pMOL30 of type strain *C. metallidurans* CH34 are already studied in detail. It was shown that the transfer frequency of both plasmids was rather low with frequencies of 10^{-8} transconjugants per recipient cell [169]. The same frequency was observed when matings were performed between *C. metallidurans* AE104 and plasmids pTOM8 and pTOM9 from *C. metallidurans* 31A, plasmids pGOE1 and pGOE2 from *C. metallidurans* KT02 and plasmid pJB4 from *C. pinatubonensis* JMP134 [169, 283]. These are much lower than the transfer frequency observed with plasmid pHG1 from *C. eutrophus* H16 [284] and the frequencies observed with the *C. metallidurans* space isolates, ranging from 10^{-5} in the case of *C. metallidurans* NE12 till 10^{-1} for *C. metallidurans* NA4. For type strain CH34, it was suggested that the genomic island CMGI-28b, located in the region for conjugative transfer, putatively plays a role in the inhibition of plasmid transfer [146]. However, comparative whole genome hybridization between 16 *C. metallidurans* isolates from different locations, and type strain CH34 showed that this genomic island is 100% conserved in *C. metallidurans* NA1 and NE12, and 90% in NA2 (see Appendix A), which all show a higher transfer frequency. Therefore, it is possible that other factors play a more important role.

Interestingly, the transfer frequency in *C. metallidurans* NA4 was putatively affected by the transposon insertion site as it is much lower in recipient

AE104_Tm2 compared to the other recipients. Overall, it seems that the transfer frequency is higher compared to the other *C. metallidurans* strains. Putatively, the small plasmid of *C. metallidurans* NA4 plays an important role herein, as it was observed in almost all transconjugants. Moreover, this plasmid was able to mobilize the IncQ plasmid pKT230 to *C. metallidurans* AE104_Tm with a frequency of 10^{-5} transconjugants per recipient cell. Preliminary analysis of the genome sequence of NA4 (Chapter 5) indicated that the putative backbone of the smallest plasmid of *C. metallidurans* NA4 is almost 100% identical to plasmid pAlide201 of *Alicycliphilus denitrificans* K601, isolated from a waste water treatment plant with cyclohexanol as sole carbon source [285], plasmid pAOVO01 from *Acidovorax* sp. JS42, isolated from a site contaminated with nitrobenzene [286], and a plasmid present in *Ralstonia* sp. 5_7_47FAA, isolated from an irritated gastrointestinal tract biopsy tissue from a 25 year old female with Crohn's disease. The plasmid of *C. metallidurans* NA4 differs from these plasmids by harbouring an additional region that contains genes involved in metal resistance. As it is a self-transmissible plasmid, the backbone harbours a complete set of mobilization genes and a type IV secretion system. Plasmid classification can be based on the sequence of the relaxase, as it is essential during conjugative DNA processing. In this way, six different MOB families each having specific characteristics could be determined namely, MOB_F, MOB_H, MOB_Q, MOB_C, MOB_P and MOB_V [287]. Phylogenetic analysis of the relaxase of many plasmids showed that the relaxase from plasmid pAOVO01 belongs to the MOB_F family of relaxases [287]. Since this protein is conserved in *C. metallidurans* NA4, we can conclude that the smallest plasmid of this isolate belongs to the MOB_F family of conjugative plasmids. Moreover, analysis of the relaxase sequence indicates the presence of conserved catalytic domains typically observed in this family. In particular, comparison of this protein with representative relaxases of the MOB_F family suggests that it belongs to the IncW incompatibility group, as it shows the

highest sequence homology with the representative relaxase of this group. However, BLAST analysis of replicon specific primers used to amplify incW plasmids suggest that no specific amplicon could be obtained [288]. Moreover, plasmids belonging to the IncW incompatibility group are considered to be broad-host range plasmids [289], what could not be confirmed for the plasmid of *C. metallidurans* NA4. However, only one experimental setup was carried out during this study. It would be interesting to examine if transconjugants could be obtained after using lower Ni^{2+} concentrations. An additional option would be to screen the plasmid profiles of obtained transconjugants after mobilizing the IncQ plasmid pKT230 to an *E. coli* strain with *C. metallidurans* NA4.

For type strain *C. metallidurans* CH34, it was already shown that a substantial part of its metal resistance determinants is located on the two megaplasmids [57, 146]. In chapter 4, it was shown that there are only a few differences in resistance to the tested metals between the *C. metallidurans* isolates and type strain CH34. Comparative whole genome hybridization between 16 *C. metallidurans* isolates from different locations, and type strain CH34, confirmed that metal resistance gene clusters present in type strain CH34 are highly conserved among all *C. metallidurans* isolates including the space isolates (see Appendix A), suggesting that they acquired it very early in their evolution. With the experiments described in this chapter, we showed that at least part of the metal resistance determinants of the *C. metallidurans* isolates are also located on their megaplasmids. Despite the energetic cost to maintain the plasmids these are still present in the isolates and thus putatively provide an advantage for the isolates to thrive in the space-related environments. Because parts of their resistance mechanisms are located on their megaplasmids, they could be disseminated to different members of the prevailing populations.

7.5 Conclusions

In this chapter, the transfer frequencies of nickel resistance determinants present in the *C. metallidurans* isolates were investigated. The observed frequencies were higher than frequencies observed after matings with plasmids from related species. As it is the case for type strain CH34, a substantial part of the metal resistance determinants carried by the *C. metallidurans* isolates are present on their megaplasmids. These resistance determinants could spread to other populations thereby providing additional features to thrive in particular environments. This is especially important in the case of *C. metallidurans* NA4, as it harbours a smaller broad-host range plasmid able to mobilize other plasmids.

PART III

CONCLUSIONS

Chapter 8

General conclusions and perspectives

8.1 Relevance to space exploration activities

The strong craving of human to explore and colonize worlds beyond our own is a complex undertaking that entails numerous challenges. Beyond all technical challenges of escaping gravity and sustaining life in an inhospitable environment, it depends also on the ability to handle the companionship of one of the oldest and 'simplest' life forms on earth. Microorganisms follow humans everywhere and thus also in in space. Even unmanned spacecrafts carry a variety of microbial contaminations introduced during the construction by human hands. During the search for life beyond Earth, one aspect is to prevent forward contamination of the destination by terrestrial microorganisms. Considering the ubiquity of microorganisms that constitute the microflora of a healthy human being, it is impossible to organize human space missions without microorganisms as fellow travellers.

Spacecrafts occupied by humans, such as the ISS, function as closed systems for long time-periods and present a number of specificities in terms of microbial prevalence and diversity. The microbial populations in these man-made environments mainly come from the crew but also environmental microorganisms are present. Unique environmental conditions such as microgravity, radiation, restricted hygienic practices and radiation favour colonization by some species rather than others. Astronauts are facing the same unique physical circumstances combined with high working pressure and psychological stressors. These factors compromise the immune system

of astronauts making them more sensitive to infections. Although most microorganisms pose no severe risks for healthy people, the hampered immune system combined with limited treatment and isolation possibilities, and no immediate return to Earth, reinforces the requirement to control microbial contamination stringently. Moreover, *in vitro* studies suggest that microorganisms may even become more pathogenic and more resistant to antibiotic treatment [153]. Next to harming the crew's health, microorganisms can also have adverse effects on the infrastructure of the space station resulting in system failure. Therefore, the contamination level as well as its diversity needs to be controlled, to guarantee adequate living quality and reduce the risks of harmful effects on the crew.

To date, no microbiological events aboard the ISS have been reported that had a critical impact on the crew [290]. However, the current biomonitoring strategy on the ISS is not sufficient to provide an accurate and complete follow-up of the spacecraft's microbial environment. Therefore, it is impossible to verify that this assumption is justified without a deeper analysis of the link between the biomonitoring strategy and crew health protection. Moreover, fluctuations in microbial concentrations and biocontamination events in the ISS, and occasional contamination hazards were reported, indicating that some specific habitat and hardware areas of the space station were apparently more prone to contamination. During this PhD project, the focus was in particular on the closely related β-proteobacterial genera *Cupriavidus* and *Ralstonia*. These genera thrive in many natural environments (soil, water, plant) and were already isolated from harsh man-made environments such as non-ferrous industry, mine areas and metal factories [139], from highly controlled clean environments such as hospitals [157], and from ultrapure industrial water systems [158]. Apparently, *Cupriavidus* and *Ralstonia* are also ubiquitously present in different space-related environments. *Cupriavidus* is one of the predominant

genera in the air of spacecraft assembly facilities before human activity [154] and *Ralstonia* belongs to the main fraction of cultivable species isolated from the surface of the Mars Odyssey Orbiter prior to flight [140]. In addition, both genera have been found in cooling and drinking water from the Mir space station [141, 156], the Shuttle [152], and the ISS [141, 156]. A four-year monitoring campaign (spread over the period 2000-2004) on the ISS SVO-ZV system – which dispenses both the Russian ground-supplied and the CWC water for consumption – showed that bacterial contamination levels were above the acceptability limit of 100 CFU/100 ml in 60% of the samples. Although these recurrent contaminations elicited a series of remediation actions, contamination levels increased always above the acceptability limit soon afterward [50]. The main objective of this study was to gain more insights in the survival and adaptation capabilities of *C. metallidurans* and *R. pickettii* strains that putatively mediate their persistence in these space-related environments.

Interestingly, the results discussed in Chapter 4 indicated that extreme resistance is not essential for surviving these harsh environments with dedicated cleaning and sanitation plans. Most of the analysed phenotypes of the isolates are common to *C. metallidurans* and *R. pickettii*, as they were similar to that of their respective type strains, which were isolated from different environments (*C. metallidurans* CH34 from soil polluted with metal and *R. pickettii* ATCC27511 from human tissue clinical origin). The first beneficial trait is that the isolates have the ability to survive in oligotrophic environments. A possible survival strategy adopted in oligotrophic conditions is to enter a reversible state of reduced metabolic activity or dormancy. These so-called persister cells decrease energetic expenditures to a minimum resulting in an increased resistance against antibiotics and disinfectants [291]. It was shown that *Ralstonia solanacearum* was able to survive over 4 years in river water, maintaining a

non-growing but cultivable population with retention of its virulence during the whole period [205]. Putatively, the *C. metallidurans* and *R. pickettii* isolates studied here adapt similarly during the long time-period in water. Dormant microorganisms exhibit a wide range of phenotypes e.g. reduction in cell size, reduced concentrations of nucleic acids, lipids fatty acids and proteins and an increase in concentration of storage compounds. It would be interesting in future studies to characterize the phenotypic behaviour of the isolates in potable water and to elucidate in detail the molecular mechanisms that are involved. A possible noteworthy aspect would be investigating the role of polyhydroxyalkanoates (PHA) such as polyhydroxybutyrate (PHB) in this survival mechanism. PHB is a polymer that is accumulated in intracellular granules to store energy when nutrient supplies are imbalanced and several genes involved in PHB synthesis are present in *C. metallidurans* CH34 [56]. Although in this study, cells could be resuscitated and proliferated during the whole period, this might be dependent on the experimental conditions (e.g. growth medium, incubation temperature) that are used. In this way, cells can putatively escape detection via culture dependent methods, which are currently used to monitor contamination levels aboard the ISS.

In addition to their capability to survive in oligotrophic conditions, all isolates acquired moderate to high resistance to several stressors (UV-C, antibiotics and metals). Metal resistance especially seems to be advantageous for the isolates in the water systems. Resistance to nickel is beneficial as an increase in nickel ions is observed in the internal active thermal control system, which removes heat from the crew and equipment, due to the general corrosion of the heat exchanger material [197]. In addition, resistance to silver is of special interest taking into account its use as water disinfectant aboard the ISS. The ISS MORD identifies 4.6 µM as the maximum tolerated silver concentration in potable water. However,

chemical analysis of samples returned from the ISS indicated that the dissolved silver concentration in SRV-K potable water was always below 0.86 µM and in SVO-ZV potable water this concentration ranged from 0.21 to 2.61 µM (both measured from Oct 2006 to Oct 2007) [201]. This decrease seems to be due to a rapid deposition of silver onto the metallic surfaces of the water distribution systems, which makes it unavailable for microbial control [197]. It was shown in Chapter 4 that the isolates could withstand silver concentrations that were often higher than those used in the ISS. Therefore, this will not eradicate the contamination nor inhibit growth when sufficient nutrients are present. Most of the isolates harbour a number of RND-driven efflux pumps shown to be involved in silver detoxification in type strain *C. metallidurans* CH34. It is therefore essential that the silver concentrations aboard the ISS are continuously monitored, and maintained close to the maximum allowed levels. However, this alone will probably not be the most suitable solution as it is shown in Chapter 5 that *C. metallidurans* is able to adapt to toxic silver concentrations. Consequently, it would be of interest to study alternative disinfectants to obtain improved control and prevention strategies. To this end, the isolates could be screened in future studies for their resistance to a wide range of possible alternative disinfectants (e.g. H_2O_2, quaternary ammonium salts, and chlorine) or combinations thereof. However, searching alternative disinfectants would not be the most straightforward task as silver has a lot of advantageous in its use as disinfection agent. Although it is shown to be highly toxic against microorganisms, silver ions seem to show limited risks towards human health. In that way, silver does not need to be removed before consumption. Moreover, it has no unfavourable effect on the colour, taste and odour of the water (Chapter 2).

Finally, the persistence of contamination and its resistance to disinfectants can be promoted by biofilm formation. It was shown in Chapter 4 that most

isolates were able to form biofilms on polystyrene and it should be further investigated if they are capable forming biofilms on other materials more relevant for space-related environments (e.g. stainless steels). However, it seems a typical feature of both species as *C. metallidurans* is able to grow in biofilms on soil particles [292] and gold grains [293], while *R. pickettii* is often found in biofilms in plastic water piping (PVC) [188], commonly used to distribute water. Biofilm formation can be promoted by the formation of pits on surfaces due to intensive cleaning, and on its turn, this will lead to higher corrosion rate [196]. Also in the water system aboard the ISS, it was observed that pitting could occur due to the deposition of the silver disinfectant onto the metallic surfaces [197]. Consequently silver concentrations decrease and cannot exert their toxic affect anymore. In addition, intervals of disinfection could lead to regrowth of biofilm communities and increased resistant to the disinfectant, reflecting the importance of a continuous disinfectant residual [294].

At this moment, it is not yet clear whether *C. metallidurans* is able to cause human infection (Chapter 4). However, *R. pickettii* strains have been reported to be opportunistic human pathogens [157, 186], and such contamination in drinking water could pose a potential threat for astronauts as the human immune system is depressed in space conditions [153]. As currently the identification methods that are available for in-flight screening of the water quality are not fully validated, consumption of contaminated water (even without pathogens) is prohibited. This type of contamination wastes tremendous amounts of crew time and Earth-based resources and require materials to be transferred both to and from the ISS with transport costs to deliver items to the ISS running up to 10,000 euros per kilogram. The ultimate challenge for the future is to develop a completely closed loop in which there is a full recycling of high quality water. However, currently, there is still a high level of resupply necessary and in-flight analysis tools are

reduced due to limited aboard technologies and crew time. Moreover, there is no remediation potential after microbial contamination. Preventing, through adequate design, and identifying critical points in the environment or system that are potentially prone to contamination build-up and biofilm formation are essential. Therefore, the current monitoring tools should be critically evaluated and optimized, as they should be able to simultaneously quantify and identify contamination aboard, and to circumvent the necessity for post-flight analyses. These molecular assays would be less time consuming for the astronauts and allow quick and autonomous decisions by the crew resulting in an accurate assessment and remediation of contamination problems aboard space stations.

8.2 Relevance to terrestrial applications

The advantages of the use of silver as disinfectants have been discussed in Chapter 2. Silver has no negative effects on odour, taste and colour of the water, and human health. Therefore, silver is used as (co-)disinfectant in many water systems on Earth. For example, it is used as disinfectant of swimming pool water, hospital hot water systems and potable water systems. Moreover, the increase in occurrence and number of antibiotic-resistant strains revived the interest in the antimicrobial effects of Ag^{+}. Today, especially AgNPs are of interest as their specific physiochemical characteristics makes them interesting not only for their antimicrobial purposes but also for use in inks, microelectronics and medical imaging. This resulted in a tremendous increase in the use of AgNPs and consequently in an increase of silver in the environment. However, the risks of AgNPs to human health are not clarified yet. Moreover, silver resistance determinants are widely spread among environmental and clinically relevant bacteria and are often located on mobile genetic elements (also in the *C. metallidurans* and *R. pickettii* isolates). This is of concern as in this way it can induce their dissemination in the environment and thereby cross-resistance to antibiotics.

Therefore, future studies are necessary to tackle the precise mechanism of Ag^+ and AgNPs toxicity and resistance. Detailed knowledge of all these factors can lead to an improvement of the many applications of silver and to a better estimation of the risks associated with human health and ecosystems (Chapter 2).

In this study, the formation of putative nanoparticles by *C. metallidurans* was observed. There already exist many chemical and physical methods to produces nanoparticles. However, these methods have the disadvantage to be expensive and labour intensive. Furthermore, it is difficult to control the size of the nanoparticles and they require toxic chemicals (Chapter 2). Therefore, the production of eco-friendly nanoparticles with use of biomaterials would be interesting and these strains could be suitable for these purposes. It was shown already that *C. metallidurans* CH34 was able to produce nanoparticles of Au by the reduction of Au^{3+} in Au^+-C compounds and nanoparticulate Au^0 [293]. In addition, *C. metallidurans* CH34 could be used as catalyst in the production of Pd^0 nanoparticles as it harbours highly active hydrogenases that nucleate Pd^{2+} reduction via H_2 oxidation [295]. In addition, about 20 years ago, it was shown already that this strain was useful for the bioremediation of Cd^{2+}, Zn^{2+}, Ni^{2+}, Cu^{2+} and Pb^{2+} from metal-contaminated wastewater and soils [296, 297]. Together with the recent data, it further strengthens the possibility to use this species for the bioremediation of heavy metals.

8.3 Novel silver resistance mechanism in *C. metallidurans*

This study discovered the adaptation of *C. metallidurans* to toxic silver concentrations not mediated by the known silver resistance mechanisms, comprising different efflux pumps. Instead, the involvement of the two-component system AgrRS that cross-regulated a small uncharacterized

protein MmmQ was discovered. Our data suggested that mutation of *agrS* leads to induction of *agrR*, which in turn affects expression of (among other) *mmmQ* resulting in an increased resistance against silver. This cross-regulation, due to a similar AgrR binding site in the *agrR* and *mmmQ* promoter, was indirectly confirmed *in vivo* in *E. coli*. Further experiments are recommended to confirm the direct binding of AgrR on the *mmmQ* promoter. Possible techniques to achieve this are electrophoretic mobility shift or pull-down assays.

Until now, the two-component system AgrRS was not linked to metal resistance [144]. The small protein MmmQ and other homologous small proteins, which are apparently only conserved in *Cupriavidus* and *Ralstonia* species, have been shown to be induced by different metals [57, 144] including silver nitrate (Chapter 4). This study shows the importance of *mmmQ* in the adaptive response to silver toxicity as deletion of the *mmmQ* results in loss of silver resistance, while resistance could be restored after plasmid-mediated complementation of *mmmQ*. In addition, MmmQ was purified, its structure was analysed and possible binding with Ag^+ was investigated (Chapter 4). It appears that MmmQ adopts a random-coil formation rather than a specific native structure. This can explain the fact that is was not able to bind Ag^+, as such intrinsically disordered proteins often undergo induced folding in the presence of the right partner molecule [217]. So far, the precise role of these proteins in the response to metals is not fully elucidated, however, our data indicate that it would be highly interesting to further study their role and function more in detail. Transcriptional expression could be screened in the presence of increasing concentrations of metals to investigate if they respond specific and/or in a dose-responsive manner. Moreover, deletion mutants can be made and the effect on metal resistance (or other stressors) could be explored. Complementary, the genes can be conditionally expressed in *E. coli* and

metal resistance can be examined. Moreover, purification of other proteins of this group and comparison of their native structure can reveal if the random-coil formation is a typical feature of these proteins. Screening for possible binding partners and analysing their effect on the native structure would be of interest. Obtained results can provide a better understanding about the role and mode of action of these unique proteins in metal resistance (or other stressors).

Interestingly, the system discovered in this study seems to be much more efficient, as it gives the strains the ability to withstand much higher silver concentrations. The latter putatively could be facilitated by the accumulation of silver ions and their reduction in nanoparticles making them unable to exert their toxic action. Further experiments are planned to explore the formation of putative nanoparticles and the involved genes and proteins, more in detail.

8.4 Mobile genetic elements

In addition to the basic problem of contamination, bacteria are capable of horizontal gene transfer, a process by which genetic material can be exchanged between individuals in the same generation, within a population or between populations that are more or less related. Horizontal gene transfer is mainly (though not exclusively) mediated by DNA entities called MGEs, which possess specialized genetic features that promote their own mobility. Additionally, they frequently encode passenger genes, genetic determinants unrelated to transfer functions but confer fitness-enhancing properties to the bacterial host, such as resistance to metals, antibiotics or the ability to degrade xenobiotic compounds. Horizontal transfer of such MGEs is a major motor of bacterial evolution, as it enables bacteria to adapt quickly and extensively to their environment [277].

Type strain *C. metallidurans* CH34 is known to carry a large diversity of MGEs, including plasmids, genomic islands, transposons, integrative and conjugative elements, and IS elements, that play an important role in its metabolic potential. Multiple genomic islands, especially those on its megaplasmids, harbour gene clusters involved in metal resistance. Its capacity to degrade toluene, to fix carbon dioxide and to oxidize hydrogen is located on Tn*4371*-like integrative and conjugative elements [56, 161]. In addition, this study revealed 9 new IS elements in *C. metallidurans* CH34. In total, 21 distinct IS elements, classified into 10 different families reaching 57 intact IS copies, were characterized. A number of these IS elements were associated with genomic islands, gene inactivation and rearrangements that alter the autotrophic growth capacities of CH34. The latter rearrangements were triggered by IS*1071*-mediated excision. That IS*1071*-mediated excision can alter the metabolic potential of a host is shown also in *C. pinatubonensis* JMP134 and *Comamonas* sp. strain JS46 were it affected the ability to degrade xenobiotic compounds [247, 298]. This IS element is often associated with organic xenobiotic degradative gene functions and recently it has been shown that it is more abundant in soils treated with pesticides. Moreover, the increased prevalence of IS*1071*-specific sequences in treated systems was accompanied by an increase in the capacity to mineralize the applied pesticides [299]. In this way, hosts containing these MGEs might contribute to the spreading of catabolic genes. Linking the presence of IS elements with the ecology of the species involved, may shed light on the evolutionary role of IS elements. Comparative whole genome hybridization illustrated that IS*1071*-like elements are present in *C. metallidurans* NA1, NA2 and NA4 (see Appendix A). Although, it is not associated with autothrophic growth in these isolates (Chapter 4), it would be interesting to investigate in future studies if it can also influence the metabolic potential of these strains. Next to IS*1071*-mediated changes, transposition of other IS elements could alter the metal resistance potential of *C. metallidurans* and

transposition could be induced by IS trapping (Chapter 6). Moreover, IS transposition was the basis of 3 out of 4 silver resistant mutants (Chapter 5). Transposition of IS elements can be induced by physical or chemical stresses. For example, in *B. cenocepacia*, IS transposition was observed after oxidative stress [300], in *Deinococcus radiodurans* increased transposition after exposure to γ- and UV irradiation [301] and in *E. coli* after nutritional stress [259]. Next to the transposition of IS elements, 10 IS elements showed differential expression to one or more metals, an environmental stress to which *C. metallidurans* CH34 is well adapted. These observations indicate, that IS elements play an active role in *C. metallidurans* CH34, its metabolic potential and adaptation under selective pressure.

The wide plethora of MGEs in type strain *C. metallidurans* CH34 is not conserved in all *C. metallidurans* isolates (although the presence of other MGEs cannot be excluded at this point), while almost all gene clusters of CH34 involved in metal resistance are present. Moreover, as in CH34, at least a part of the metal resistance determinants is located on one of their megaplasmids (Chapter 7). In at least all *C. metallidurans* isolates, *silCBA*, a HME-RND efflux pump involved in silver resistance is located on their megaplasmids. These plasmids were able to transfer to another *C. metallidurans* strains and in addition, the smallest plasmid of *C. metallidurans* NA4 was able to mobilize other plasmids (Chapter 7). As it is shown that the frequency of conjugative transfer and mobilization of plasmids does not differ in Gram-negative bacteria under space flight conditions [302] they could be disseminated to different members of the contaminating population, making disinfection more difficult. Mechanisms necessary to resist metals are generally the same as those of antibiotic resistance [198] and co-selection between them has been frequently reported [for a comprehensive overview, see 129]. Therefore, tolerance to heavy metals can be an additional advantage as it can putatively influence

antibiotic resistance and vice versa. Furthermore, many species that thrive on building materials, causing damage to the infrastructure, are also capable of spreading their genetic material by horizontal transfer [152].

8.5 Conclusion

With this study, some pieces of the puzzle that hold the key to how *C. metallidurans* and *R. pickettii* isolates are able to thrive in harsh and strictly controlled space-related environments were put together. It seems that tolerance to several stressors, combined with the ability to grow in oligotrophic conditions seems to be beneficial for surviving in these environments. In addition, a novel silver resistance mechanism in *C. metallidurans* was discovered that gives the strains the ability to withstand very high silver concentrations. These observations have implications for (1) long-term manned space missions, as silver is used as disinfectant in potable water systems aboard the ISS and (2) terrestrial applications, as silver and silver nanoparticles are increasingly used in many applications because of their antimicrobial purposes.

Bibliography

1. Aponte VM, Finch DS, Klaus DM (2006) Considerations for non-invasive in-flight monitoring of astronaut immune status with potential use of MEMS and NEMS devices. Life Sci 79: 1317-1333
2. Aviles H, Belay T, Fountain K, Vance M, Sonnenfeld G (2003) Increased susceptibility to *Pseudomonas aeruginosa* infection under hindlimb-unloading conditions. J Appl Physiol 95: 73-80
3. Mehta SK, Pierson DL, Cooley H, Dubow R, Lugg D (2000) Epstein-Barr virus reactivation associated with diminished cell-mediated immunity in antarctic expeditioners. J Med Virol 61: 235-240
4. Duncan JM, Bogomolov VV, Castrucci F, Koike Y, Comtois JM, Sargsyan AE (2008) Organization and management of the International Space Station (ISS) multilateral medical operations. Acta Astronautica 63: 1137-1147
5. ISS MORD (2009) SSP 50260: ISS Medical Operations Requirement Document. Houston.
6. Sessa R, Di PM, Schiavoni G, Santino I, Altieri A, Pinelli S, Del PM (2002) Microbiological indoor air quality in healthy buildings. New Microbiol 25: 51-56
7. Dacarro C, Picco AM, Grisoli P, Rodolfi M (2003) Determination of aerial microbiological contamination in scholastic sports environments. J Appl Microbiol 95: 904-912
8. Brief RS, Bernath T (1988) Indoor pollution: Guidelines for prevention and control of microbiological respiratory hazards associated with air conditioning and ventilation system. Applied Industrial Hygiene 3: 5-10
9. Verhoeff A (1993) Biological Particles in Indoor Environments. European Collaborative Action, Indoor Air Quality and Its Impact on Man, COST Project 613, Report N 12, EUR 14988 EN1993, Luxembourg.
10. WHO (2008) World Health Organization: Guidelines for drinking-water quality: incorporating 1st and 2nd addenda, Vol.1, Recommendations., Geneva
11. Dawson DJ, Sartory DP (2000) Microbiological safety of water. Br Med Bull 56: 74-83
12. Mulvey D, Redding P, Robertson C, Woodall C, Kingsmore P, Bedwell D, Dancer SJ (2011) Finding a benchmark for monitoring hospital cleanliness. J Hosp Infect 77: 25-30
13. Kemp PC, Neumeister-Kemp HG (2005) Australian Mould Guideline: AMG-2005-1. Myco Logia Australia Pty Ltd

14. Husman T (1996) Health effects of indoor-air microorganisms. Scand J Work Environ Health 22: 5-13
15. Cox CS (1995) Physical aspects of bioareosol particles. In: Cox, CS, Wathes, CM (eds.) Bioaerosols Handbook. CRC Press, Boca Rotan, Florida, pp. 15-25
16. Morawska L (2006) Droplet fate in indoor environments, or can we prevent the spread of infection? Indoor Air 16: 335-347
17. Cox CS (1995) Stability of airborne microbes and allergens. In: Cox, CS, Wathes, CM (eds.) Bioaerosols Handbook. CRC Press, Boca Rotan, Florida, pp. 77-99
18. Eames I, Tang JW, Li Y, Wilson P (2009) Airborne transmission of disease in hospitals. J R Soc Interface 6 Suppl 6: S697-702
19. Tang JW (2009) The effect of environmental parameters on the survival of airborne infectious agents. Journal of the Royal Society Interface 6: S737-S746
20. Castro VA, Bruce RJ, Ott CM, Pierson DL (2006) The Influence of Microbiology on Spacecraft Design and Controls: A Historical Perspective of the Shuttle and International Space Station Programs. International Conference On Environmental Systems, Norfolk, VA, USA.
21. NASA (2005) International Space Station bacteria filter element service life evaluation. Houston.
22. Volodina E, Nagolkin A, Fedotov A (2003) Air cleaning device for destruction of microbes based on electroporation effect. In: Wirtanen, G, Salo, S (eds.) 34th R3-Nordic Contamination Control Symposium, Turku, Finland, pp. 199-204.
23. NASA (2005) MR052L, Microbial Analysis of ISS Air Using the Microbial Air Sampler (MAS). Houston.
24. Van Houdt R, Michiels CW (2010) Biofilm formation and the food industry, a focus on the bacterial outer surface. J Appl Microbiol 109: 1117-1131
25. Van Houdt R, Michiels CW (2005) Role of bacterial cell surface structures in *Escherichia coli* biofilm formation. Res Microbiol 156: 626-633
26. Debus A (2006) The European standard on planetary protection requirements. Res Microbiol 157: 13-18
27. NASA (2005) MR050L, Microbial Analysis of ISS Surfaces Using the Surface Sampler Kit (SSK). Houston.
28. Berry D, Xi C, Raskin L (2006) Microbial ecology of drinking water distribution systems. Curr Opin Biotechnol 17: 297-302
29. Szewzyk U, Szewzyk R, Manz W, Schleifer KH (2000) Microbiological safety of drinking water. Annu Rev Microbiol 54: 81-127

30. Wingender J, Flemming HC (2004) Contamination potential of drinking water distribution network biofilms. Water Sci Technol 49: 277-286
31. Emtiazi F, Schwartz T, Marten SM, Krolla-Sidenstein P, Obst U (2004) Investigation of natural biofilms formed during the production of drinking water from surface water embankment filtration. Water Res 38: 1197-1206
32. Stewart PS, Rayner J, Roe F, Rees WM (2001) Biofilm penetration and disinfection efficacy of alkaline hypochlorite and chlorosulfamates. J Appl Microbiol 91: 525-532
33. Straub JE, Plumlee DK, Schultz JR (2009) Chemical analysis results for potable water returned from ISS Expeditions 14 and 15. SAE Int J Aerosp 1: 556-577
34. Bruce RJ, Ott CM, Skuratov VM, Pierson DL (2005) Microbial surveillance of potable water sources of the International Space Station. SAE transactions 114: 283-292
35. James JT, Parmet AJ, Pierson DL (2008) Aerospace toxicology and microbiology. In: Davis, JR, Johnson, R, Stepanek, J, Fogarty, JA (eds.) Fundamentals of aerospace medicine, 4th edn. Lippincott, Williams & Wilkins, Philadelphia, pp. 236-250
36. Jenkins DR (1996) Space Shuttle: The History of Developing the National Space Transportation System. Motorbooks International, Minneapolis
37. NASA (2005) MR051L, Microbial Analysis of ISS Water using the Water Microbiology Kit (WMK) and the Microbiology Water Analysis Kit. Houston.
38. Perchonok M, Douglas G (2008) Risk Factor of an Inadequate Food SystemHuman Research Evidence Book. National Aeronautics and Space Administration, Houston
39. NASA (2006) SD-T-0251, Microbiological Specification and Testing Procedure for Foods Which Are Not Commercially Sterile. Houston.
40. Lachance PA (1997) How HACCP started. Food Technology 51: 35
41. Novikova ND (2004) Review of the knowledge of microbial contamination of the Russian manned spacecraft. Microb Ecol 47: 127-132
42. Novikova N, De Boever P, Poddubko S, Deshevaya E, Polikarpov N, Rakova N, Coninx I, Mergeay M (2006) Survey of environmental biocontamination on board the International Space Station. Res Microbiol 157: 5-12
43. Castro VA, Thrasher AN, Healy M, Ott CM, Pierson DL (2004) Microbial characterization during the early habitation of the International Space Station. Microb Ecol 47: 119-126

44. Osman S, La Duc MT, Dekas A, Newcombe D, Venkateswaran K (2008) Microbial burden and diversity of commercial airline cabin air during short and long durations of travel. ISME J 2: 482-497
45. Van Houdt R, De Boever P, Coninx I, Le Calvez C, Dicasillati R, Mahillon J, Mergeay M, Leys N (2009) Evaluation of the airborne bacterial population in the periodically confined Antarctic base Concordia. Microb Ecol 57: 640-648
46. Berry CA (1973) View of human problems to be addressed for long-duration space flights. Aerosp Med 44: 1136-1146
47. Pasanen AL, Heinonentanski H, Kalliokoski P, Jantunen MJ (1992) Fungal microcolonies on indoor surfaces - An explanation for the base-level fungal spore counts in indoor air. Atmospheric Environment Part B-Urban Atmosphere 26: 117-120
48. Cabral JP (2010) Can we use indoor fungi as bioindicators of indoor air quality? Historical perspectives and open questions. Sci Total Environ 408: 4285-4295
49. Hardin BD, Kelman BJ, Saxon A (2003) Adverse human health effects associated with molds in the indoor environment. J Occup Environ Med 45: 470-478
50. Bruce RJ, Ott CM, Skuratov VM, Pierson DL (2005) Microbial Surveillance of Potable Water Sources of the International Space Station. SAE transactions 114: 283-292
51. Morris HC, Monaco LA, Steele A, Wainwright N (2010) Setting a standard: the limulus amebocyte lysate assay and the assessment of microbial contamination on spacecraft surfaces. Astrobiology 10: 845-852
52. Maule J, Wainwright N, Steele A, Monaco L, Morris H, Gunter D, Damon M, Wells M (2009) Rapid culture-independent microbial analysis aboard the International Space Station (ISS). Astrobiology 9: 759-775
53. McAlister MB, Kulakov LA, O'Hanlon JF, Larkin MJ, Ogden KL (2002) Survival and nutritional requirements of three bacteria isolated from ultrapure water. J Ind Microbiol Biotechnol 29: 75-82
54. Alvarez B, Lopez MM, Biosca EG (2008) Survival strategies and pathogenicity of *Ralstonia solanacearum* phylotype II subjected to prolonged starvation in environmental water microcosms. Microbiol 154: 3590-3598
55. Mergeay M, Monchy S, Janssen P, Van Houdt R, Leys N (2009) Megaplasmids in *Cupriavidus* genus and metal resistance. In: Schwartz, E (ed.) Microbial megaplasmids. Springer, Berlin, pp. 209-238
56. Janssen PJ, Van Houdt R, Moors H, Monsieurs P, Morin N, Michaux A, Benotmane MA, Leys N, Vallaeys T, Lapidus A, Monchy S, Medigue C, Taghavi S, McCorkle S, Dunn J, van der Lelie D, Mergeay M (2010) The complete genome sequence of

Cupriavidus metallidurans strain CH34, a master survivalist in harsh and anthropogenic environments. PLoS One 5: e10433

57. Monchy S, Benotmane MA, Janssen P, Vallaeys T, Taghavi S, van der Lelie D, Mergeay M (2007) Plasmids pMOL28 and pMOL30 of *Cupriavidus metallidurans* are specialized in the maximal viable response to heavy metals. J Bacteriol 189: 7417-7425
58. Alexander JW (2009) History of the medical use of silver. Surg Infect (Larchmt) 10: 289-292
59. Klasen HJ (2000) Historical review of the use of silver in the treatment of burns. I. Early uses. Burns 26: 117-130
60. Yahya MT, Landeen LK, Messina MC, Kutz SM, Schulze R, Gerba CP (1990) Disinfection of bacteria in water systems by using electrolytically generated copper:silver and reduced levels of free chlorine. Can J Microbiol 36: 109-116
61. Jung WK, Kim SH, Koo HC, Shin S, Kim JM, Park YK, Hwang SY, Yang H, Park YH (2007) Antifungal activity of the silver ion against contaminated fabric. Mycoses 50: 265-269
62. Chopra I (2007) The increasing use of silver-based products as antimicrobial agents: a useful development or a cause for concern? J Antimicrob Chemother 59: 587-590
63. McHugh GL, Moellering RC, Hopkins CC, Swartz MN (1975) *Salmonella typhimurium* resistant to silver nitrate, chloramphenicol, and ampicillin. Lancet 1: 235-240
64. Silver S (2003) Bacterial silver resistance: molecular biology and uses and misuses of silver compounds. FEMS Microbiol Rev 27: 341-353
65. Haefeli C, Franklin C, Hardy K (1984) Plasmid-determined silver resistance in *Pseudomonas stutzeri* isolated from a silver mine. J Bacteriol 158: 389-392
66. Silver S, Gupta A, Matsui K, Lo JF (1999) Resistance to Ag^+ cations in bacteria: environments, genes and proteins. Metal Based Drugs 6: 315-320
67. Drake PL, Hazelwood KJ (2005) Exposure-related health effects of silver and silver compounds: a review. Ann Occup Hyg 49: 575-585
68. Lansdown AB (2010) A pharmacological and toxicological profile of silver as an antimicrobial agent in medical devices. Adv Pharmacol Sci 2010: 910686
69.
70. World Health Organization (1996) Silver in drinking water: Background document for the development of WHO Guidelines for drinking water quality: WHO, Geneva, Switzerland, WHO/SDE/WSH/03.04/14
71. Flegal AR, Brown CL, Squire S, Ross JR, Scelfo GM, Hibdon S (2007) Spatial and temporal variations in silver contamination and toxicity in San Francisco Bay. Environ Res 105: 34-52

72. Yudkins J (1937) The effect of silver ions on some enzymes of *Bacterium coli*. Enzymologia 2: 161-170
73. Chambers C, Proctor C, Kabler P (1962) Bactericidal effect of low concentrations of silver. American Water Works Association 54: 208-216
74. Russell AD, Hugo WB (1994) Antimicrobial activity and action of silver. Prog Med Chem 31: 351-370
75. Gordon O, Vig Slenters T, Brunetto PS, Villaruz AE, Sturdevant DE, Otto M, Landmann R, Fromm KM (2010) Silver coordination polymers for prevention of implant infection: thiol interaction, impact on respiratory chain enzymes, and hydroxyl radical induction. Antimicrob Agents Chemother 54: 4208-4218
76. Dibrov P, Dzioba J, Gosink KK, Hase CC (2002) Chemiosmotic mechanism of antimicrobial activity of Ag^+ in *Vibrio cholerae*. Antimicrob Agents Chemother 46: 2668-2670
77. Schreurs WJ, Rosenberg H (1982) Effect of silver ions on transport and retention of phosphate by *Escherichia coli*. J Bacteriol 152: 7-13
78. Bragg PD, Rainnie DJ (1974) Effect of silver ions on the respiratory chain of *Escherichia coli*. Can J Microbiol 20: 883-889
79. Hayashi M, Miyoshi T, Sato M, Unemoto T (1992) Properties of respiratory chain-linked Na^+-independent NADH-Quinone reductase in a marine *Vibrio alginolyticus*. Biochim Biophys Acta 1099: 145-151
80. Semeykina AL, Skulachev VP (1990) Submicromolar Ag^+ increases passive Na^+ permeability and inhibits the respiration-supported formation of Na^+ gradient in *Bacillus* FTU vesicles. FEBS Letters 269: 69-72
81. Liau SY, Read DC, Pugh WJ, Furr JR, Russell AD (1997) Interaction of silver nitrate with readily identifiable groups: relationship to the antibacterial action of silver ions. Lett Appl Microbiol 25: 279-283
82. Cabiscol E, Tamarit J, Ros J (2000) Oxidative stress in bacteria and protein damage by reactive oxygen species. Int Microbiol 3: 3-8
83. Park HJ, Kim JY, Kim J, Lee JH, Hahn JS, Gu MB, Yoon J (2009) Silver-ion-mediated reactive oxygen species generation affecting bactericidal activity. Water Research 43: 1027-1032
84. Matsumura Y, Yoshikata K, Kunisaki S, Tsuchido T (2003) Mode of bactericidal action of silver zeolite and its comparison with that of silver nitrate. Appl Environ Microbiol 69: 4278-4281
85. Xiu ZM, Ma J, Alvarez PJ (2011) Differential effect of common ligands and molecular oxygen on antimicrobial activity of silver nanoparticles versus silver ions. Environ Sci Technol 45: 9003-9008
86. Kim JY, Lee C, Cho M, Yoon J (2008) Enhanced inactivation of *E. coli* and MS-2 phage by silver ions combined with UV-A and visible light irradiation. Water Res 42: 356-362

87. Gupta A, Maynes M, Silver S (1998) Effects of halides on plasmid-mediated silver resistance in *Escherichia coli*. Appl Environ Microbiol 64: 5042-5045
88. Edwards-Jones V (2009) The benefits of silver in hygiene, personal care and healthcare. Lett Appl Microbiol 49: 147-152
89. Li XZ, Nikaido H, Williams KE (1997) Silver-resistant mutants of *Escherichia coli* display active efflux of Ag^+ and are deficient in porins. J Bacteriol 179: 6127-6132
90. Rai MK, Deshmukh SD, Ingle AP, Gade AK (2012) Silver nanoparticles: the powerful nanoweapon against multidrug-resistant bacteria. J Appl Microbiol 112: 841-852
91. Perelaer J, Hendriks CE, de Laat AW, Schubert US (2009) One-step inkjet printing of conductive silver tracks on polymer substrates. Nanotechnology 20: 165303
92. Wu HP, Liu JF, Wu XJ, Ge MY, Wang YW, Zhang GQ, Jiang JZ (2006) High conductivity of isotropic conductive adhesives filled with silver nanowires. Int J Adhes Adhes 26: 617-621
93. Jain PK, Huang XH, El-Sayed IH, El-Sayed MA (2008) Noble metals on the nanoscale: optical and photothermal properties and some applications in imaging, sensing, biology, and medicine. Accounts Chem Res 41: 1578-1586
94. Fabrega J, Luoma SN, Tyler CR, Galloway TS, Lead JR (2011) Silver nanoparticles: behaviour and effects in the aquatic environment. Environ Int 37: 517-531
95. Pokhrel LR, Dubey B (2012) Potential impact of low-concentration silver nanoparticles on predator-prey interactions between predatory dragonfly nymphs and *Daphnia magna* as a Prey. Environ Sci Technol 46: 7755-7762
96. Elechiguerra JL, Burt JL, Morones JR, Camacho-Bragado A, Gao X, Lara HH, Yacaman MJ (2005) Interaction of silver nanoparticles with HIV-1. J Nanobiotechnology 3: 6
97. Rogers JV, Parkinson CV, Choi YW, Speshock JL, Hussain SM (2008) A preliminary assessment of silver nanoparticle inhibition of monkeypox virus plaque formation. Nanoscale Research Letters 3: 129-133
98. De Gusseme B, Hennebel T, Christiaens E, Saveyn H, Verbeken K, Fitts JP, Boon N, Verstraete W (2011) Virus disinfection in water by biogenic silver immobilized in polyvinylidene fluoride membranes. Water Res 45: 1856-1864
99. Pal S, Tak YK, Song JM (2007) Does the antibacterial activity of silver nanoparticles depend on the shape of the nanoparticle? A study of the Gram-negative bacterium *Escherichia coli*. Appl Environ Microbiol 73: 1712-1720

100. El Badawy AM, Silva RG, Morris B, Scheckel KG, Suidan MT, Tolaymat TM (2011) Surface charge-dependent toxicity of silver nanoparticles. Environ Sci Technol 45: 283-287
101. Panacek A, Kvitek L, Prucek R, Kolar M, Vecerova R, Pizurova N, Sharma VK, Nevecna T, Zboril R (2006) Silver colloid nanoparticles: synthesis, characterization, and their antibacterial activity. J Phys Chem B 110: 16248-16253
102. Sotiriou GA, Pratsinis SE (2010) Antibacterial activity of nanosilver ions and particles. Environmental Science & Technology 44: 5649-5654
103. Morones JR, Elechiguerra JL, Camacho A, Holt K, Kouri JB, Ramirez JT, Yacaman MJ (2005) The bactericidal effect of silver nanoparticles. Nanotechnology 16: 2346-2353
104. Xiu ZM, Zhang QB, Puppala HL, Colvin VL, Alvarez PJ (2012) Negligible particle-specific antibacterial activity of silver nanoparticles. Nano Lett 12: 4271-4275
105. El Badawy AM, Luxton TP, Silva RG, Scheckel KG, Suidan MT, Tolaymat TM (2010) Impact of environmental conditions (pH, ionic strength, and electrolyte type) on the surface charge and aggregation of silver nanoparticles suspensions. Environ Sci Technol 44: 1260-1266
106. Schacht VJ, Neumann LV, Sandhi SK, Chen L, Henning T, Klar PJ, Theophel K, Schnell S, Bunge M (2013) Effects of silver nanoparticles on microbial growth dynamics. J Appl Microbiol 114: 25-35
107. Nanda A, Saravanan M (2009) Biosynthesis of silver nanoparticles from *Staphylococcus aureus* and its antimicrobial activity against MRSA and MRSE. Nanomed-Nanotechnol 5: 452-456
108. Saravanan M, Vemu AK, Bank SK (2011) Rapid biosynthesis of silver nanoparticles from *Bacillus megaterium* (NCIM 2326) and their antibacterial activity on multi drug resistant clinical pathogens. Colloids and Surfaces B-Biointerfaces 88: 325-331
109. Kumar CG, Mamidyala SK (2011) Extracellular synthesis of silver nanoparticles using culture supernatant of *Pseudomonas aeruginosa*. Colloids and Surfaces B-Biointerfaces 84: 462-466
110. Shahverdi AR, Fakhimi A, Shahverdi HR, Minaian S (2007) Synthesis and effect of silver nanoparticles on the antibacterial activity of different antibiotics against *Staphylococcus aureus* and *Escherichia coli*. Nanomed-Nanotechnol 3: 168-171
111. Klaus T, Joerger R, Olsson E, Granqvist CG (1999) Silver-based crystalline nanoparticles, microbially fabricated. Proc Natl Acad Sci U S A 96: 13611-13614
112. Sedlak RH, Hnilova M, Grosh C, Fong H, Baneyx F, Schwartz D, Sarikaya M, Tamerler C, Traxler B (2012) Engineered Escherichia

coli silver-binding periplasmic protein that promotes silver tolerance. Appl Environ Microbiol 78: 2289-2296
113. Jelenko C, 3rd (1969) Silver nitrate resistant *E. coli*: report of case. Ann Surg 170: 296-299
114. Kremer AN, Hoffmann H (2012) Subtractive hybridization yields a silver resistance determinant unique to nosocomial pathogens in the *Enterobacter cloacae* complex. J Clin Microbiol 50: 3249-3257
115. Davis IJ, Richards H, Mullany P (2005) Isolation of silver- and antibiotic-resistant *Enterobacter cloacae* from teeth. Oral Microbiol Immunol 20: 191-194
116. Holland SL, Dyer PS, Bond CJ, James SA, Roberts IN, Avery SV (2011) *Candida argentea* sp. nov., a copper and silver resistant yeast species. Fungal Biol 115: 909-918
117. Gupta A, Matsui K, Lo JF, Silver S (1999) Molecular basis for resistance to silver cations in *Salmonella*. Nat Med 5: 183-188
118. Silver S, Phung le T, Silver G (2006) Silver as biocides in burn and wound dressings and bacterial resistance to silver compounds. J Ind Microbiol Biotechnol 33: 627-634
119. Franke S (2007) Microbiology of the toxic noble metal silver. In: Nies, D, Silver, S (eds.) Molecular Biology of Heavy Metals. Microbiology Monographs, pp. 343-355
120. Franke S, Grass G, Rensing C, Nies DH (2003) Molecular analysis of the copper-transporting efflux system CusCFBA of *Escherichia coli*. J Bacteriol 185: 3804-3812
121. Franke S, Grass G, Nies DH (2001) The product of the *ybdE* gene of the *Escherichia coli* chromosome is involved in detoxification of silver ions. Microbiology 147: 965-972
122. Munson GP, Lam DL, Outten FW, O'Halloran TV (2000) Identification of a copper-responsive two-component system on the chromosome of *Escherichia coli* K-12. J Bacteriol 182: 5864-5871
123. Long F, Su CC, Zimmermann MT, Boyken SE, Rajashankar KR, Jernigan RL, Yu EW (2010) Crystal structures of the CusA efflux pump suggest methionine-mediated metal transport. Nature 467: 484-488
124. Zimmermann M, Udagedara SR, Sze CM, Ryan TM, Howlett GJ, Xiao Z, Wedd AG (2012) PcoE - A metal sponge expressed to the periplasm of copper resistance *Escherichia coli*. Implication of its function role in copper resistance. Journal of inorganic biochemistry 115: 186-197
125. Lok CN, Ho CM, Chen R, Tam PK, Chiu JF, Che CM (2008) Proteomic identification of the Cus system as a major determinant of constitutive *Escherichia coli* silver resistance of chromosomal origin. J Proteome Res 7: 2351-2356

126. Gudipaty SA, Larsen AS, Rensing C, McEvoy MM (2012) Regulation of Cu(I)/Ag(I) efflux genes in *Escherichia coli* by the sensor kinase CusS. FEMS Microbiol Lett 330: 30-37
127. Cunningham JH, Lin LS (2010) Fate of amoxicillin in mixed-culture bioreactors and its effects on microbial growth and resistance to silver ions. Environmental Science & Technology 44: 1827-1832
128. Nakajima H, Kobayashi K, Kobayashi M, Asako H, Aono R (1995) Overexpression of the robA gene increases organic solvent tolerance and multiple antibiotic and heavy metal ion resistance in Escherichia coli. Appl Environ Microbiol 61: 2302-2307
129. Baker-Austin C, Wright MS, Stepanauskas R, McArthur JV (2006) Co-selection of antibiotic and metal resistance. Trends Microbiol 14: 176-182
130. Gupta A, Phung LT, Taylor DE, Silver S (2001) Diversity of silver resistance genes in IncH incompatibility group plasmids. Microbiology 147: 3393-3402
131. Starodub ME, Trevors JT (1989) Silver resistance in *Escherichia coli* R1. Journal of medical microbiology 29: 101-110
132. Deshpande LM, Chopade BA (1994) Plasmid mediated silver resistance in *Acinetobacter baumannii*. Biometals 7: 49-56
133. Van Houdt R, Toussaint A, Ryan M, Pembroke J, Mergeay M, Adley CC (2012) The Tn*4371* ICE family of bacterial mobile genetic elements. In: Roberts, AP, Mullany, P (eds.) Bacterial Integrative Mobile Genetic Elements. Landes Bioscience, Austin, United States, Austin, TX, pp. 1-22
134. Tappin AD, Barriada JL, Braungardt CB, Evans EH, Patey MD, Achterberg EP (2010) Dissolved silver in European estuarine and coastal waters. Water Res 44: 4204-4216
135. Bryan GW, Langston WJ (1992) Bioavailability, accumulation and effects of heavy metals in sediments with special reference to United Kingdom estuaries: a review. Environmental pollution 76: 89-131
136. Kaegi R, Voegelin A, Ort C, Sinnet B, Thalmann B, Krismer J, Hagendorfer H, Elumelu M, Mueller E (2013) Fate and transformation of silver nanoparticles in urban wastewater systems. Water Res
137. Aminov RI (2011) Horizontal gene exchange in environmental microbiota. Front Microbiol 2: 158
138. Heuer H, Kopmann C, Binh CT, Top EM, Smalla K (2009) Spreading antibiotic resistance through spread manure: characteristics of a novel plasmid type with low % G+C content. Environ Microbiol 11: 937-949
139. Goris J, De Vos P, Coenye T, Hoste B, Janssens D, Brim H, Diels L, Mergeay M, Kersters K, Vandamme P (2001) Classification of metal-resistant bacteria from industrial biotopes as *Ralstonia campinensis* sp. nov., *Ralstonia metallidurans* sp. nov. and *Ralstonia*

basilensis Steinle et al. 1998 emend. Int J Syst Evol Microbiol 51: 1773-1782

140. La Duc MT, Nicholson W, Kern R, Venkateswaran K (2003) Microbial characterization of the Mars Odyssey spacecraft and its encapsulation facility. Environ Microbiol 5: 977-985
141. Ott CM, Bruce RJ, Pierson DL (2004) Microbial characterization of free floating condensate aboard the Mir space station. Microb Ecol 47: 133-136
142. Coenye T, Spilker T, Reik R, Vandamme P, Lipuma JJ (2005) Use of PCR analyses to define the distribution of *Ralstonia* species recovered from patients with cystic fibrosis. J Clin Microbiol 43: 3463-3466
143. Langevin S, Vincelette J, Bekal S, Gaudreau C (2011) First case of invasive human infection caused by *Cupriavidus metallidurans*. J Clin Microbiol 49: 744-745
144. Monsieurs P, Moors H, Van Houdt R, Janssen PJ, Janssen A, Coninx I, Mergeay M, Leys N (2011) Heavy metal resistance in *Cupriavidus metallidurans* CH34 is governed by an intricate transcriptional network. Biometals 24: 1133-1151
145. Van Houdt R, Mergeay M (2012) Plasmids as Secondary Chromosomes. In: Bell, E, Bond, PJS, Klinman, PJP, Masters, DBSS, Wells, PRD (eds.) Molecular Life Sciences: An Encyclopedic Reference. Springer-Verlag Berlin Heidelberg, Germany, pp. 1-4.
146. Mergeay M, Monchy S, Vallaeys T, Auquier V, Benotmane A, Bertin P, Taghavi S, Dunn J, van der Lelie D, Wattiez R (2003) *Ralstonia metallidurans*, a bacterium specifically adapted to toxic metals: towards a catalogue of metal-responsive genes. FEMS Microbiol Rev 27: 385-410
147. Auquier V (2006) Identification et caractérisation de protéines membranaires impliquées dans les systèmes de résistance aux métaux lourds chez *Cupriavidus metallidurans* CH34. Université Libre de Bruxelles
148. Bersch B, Derfoufi KM, De Angelis F, Auquier V, Ngonlong Ekende E, Mergeay M, Ruysschaert JM, Vandenbussche G (2011) Structural and Metal Binding Characterization of the C-Terminal Metallochaperone Domain of Membrane Fusion Protein SilB from *Cupriavidus metallidurans* CH34. Biochemistry 50: 2194-2204
149. Van Houdt R, Monsieurs P, Mijnendonckx K, Provoost A, Janssen A, Mergeay M, Leys N (2012) Variation in genomic islands contribute to genome plasticity in *Cupriavidus metallidurans*. BMC Genomics 13: 111
150. Mijnendonckx K, Provoost A, Ott CM, Venkateswaran K, Mahillon J, Leys N, Van Houdt R (2013) Characterization of the survival

ability of *Cupriavidus metallidurans* and *Ralstonia pickettii* from space-related environments. Microb Ecol 56: 347-360
151. Van Houdt R, Mijnendonckx K, Leys N (2012) Microbial contamination monitoring and control during human space missions. Planetary and Space Science 60: 115-120
152. Pierson DL (2001) Microbial contamination of spacecraft. Gravit Space Biol Bull 14: 1-6
153. Klaus DM, Howard HN (2006) Antibiotic efficacy and microbial virulence during space flight. Trends Biotechnol 24: 131-136
154. Newcombe D, Duc ML, Vaishampayan P, Venkateswaran K (2008) Impact of assembly, testing and launch operations on the airborne bacterial diversity within a spacecraft assembly facility clean-room. Int J Astrobiol 7: 223–236
155. La Duc MT, Kern R, Venkateswaran K (2004) Microbial monitoring of spacecraft and associated environments. Microb Ecol 47: 150-158
156. Baker PW, Leff L (2004) The effect of simulated microgravity on bacteria from the Mir space station. Microgravity Sci Technol 15: 35-41
157. Ryan MP, Pembroke JT, Adley CC (2006) *Ralstonia pickettii:* a persistent gram-negative nosocomial infectious organism. J Hosp Infect 62: 278-284
158. Kulakov LA, McAlister MB, Ogden KL, Larkin MJ, O'Hanlon JF (2002) Analysis of bacteria contaminating ultrapure water in industrial systems. Appl Environ Microbiol 68: 1548-1555
159. Van Houdt R, Michiels CW (2010) Biofilm formation and the food industry, a focus on the bacterial outer surface. J Appl Microbiol 109: 1117-1131
160. Mergeay M, Monchy S, Janssen P, Van Houdt R, Leys N (2009) Megaplasmids in *Cupriavidus* Genus and Metal ResistanceMicrobial Megaplasmids, 1 edn. Springer-Verlag, Berlin Heidelberg, Germany, pp. 209 - 238
161. Van Houdt R, Monchy S, Leys N, Mergeay M (2009) New mobile genetic elements in *Cupriavidus metallidurans* CH34, their possible roles and occurrence in other bacteria. Antonie Van Leeuwenhoek 96: 205-226
162. Schwartz E, Henne A, Cramm R, Eitinger T, Friedrich B, Gottschalk G (2003) Complete nucleotide sequence of pHG1: a *Ralstonia eutropha* H16 megaplasmid encoding key enzymes of H(2)-based ithoautotrophy and anaerobiosis. J Mol Biol 332: 369-383
163. Trefault N, De la Iglesia R, Molina AM, Manzano M, Ledger T, Perez-Pantoja D, Sanchez MA, Stuardo M, Gonzalez B (2004) Genetic organization of the catabolic plasmid pJP4 from *Ralstonia eutropha* JMP134 (pJP4) reveals mechanisms of adaptation to chloroaromatic pollutants and evolution of specialized chloroaromatic degradation pathways. Environ Microbiol 6: 655-668

164. Mergeay M, Houba C, Gerits J (1978) Extrachromosomal inheritance controlling resistance to cadmium, cobalt, copper and zinc ions: evidence from curing in a *Pseudomonas* [proceedings]. Arch Int Physiol Biochim 86: 440-442
165. Ralston E, Palleron.Nj, Doudorof.M (1973) Pseudomonas-pickettii, a new species of clinical origin related to Pseudomonas-solanacearum. Int J Syst Bacteriol 23: 15-19
166. Blattner FR, Plunkett G, 3rd, Bloch CA, Perna NT, Burland V, Riley M, Collado-Vides J, Glasner JD, Rode CK, Mayhew GF, Gregor J, Davis NW, Kirkpatrick HA, Goeden MA, Rose DJ, Mau B, Shao Y (1997) The complete genome sequence of *Escherichia coli* K-12. Science 277: 1453-1462
167. Bobe L, Kochetkov A, Soloukhin V, Andreichuk P, Protasov N, Sinyak Y (2008) International Conference On Environmental Systems. SAE International: San Francisco, CA, USA
168. Benardini J, Ballinger J, Crawford RL, Roman M, Sumner R, Venkateswaran K (2005) International Space Station Internal active thermal control system: an initial assessment of the microbial communities within fluid from ground support and flight hardware. SAE International papers 2005-01-3094: 1-8
169. Mergeay M, Nies D, Schlegel HG, Gerits J, Charles P, Van Gijsegem F (1985) *Alcaligenes eutrophus* CH34 is a facultative chemolithotroph with plasmid-bound resistance to heavy metals. J Bacteriol 162: 328-334
170. Hulton CS, Higgins CF, Sharp PM (1991) ERIC sequences: a novel family of repetitive elements in the genomes of *Escherichia coli*, *Salmonella typhimurium* and other enterobacteria. Mol Microbiol 5: 825-834
171. Andrup L, Barfod KK, Jensen GB, Smidt L (2008) Detection of large plasmids from the *Bacillus cereus* group. Plasmid 59: 139-143
172. O'Toole GA, Kolter R (1998) Initiation of biofilm formation in *Pseudomonas fluorescens* WCS365 proceeds via multiple, convergent signalling pathways: a genetic analysis. Mol Microbiol 28: 449-461
173. Christensen GD, Simpson WA, Younger JJ, Baddour LM, Barrett FF, Melton DM, Beachey EH (1985) Adherence of coagulase-negative *staphylococci* to plastic tissue culture plates: a quantitative model for the adherence of *staphylococci* to medical devices. J Clin Microbiol 22: 996-1006
174. Aertsen A, Van Houdt R, Vanoirbeek K, Michiels CW (2004) An SOS response induced by high pressure in *Escherichia coli*. J Bacteriol 186: 6133-6141
175. Coohill TP, Sagripanti JL (2008) Overview of the inactivation by 254 nm ultraviolet radiation of bacteria with particular relevance to biodefense. Photochem Photobiol 84: 1084-1090

176. Moissl C, Osman S, La Duc MT, Dekas A, Brodie E, DeSantis T, Venkateswaran K (2007) Molecular bacterial community analysis of clean rooms where spacecraft are assembled. FEMS Microbiol Ecol 61: 509-521
177. Newcombe DA, Schuerger AC, Benardini JN, Dickinson D, Tanner R, Venkateswaran K (2005) Survival of spacecraft-associated microorganisms under simulated martian UV irradiation. Appl Environ Microbiol 71: 8147-8156
178. Osman S, Peeters Z, La Duc MT, Mancinelli R, Ehrenfreund P, Venkateswaran K (2008) Effect of shadowing on survival of bacteria under conditions simulating the Martian atmosphere and UV radiation. Appl Environ Microbiol 74: 959-970
179. Brim H, Heyndrickx M, de Vos P, Wilmotte A, Springael D, Schlegel HG, Mergeay M (1999) Amplified rDNA restriction analysis and further genotypic characterization of metal-resistant soil bacteria and related facultative hydrogenotrophs. Syst Appl Microbiol 22: 258-268
180. Taghavi S, Mergeay M, van der Lelie D (1997) Genetic and physical maps of the *Alcaligenes eutrophus* CH34 megaplasmid pMOL28 and its derivative pMOL50 obtained after temperature-induced mutagenesis and mortality. Plasmid 37: 22-34
181. Mijnendonckx K, Provoost A, Monsieurs P, Leys N, Mergeay M, Mahillon J, Houdt RV (2011) Insertion sequence elements in *Cupriavidus metallidurans* CH34: Distribution and role in adaptation. Plasmid 65: 193-203
182. Lejeune P, Mergeay M, Van Gijsegem F, Faelen M, Gerits J, Toussaint A (1983) Chromosome transfer and R-prime plasmid formation mediated by plasmid pULB113 (RP4::mini-Mu) in *Alcaligenes eutrophus* CH34 and *Pseudomonas fluorescens* 6.2. J Bacteriol 155: 1015-1026
183. Mergeay M, Sadouk A, Diels L, Faelen M, Gerits J, Denecke J, Powell B (1987) High-level spontaneous mutagenesis revealed by survival at nonoptimal temperature in *Alcaligenes eutrophus* CH34. Arch Int Physiol Biochim Biophys 95: B36-B36
184. Dong Q, Sadouk A, van der Lelie D, Taghavi S, Ferhat A, Nuyten JM, Borremans B, Mergeay M, Toussaint A (1992) Cloning and sequencing of IS*1086*, an *Alcaligenes eutrophus* insertion element related to IS*30* and IS*4351*. J Bacteriol 174: 8133-8138
185. Langevin S, Vincelette J, Bekal S, Gaudreau C (2010) A first case of invasive human infection caused by *Cupriavidus metallidurans*. J Clin Microbiol
186. Coenye T, Goris J, Spilker T, Vandamme P, LiPuma JJ (2002) Characterization of unusual bacteria isolated from respiratory secretions of cystic fibrosis patients and description of *Inquilinus limosus* gen. nov., sp. nov. J Clin Microbiol 40: 2062-2069

187. Van Houdt R, Monsieurs P, Mijnendonckx K, Provoost A, Janssen A, Mergeay M, Leys N (2012) Variation in genomic islands contribute to genome plasticity in Cupriavidus metallidurans. BMC Genomics 13: 111
188. Anderson RL, Holland BW, Carr JK, Bond WW, Favero MS (1990) Effect of disinfectants on *Pseudomonads* colonized on the interior surface of PVC pipes. Am J Public Health 80: 17-21
189. Ryan MP, Pembroke JT, Adley CC (2007) *Ralstonia pickettii* in environmental biotechnology: potential and applications. J Appl Microbiol 103: 754-764
190. Amadou C, Pascal G, Mangenot S, Glew M, Bontemps C, Capela D, Carrere S, Cruveiller S, Dossat C, Lajus A, Marchetti M, Poinsot V, Rouy Z, Servin B, Saad M, Schenowitz C, Barbe V, Batut J, Medigue C, Masson-Boivin C (2008) Genome sequence of the beta-rhizobium *Cupriavidus taiwanensis* and comparative genomics of rhizobia. Genome Res 18: 1472-1483
191. Venkateswaran K, Kempf M, Chen F, Satomi M, Nicholson W, Kern R (2003) *Bacillus nealsonii* sp. nov., isolated from a spacecraft-assembly facility, whose spores are gamma-radiation resistant. Int J Syst Evol Microbiol 53: 165-172
192. Venkateswaran K, Satomi M, Chung S, Kern R, Koukol R, Basic C, White D (2001) Molecular microbial diversity of a spacecraft assembly facility. Syst Appl Microbiol 24: 311-320
193. Silver S, Phung LT (1996) Bacterial heavy metal resistance: new surprises. Annu Rev Microbiol 50: 753-789
194. Finney LA, O'Halloran TV (2003) Transition metal speciation in the cell: insights from the chemistry of metal ion receptors. Science 300: 931-936
195. Schmidt T, Schlegel HG (1994) Combined nickel-cobalt-cadmium resistance encoded by the ncc locus of *Alcaligenes xylosoxidans* 31A. J Bacteriol 176: 7045-7054
196. Junker B (2009) Corrosion in bioprocessing applications. Bioprocess Biosyst Eng 32: 1-29
197. Roman M, Macuch P, McKrell T, Van der Schijf O (2005) Assessment of microbiologically influenced corrosion potential in the international space station internal active thermal control system heat exchanger materials: a 6-month study. SAE International papers: 1-12
198. van Hoek AH, Mevius D, Guerra B, Mullany P, Roberts AP, Aarts HJ (2011) Acquired antibiotic resistance genes: an overview. Front Microbiol 2: 203
199. Klasen HJ (2000) A historical review of the use of silver in the treatment of burns. II. Renewed interest for silver. Burns 26: 131-138

200. Lin YS, Vidic RD, Stout JE, Yu VL (2002) Negative effect of high pH on biocidal efficacy of copper and silver ions in controlling *Legionella pneumophila*. Appl Environ Microbiol 68: 2711-2715
201. Straub J, Plumlee D, Schultz J (2008) Chemical analysis results for potable water returned from ISS expediotions 14 and 15. SAE International Journal of Aerospace 1: 556-577
202. Lehtola MJ, Miettinen IT, Martikainen PJ (2002) Biofilm formation in drinking water affected by low concentrations of phosphorus. Can J Microbiol 48: 494-499
203. Miettinen IT, Vartiainen T, Martikainen PJ (1997) Phosphorus and bacterial growth in drinking water. Appl Environ Microbiol 63: 3242-3245
204. Jayaraman R (2008) Bacterial persistence: some new insights into an old phenomenon. J Biosci 33: 795-805
205. Alvarez B, Lopez MM, Biosca EG (2008) Survival strategies and pathogenicity of *Ralstonia solanacearum* phylotype II subjected to prolonged starvation in environmental water microcosms. Microbiology 154: 3590-3598
206. Bennett PM (2008) Plasmid encoded antibiotic resistance: acquisition and transfer of antibiotic resistance genes in bacteria. Br J Pharmacol 153 Suppl 1: S347-357
207. Schafer A, Tauch A, Jager W, Kalinowski J, Thierbach G, Puhler A (1994) Small mobilizable multi-purpose cloning vectors derived from the *Escherichia coli* plasmids pK18 and pK19: selection of defined deletions in the chromosome of *Corynebacterium glutamicum*. Gene 145: 69-73
208. Kovach ME, Elzer PH, Hill DS, Robertson GT, Farris MA, Roop RM, Peterson KM (1995) 4 New Derivatives of the Broad-Host-Range Cloning Vector pBBR1MCS, Carrying Different Antibiotic-Resistance Cassettes. Gene 166: 175-176
209. Miller WG, Leveau JH, Lindow SE (2000) Improved *gfp* and *inaZ* broad-host-range promoter-probe vectors. Mol Plant Microbe Interact 13: 1243-1250
210. Guzman LM, Belin D, Carson MJ, Beckwith J (1995) Tight Regulation, Modulation, and High-Level Expression by Vectors Containing the Arabinose PBAD Promoter. Journal of Bacteriology 177: 4121-4130
211. Cardona ST, Valvano MA (2005) An expression vector containing a rhamnose-inducible promoter provides tightly regulated gene expression in *Burkholderia cenocepacia*. Plasmid 54: 219-228
212. Goormaghtigh E, Raussens V, Ruysschaert JM (1999) Attenuated total reflection infrared spectroscopy of proteins and lipids in biological membranes. Bba-Rev Biomembranes 1422: 105-185
213. Laub MT, Goulian M (2007) Specificity in two-component signal transduction pathways. Annu Rev Genet 41: 121-145

214. Perron K, Caille O, Rossier C, Van Delden C, Dumas JL, Kohler T (2004) CzcR-CzcS, a two-component system involved in heavy metal and carbapenem resistance in *Pseudomonas aeruginosa*. J Biol Chem 279: 8761-8768
215. Dieppois G, Ducret V, Caille O, Perron K (2012) The transcriptional regulator CzcR modulates antibiotic resistance and quorum sensing in *Pseudomonas aeruginosa*. PLoS One 7: e38148
216. Monchy S, Benotmane MA, Wattiez R, van Aelst S, Auquier V, Borremans B, Mergeay M, Taghavi S, van der Lelie D, Vallaeys T (2006) Transcriptomic and proteomic analyses of the pMOL30-encoded copper resistance in *Cupriavidus metallidurans* strain CH34. Microbiology 152: 1765-1776
217. Kovacs D, Szabo B, Pancsa R, Tompa P (2013) Intrinsically disordered proteins undergo and assist folding transitions in the proteome. Archives of biochemistry and biophysics 531: 80-89
218. Uversky VN (2013) The most important thing is the tail: Multitudinous functionalities of intrinsically disordered protein termini. FEBS Lett 587: 1891-1901
219. Top E, De Smet I, Verstraete W, Dijkmans R, Mergeay M (1994) Exogenous isolation of mobilizing plasmids from polluted soils and sludges. Appl Environ Microbiol 60: 831-839
220. Van der Auwera GA, Krol JE, Suzuki H, Foster B, Van Houdt R, Brown CJ, Mergeay M, Top EM (2009) Plasmids captured in *C. metallidurans* CH34: defining the PromA family of broad-host-range plasmids. Antonie Van Leeuwenhoek 96: 193-204
221. Diels L, Springael D, van der Lelie N, Top E, Mergeay M (1993) Use of DNA probes and plasmid capture in a search for new interesting environmental genes. Sci Total Environ 139-140: 471-478
222. Craig JW, Chang FY, Brady SF (2009) Natural products from environmental DNA hosted in *Ralstonia metallidurans*. ACS Chem Biol 4: 23-28
223. Craig JW, Chang FY, Kim JH, Obiajulu SC, Brady SF (2010) Expanding small-molecule functional metagenomics through parallel screening of broad-host-range cosmid environmental DNA libraries in diverse proteobacteria. Appl Environ Microbiol 76: 1633-1641
224. Leys N, Baatout S, Rosier C, Dams A, s'Heeren C, Wattiez R, Mergeay M (2009) The response of *Cupriavidus metallidurans* CH34 to spaceflight in the international space station. Antonie Van Leeuwenhoek 96: 227-245
225. Fricke WF, Kusian B, Bowien B (2009) The genome organization of *Ralstonia eutropha* strain H16 and related species of the *Burkholderiaceae*. J Microbiol Biotechnol 16: 124-135

226. Diels L, Mergeay M (1990) DNA probe-mediated detection of resistant bacteria from soils highly polluted by heavy metals. Appl Environ Microbiol 56: 1485-1491
227. Van der Lelie D, *al. e* (1992) Stress and survival in *Alcaligenus eutrophus* CH34: effect of temperature and genetic rearrangements In: Gauthier, M (ed.) Gene Transfers and Environment. Springer-Verlag, Heidelberg
228. Mahillon J, Chandler M (1998) Insertion sequences. Microbiol Mol Biol Rev 62: 725-774
229. Bickhart DM, Gogarten JP, Lapierre P, Tisa LS, Normand P, Benson DR (2009) Insertion sequence content reflects genome plasticity in strains of the root nodule actinobacterium Frankia. BMC Genomics 10: 468
230. Bentley SD, Corton C, Brown SE, Barron A, Clark L, Doggett J, Harris B, Ormond D, Quail MA, May G, Francis D, Knudson D, Parkhill J, Ishimaru CA (2008) Genome of the actinomycete plant pathogen *Clavibacter michiganensis* subsp. sepedonicus suggests recent niche adaptation. J Bacteriol 190: 2150-2160
231. Lin H, Li TY, Xie MH, Zhang Y (2007) Characterization of the variants, flanking genes, and promoter activity of the *Leifsonia xyli* subsp. cynodontis insertion sequence IS*1237*. J Bacteriol 189: 3217-3227
232. Hubner A, Hendrickson W (1997) A fusion promoter created by a new insertion sequence, IS*1490*, activates transcription of 2,4,5-trichlorophenoxyacetic acid catabolic genes in *Burkholderia cepacia* AC1100. J Bacteriol 179: 2717-2723
233. Mira A, Klasson L, Andersson SG (2002) Microbial genome evolution: sources of variability. Curr Opin Microbiol 5: 506-512
234. Schneider D, Lenski RE (2004) Dynamics of insertion sequence elements during experimental evolution of bacteria. Res Microbiol 155: 319-327
235. Schneider D, Faure D, Noirclerc-Savoye M, Barriere AC, Coursange E, Blot M (2000) A broad-host-range plasmid for isolating mobile genetic elements in gram-negative bacteria. Plasmid 44: 201-207
236. Choi KH, Kumar A, Schweizer HP (2006) A 10-min method for preparation of highly electrocompetent *Pseudomonas aeruginosa* cells: application for DNA fragment transfer between chromosomes and plasmid transformation. J Microbiol Methods 64: 391-397
237. Vallenet D, Labarre L, Rouy Z, Barbe V, Bocs S, Cruveiller S, Lajus A, Pascal G, Scarpelli C, Medigue C (2006) MaGe: a microbial genome annotation system supported by synteny results. Nucleic Acids Res 34: 53-65
238. Siguier P, Perochon J, Lestrade L, Mahillon J, Chandler M (2006) ISfinder: the reference centre for bacterial insertion sequences. Nucleic Acids Res 34: D32-36

239. Rice P, Longden I, Bleasby A (2000) EMBOSS: the European Molecular Biology Open Software Suite. Trends Genet 16: 276-277
240. Wagner A, Lewis C, Bichsel M (2007) A survey of bacterial insertion sequences using IScan. Nucleic Acids Res 35: 5284-5293
241. Touchon M, Rocha EP (2007) Causes of insertion sequences abundance in prokaryotic genomes. Mol Biol Evol 24: 969-981
242. De Palmenaer D, Siguier P, Mahillon J (2008) IS*4* family goes genomic. BMC evolutionary biology 8: 18
243. Mathee K, Narasimhan G, Valdes C, Qiu X, Matewish JM, Koehrsen M, Rokas A, Yandava CN, Engels R, Zeng E, Olavarietta R, Doud M, Smith RS, Montgomery P, White JR, Godfrey PA, Kodira C, Birren B, Galagan JE, Lory S (2008) Dynamics of *Pseudomonas aeruginosa* genome evolution. Proc Natl Acad Sci U S A 105: 3100-3105
244. Yang F, Pecina DA, Kelly SD, Kim SH, Kemner KM, Long DT, Marsh TL (2010) Biosequestration via cooperative binding of copper by *Ralstonia pickettii*. Environmental technology 31: 1045-1060
245. Nelson MJ, Montgomery SO, Mahaffey WR, Pritchard PH (1987) Biodegradation of trichloroethylene and involvement of an aromatic biodegradative pathway. Appl Environ Microbiol 53: 949-954
246. Schleheck D, Knepper TP, Fischer K, Cook AM (2004) Mineralization of individual congeners of linear alkylbenzenesulfonate by defined pairs of heterotrophic bacteria. Appl Environ Microbiol 70: 4053-4063
247. Providenti MA, Shaye RE, Lynes KD, McKenna NT, O'Brien JM, Rosolen S, Wyndham RC, Lambert LB (2006) The locus coding for the 3-nitrobenzoate dioxygenase of *Comamonas* sp strain JS46 is flanked by IS*1071* elements and is subject to deletion and inversion events. Applied and Environmental Microbiology 72: 2651-2660
248. Collard JM, Provoost A, Taghavi S, Mergeay M (1993) A new type of *Alcaligenes eutrophus* CH34 zinc resistance generated by mutations affecting regulation of the *cnr* cobalt-nickel resistance system. J Bacteriol 175: 779-784
249. Grass G, Grosse C, Nies DH (2000) Regulation of the *cnr* cobalt and nickel resistance determinant from *Ralstonia sp*. strain CH34. J Bacteriol 182: 1390-1398
250. Tibazarwa C, Wuertz S, Mergeay M, Wyns L, van Der Lelie D (2000) Regulation of the *cnr* cobalt and nickel resistance determinant of *Ralstonia eutropha* (*Alcaligenes eutrophus*) CH34. J Bacteriol 182: 1399-1409
251. Talat M-e- (2000) Genetic mechanism of heavy metal resistance of *Pseudomonas aeruginosa* CMG103. PhD thesis, University of Karachi

252. Nagy Z, Chandler M (2004) Regulation of transposition in bacteria. Res Microbiol 155: 387-398
253. Haritha A, Sagar KP, Tiwari A, Kiranmayi P, Rodrigue A, Mohan PM, Singh SS (2009) MrdH, a novel metal resistance determinant of *Pseudomonas putida* KT2440, is flanked by metal-inducible mobile genetic elements. J Bacteriol 191: 5976-5987
254. Brocklehurst KR, Morby AP (2000) Metal-ion tolerance in *Escherichia coli*: analysis of transcriptional profiles by gene-array technology. Microbiology 146: 2277-2282
255. Ohtsubo Y, Genka H, Komatsu H, Nagata Y, Tsuda M (2005) High-temperature-induced transposition of insertion elements in *burkholderia multivorans* ATCC 17616. Appl Environ Microbiol 71: 1822-1828
256. Tachdjian S, Kelly RM (2006) Dynamic metabolic adjustments and genome plasticity are implicated in the heat shock response of the extremely thermoacidophilic archaeon *Sulfolobus solfataricus*. J Bacteriol 188: 4553-4559
257. Eichenbaum Z, Livneh Z (1998) UV light induces IS*10* transposition in *Escherichia coli*. Genetics 149: 1173-1181
258. Del Re B, Garoia F, Mesirca P, Agostini C, Bersani F, Giorgi G (2003) Extremely low frequency magnetic fields affect transposition activity in *Escherichia coli*. Radiat Environ Biophys 42: 113-118
259. Twiss E, Coros AM, Tavakoli NP, Derbyshire KM (2005) Transposition is modulated by a diverse set of host factors in *Escherichia coli* and is stimulated by nutritional stress. Molecular Microbiology 57: 1593-1607
260. Christie-Oleza JA, Lanfranconi MP, Nogales B, Lalucat J, Bosch R (2009) Conjugative interaction induces transposition of IS*Pst9* in *Pseudomonas stutzeri* AN10. J Bacteriol 191: 1239-1247
261. Tibazarwa C, Wuertz S, Mergeay M, Wyns L, van der Lelie D (2000) Regulation of the *cnr* cobalt and nickel resistance determinant of *Ralstonia eutropha* (*Alcaligenes eutrophus*) CH34. J Bacteriol 182: 1399-1409
262. Brzostowicz PC, Walters DM, Jackson RE, Halsey KH, Ni H, Rouviere PE (2005) Proposed involvement of a soluble methane monooxygenase homologue in the cyclohexane-dependent growth of a new *Brachymonas* species. Environ Microbiol 7: 179-190
263. Tuskan GA, Difazio S, Jansson S, Bohlmann J, Grigoriev I, Hellsten U, Putnam N, Ralph S, Rombauts S, Salamov A, Schein J, Sterck L, Aerts A, Bhalerao RR, Bhalerao RP, Blaudez D, Boerjan W, Brun A, Brunner A, Busov V, Campbell M, Carlson J, Chalot M, Chapman J, Chen GL, Cooper D, Coutinho PM, Couturier J, Covert S, Cronk Q, Cunningham R, Davis J, Degroeve S, Dejardin A, Depamphilis C, Detter J, Dirks B, Dubchak I, Duplessis S, Ehlting J, Ellis B, Gendler K, Goodstein D, Gribskov M, Grimwood J,

Groover A, Gunter L, Hamberger B, Heinze B, Helariutta Y, Henrissat B, Holligan D, Holt R, Huang W, Islam-Faridi N, Jones S, Jones-Rhoades M, Jorgensen R, Joshi C, Kangasjarvi J, Karlsson J, Kelleher C, Kirkpatrick R, Kirst M, Kohler A, Kalluri U, Larimer F, Leebens-Mack J, Leple JC, Locascio P, Lou Y, Lucas S, Martin F, Montanini B, Napoli C, Nelson DR, Nelson C, Nieminen K, Nilsson O, Pereda V, Peter G, Philippe R, Pilate G, Poliakov A, Razumovskaya J, Richardson P, Rinaldi C, Ritland K, Rouze P, Ryaboy D, Schmutz J, Schrader J, Segerman B, Shin H, Siddiqui A, Sterky F, Terry A, Tsai CJ, Uberbacher E, Unneberg P, Vahala J, Wall K, Wessler S, Yang G, Yin T, Douglas C, Marra M, Sandberg G, Van de Peer Y, Rokhsar D (2006) The genome of black cottonwood, *Populus trichocarpa* (Torr. & Gray). Science 313: 1596-1604

264. Astua-Monge G, Lyznik A, Jones V, Mackenzie SA, Vallejos CE (2002) Evidence for a prokaryotic insertion-sequence contamination in eukaryotic sequences registered in different databases. Theor Appl Genet 104: 48-53
265. Binns M (1993) Contamination of DNA database sequence entries with *Escherichia coli* insertion sequences. Nucleic Acids Res 21: 779
266. Sota M, Yano H, Nagata Y, Ohtsubo Y, Genka H, Anbutsu H, Kawasaki H, Tsuda M (2006) Functional analysis of unique class II insertion sequence IS*1071*. Appl Environ Microbiol 72: 291-297
267. Nakatsu C, Ng J, Singh R, Straus N, Wyndham C (1991) Chlorobenzoate catabolic transposon Tn*5271* is a composite class I element with flanking class II insertion sequences. Proc Natl Acad Sci U S A 88: 8312-8316
268. Martinez B, Tomkins J, Wackett LP, Wing R, Sadowsky MJ (2001) Complete nucleotide sequence and organization of the atrazine catabolic plasmid pADP-1 from *Pseudomonas* sp. strain ADP. J Bacteriol 183: 5684-5697
269. Providenti MA, Shaye RE, Lynes KD, McKenna NT, O'Brien J M, Rosolen S, Wyndham RC, Lambert IB (2006) The locus coding for the 3-nitrobenzoate dioxygenase of *Comamonas* sp. strain JS46 is flanked by IS*1071* elements and is subject to deletion and inversion events. Appl Environ Microbiol 72: 2651-2660
270. Junker F, Cook AM (1997) Conjugative plasmids and the degradation of arylsulfonates in *Comamonas testosteroni*. Appl Environ Microbiol 63: 2403-2410
271. Boon N, Goris J, De Vos P, Verstraete W, Top EM (2001) Genetic diversity among 3-chloroaniline- and aniline-degrading strains of the *Comamonadaceae*. Appl Environ Microbiol 67: 1107-1115

272. Sota M, Kawasaki H, Tsuda M (2003) Structure of haloacetate-catabolic IncP-1β plasmid pUO1 and genetic mobility of its residing haloacetate-catabolic transposon. J Bacteriol 185: 6741-6745
273. Clement P, Pieper DH, Gonzalez B (2001) Molecular characterization of a deletion/duplication rearrangement in *tfd* genes from *Ralstonia eutropha* JMP134(pJP4) that improves growth on 3-chlorobenzoic acid but abolishes growth on 2,4-dichlorophenoxyacetic acid. Microbiology 147: 2141-2148
274. Mattes TE, Alexander AK, Richardson PM, Munk AC, Han CS, Stothard P, Coleman NV (2008) The genome of *Polaromonas* sp. strain JS666: insights into the evolution of a hydrocarbon- and xenobiotic-degrading bacterium, and features of relevance to biotechnology. Appl Environ Microbiol 74: 6405-6416
275. Leveau JH, van der Meer JR (1996) The *tfdR* gene product can successfully take over the role of the insertion element-inactivated TfdT protein as a transcriptional activator of the *tfdCDEF* gene cluster, which encodes chlorocatechol degradation in *Ralstonia eutropha* JMP134(pJP4). J Bacteriol 178: 6824-6832
276. Lloyd-Jones G, Lau PC (1997) Glutathione S-transferase-encoding gene as a potential probe for environmental bacterial isolates capable of degrading polycyclic aromatic hydrocarbons. Appl Environ Microbiol 63: 3286-3290
277. Frost LS, Leplae R, Summers AO, Toussaint A (2005) Mobile genetic elements: The agents of open source evolution. Nature Reviews Microbiology 3: 722-732
278. Top EM, Springael D (2003) The role of mobile genetic elements in bacterial adaptation to xenobiotic organic compounds. Curr Opin Biotechnol 14: 262-269
279. Mavrodi DV, Loper JE, Paulsen IT, Thomashow LS (2009) Mobile genetic elements in the genome of the beneficial rhizobacterium Pseudomonas fluorescens Pf-5. BMC Microbiol 9: 8
280. Cardona ST, Mueller CL, Valvano MA (2006) Identification of essential operons with a rhamnose-inducible promoter in *Burkholderia cenocepacia*. Appl Environ Microbiol 72: 2547-2555
281. Figurski DH, Helinski DR (1979) Replication of an origin-containing derivative of plasmid RK2 dependent on a plasmid function provided in trans. Proc Natl Acad Sci U S A 76: 1648-1652
282. Bagdasarian M, Lurz R, Ruckert B, Franklin FCH, Bagdasarian MM, Frey J, Timmis KN (1981) Specific-Purpose Plasmid Cloning Vectors .2. Broad Host Range, High Copy Number, RSF1010-Derived Vectors, and a Host-Vector System for Gene Cloning in *Pseudomonas*. Gene 16: 237-247

283. Schmidt T, Stoppel RD, Schlegel HG (1991) High-Level Nickel Resistance in *Alcaligenes xylosoxydans* 31A and *Alcaligenes eutrophus* KTO2. Appl Environ Microbiol 57: 3301-3309
284. Friedrich B, Hogrefe C, Schlegel HG (1981) Naturally occurring genetic transfer of hydrogen-oxidizing ability between strains of *Alcaligenes eutrophus*. J Bacteriol 147: 198-205
285. Oosterkamp MJ, Veuskens T, Plugge CM, Langenhoff AA, Gerritse J, van Berkel WJ, Pieper DH, Junca H, Goodwin LA, Daligault HE, Bruce DC, Detter JC, Tapia R, Han CS, Land ML, Hauser LJ, Smidt H, Stams AJ (2011) Genome sequences of *Alicycliphilus denitrificans* strains BC and K601T. J Bacteriol 193: 5028-5029
286. Haigler BE, Wallace WH, Spain JC (1994) Biodegradation of 2-nitrotoluene by *Pseudomonas* sp. strain JS42. Appl Environ Microbiol 60: 3466-3469
287. Garcillan-Barcia MP, Francia MV, de la Cruz F (2009) The diversity of conjugative relaxases and its application in plasmid classification. FEMS Microbiol Rev 33: 657-687
288. Gotz A, Pukall R, Smit E, Tietze E, Prager R, Tschape H, vanElsas JD, Smalla K (1996) Detection and characterization of broad-host-range plasmids in environmental bacteria by PCR. Applied and Environmental Microbiology 62: 2621-2628
289. Fernandez-Lopez R, Garcillan-Barcia MP, Revilla C, Lazaro M, Vielva L, de la Cruz F (2006) Dynamics of the IncW genetic backbone imply general trends in conjugative plasmid evolution. Fems Microbiology Reviews 30: 942-966
290. Mermel LA (2013) Infection prevention and control during prolonged human space travel. Clin Infect Dis 56: 123-130
291. Lennon JT, Jones SE (2011) Microbial seed banks: the ecological and evolutionary implications of dormancy. Nat Rev Microbiol 9: 119-130
292. Diels L, Van Roy S, Taghavi S, Van Houdt R (2009) From industrial sites to environmental applications with *Cupriavidus metallidurans*. Antonie Van Leeuwenhoek 96: 247-258
293. Reith F, Etschmann B, Grosse C, Moors H, Benotmane MA, Monsieurs P, Grass G, Doonan C, Vogt S, Lai B, Martinez-Criado G, George GN, Nies DH, Mergeay M, Pring A, Southam G, Brugger J (2009) Mechanisms of gold biomineralization in the bacterium *Cupriavidus metallidurans*. Proc Natl Acad Sci U S A 106: 17757-17762
294. Codony F, Morato J, Mas J (2005) Role of discontinuous chlorination on microbial production by drinking water biofilms. Water Res 39: 1896-1906
295. Gauthier D, Sobjerg LS, Jensen KM, Lindhardt AT, Bunge M, Finster K, Meyer RL, Skrydstrup T (2010) Environmentally benign

recovery and reactivation of palladium from industrial waste by using gram-negative bacteria. ChemSusChem 3: 1036-1039

296. Diels L, De Smet M, Hooyberghs L, Corbisier P (1999) Heavy metals bioremediation of soil. Molecular biotechnology 12: 149-158
297. Diels L, Vanroy S, Somers K, Willems I, Doyen W, Mergeay M, Springael D, Leysen R (1995) The Use of Bacteria Immobilized in Tubular Membrane Reactors for Heavy-Metal Recovery and Degradation of Chlorinated Aromatics. J Membrane Sci 100: 249-258
298. Clement P, Pieper DH, Gonzalez B (2001) Molecular characterization of a deletion/duplication rearrangement in *tfd* genes from *Ralstonia eutropha* JMP134 (pJP4) that improves growth on 3-chlorobenzoic acid but abolishes growth on 2,4-dichlorophenoxyacetic acid. Microbiology 147: 2141-2148
299. Dunon V, Sniegowski K, Bers K, Lavigne R, Smalla K, Springael D (2013) High prevalence of IncP-1 plasmids and IS*1071* insertion sequences in on-farm biopurification systems and other pesticide polluted environments. FEMS Microbiol Ecol
300. Drevinek P, Baldwin A, Lindenburg L, Joshi LT, Marchbank A, Vosahlikova S, Dowson CG, Mahenthiralingam E (2010) Oxidative stress of *Burkholderia cenocepacia* induces insertion sequence-mediated genomic rearrangements that interfere with macrorestriction-based genotyping. J Clin Microbiol 48: 34-40
301. Mennecier S, Servant P, Coste G, Bailone A, Sommer S (2006) Mutagenesis via IS transposition in *Deinococcus radiodurans*. Mol Microbiol 59: 317-325
302. Boever PD, Ilyin V, Forget-Hanus D, Auwera GVd, Mahillon J, Mergeay M (2007) Conjugation-mediated plasmid exchange between bacteria grown under space flight conditions. Microgravity sci technol XIX-2: 45-51
303. Silver S, Phung le T (2005) A bacterial view of the periodic table: genes and proteins for toxic inorganic ions. J Ind Microbiol Biotechnol 32: 587-605
304. Mergeay M (2000) Bacteria adapted to industrial biotopes: the metal resistant *Ralstonia*. In: Storz, G, Hengge, R (eds.) Bacterial Stress Responses. ASM Press, Washington D.C., pp. 403-414
305. Ryan MP, Pembroke JT, Adley CC (2009) Novel Tn*4371*-ICE like element in Ralstonia pickettii and genome mining for comparative elements. BMC Microbiol 9: 242
306. Toussaint A, Merlin C, Monchy S, Benotmane MA, Leplae R, Mergeay M, Springael D (2003) The biphenyl- and 4-chlorobiphenyl-catabolic transposon Tn*4371*, a member of a new family of genomic islands related to IncP and Ti plasmids. Appl Environ Microbiol 69: 4837-4845

307. La Duc M, Sumner R, Pierson D, Venkateswaran K (2003) Characterization and Monitoring of Microbes in the International Space Station Drinking Water. Environ Microbiol 5: 977-985
308. Konopka A, Zakharova T (1999) Quantification of bacterial lead resistance via activity assays. J Microbiol Methods 37: 17-22
309. Timotius K, schlegel HG (1987) Aus abwässern isolierte nickel-resistente bakterien. Nacht Akod Wiss Göttingen II Moth-Physik Klasse 3: 15-23
310. Bobe L, Kochetkov A, Soloukhin V, Ancreichuk P, Protasov N, Sinyak Y (2008) SRV-K Status Aboard the International Space Station during Missions 15 and 16. International Conference On Environmental Systems. SAE International, San Fransisco, CA, USA.
311. Smyth GK (2005) Limma: linear models for microarray data. In: Gentleman, R, Carey, V, Docoit, S, Irizarry, R, Huber, W (eds.) Bioinformatics and Computational Biology Solutions using R and Bioconductor. Springer, New York, pp. 397-420
312. Ritchie ME, Silver J, Oshlack A, Holmes M, Diyagama D, Holloway A, Smyth GK (2007) A comparison of background correction methods for two-colour microarrays. Bioinformatics 23: 2700-2707
313. Smyth GK, Speed T (2003) Normalization of cDNA microarray data. Methods 31: 265-273
314. Suzuki R, Shimodaira H (2006) Pvclust: an R package for assessing the uncertainty in hierarchical clustering. Bioinformatics 22: 1540-1542
315. Vallenet D, Labarre L, Rouy Z, Barbe V, Bocs S, Cruveiller S, Lajus A, Pascal G, Scarpelli C, Medigue C (2006) MaGe: a microbial genome annotation system supported by synteny results. Nucleic Acids Research 34: 53-65
316. Schmidt T, Schlegel HG (1989) Nickel and Cobalt Resistance of Various Bacteria Isolated from Soil and Highly Polluted Domestic and Industrial-Wastes. Fems Microbiology Ecology 62: 315-328
317. Klockgether J, Wurdemann D, Reva O, Wiehlmann L, Tummler B (2007) Diversity of the abundant pKLC102/PAGI-2 family of genomic islands in *Pseudomonas aeruginosa*. Journal of Bacteriology 189: 2443-2459
318. Kill K, Binnewies TT, Sicheritz-Ponten T, Willenbrock H, Hallin PF, Wassenaart TM, Ussery DW (2005) Genome update: sigma factors in 240 bacterial genomes. Microbiology-Sgm 151: 3147-3150
319. Scherer J, Nies DH (2009) CzcP is a novel efflux system contributing to transition metal resistance in *Cupriavidus metallidurans* CH34. Molecular Microbiology 73: 601-621

320. Bavishi A, Abhishek A, Lin L, Choudhary M (2010) Complex prokaryotic genome structure: rapid evolution of chromosome II. Genome 53: 675-687
321. Sato Y, Nishihara H, Yoshida M, Watanabe M, Rondal JD, Concepcion RN, Ohta H (2006) *Cupriavidus pinatubonensis* sp nov and *Cupriavidus laharis* sp nov., novel hydrogen-oxidizing, facultatively chemolithotrophic bacteria isolated from volcanic mudflow deposits from Mt. Pinatubo in the Philippines. International Journal of Systematic and Evolutionary Microbiology 56: 973-978
322. Wachtershauser G (2006) From volcanic origins of chemoautotrophic life to Bacteria, Archaea and Eukarya. Philos T R Soc B 361: 1787-1806
323. Gribble G (2010) Naturally occurring organohalogen compounds - a comprehensive update. Springer, New York
324. Parks AR, Peters JE (2007) Transposon Tn*7* is widespread in diverse bacteria and forms genomic islands. J Bacteriol 189: 2170-2173
325. Parks AR, Peters JE (2009) Tn*7* elements: engendering diversity from chromosomes to episomes. Plasmid 61: 1-14
326. Grosse C, Friedrich S, Nies DH (2007) Contribution of extracytoplasmic function sigma factors to transition metal homeostasis in *Cupriavidus metallidurans* strain CH34. Journal of molecular microbiology and biotechnology 12: 227-240

Appendix A

Variation in genomic islands contribute to genome plasticity in *Cupriavidus metallidurans*

Different *Cupriavidus metallidurans* strains isolated from metal-contaminated and other anthropogenic environments were genotypically and phenotypically compared with *C. metallidurans* type strain CH34. Comparative genomic hybridization indicated that the extensive arsenal of determinants involved in metal resistance was well conserved among the different *C. metallidurans* strains. Contrary, the mobile genetic elements identified in type strain CH34 were not present in all strains but clearly showed a pattern, although, not directly related to a particular biotope nor location (geographical). One group of strains carried almost all mobile genetic elements, while these were much less abundant in the second group. In addition, the clear pattern of genomic islands distribution allowed to identify new putative genomic islands on chromosome 1 and 2 of *C. metallidurans* CH34.

This chapter was based on the following publication:

Van Houdt R., Monsieurs P., Mijnendonckx K., Provoost A., Janssen A., Mergeay M., Leys N (2012) Variation in genomic islands contribute to genome plasticity in *Cupriavidus metallidurans BMC Genomics* (13): 111

A.1 Introduction

Metals are common in our environment and diet. Rocks and soils are the principal and natural sources of metals in the environment. These sources lead to natural background levels in soils, sediments, waters and organisms that are supplemented by many human activities like agriculture (fertilizers, manure and pesticides) and industrial activities (petrochemical, extractive, metallurgic). Some metals are essential trace elements, however, many are toxic to organisms. The essential elements are acquired from the environment depending on the necessities and their uptake is strictly controlled by homeostasis. Failure of these regulation mechanisms due to metal deficiency or toxicity (excess) results in harmful effects on the organism. Mechanisms to resist metals are abundant and widespread in bacteria, with resistance determinants occurring in a few percent in pristine environments to in nearly all isolates in heavily polluted environments [303].

Cupriavidus metallidurans is a species characterized by multiple metal-resistances [139, 146, 304]. For *C. metallidurans* type strain CH34 a substantial part of the metal resistance mechanisms are carried by its two megaplasmids pMOL28 and pMOL30 [57, 160]. However, next to these specialized plasmids also chromosomally-encoded metal responsive gene clusters have been identified [144]. The *C. metallidurans* CH34 genome [56] hosts in addition a large diversity of MGEs including genomic islands (GIs), integrative and conjugative elements, transposons and IS elements [161, 181]. Both the number and diversity of genes related to MGEs is larger in type strain CH34 than in related strains from other *Cupriavidus* and *Ralstonia* genera [56, 161]. Multiple GIs, in particular on both plasmids, contain genes for heavy metal resistance [160, 161]. Its capacity to degrade toluene, to fix carbon dioxide and to oxidize hydrogen is located on Tn*4371*-like integrative and conjugative elements [161, 305, 306].

C. metallidurans strains were often isolated from industrial sites linked to mining-, metallurgical-, and chemical industries [139, 179, 226]. Next to this, *C. metallidurans* strains were isolated from environments not typified by metal contamination like, for instance, from different spacecraft-related environments [141, 152, 155, 156, 307], from patients with cystic fibrosis [142] or even as the causative agent of an invasive human infection [143].

In this study, we aimed to gain insight in the dispersion and horizontal transfer of genes and the evolutionary forces shaping this species. Therefore, whole-genome oligonucleotide DNA microarrays based on the genome of CH34 were used to compare 16 *C. metallidurans* strains isolated from diverse metal-contaminated biotopes, from other anthropogenic environments and from human cerebrospinal fluid with type strain CH34.

A.2 Materials and Methods

A.2.1 Strains, media and culture conditions

C. metallidurans strains used in this study are summarized in Table A.1 and were routinely cultured at 30°C in Tris-buffered mineral medium (MM284) supplemented with 0.2% (wt/vol) gluconate as described previously [169]. Autotrophic growth on H_2 and CO_2 was scored by incubating on MM284 agar medium (without gluconate) under an atmosphere of $H_2/CO_2/O_2$ (approximately 75:15:10; by vol.). Growth on toluene was scored by growing strains on MM284 agar medium (without gluconate) in a closed container saturated with toluene vapor. The maximum tolerable concentration (MTC), which is the highest tested concentration of a substance for which bacterial growth could be observed, was determined for $ZnSO_4$, $SrCl_2$, $CoCl_2$, $NiCl_2$ and K_2CrO_4 in liquid MM284. A stationary phase culture of each isolate was diluted 100-fold in liquid MM284 containing the metal concentration of interest. Cultures were incubated at 30°C and after 72 hours the MTC was scored. The MTC for $Pb(NO_3)_2$ was

determined similarly except the analysis medium contained 0.4 g/l peptone, 0.4 g/l yeast extract, 0.4 g/l tryptone and 10 mM 2-N-morpholinoethanesulfonic acid to buffer the pH at 6.5 [adapted from [308]].

Table A.1: Strains used in this study

Strain	Isolation site	Isolation place	Reference
AS39	Mine tailings	Likasi-Sud, Congo	[226]
AS167	Mine tailings	Likasi-Sud, Congo	[179]
AS168	Mine tailings	Likasi-Sud, Congo	[226]
KT01	Wastewater treatment plant	Göttingen, Germany	[309]
KT02	Wastewater treatment plant	Göttingen, Germany	[283]
KT21	Wastewater treatment plant	Göttingen, Germany	[309]
SV661	Non-ferrous industry	Beerse, Belgium	[226]
$CH34^T$	Decantation tank, zinc factory	Liège, Belgium	[164]
CH42	Polluted sediments, zinc factory	Liège, Belgium	[179]
CH79	Polluted sediments, zinc factory	Liège, Belgium	[179]
31A	Galvanization tank, metal factory	Holzminden, Germany	[283]
NE12	Cleanroom Kennedy Space Center	Florida, USA	[154]
NA1	Water storage system	International Space Station	[310]
NA2	Contingency water container	International Space Station	[310]
NA4	Water recovery system	International Space Station	[310]
43015	Human cerebrospinal fluid	Göteborg, Sweden	CCUG*
45957	Pharmaceutical industry	Sweden	CCUG

*Culture Collection, University of Göteborg, Sweden

A.2.2 Molecular analyses

Standard techniques were used for PCR and agarose gel electrophoresis. The oligonucleotides used for PCR were synthesized by Eurogentec (Seraing, Belgium) and are listed in Table A.2. Genomic DNA (gDNA) was prepared using the QIAamp DNA mini kit (Qiagen, Venlo, The Netherlands). Extraction of megaplasmids was based on the method of Andrup *et al*. [171].

A.2.3 Genomic DNA labeling, array hybridization, washing and scanning

Four µg of gDNA was fragmented to 50 to 150 bp by partial digestion with *Sau*3AI (Fermentas, St. Leon-Rot, Germany). Next, gDNA was labeled with the BioPrime® Array CGH Genomic Labeling System (Invitrogen, Merelbeke, Belgium). Labeled gDNA was re-suspended in the universal hybridization buffer of the Pronto kit (Promega, United States), mixed and added to the spotted slide (GEO accession number Platform GPL4980) for overnight hybridization at 42°C in a Tecan HS4800 Pro hybridization station (Tecan Group Ltd, Switzerland). Afterwards, slides were washed according to Pronto kit's protocol. Slides were scanned (at 532 and 635 nm) using the GenePix Personal 4100A microarray scanner (Molecular Devices©, USA).

Table A.2: PCR Primers used in this study

Primer name	**Sequence (5' → 3')**	**Primer annealing coordinates**
hmyB_FW	GAAGGGCAGAGCGTCGATATC	692049-692069 (CHR2)
hmyA_RV	GCATAGCGCACCGAATTGA	696246-696264 (CHR2)
mmmQ_FW	AGTCTCTAGAACGCGAGCTACTTCTTCGAG	1058076-1058097 (CHR2)
czcR2i_RV	CTAGAAGCTTGGTGTTGCTGTCGAAGTTCA	1062197-1062218 (CHR2)
czcA1(c711)_FW	CGTGGTCTACGGTTTCACG	2438423-2438441 (CHR2)
czcA2(c711)_RV	CACACCGTTGATCTTGCGTA	2436991-2437010 (CHR2)
czcC2	TGTACACAGCCATCCGTCAG	1217038-1217057 (CHR2)
czcA2R	GTACGAGGCCAGCTTTTCAG	1066866-1066885 (CHR2)
pbrUa_FW	GTCTTCTGGGTGGCAGTCAT	117837-117856 (pMOL30)
pbrUb_RV	GCACCTGCATAGAACGTGAA	121954-121973 (pMOL30)

A.2.4 Array data and clustering analysis

Microarray spot-signals were analysed using the GenePix Pro v.6.0.1 software and flagged according to build-in quality criteria. Raw median intensity data were imported into R version 2.13.1 for statistical analysis using the LIMMA package version 2.15.15 [311] as available from BioConductor. Raw data were background-corrected based on convolution of normal and exponential distributions with an offset of 50 [312]. Data were normalized within each array using the printing-tip loess normalization algorithm [313]. The microarray data have been deposited in the Gene Expression Omnibus website (http://www.ncbi.nlm.nih.gov/geo/) under accession number GSE36303. Analysis of previously characterized *C. metallidurans* CH34 derivatives (loss of either pMOL28 or pMOL30 [57], IS*1071*-mediated loss of growth on CO_2 and H_2 [181]) allowed us to validate and optimize the trade-off between the number of false-positives and false-negatives. In the final analyses, a cut-off of 20-fold change in hybridization intensity compared to the background was used (GSE36303). Hierarchical clustering was performed using the complete linkage method with the hclust software from the R-package stats (version 2.13.1). Hierarchical clustering was obtained based on the pair-wise correlation between the different strains of the percentage of overlapping genes and percentage of GI genes conserved in Figures A.1 and A.3, respectively. Bootstrap values (n = 1,000) were obtained using the R-package pvclust [314]. Heatmaps were produced using the heatmap.2 function as implemented in the R-package gplots (version 2.10.1). Gene annotations were retrieved from the up-to-date annotation of the different replicons of *C. metallidurans* CH34 available on GenoScope's MaGe system [315].

A.3 Results

A.3.1 General comparison

Comparative whole-genome hybridization (CGH) was applied to compare sixteen *C. metallidurans* strains (Table A.1) with type strain CH34 and showed that all strains shared a core of 3,387 coding sequences (CDS), which represents 54.6% of the 6,205 oligonucleotide probes present on the CH34 microarray. This common gene pool represented 58.2%, 53.7%, 16.4% and 31.0% of chromosome 1 (CHR1), chromosome 2 (CHR2), pMOL28 and pMOL30, respectively. Thus, although the main replicon (CHR1) carries most of the housekeeping genes [56], only a slightly higher percentage of CDS is conserved in CHR1 compared to CHR2. This is different when comparing the sequenced *Cupriavidus* species (*C. metallidurans*, *C. eutrophus*, *C. pinatubonensis*, *C. taiwanensis*), for which the percentage of common genes is much larger for CHR1 than for CHR2 [56].

Within this conserved group, 2,760 CDS were assigned to a Cluster of Orthologous Groups (COG). The most abundant COG functional categories were function unknown (Category S; 12.4%), amino acid transport and metabolism (Cat. E; 9.3%), general function prediction only (Cat. R; 9.0%), transcription (Cat. K; 8.5%) and energy production and conversion (Cat. C; 8.4%), respectively.

Cluster analysis based on the pairwise number of overlapping orthologs indicated that all strains can clearly be clustered into two main groups (Figure A.1). The strains isolated from the mine tailings in Congo (AS39, AS167 and AS168) grouped together with SV661 isolated from a metal factory in Belgium and with KT01 from a wastewater treatment plant in Germany. This cluster grouped together with a cluster comprising type strain

CH34 and the other two isolates KT02 and KT21 from the wastewater treatment plant in Germany forming group I (Figure A.1). Group II included the strains isolated from the spacecraft-related environments (NE12, NA1, NA2 and NA4), as well as 31A (Germany) and CH42 (Belgium) from metal factories, the clinical strain 43015 (Sweden), and strain 45957 from pharmaceutics (Sweden). Interestingly, type strain CH34 did not group with the two other strains (CH42 and CH79) isolated from the same site in Belgium.

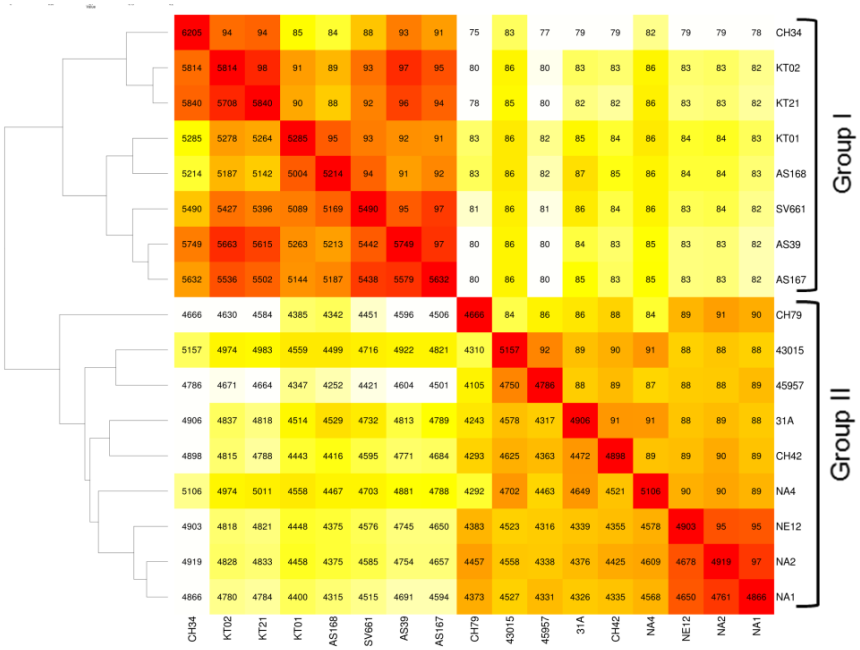

Figure A.1: Graphical representation and clustering analysis of *C. metallidurans* strains. Hierarchically (complete-linkage) clustered heat map based on CGH results of 17 different *C. metallidurans* strains to a whole-genome oligonucleotide DNA microarray of type strain CH34. The numbers indicated on the heat map are the total number (below diagonal) and percentage (above diagonal) of genes shared between two corresponding strains. The numbers on the diagonal represent the maximal number of genes within one species that gave a detectable signal on the DNA microarray. Bootstrap values (%) from 1,000 times resampling are shown at each dendrogram node.

A.3.2 Mobile genetic elements

All strains (except CH42) carried one or more megaplasmids (Figure A.2). Concordantly, a good overall conservation of pMOL28 and pMOL30 genes was observed. CGH indicated that for pMOL30 genes in general between 80 and 99% of the probes showed a positive hybridization signal except for CH42 (55.6%), 31A (55.6%), 43015 (51.4%) and 45957 (42.6%) (Figure A.3, Table A.3). For KT02, 99% or 214 out of 216 gave a positive hybridization signal. For CH42, 31A, 43015 and 45957, a higher percentage of positive hybridization signals was observed for the genomic islands CMGI-30a and CMGI-30b carried by pMOL30 than for the plasmid backbone, indicating that the megaplasmid(s) in these strains probably do not carry a backbone similar to pMOL30. The pMOL28 genes are less conserved than those from pMOL30 but still in general between 71 and 95% with the highest number of positive CGH signals for KT21 (95%) and KT02 (94%) (Figure A.3, Table A.3). Conservation below 70% was observed for CH42 (29.6%), CH79 (31.6%), NE12 (38.8%) and NA2 (55.9%). More positive hybridization signals were found for the GIs on pMOL28 than the plasmid backbone, indicating that their megaplasmids probably do not carry a backbone similar to pMOL28. Concordantly, strains lacking either the pMOL28 backbone (CH79, NE12 and NA2), the pMOL30 backbone (43015 and 45957) or both (CH42) have only one or no megaplasmid (Figure A.2). Strain 31A, which carries two megaplasmids pTOM8 and pTOM9 [316], showed only a positive hybridization signal with the pMOL28 backbone, indicating that the one of both has a backbone related to pMOL28 while the other has a backbone unrelated to pMOL30.

The strong conservation of the GIs on pMOL28 (especially CMGI-28a) and pMOL30, which carry all the metal resistance determinants of these plasmids, already indicated a high conservation of the metal responsive clusters (see below).

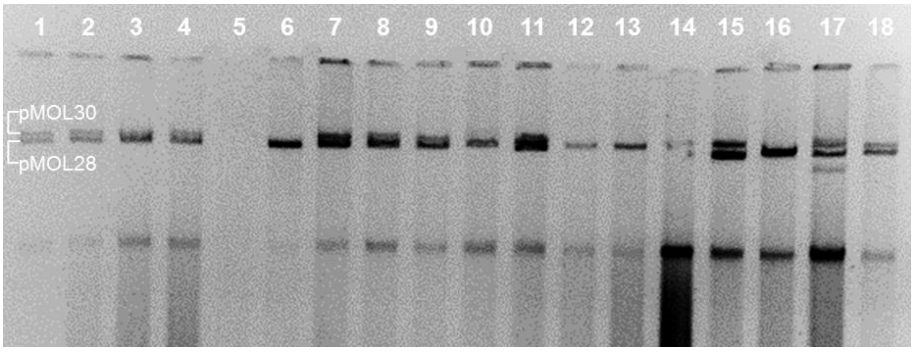

Figure A.2: Plasmid patterns of *C. metallidurans* strains. Agarose gel electrophoresis of plasmid extracts from strains CH34 (1 and 18), KT01 (2), KT02 (3), KT21 (4), CH42 (5), CH79 (6), AS39 (7), AS167 (8), AS168 (9), 31A (10), SV661 (11), 43015 (12), 45957 (13), NE12 (14), NA1 (15), NA2 (16), and NA4 (17). Lower band represents chromosomal DNA.

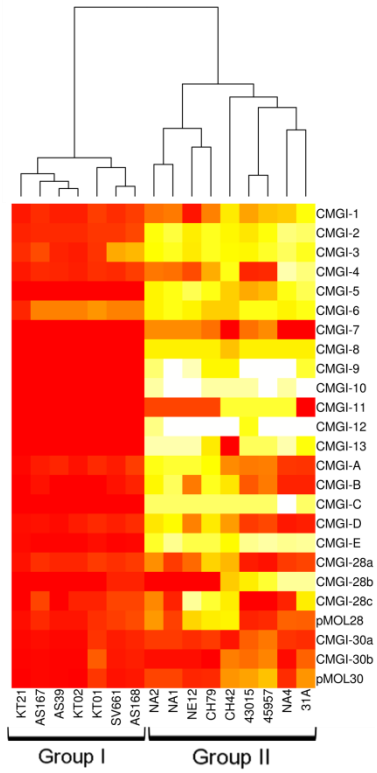

Figure A.3: Graphical representation and clustering analysis of MGEs in *C. metallidurans* strains**.** Hierarchically (complete-linkage) clustered heat map based on CGH results related to plasmids, previously and newly identified genomic islands of 16 different *C. metallidurans* strains to a whole-genome oligonucleotide DNA microarray of type strain CH34. Bootstrap values (%) from 1,000 times resampling are shown at each dendrogram node.

Table A.3: Relative occurrence of *C. metallidurans* CH34 genomic islands and plasmids in *C. metallidurans* strains as indicated by CGH. Percentage of genes related to a particular genomic island (CMGI) or plasmid (pMOL) displaying a positive hybridization signal by CGH. [§]Genomic islands identified in this study.

CMGI	**AS39**	**AS167**	**AS168**	**KT01**	**KT02**	**KT21**	**SV661**	**CH42**	**CH79**	**31A**	**NE12**	**NA1**	**NA2**	**NA4**	**43015**	**45957**
CMGI-1	90.8	87.5	81.7	81.7	90.8	91.7	86.7	29.2	62.5	23.3	92.5	63.3	65.8	37.5	50.0	41.7
CMGI-2	86.6	86.6	78.6	83.0	86.6	89.3	83.0	27.7	22.3	15.2	30.4	18.8	24.1	12.5	32.1	25.0
CMGI-3	89.5	77.9	47.7	84.9	91.9	87.2	51.2	26.7	22.1	20.9	30.2	26.7	29.1	20.9	30.2	24.4
CMGI-4	88.7	86.8	81.1	84.9	90.6	92.5	86.8	22.6	47.2	13.2	77.4	66.0	64.2	7.5	88.7	86.8
CMGI-5	**100**	**100**	**100**	**100**	**100**	**100**	**100**	38.9	22.2	16.7	16.7	22.2	27.8	22.2	50.4	44.4
CMGI-6	46.2	46.2	46.2	38.5	46.2	84.6	46.2	23.1	30.8	15.4	7.7	0	7.7	7.7	0	0
CMGI-7	**100**	**100**	**100**	**100**	**100**	**100**	**100**	**100**	69.2	**100**	61.5	53.8	61.5	**100**	69.2	53.8
CMGI-8	**100**	**100**	**100**	**100**	**100**	**100**	**100**	42.9	28.6	28.6	28.6	28.6	28.6	28.6	28.6	28.6
CMGI-9	**100**	**100**	**100**	**100**	**100**	**100**	**100**	20.0	20.0	13.3	6.7	0	13.3	0	0	0
CMGI-10	**100**	**100**	**100**	**100**	**100**	**100**	**100**	7.1	7.1	0	0	0	7.1	7.1	7.1	0
CMGI-11	**100**	**100**	**100**	**100**	**100**	**100**	**100**	14.3	57.1	**100**	57.1	57.1	57.1	28.6	28.6	28.6
CMGI-12[§]	**100**	**100**	**100**	**100**	**100**	**100**	**100**	0	0	0	0	0	11.1	0	22.2	0
CMGI-13[§]	**100**	**100**	**100**	**100**	**100**	**100**	**100**	**100**	31.3	25.0	6.3	6.3	12.5	12.5	18.8	18.8
CMGI-A[§]	89.0	91.8	82.2	87.7	94.5	97.3	91.8	57.5	24.7	84.9	19.2	19.2	21.9	83.6	63.0	61.6

CMGI-B[§]	**100**	95.2	85.7	**100**	**100**	**100**	95.2	28.6	19.0	85.7	61.9	14.3	23.8	85.7	71.4	61.9
CMGI-C[§]	**100**	**100**	**100**	**100**	**100**	**100**	**100**	14.3	14.3	14.3	14.3	14.3	14.3	0	14.3	14.3
CMGI-D[§]	96.2	95.2	86.5	87.5	91.3	95.2	91.3	52.9	31.7	91.3	63.5	26.9	32.7	95.2	82.7	77.9
CMGI-E[§]	99.0	98.0	98.0	96.0	99.0	97.0	99.0	25.7	17.8	9.9	17.8	10.9	20.8	10.9	10.9	8.9
CMGI-28a	91.1	88.9	86.7	86.7	91.1	95.6	88.9	53.3	44.4	73.3	71.1	86.7	66.7	86.7	93.3	95.6
CMGI-28b	**100**	**100**	83.3	91.7	**100**	**100**	91.7	33.3	**100**	8.3	**100**	**100**	91.7	8.3	25.0	16.7
CMGI-28c	**100**	83.3	75.0	83.3	83.3	91.7	83.3	25.0	16.7	33.3	8.3	75.0	50.0	75.0	91.7	91.7
pMOL28	93.4	87.5	77.6	86.2	94.1	95.4	82.2	29.6	31.6	72.4	38.8	81.6	55.9	71.7	90.1	88.2
CMGI-30a	98.4	96.8	91.9	88.7	98.4	98.4	93.5	93.5	83.9	83.9	88.7	85.5	85.5	87.1	77.4	72.6
CMGI-30b	98.8	97.6	90.4	73.5	98.8	98.8	92.8	61.4	**100**	71.1	95.2	95.2	95.2	96.4	66.3	59.0
pMOL30	98.6	97.2	92.6	83.3	99.1	99.1	94.4	55.6	88.0	55.6	88.4	80.1	80.1	86.6	51.4	42.6

Next to the megaplasmids and their GIs, CH34 carries 11 previously identified GIs on chromosome 1 [160, 161]. Based on CGH data analysis for the presence of GIs, the strains could again be divided into two main groups. One group (KT01, KT02, KT21, AS39, AS167, AS168 and SV661) carried almost all GIs identified in CH34, while these GIs were much less abundant in the second group (31A, CH42, CH79, NE12, NA1, NA2, NA4, 43015 and 45957) (Table A.3, Figure A.3). This clustering (Figure A.3) resembled the clustering based on all oligonucleotide probes (Figure A.1), which indicated that the presence of GIs is the main source of divergence in these strains. At least 11 strains carried CMGI-1 (or a large part of it). CMGI-1 of CH34 is a 109 kb GI of the PAGI-2 family and is almost 100% identical to PAGI-2C of *P. aeruginosa* clone C isolated from a cystic fibrosis patient [161, 317]. These data are in agreement with the analysis of the KT and CH strains by Klockgether *et al*. [317]. The relative occurrence also indicated that CMGI-5 and CMGI-7 to CMGI-11 were highly conserved when present. CMGI-2 to CMGI-4 belong to the Tn*4371* family [133, 161, 305, 306] and were previously designated $ICE_{Tn4371}6054$, $ICE_{Tn4371}6055$ and $\Delta ICE_{Tn4371}6056$, respectively [133]. CMGI-2 ($ICE_{Tn4371}6054$) and CMGI-3 ($ICE_{Tn4371}6055$) are responsible for CH34's ability to grow on aromatic compounds and to fix carbon dioxide, respectively. The presence of these GIs in the *C. metallidurans* strains is in accordance with their ability to degrade toluene or to grow on hydrogen gas and carbon dioxide (Table A.4). Except for NE12 that apparently lacks the genes involved in degradation of aromatic compounds but is able to degrade toluene and vice versa for AS39 that apparently carries the genes but lacked degradation ability. Therefore, NE12 putatively carries other functional genes, while for AS39 functionality is probably lost. Finally, the presence of other Tn*4371*-like elements in these strains can not be excluded. Especially since all strains except CH42, 31A and NA4 displayed good conservation of the partial CMGI-4

(ΔICE$_{Tn4371}$6056), which lacks the transfer module [161], and displayed positive hybridization signals related to the transfer module of CMGI-2.

Table A.4: Relative occurrence of *C. metallidurans* CH34 genomic islands CMGI-2 and CMGI-3 and associated phenotypes in *C. metallidurans* strains

Strain	**CMGI-2[a]**	**AccMod[b]**	**Toluene[c]**	**CMGI-3[a]**	**AccMod[b]**	**H_2 + CO_2[c]**
AS39	86.6	86.1	-	89.5	93.6	+
AS167	86.6	87.5	+	77.9	72.3	+
AS168	78.6	77.8	+	47.7	21.3	-
KT01	83.0	83.3	+	84.9	91.5	+
KT02	86.6	86.1	+	91.9	95.7	+
KT21	89.3	88.9	+	87.2	91.5	+
SV661	83.0	83.3	+	51.2	23.4	+
CH42	27.7	16.7	-	26.7	21.3	-
CH79	22.3	12.5	-	22.1	17.0	-
31A	15.2	8.3	-	20.9	17.0	-
NE12	30.4	11.1	+	30.2	17.0	-
NA1	18.8	8.3	-	26.7	17.0	-
NA2	24.1	9.7	-	29.1	17.0	-
NA4	12.5	8.3	-	20.9	14.9	-
43015	32.1	18.1	ND	30.2	17.0	-
45957	25.0	8.3	ND	24.4	10.6	-

Percentage of genes related to the GI([a]) or its accessory module ([b]) displaying a positive hybridization signal by CGH. [c]Growth capability on toluene and H_2 and CO_2, respectively.

The mosaic structure of the second chromosome of *C. metallidurans* CH34, but also other *Cupriavidus*, *Ralstonia* and *Burkholderia* strains, made it complicated to clearly identify GIs on this replicon. Consequently, no GIs on chromosome 2 of *C. metallidurans* CH34 were defined in a previous study [161]. Here we took advantage of the clear pattern of GI distribution in chromosome 1 over the 16 different *C. metallidurans* strains to scan chromosome 2 for similar patterns, which could be an indication for the

presence of a genomic island. Five different GIs could be identified (Tables A.3 and A.5, Figure A.3). Interestingly, in CH34 both CMGI-B and CMGI-D flank a copy of the Tn*6050* transposon. It was previously shown that in CH34 a chromosomal inversion occurred by recombination between the pair of Tn*6050* transposons [161]. Therefore, CMGI-B and CMGI-D are in fact two parts of the same genomic island of 160.7 kb with at one extremity multiple genes coding for phage-related proteins (associated to phages of *Ralstonia solanacearum*) and at the other extremity a cluster of 22 genes in synteny with *R. solanacearum*. Accordingly, the relative occurrence of CMGI-B was comparable to that of CMGI-D for each strain, and both were conserved (> 60%) in 13 strains (Table A.3, Figure A.3). In CH34, the 120 kb CMGI-E carries at one extremity an IS*Rme3*, three Tn*7*-related genes (*tnsABC*) and an IS*Rme11* inserted into *tnsC*. In fact a very small gene cluster (located approximately 1.89 Mb upstream (or +/- 687 kb downstream) in chromosome 2 carried a IS*Rme3* and two Tn*7*-related genes (*tnsD1 tnsD2*). Furthermore, for each strain the presence of these genes coincides with the presence of *tnsABC*. To determine the relation between these distant Tn*7*-related genes, the STRING database (version 8.3; http://string.embl.de) was used to find genomes where these genes occur as immediate neighbours. This identified with high confidence (based on STRING parameters) orthologous groups of TnsABCD2 in *Anabaena variabilis* and of TnsABCD1 in *Hahella chejuensis*, *Shigella sonnei* and *Idiomarina loihiensis*. Additional BLASTP searches indicated the presence of this cluster also in strains more closely related to CH34 such as *Burkholderia phymatum* and *Herminiimonas arsenicoxydans* (both β-Proteobacteria). These results evidenced that a putative chromosomal inversion of a very large region (+/- 687 kb) occurred in CH34 by recombination between the pair of IS*Rme3* elements. In fact, before inversion the region formed a genomic island with a set of Tn*7*-encoded

proteins (TnsABCD1D2) at one extremity and accessory genes putatively involved in the degradation of aromatic compounds.

Table A.5: Newly identified putative genomic islands on chromosome 1 and chromosome 2 of *C. metallidurans* CH34

GI	Replicon	Size (kb)	Coordinates	Features
CMGI-12	CHR1	9.1	2,895,950 - 2,905,048	Direct repeats (3′ end sequence of a boundary tRNA gene), genes coding for hypothetical proteins
CMGI-13	CHR1	15.9	2,957,898 - 2,973,796	Genes involved in polysaccharide biosynthesis
CMGI-A	CHR2	87.1	813,173 - 900,292	IS*Rme1* at one extremity
CMGI-B	CHR2	19.5	1,075,185 - 1,094,655	Multiple genes coding for phage-related proteins (associated to phages of *Ralstonia solanacearum*)
CMGI-C	CHR2	7.1	1,160,750 - 1,167,881	Fragment of tyrosine-based site-specific recombinase at one extremity, direct repeats (41 bp), gene coding for mannose-binding lectin
CMGI-D	CHR2	141.2	1,217,667 - 1,358,908	At one extremity 22 genes in synteny with *R. solanacearum*
CMGI-E	CHR2	120.2	2,202,142 – 2,322,293	Tn*7*-related genes at one extremity, genes putatively involved in degradation of aromatic compounds

The above described observations also encouraged us to scrutinize once more chromosome 1 of CH34 for putative genomic islands. In addition to the previously identified islands [161], at least two other putative GIs could be identified (Tables A.3 and A.5, Figure A.3). CMGI-12 carries genes coding for hypothetical proteins and is flanked by direct repeats (3′ end sequence of a boundary tRNA gene). CMGI-13 carries genes involved in polysaccharide biosynthesis, however, no genes putatively involved in mobility could be identified.

The occurrence of insertion sequences in the different *C. metallidurans* strains followed the same trend as that of the GIs. Based on CGH the same two main clusters could be derived. One group (KT01, KT02, KT21, AS39, AS168, AS169 and SV661) displayed positive hybridization signals for 90 to 98% of the 42 probes related to IS elements, while the second group (31A, CH42, CH79, NE12, NA1, NA2, NA4, 43015 and 45957) only displayed 43 to 62% positive signals (data not shown).

The occurrence of transposon Tn*6048* displayed the same pattern as for the IS elements and GIs, however, Tn*6049* and the mercury transposons (Tn*4378* and Tn*4380*) appear to be present in all strains (data not shown).

A.3.3 Heavy metal resistance genes

The presence of all gene clusters, which are identified in CH34 as involved in heavy metal detoxification, was evaluated in the genomes of the other strains (Table A.6). Almost all metal responsive clusters were found in the other isolates, however, some clusters did not fully correspond to those from CH34. The metal resistance arsenal of CH34 is most conserved in KT21 followed by KT02, AS39, AS167 and SV661. These strains also grouped into a separate cluster based on total genome comparison (Figure A.1).

Table A.6: Occurrence of *C. metallidurans* CH34 metal resistance gene clusters in *C. metallidurans* strains as indicated by CGH[a,b].

Gene cluster in CH34[c,d]	**AS39**	**AS167**	**AS168**	**KT01**	**KT02**	**KT21**	**SV661**	**CH42**	**CH79**	**31A**	**NE12**	**NA1**	**NA2**	**NA4**	**43015**	**45957**
cdfX, pbrR$_2$cadA pbrC$_2$, pbrR$_3$								*XAC$_2$*	*XAC$_2$*	*XAC$_2$*		*XAC$_2$*	*XAC$_2$*	*XAC$_2$*	*XAC$_2$*	*XAC$_2$*
pbrU$_b$|U$_a$TR pbrABCD				*R*					*U$_b$U$_a$*						*U$_b$RAD*	*U$_b$RABCD*
merRTPA'A"			*R*	*R*				*R*	*R*	*R*		*RPA*	*RPA*	*R*	*R*	*RA*
merRTPADE urf-2																
merRTPADE urf-2																
merRTΔP								*RTΔP*	*RTΔP*	*RTΔP*	*RTΔP*	*RTΔP*	*RTΔP*	*RTΔP*	*RTΔP*	*RTΔP*
chrBAF			*F*	*F*					*BF*		*BF*	*BF*	*BF*			
chrIBACEFONPYZ								*IBACEOY*	*IBACEFOY*		*Z*		*BO*		*O*	
cusDCBAF			*D*	*D*			*D*	*DB*	*D*	*D*			*D*			*D*
silDCBA cusΔF				*C*											*ΔF*	*ΔF*
copSRABCD	*S*	*S*	*SC*	*SC*	*C*	*C*	*SC*	*SC*	*C*	*SC*	*C*	*C*	*C*		*SC*	*C*
copV-W$^{(*)}$			*IJF*	*KCIJFOH*			*FH*									
czcLRS ubiG czcB$_a$|B$_b$CI zntA			*I*	*I*					*I*						*I*	*I*
czcMNICBADRSEJ ompP czcP			*B*	*BS*					*ompP*			*S ompP*	*S ompP*	*S*		
nimBA$_a$|A$_b$C	*C*	*C*	*BC*	*BC*	*C*		*C*	*C*	*BC*	*BC*					*C*	*C*
cnrYXHCBAT	*HC*	*HC*	*YHC*	*HC*	*HC*	*C*	*HC*	*YXHCBA*	*YXHCBAT*	*C*	*HC*	*HC*	*YXHCA*	*C*	*C*	

nccCB"B'A nreB			*CB'*	*CB*			*B'*	*CB"B'A*			*B"*	*B"*			*CB'*	*CB"B'A*
arsPHC$_1$BC$_2$IRM																
cupRAC				*R*					*R*							
agrCBA<u>RS</u>		*S*	*S*									*B*				
hmz<u>RS</u> hmzBΔA	*RB*	*RB*	*RBA*	*RBA*	*R*	*R*	*B*	*RSBΔA*	*RSBΔA*	*RSBΔA*	*R*	*R*	*B*	*RSBΔA*	*R*	*R*
hmvCBΔA				*CB*					*C*		*BA*	*BA*	*BA*	*BA*		*A*
zniABC<u>SR</u> zneP<u>RS</u>CAB[(#)]	*C*^{i}	*C*^{i}	*C*^{i}	*C*^{i}	*C*^{i}	*C*^{i}	*C*^{i}	*C*^{i}	*C*^{i}	*C*^{i}	*C*^{i}	*C*^{i}*C*^{e}	*C*^{i}*C*^{e}	*C*^{i}		
hmyCB|hmyA			*C*	*C*							*A*	*A*				

[a]Only genes that did not display positive hybridization signals are shown. [b]See ref. [56] for the extensive and descriptive table with metal detoxifications in *C. metallidurans* CH34. [c]Underlined genes are regulators; [d]Insertion (IS or Tn), frameshift and truncation are indicated by (|), (',") and (Δ), respectively. *Complete cluster is *copVTKMN<u>SR</u>ABCDIJGFOLQHEW*; [#]*zniC* (*C*^{i}) and *zneC* (*C*^{e}).

A noticeable phenotypic difference was observed for nickel, chromate and lead resistance compared to CH34 (Table A.7). For most isolates, including CH34, the maximum tolerable nickel concentration is around 4 mM, however, this concentration is much higher for NA4, KT01, KT02, KT21 and 31A (Table A.7). For strains 31A and KT02, it has been shown that the *nccYXHCBAN* locus is responsible for the resistance to 40 mM nickel [195]. The *nccCBA* locus in CH34 bears a frameshift in *nccB* indicating that the *ncc* genes probably are not functional [57]. The pMOL28-encoded chromate cluster (*chrIchrBACEFONPYZ*) is almost completely absent in strains CH42 and CH79 (Table A.6). Concordantly, the maximum tolerable chromate concentration for these strains is around 0.1 mM, while this concentration is around 0.2 mM for the other strains. Similarly, the pMOL30-encoded lead cluster (*pbrABCD*) is almost complete absent in strains 43015 and 45957 (Table A.6), resulting in a lower MTC compared to the other strains (Table A.7).

Strain CH34 carries several metal resistance genes that are putatively inactivated by frame shift mutation (like *nccB*, see above), truncation or insertion by an IS element or transposon (Table A.6). The presence of three different insertions was evaluated for all isolates, specifically (*i*) insertion of IS*1088* between *hmyA* and *hmyB* (coding for part of a RND transporter), (*ii*) insertion of IS*Rme3* in *nimA* (coding part of system), and (*iii*) insertion of Tn*6049* in *pbrU* (encoding a Major Facilitator Superfamily permease).

The presence of these insertions followed the same trend as the occurrence of insertion sequences (described above). Insertions of IS*1088*, IS*Rme3* and Tn*6049* were present in strains KT01, KT02, KT21, AS39, AS167, AS168 and SV661 but not in strains CH42, CH79, 31A, NE12, NA1, NA2, NA4, 43015 and 45957 (data not shown). The occurrence of an insertion in *nimBAC*, which codes for a RND transporter putatively involved in the resistance to Ni^{2+} and Co^{2+} [56, 146], does not clearly influence the MTC of

nickel or cobalt, however, the presence of other (plasmid-encoded) Ni^{2+} and Co^{2+} resistance determinants could mask this. Similarly, the occurrence of an insertion in *pbrU* is not univocally related to a lower MTC (Table 1.7). Finally, it should be noted that potentially additional metal resistance determinants could be present in the other strains, which are undetectable with a CGH array based on the CH34 genome.

Table A.7: Maximum tolerable concentrations (mM) for tested metals

	CrO_4^{2-}	**Ni^{2+}**	**Co^{2+}**	**Pb^{2+}**
CH34	0.2	4	12.5	0.7
AS39	0.4	4	12.5	0.7
AS167	0.2	4	12.5	0.6
AS168	0.2	4	12.5	0.6
KT01	0.2	10	12.5	0.7
KT02	0.2	40	12.5	0.6
KT21	0.2	20	12.5	0.7
SV661	0.2	4	12.5	0.6
CH42	0.1	4	6.25	0.6
CH79	0.1	4	12.5	0.7
31A	0.4	40	12.5	0.7
NE12	0.2	4	6.25	0.7
NA1	0.2	3	6.25	0.7
NA2	0.2	3.5	6.25	0.7
NA4	0.2	20	6.25	0.6
43015	0.2	>16	12.5	0.3
45957	0.2	>16	12.5	0.3

A.3.4 Genes encoding sigma factors and small stress responsive proteins

No less than 18 different sigma factors were identified in *C. metallidurans* CH34, which enable specific binding of RNA polymerase to promoters, and are activated in response to different environmental changes [56]. Generally, the number and diversity of sigma factor genes in a certain genome relates to the environmental variation allowing growth [318], which thus indicates that

C. metallidurans CH34 is able to respond to a broad range of environmental changes. CGH showed for all *C. metallidurans* strains positive signals for 12 sigma factors. Hybridization signals below the threshold were found for the housekeeping sigma-70 factors RpoD1 and RpoD2 for strain AS168, KT01 and CH79, and NE12, NA1 and 45957, respectively. Sigma factor CnrH carried by plasmid pMOL28 and encoded by the *cnr* gene cluster, which is involved in nickel resistance, was only observed for KT21, 31A, NA4, 43015 and 45957. Next to these, differences were observed for RpoR (for strains KT01, CH79, AS39, AS167, AS168, 31A, SV661), RpoP (for strains CH79, NE12, NA1, NA2, 43015 and 45957) and RpoJ (for strain NA4).

Another interesting group of genes in CH34 consists of 19 homologous genes encoding for putative small (between 69 and 165 amino acids) stress responsive proteins in CH34, which are likely to be secreted since all have a distinctive signal peptide and are apparently only found in *Cupriavidus* and *Ralstonia* species [56]. Ten of these genes were found to be induced in response to different heavy metals [144] like the pMOL30-encoded *copQ* [216] and *czcJ* [319], while three others were induced by hydrogen peroxide (Saiful Islam Muhammed, pers. comm.). CGH indicated that these genes are well conserved among *C. metallidurans* strains (Table A.8).

Table A.8: Occurrence of CH34 genes coding small stress responsive proteins in *C. metallidurans* strains as indicated by CGH.

CH34 locus tag	AS39	AS167	AS168	KT01	KT02	KT21	SV661	CH42	CH79	31A	NE12	NA1	NA2	NA4	43015	45957
Rmet_0477	+	+	+	+	+	+	+	+	+	+	+	+	+	+	+	+
Rmet_1183	+	+	+	+	+	+	+	+	+	+	+	+	+	+	+	+
Rmet_1797	+	+	-	-	+	+	+	+	-	-	+	+	+	+	+	-
Rmet_3454	+	-	-	+	+	+	-	+	+	-	+	+	+	+	+	+
Rmet_3571	+	+	+	+	+	+	+	+	+	+	+	+	+	+	+	+
Rmet_3641	+	+	+	+	+	+	+	+	+	+	+	+	+	+	+	+
Rmet_3715	+	+	+	+	+	+	+	+	+	+	+	+	+	+	+	+
Rmet_3909	+	+	+	+	+	+	+	+	+	+	+	+	+	+	+	+
Rmet_4187	+	+	+	+	+	+	+	+	+	+	+	+	+	+	+	+
Rmet_4264*																
Rmet_4461	+	+	+	+	+	+	+	+	+	+	+	+	+	+	+	+
Rmet_4908[#]	+	+	+	+	+	+	+	+	+	+	+	+	+	+	+	+
Rmet_5281	+	+	+	+	+	+	+	+	+	+	+	+	+	+	+	+
Rmet_5594[#]	+	+	+	+	+	+	+	+	+	+	+	+	+	+	+	+
Rmet_5620	+	+	+	+	+	+	+	+	+	+	+	+	+	+	+	+
Rmet_5975	+	+	+	+	+	+	+	+	+	+	+	+	+	+	+	+
Rmet_6121	+	+	+	+	+	+	+	+	+	+	+	+	+	+	+	+
Rmet_6124*																
Rmet_6143	+	+	+	+	+	+	+	-	+	+	+	+	+	+	+	-

*No oligonucleotide probe available on microarray, [#]identical genes.

A.4 Discussion

Comparative whole-genome hybridization was used to compare sixteen *C. metallidurans* strains isolated from different biotopes with type strain CH34. Although the nature of these sites differs, ranging from pharmaceutical and space industry to metal mining and metal industries, waste treatment plants and even human infection, at least the oligotrophic aspect is common.

The global comparison indicated that while chromosome 1 is the ancestral replicon of the *Cupriavidus* genus, chromosome 2 appears to be more specific to and conserved within the *C. metallidurans* species. These results are in agreement with the study of Bavishi and colleagues [320], which indicated that chromosome 2 evolves faster than chromosome 1, leading to different conservation on inter- and intraspecies level. This global comparison also indicated that strain CH34 is more closely related to strains isolated from Congo than with the two other strains (CH42 and CH79) isolated in Belgium. This supports an old assumption that strain CH34 was transported into Belgium by the import of ores from Congo, which was a Belgian colony from 1908 until 1960.

The incidence of MGEs showed a clear pattern as well as evident phenotypes carried by them like the degradation of toluene or the ability to grow on H_2 and CO_2. No clear correlation was found between the occurrence of some MGEs and isolation site characteristics and location (geographic). However, it was apparent that strains carried either most of the MGEs or only a few. Interestingly, strains isolated from more hygienic settings like clinical, pharmaceutical or spacecraft environments carried almost no MGEs contrary to strains isolated from sites related to raw materials or environmental sources. This could indicate that either acquisition or loss of these MGEs was advantageous at one point enabling their spread in numerous environments and locations. For example, the MGEs related to

hydrogenotrophy and degradation of toluene may recall to the volcanic origin [321-323] and such MGEs may have been dispensable and lost in technologized environments. Whereas MGEs with a putative link (however without direct evidence at this time) to opportunistic infection were maintained, such as CMGI-1, which is almost identical to the PAGI-2C island identified in *Pseudomonas aeruginosa* clone C (isolated from a cystic fibrosis patient), and CMGI-11, which carries fimbrial genes.

The clear presence or absence of a multitude of MGEs in this group of *C. metallidurans* strains allowed us to further scrutinize the genome of CH34 for MGEs, especially in the second chromosome. At least five additional regions could be identified with one island formed by a Tn*7*-like transposon carrying accessory genes putatively involved in the degradation of certain aromatic compounds. Genomic islands formed by Tn*7*-like transposons have been identified in *H. chejuensis*, *S. sonnei* and *I. loihiensis*, in which Tn*7* inserted into the *att*Tn*7* site adjacent to a *glmS* gene [324]. In *C. metallidurans* CH34 this Tn*7*-like element is not found within the *att*Tn*7* site and in addition lacks the *tnsE* gene and possesses two distinct *tnsD* genes. Parks and Peters [325] showed that the presence of two distinct *tnsD* genes is common in Tn*7*-like elements that are not found within the *att*Tn*7* site and hypothesized that one of the TnsD proteins might actually allow non-specific target site recognition.

Both the CGH and physiological data indicated that the heavy metal resistance determinants identified in *C. metallidurans* CH34 are well conserved among other *C. metallidurans* strains. This strong conservation was also observed for genes encoding small stress responsive proteins and sigma factors, of which at least a part are involved in metal resistance [144, 326].

The incidence of these metal resistance determinants could, however, not be directly related to their isolation source (biotype) nor location (geographic). This indicates that these resistance determinants are probably acquired earlier in evolution, which is consistent with the hypothesis that toxic metal resistance systems are preexistent to the recent anthropogenic activities and arose soon after life began, in a world already polluted by volcanic activities [193]. However, taking into account that most of the metal determinants are on the native megaplasmids and the GIs thereon, it could be argued that anthropogenic activities and technologized environments provided a selective pressure for the conservation of these determinants or even the acquisition of some, considering both the arsenal of determinants as well as the level of resistance to metals. Putatively, these determinants may even render a higher fitness in infections as these megaplasmids, despite their fitness cost, are also present in strains isolated from human infections. The structural and functional characteristics that metal resistance systems share with antibiotic resistance systems could be significant for this [129].

A.5 Conclusions

Our comparative study showed that most metal resistance determinants identified in *C. metallidurans* CH34 are common to all *C. metallidurans* strains irrespective of the strain's isolation type and place. *C. metallidurans* strains do display considerable differences in the diversity and size of their mobile gene pool, which reflects at least some metabolic properties.

Appendix B

Curriculum vitae

Kristel Mijnendonckx

Born	25th of December 1984
Phone	+32 498 24 14 58
Email	kristel.mijnendonckx@gmail.com
Nationality	Belgian

Education and Scientific career

2009 – present **PhD student**

Title: Adaptive silver resistance in *C. metallidurans*

Promotors: Prof. J. Mahillon and Dr. Ir. R. Van Houdt
Catholic University of Louvain-la-Neuve (UCL), Laboratory of Food and Environmental Microbiology and Belgian Nuclear Research Center (SCK•CEN), Expertise Group Molecular and Cellular Biology, Unit Microbiology

2008 –2009 **Bio-Plus Services BVBA**
Run and analyse biochemical and cellular assays for drug discovery projects in oncology at Janssen Pharmaceutica. More in detail: study of the glycolytic- and fatty acid synthesis pathway in cancer cells.

2007-2008 **Master Molecular Biotechnology *option* Medical**
Ghent University

Thesis: Studies on the effect of Bax-inhibitor 1 on apoptotic and necrotic cell death

Promoter: Prof. Dr. P. Vandenabeele

2002-2007 **Master Biology *option* Physiology and Molecular Biology of animals**
Catholic University of Leuven

Thesis: The role of ghrelin in the food intake of chicken

Promoter: Prof. V. Darras

Publications

Mijnendonckx K., Leys N., Mahillon J., Silver S., Van Houdt R. (2013) Antimicrobial silver: uses, toxicity and potential for resistance *Biometals* 26 (3)

Mijnendonckx K., Provoost A., Ott C., Venkateswaran K., Mahillon J., Leys N., Van Houdt R. (2013) Characterization of the Survival Ability of *Cupriavidus metallidurans* and *Ralstonia pickettii* from Space-Related Environments *Microbial Ecology* 65(2): 347-360

Van Houdt R., Monsieurs P., **Mijnendonckx K**., Provoost A., Janssen A., Mergeay M., Leys N (2012) Variation in genomic islands contribute to genome plasticity in *Cupriavidus metallidurans BMC Genomics* (13): 111

Van Houdt R., **Mijnendonckx K**., Leys N. (2012) Microbial contamination monitoring and control during human space missions *Planetary and Space Science* 60(1):115-120

Mijnendonckx K., Provoost A., Monsieurs P., Leys N., Mergeay M., Mahillon J., Van Houdt R. (2011) Insertion sequence elements in *Cupriavidus metallidurans* CH34: Distribution and role in adaptation *Plasmid* 65(3): 193-203

Oral presentations

Mijnendonckx K., Monsieurs P., Leys N., Mahillon J., Van Houdt R.- Dynamic genetic adaptation of Cupriavidus metallidurans in response to silver toxicity.- *Posttranscriptional regulation and epigenetics in microorganisms*.- Brussels, Belgium, 30 November 2012

Mijnendonckx K., Monsieurs P., Mergeay M., Leys N., Mahillon J., Van Houdt R.- Increased resistance to the silver disinfectant is acquired by endogenous insertion sequence elements and cross regulation in the bacterium *Cupriavidus Metallidurans* CH34.- *ELGRA Biennial Symposium and General Assembly: "Gravity: from µ to x !"*.- Antwerp, Belgium, 6-9 September 2011

Mijnendonckx K., Provoost A., Ott M.C., Venkateswaran K., Leys N., Mahillon J. and Van Houdt R. - *Cupriavidus* and *Ralstonia* bacteria just 'have it in them' to make from ultra-clean spacecraft environments their home - *7th International Microbial Space Workshop* – Clermont-Ferrand, France, 17-19 May 2011

Mijnendonckx K.- Metal Resistant *Cupriavidus metallidurans* isolates mainly differ in mobile genetic elements content.- *Consortium Cupriavidus metallidurans CH34*.- Brussels, Belgium, 5 April 2011

Mijnendonckx K., Van Houdt R., Provoost A., Bossus A., Ott M., Venkateswaran K., Leys N.- Inventorying the molecular potential of *Cupriavidus* and *Ralstonia* strains surviving harsh space-related environments.- *38th COSPAR scientific assembly*.- Bremen, Germany, 18-25 July 2010

Poster presentations

Mijnendonckx K., Monsieurs P., Leys N., Mahillon J., Van Houdt R.- Dynamic genetic adaptation of *Cupriavidus metallidurans* in response to silver toxicity.- *FEMS* - Leipzig, Germany 21-25 July 2013 (**selected for travel grant**)

Mijnendonckx K., Monsieurs P., Leys N., Mahillon J., Van Houdt R.- Dynamic genetic adaptation of *Cupriavidus metallidurans* in response to silver toxicity.- *Posttranscriptional regulation and epigenetics in microorganisms*.- Brussels, Belgium, 30 November 2012 (**Winner of the "Merck Sharp & Dohme" Poster Award for Bacteriology**)

Mijnendonckx K., Provoost A., Ott C.M., Venkateswaran K., Leys N., Mahillon J., and Van Houdt R. – Metal resistance in *Cupriavidus metallidurans* and *Ralstonia pickettii* isolates. - *8th International Biometals Symposium*, Brussels, Belgium, 15-19 July 2012

Mijnendonckx K., Provoost A., Ott M., Venkateswaran K., Leys N., Mahillon J., Van Houdt R.- Silver resistance in *Cupriavidus metallidurans* and *Ralstonia* pickettii bacterial isolates obtained from water supplies of the International Space Station.- *BelTox*.- Mechelen, Belgium, 8 December 2011

Mijnendonckx K., Monsieurs P., Mergeay M., Leys N., Mahillon J., Van Houdt R.- Silver resistance in *Cupriavidus metallidurans* CH34 is affected by endogenous Insertion Sequence elements and cross regulation.- *Life, death and survival of Micro-organisms*.- Brussels, Belgium, 16 November 2011

Mijnendonckx K., Provoost A., Ott M., Venkateswaran K., Leys N., Mahillon J., Van Houdt R- *Cupriavidus* and *Ralstonia bacteria* just 'have it in them' to make from ultra-clean spacecraft environments their home.- *ELGRA Biennial Symposium and General Assembly: "Gravity: from µ to x !"*.- Antwerp, Belgium, 6-9 September 2011

Mijnendonckx K., Monsieurs P., Mergeay M., Leys N., Mahillon J., and Van Houdt R. - Silver resistance in *Cupriavidus metallidurans* CH34 is affected by endogenous insertion sequence elements and cross regulation – *11th ICOBTE conference* – Florence, Italy, 03-07 July 2011

Mijnendonckx K., Monsieurs P., Mergeay M., Leys N., Mahillon J., and Van Houdt R. - Silver resistance in *Cupriavidus metallidurans* CH34 is affected by endogenous insertion sequence elements and cross regulation - *FEMS* – Geneve, Switserland, 26-30 June 2011

Mijnendonckx K., Provoost A., Ott M.C., Venkateswaran K., Leys N., Mahillon J. and Van Houdt R. - *Cupriavidus* and *Ralstonia* bacteria just 'have it in them' to make from ultra-clean spacecraft environments their home - *FEMS* – Geneve, Switserland, 26-30 June 2011

Mijnendonckx K., Provoost A., Saiful I., Ott M.C., Venkateswaran K., Leys N., Mahillon J. and Van Houdt R. - *Cupriavidus* and *Ralstonia* bacteria just 'have it in them' to make from ultra-clean spacecraft environments their home - *8th International congress on Extremophiles* - Azores, Portugal, 12-16 September 2010

Mijnendonckx K., Provoost A., Monsieurs P., Leys N., Mergeay M., Mahillon J., Van Houdt R - Identification, characterization and distribution of insertion sequence elements in *Cupriavidus metallidurans* CH34.- *annual BSM meeting*.- Brussels, Belgium, 11-11 December 2009

Mentor of students:

Mollaei M. - 'Study of Microbial resistance to silver and survival in pure water' – Master Level Apprenticeship – 1 August - 31 December 2010

Renckens W.- Temperatuurgeïnduceerde mutagenese en mortaliteit van *Cupriavidus metallidurans* CH34.- Diepenbeek, Belgium: Provinciale Hogeschool Limburg (PHL), 2011.- 66 p.- Bachelor thesis

Soetemans L. – Mobilisatie en karakterisatie van megaplasmiden in *Cupriavidus metallidurans* - Diepenbeek, Belgium: Provinciale Hogeschool Limburg (PHL), 2012.- 81 p.- Bachelor thesis